GRAN SASSO
hands-on 2025
PhD school on experimental astroparticle physics
September 8th - 18th, 2025

Cosmic rays experiments

Lorenzo Perrone - Università del Salento e INFN Sezione di Lecce

image: credits to the Pierre Auger Observatory

Why studying cosmic rays?!

They are very…..”natural”

~ 300 particles/s/m^2 20% of natural radioactivity

→ Unveil the nature and origin of galactic and extra-galactic **astrophysical sources** along with the understanding of high-energy particles production and acceleration mechanisms

→ Study of **fundamental interactions** up to energies well beyond man-made accelerators nowadays

→ Long record of pioneering discoveries → insight into new physics is in their DNA

messengers of **new/exotic/unknown physics (dark matter, dark energy)**

→ the highest energy particles ever observed in the Universe

Cosmic rays and society

Cheope Pyramid

Northern lights

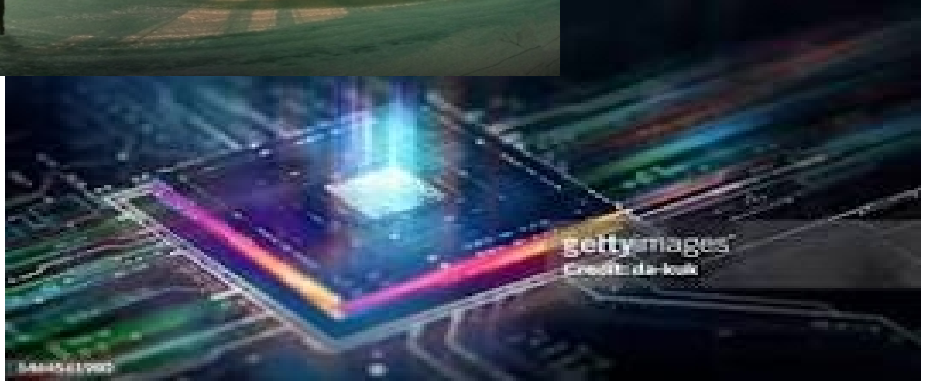

Quantum computing

Cosmic rays and gammas energy spectrum

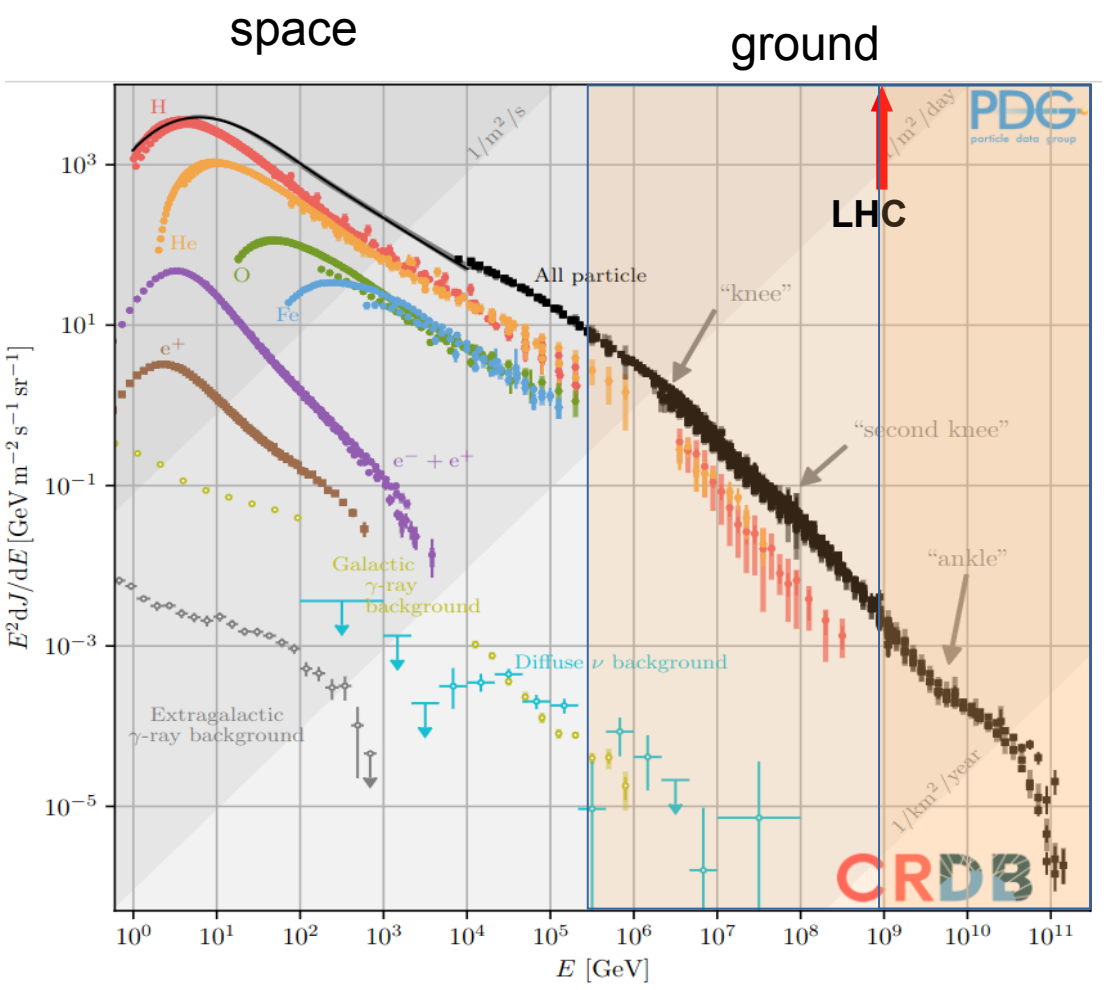

Wide range of energy/flux

Diverse measurement techniques

Impressive improvement of the knowledge in the past decade
still many open problems

Such as: origin and nature of ultra-high energy cosmic rays, acceleration mechanisms, propagation effects...

Unprecedented statistics and precision!

The multi-messenger astronomy landscape

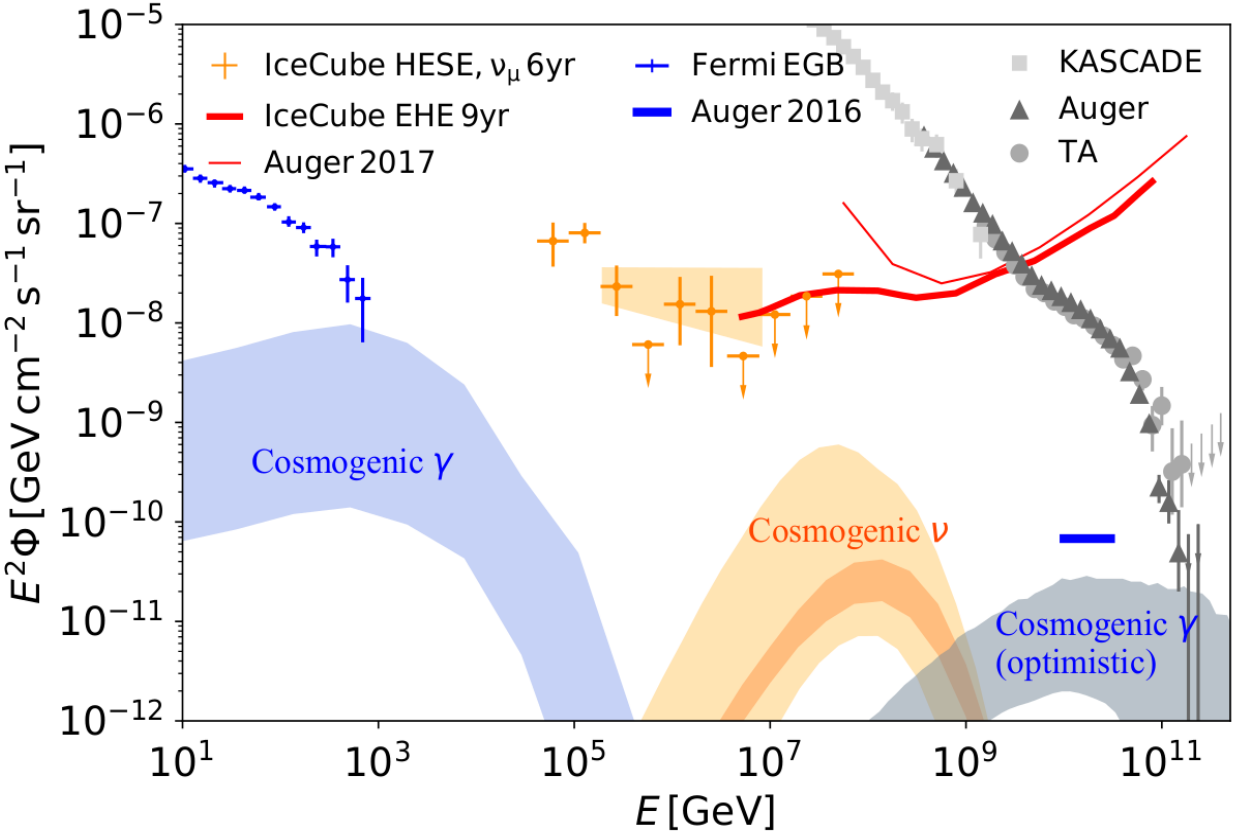

Strong interplay between different “cosmic” actors

Broader context is essential to have a scientifically coherent picture

Exploring and exploiting the potential of these tools in fundamental physics

The cosmic horizon

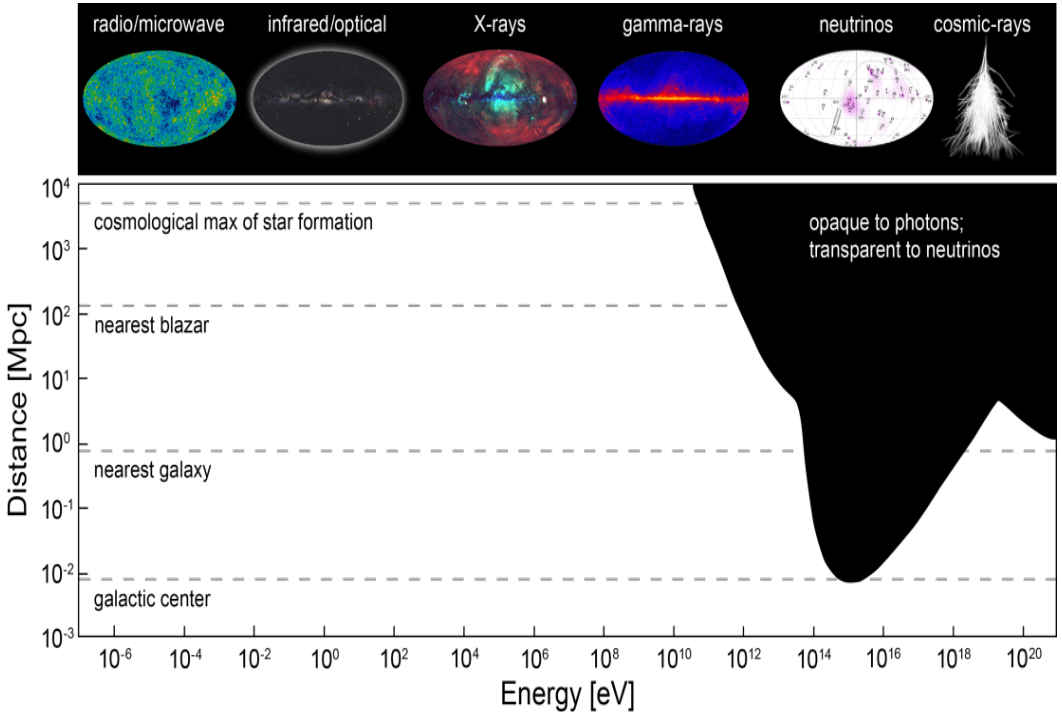

→ **UHE photons:**
limited horizon (local universe)
or hints for new physics (SHDM, LIV)

→ **Gravitational Waves:**
Multi wavelength searches in combination with mergers

→ **Charged CR:**
magnetic fields deflection
propagation effect (~100 Mpc at 10^{20} eV)

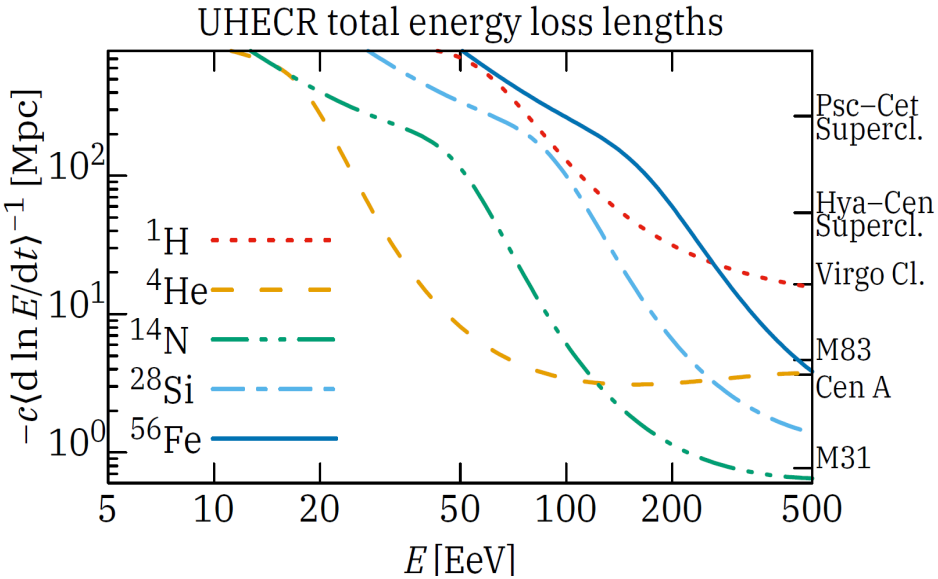

→ **UHE neutrinos:** probing the most distant UHECR sources. Elusive particles need large exposure

Historical retrospective

1896- 1903: Discovery of natural radioactivity (H. Bequerel) and first measurements (E. Rutherford)

1910: T. Wulf goes on top of the Eiffel tower and measures the concentration of radioactivity at high altitude (using an electroscope)

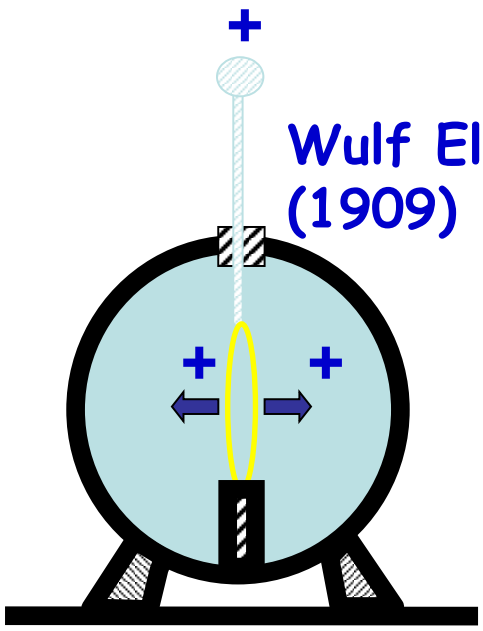

Wulf Electroscope (1909)

At the same time D. Pacini was performing similar measurements in deep water in front of Livorno (Italy)

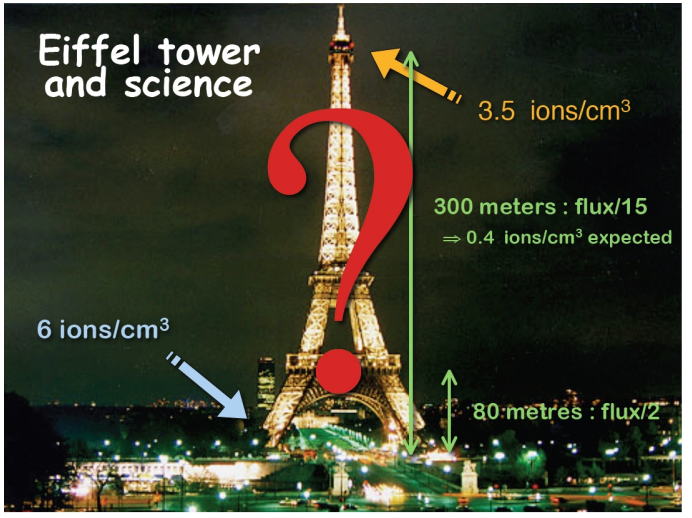

Smaller flux than at ground level

BUT….Not as small as predicted

First puzzle…..

Victor F. Hess: the 1912 flight (5350 m)

Cosmic rays come from outside Earth atmosphere

Nobel prize in 1936 for the discovery of Cosmic Rays

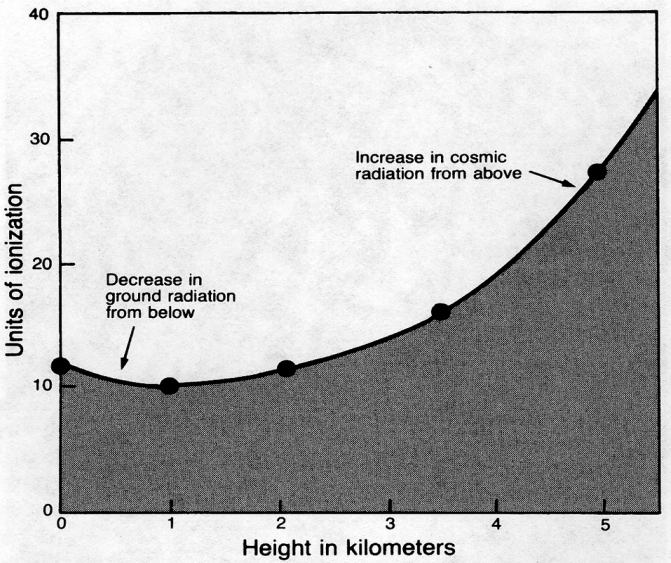

Readings on ionization chamber Victor Hess carried aloft in the Böhmen. Above four kilometers the ionization rose rapidly indicating "that rays of very great penetrating power are entering our atmosphere from above". These cosmic rays contain the only modern samples of matter from outside our solar system which can be investigated directly.

What are they? Radiation or particles?

1930: B. Rossi predicts a east-west asymmetry if they were charged particles due to the geomagnetic field. Later (1934) he observs a time coincidence at large distance, first hints of extensive air showers

1932: Millikan vs Compton. Photons or charged particles?

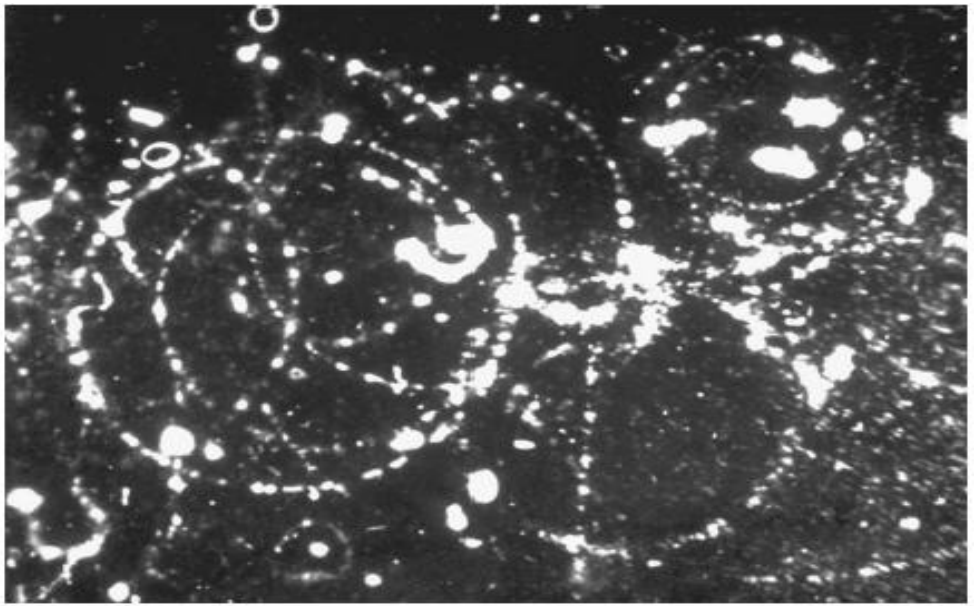

D. Skobeltsyn: picture of cosmic ray event in cloud chamber with B-field

The beginning of particle physics!

1932: Carl Anderson, positron (antimatter) discovery in CR Nobel prize in 1936 (shared with Hess)

1937: Neddermeyer and **Anderson,** muon discovery

1940's: several discoveries, pions and strange particles

Extensive Cosmic-Ray Showers

PIERRE AUGER
In collaboration with
P. EHRENFEST, R. MAZE, J. DAUDIN, ROBLEY, A. FRÉON
Paris, France

Pierre Auger

LONG DISTANCE COINCIDENCES

If two or three counters are arranged in coincidence in free air, a small number of coincidences is observable, due to "air showers" and this number decreases quickly when the horizontal distance of the counters is increased. Schmeiser and Bothe have studied these local showers with counter separations up to half a meter.[2] If the distance is increased further, the

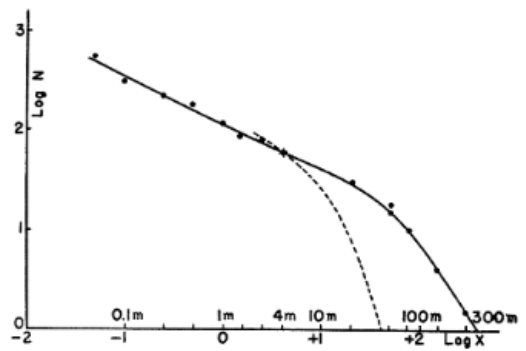

FIG. 1. Results with two parallel and horizontal counters.

ENERGY SPECTRUM OF PRIMARIES

It is interesting to see if our measurements are consistent with the spectral distribution which has been found in the case of the penetrating particles. The number N of particles with an energy higher than E is proportional to E^{-2}, so

CONCLUSION

One of the consequences of the extension of the energy spectrum of cosmic rays up to 10^{15} ev is that it is actually impossible to imagine a single process able to give to a particle such an energy. It seems much more likely that the charged particles which constitute the primary cosmic radiation acquire their energy along electric fields of a very great extension.

John Linsley

PHYSICAL REVIEW VOLUME 128, NUMBER 5 DECEMBER 1, 1962

Arrival Times of Air Shower Particles at Large Distances from the Axis*

JOHN LINSLEY AND LIVIO SCARSI†
Laboratory for Nuclear Science, Massachusetts Institute of Technology, Cambridge, Massachusetts

(Received July 5, 1962)

A study has been made of the relative times of arrival of shower particles at large distances (200 to 1500 m) from the shower axis. Data were obtained at the MIT Volcano Ranch Station, using an array of 20 scintillation detectors, one of which was shielded part of the time. The shower size, direction, and core location were determined for each event. We describe the spatial distribution of shower particles at a given instant by means of three curved surfaces: the median surface for the penetrating particles (muons), the median surface for the electrons, and the extreme front. We find that the average median surface for the muons is approximately spherical, the center being located at an atmospheric depth of 320±70 g cm^{-2}, and that the average median surface for the electrons has a radius of curvature of about 1 km at a distance from the axis of 450 m. The electron radius of curvature increases at greater distances. Assuming that the extreme front is spherical, its average center must be located above 320 g cm^{-2}. We measured the radius for curvature of the extreme front for a small number of individual showers, but were not able to improve upon that limit.

EVIDENCE FOR A PRIMARY COSMIC-RAY PARTICLE WITH ENERGY 10^{20} eV†

John Linsley
Laboratory for Nuclear Science, Massachusetts Institute of Technology, Cambridge, Massachusetts
(Received 10 January 1963)

Analysis of a cosmic-ray air shower recorded at the MIT Volcano Ranch station in February 1962 indicates that the total number of particles in the shower (Serial No. 2-4834) was 5×10^{10}. The total energy of the primary particle which produced the shower was 1.0×10^{20} eV. The shower was about twice the size of the largest we had reported previously (No. 1-15832, recorded in March 1961).[1]

The existence of cosmic-ray particles having such a great energy is of importance to astrophysics because such particles (believed to be atomic nuclei) have very great magnetic rigidity. It is believed that the region in which such a particle originates must be large enough and possess a strong enough magnetic field so that $RH \gg (1/300)\times(E/Z)$, where R is the radius of the region (cm) and H is the intensity of the magnetic field (gauss). E is the total energy of the particle (eV) and Z is its charge. Recent evidence favors the choice $Z=1$ (proton primaries) for the region of highest cosmic-ray energies.[2] For the present event one obtains the condition $RH \gg 3\times10^{17}$. This condition is not satisfied by our galaxy (for which $RH=5\times10^{17}$, halo included) or known objects within it, such as supernovae.

The technique we use has been described elsewhere.[1] An array of scintillation detectors is used to find the direction (from pulse times) and size (from pulse amplitudes) of shower events which satisfy a triggering requirement. In the present case, the direction of the shower was nearly vertical (zenith angle $10\pm5°$). The values of shower density registered at the various points of the array are shown in Fig. 1. It can be verified by close inspection of the figure that the core of the shower must have struck near the point marked "*A*," assuming only (1) that shower particles are distributed symmetrically about an axis (the "core"), and (2) that the density of particles decreases monotonically with increasing distance from the axis. The observed densities

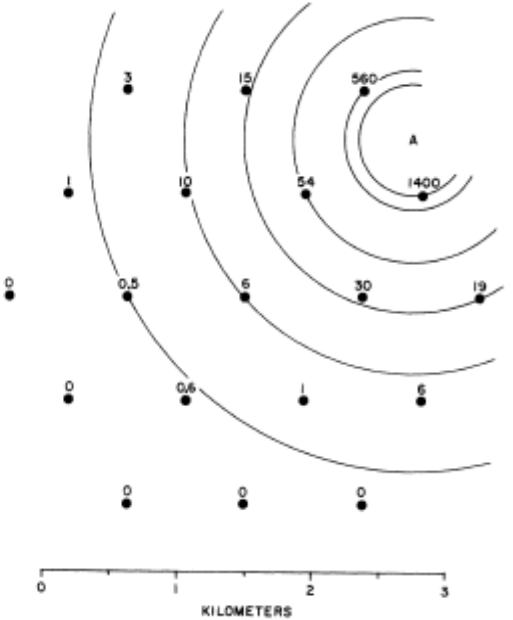

FIG. 1. Plan of the Volcano Ranch array in February 1962. The circles represent 3.3-m^2 scintillation detectors. The numbers near the circles are the shower densities (particles/m^2) registered in this event, No. 2-4834. Point "*A*" is the estimated location of the shower core. The circular contours about that point aid in verifying the core location by inspection.

Cosmic rays sources

Colliding galaxies

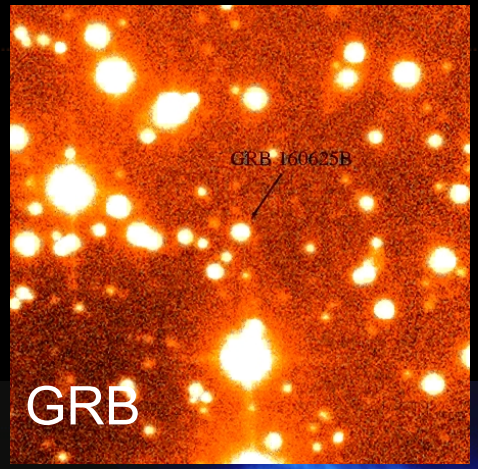

GRB

AGN

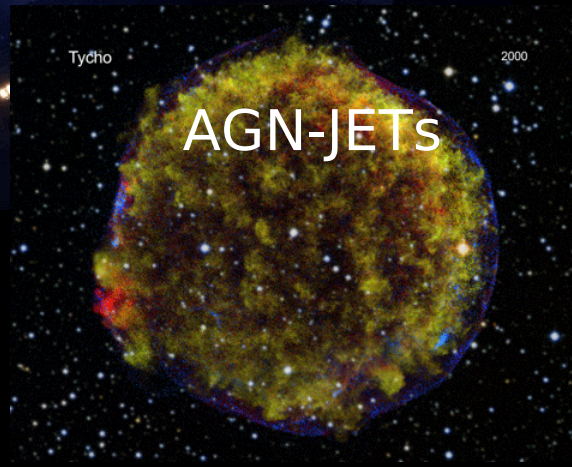

AGN-JETs

Blazar

Acceleration mechanisms (Fermi theory)

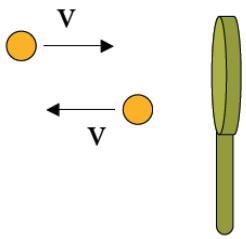

No acceleration

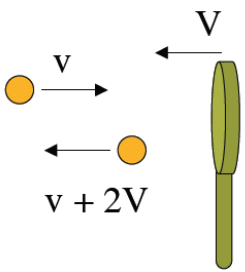

acceleration

Momentum conservation

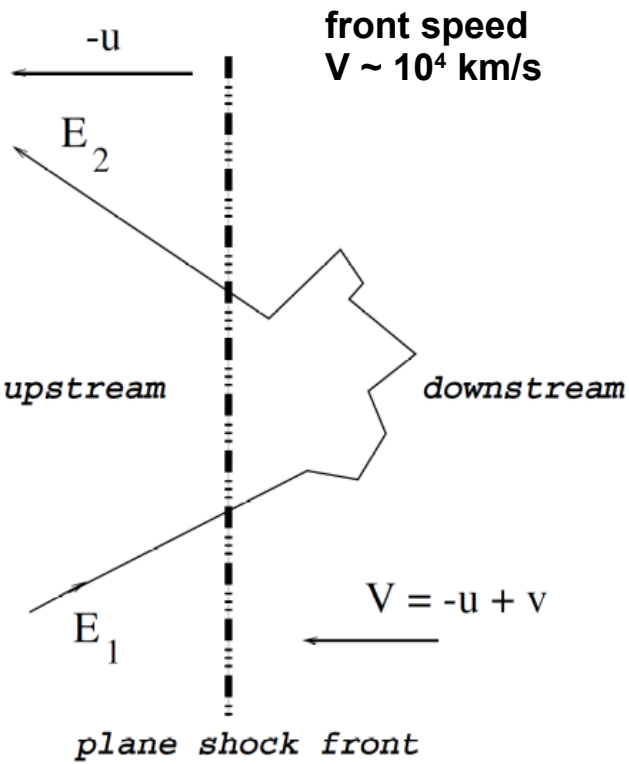

Particles go back and forth across a shock wave (i.e. *Supernovae shocks*)
Energy transfer→ net energy gain for the crossing particles

Main acceleration processes

$V \sim 10^4$ km/s

Fermi model

Random moving magnetic clouds

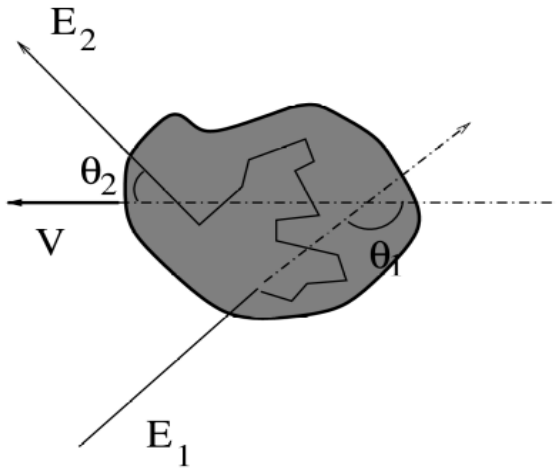

also magnetic reconnection

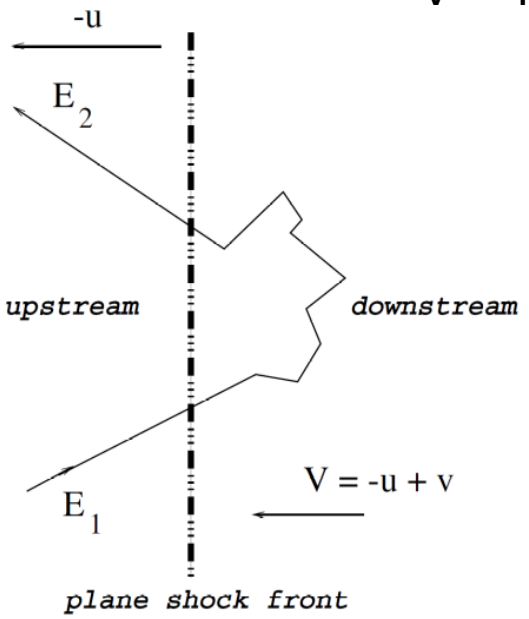

Stochastic → $dE/E \sim (V/c)^2$
second order, less effective

Diffusive → $dE/E \sim V/c$
first order, more effective

Expected flux of accelerated particles → **$dN/dE \sim E^{-2}$**

Where do they come from?

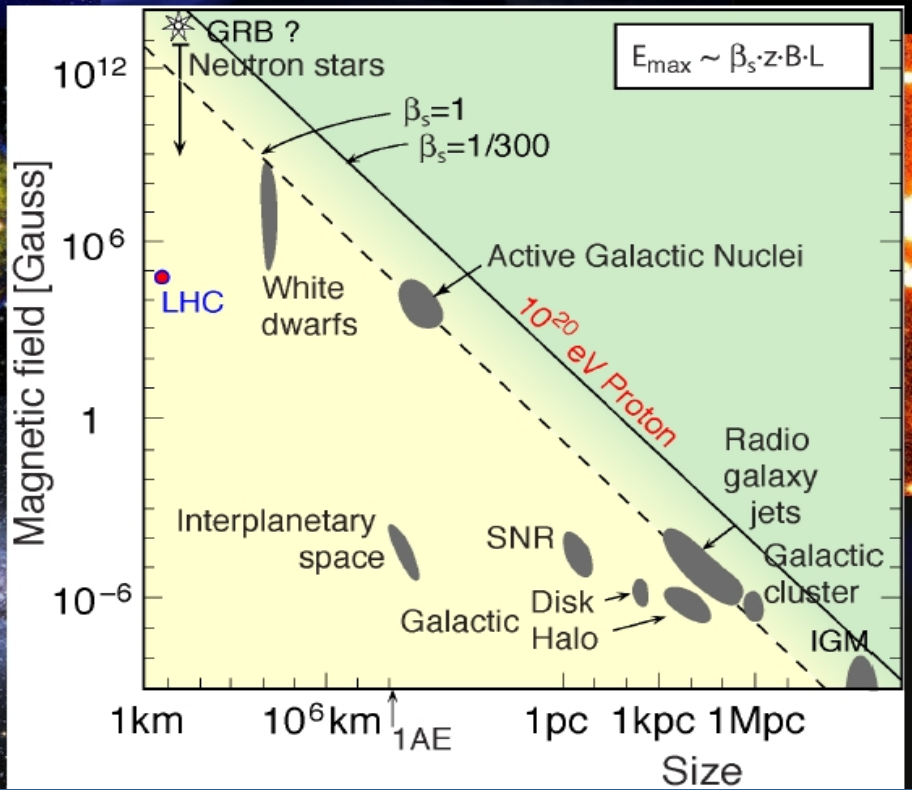

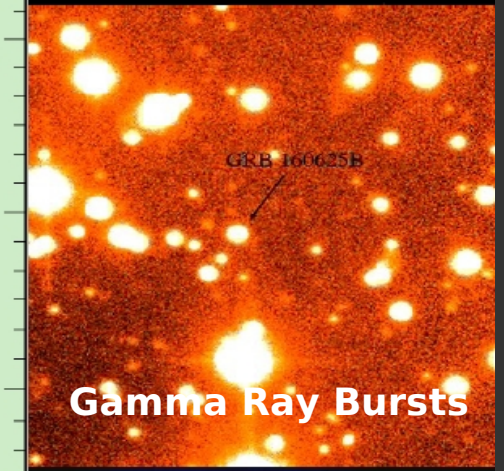

Inside the engine of an astrophysical source….

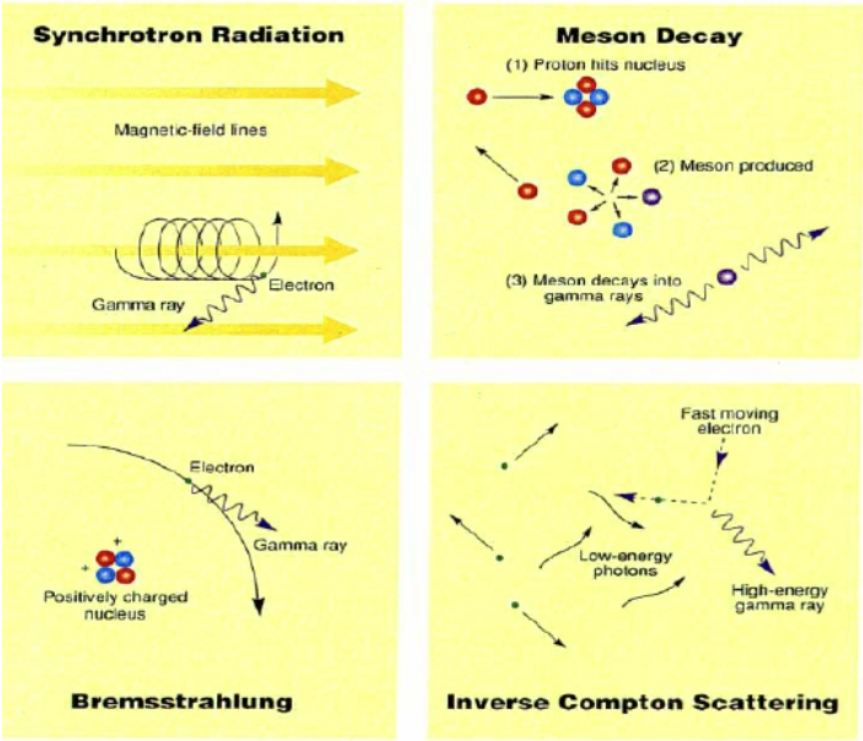

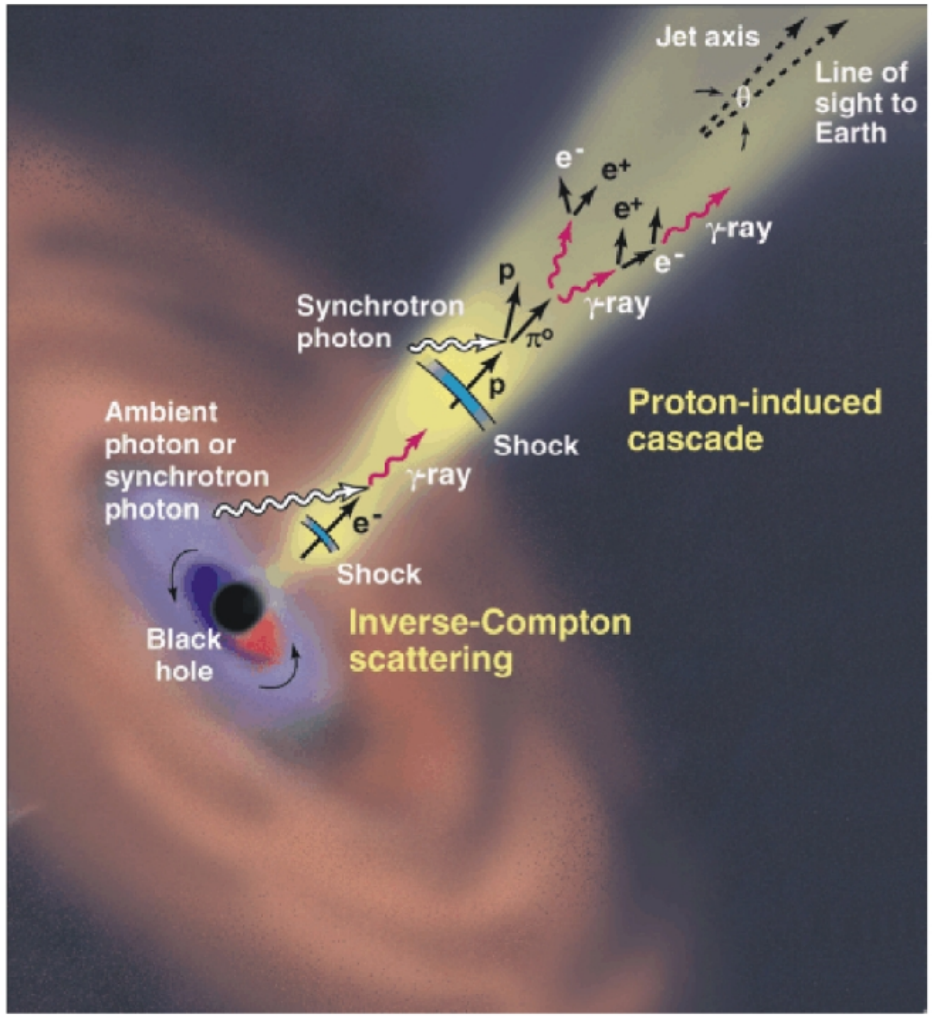

Gamma rays of leptonic origin ...

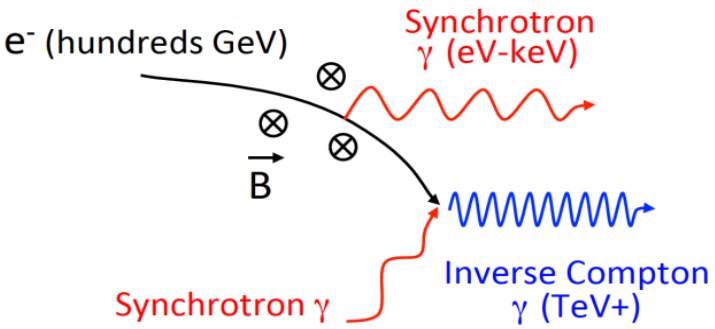

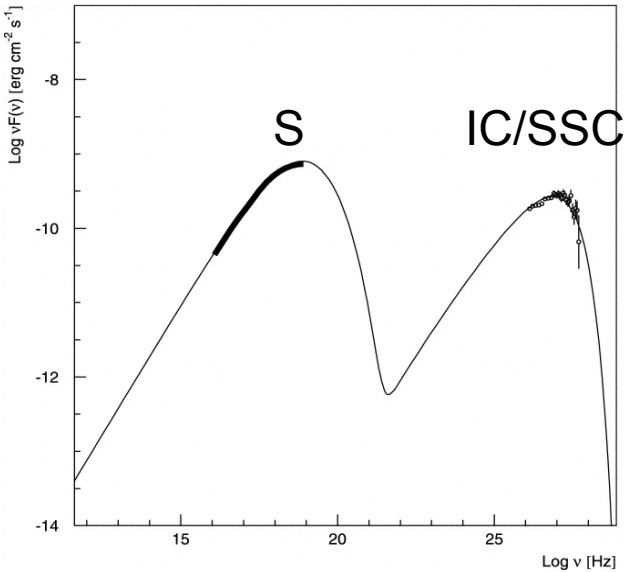

Inverse-compton (IC)

Syncrotron (S)

Synchrotron Self-Compton (SSC)

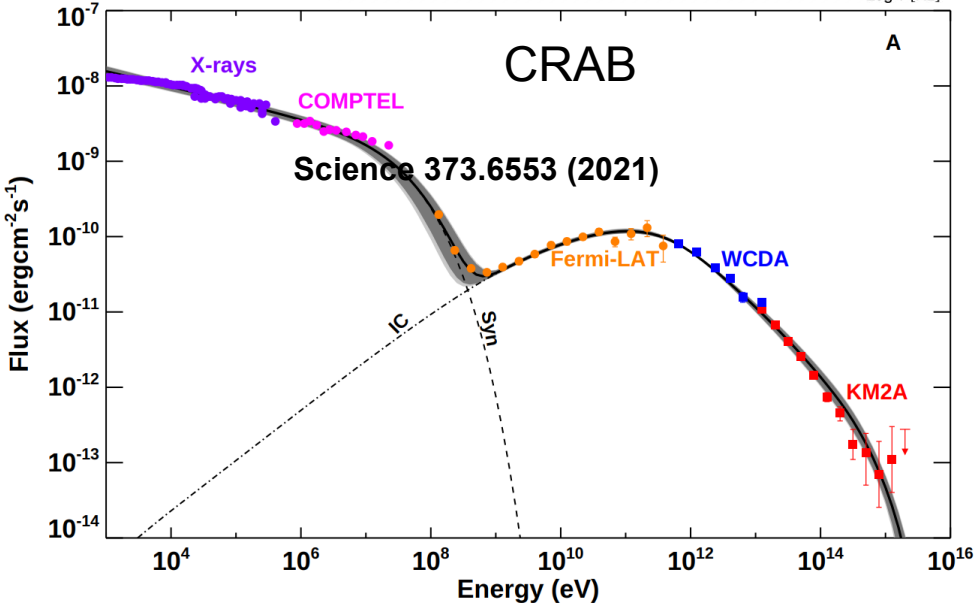

...or hadronic origin

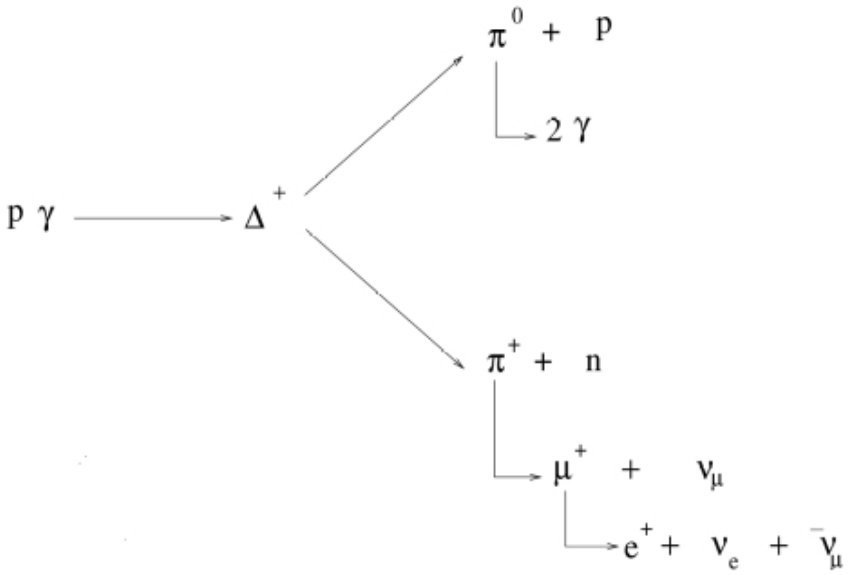

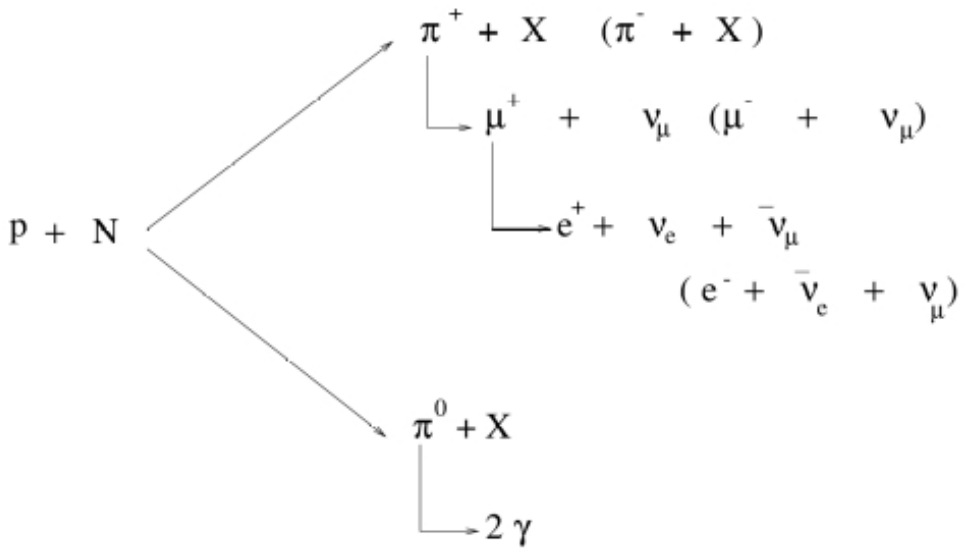

High-energy **photons and neutrinos** produced by hadronic interactions with the surrounding gas and radiation → pN, pɣ

Elemental composition of charged CRs at GeV energy

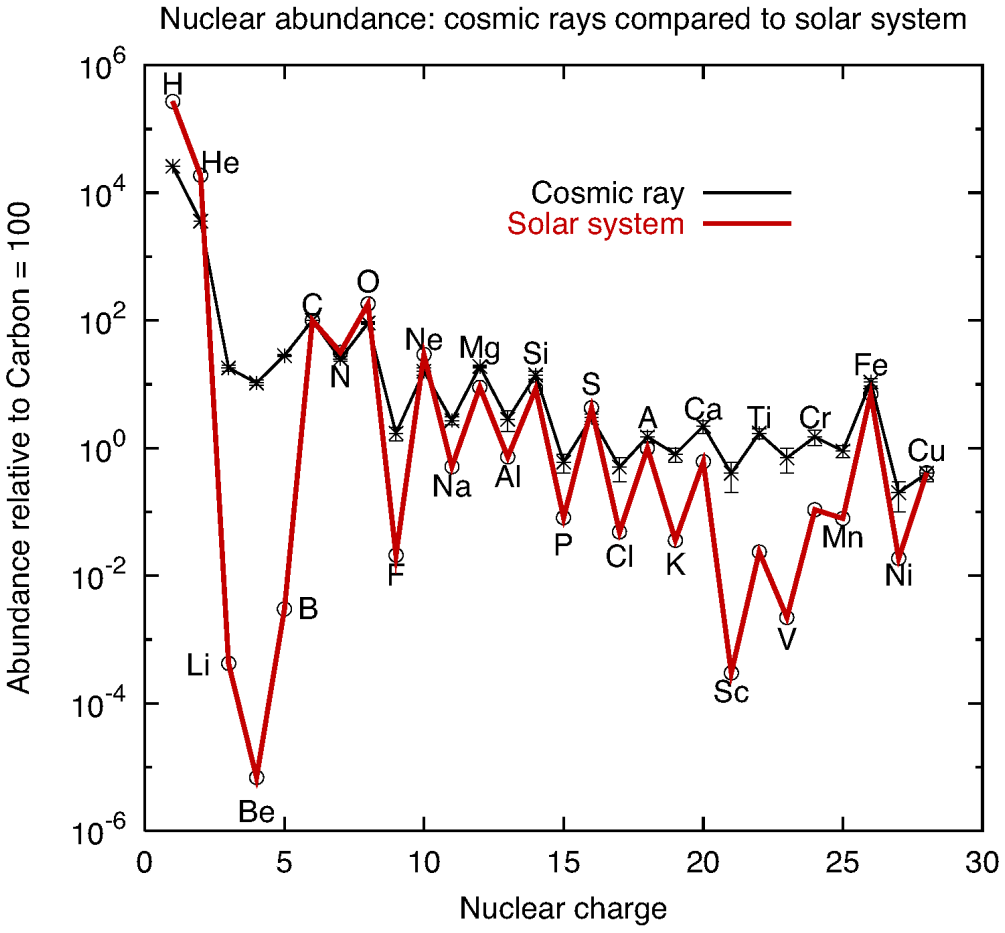

Most of Li, Be, B produced by spallation of CNO

[Sc, T, Cr by spallation of Fe]

The more reactions the higher their abundances
Memory of the propagation
Importance of the relative abundances (i.e. B/C ratio)

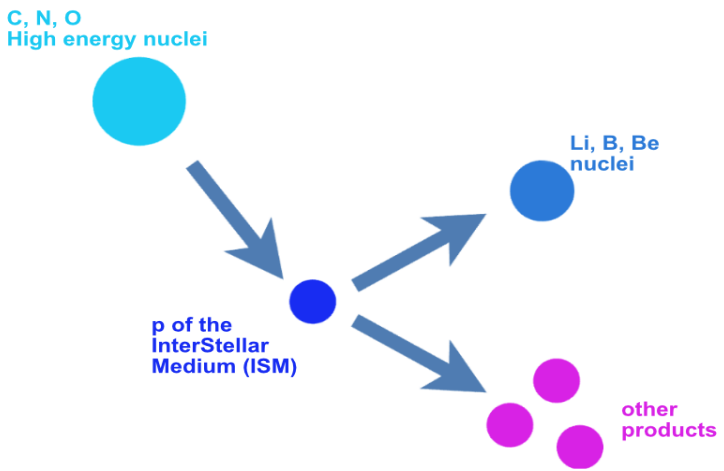

The Review of Particle Physics (2018) M. Tanabashi et al.(Particle Data Group), Phys. Rev. D 98, 030001 (2018).

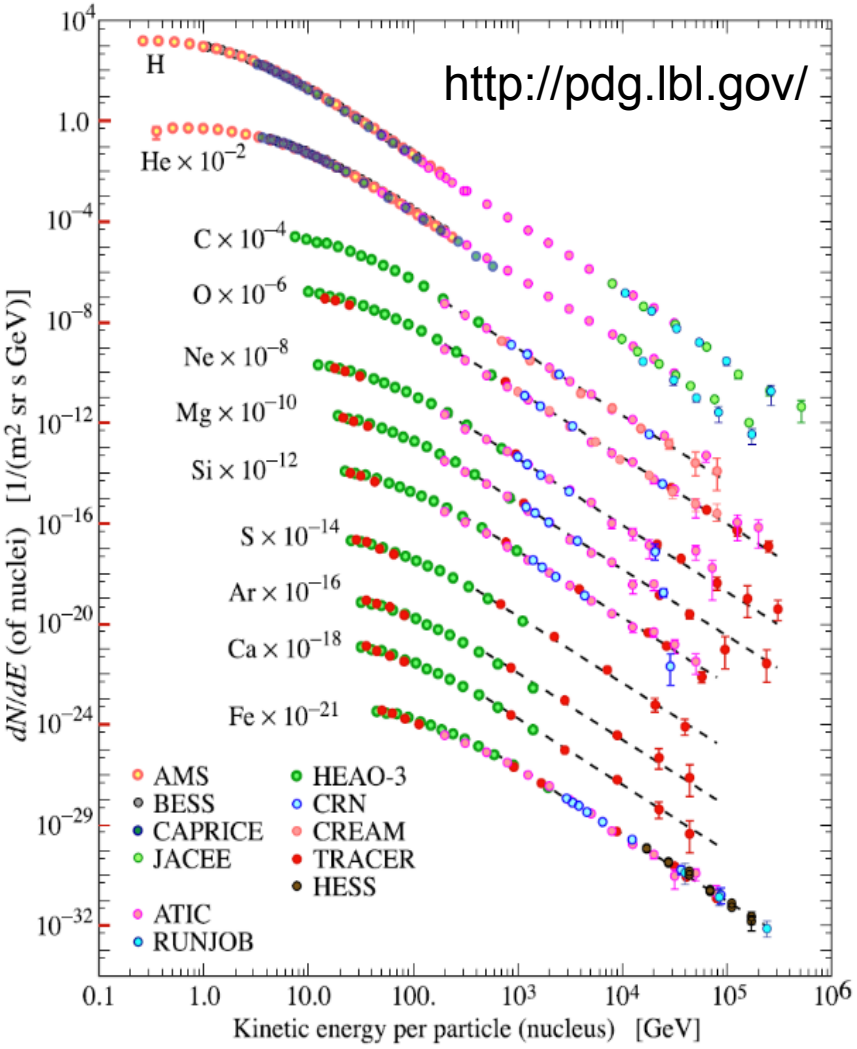

At ~ GeV energies

~ 79% protons

~ 15% He nuclei

~ 5% heavier nuclei

~ 1% free electrons

~ 10^{-5} 10^{-4} antiprotons

- composition changes with energies
still mixed at $10^{19.5}$ eV

- galactic origin energy <~ $10^{16\text{-}17}$ eV
- most likely extragalactic energy >~ 10^{18} eV

- isotropic ?
Anisotropy is still an open point

Cosmic Rays Propagation through the Milky Way

Magnetic fields drive the path of CR

Confinement depends on energy and rigidity

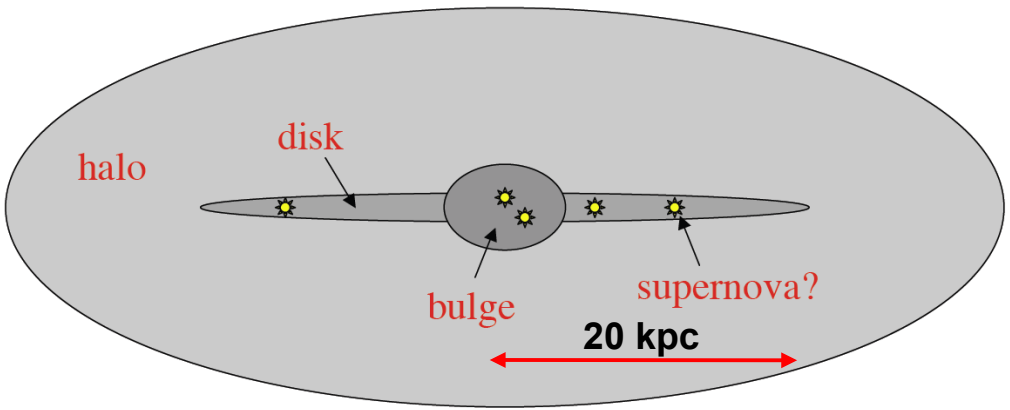

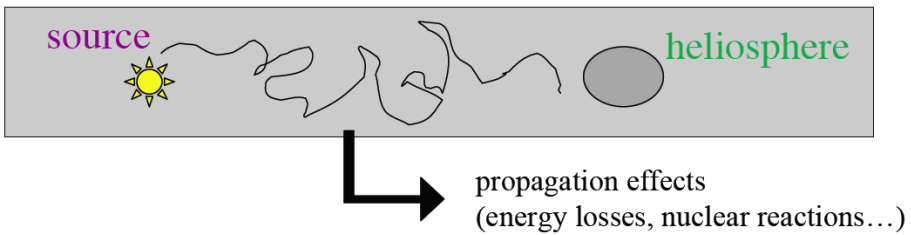

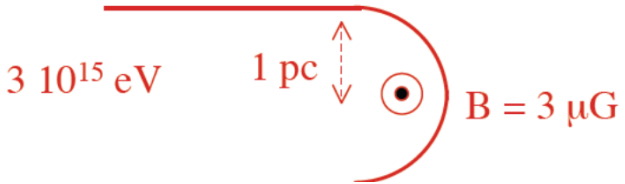

$$R_{gyro} = \frac{cp_{\perp}}{ZeB}$$

High-energy and low Z particles likely escape the galaxy for energy larger than 3 10^{15} eV ***knee region***

CRs spend **20 million years in our Galaxy**
constant flux of CRs requires an **injection power of ~2 10^{41} erg/s**

3 supernovae/century may provide this power

Propagation at the highest energies

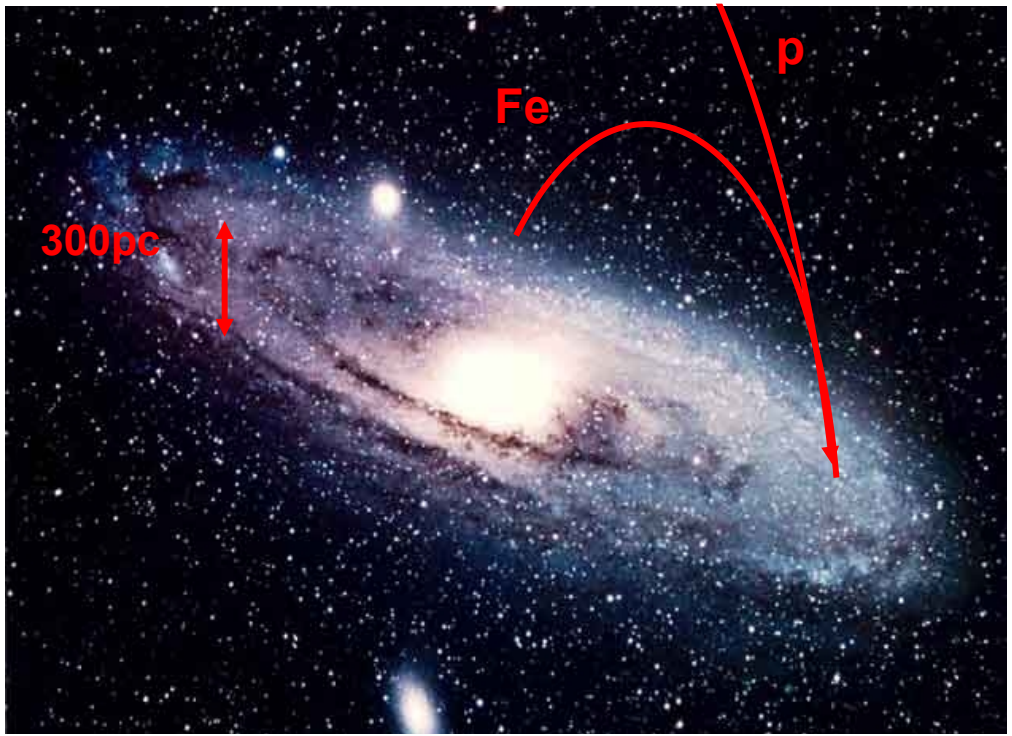

Gyroradius exceeds the size of our Galaxy

$$r_L \sim \frac{E_{18}}{Z B_{\mu G}} kpc$$

Particles with energies above few EeV (1 EeV = 10^{18} eV) are most likely of extragalactic origin

$$d\theta(E,d) \simeq \frac{d}{r_L} \simeq 0.52^\circ \cdot \mathrm{Z} \cdot \left(\frac{E}{10^{20}\ \mathrm{eV}}\right)^{-1} \cdot \left(\frac{B}{10^{-9}\ \mathrm{G}}\right) \cdot \left(\frac{d}{\mathrm{Mpc}}\right)$$

Proton, 10^{20} eV, less than 1 degree deflection along 1kpc (1 Mpc) with B ~ 10^{-6} (10^{-9}) Gauss

Magnetic deflection reduced at the highest energies:

ASTRONOMY with charged Cosmic-Rays

Gravitational waves!

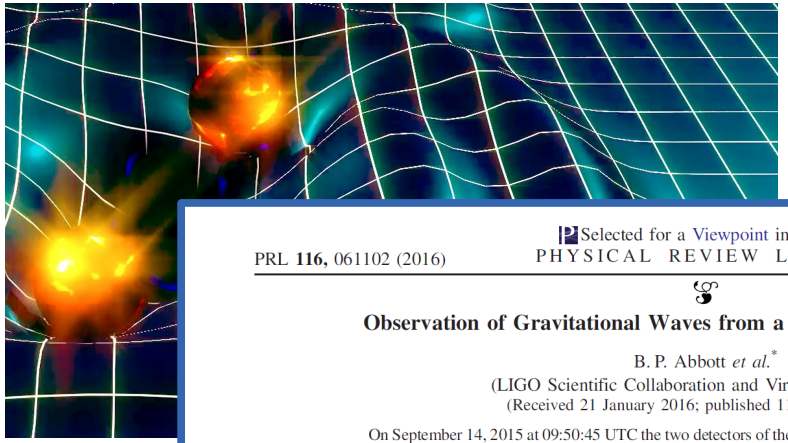

PRL **116,** 061102 (2016)

Selected for a Viewpoint in *Physics*
PHYSICAL REVIEW LETTERS

week ending
12 FEBRUARY 2016

Observation of Gravitational Waves from a Binary Black Hole Merger

B. P. Abbott *et al.*[*]
(LIGO Scientific Collaboration and Virgo Collaboration)
(Received 21 January 2016; published 11 February 2016)

On September 14, 2015 at 09:50:45 UTC the two detectors of the Laser Interferometer Gravitational-Wave Observatory simultaneously observed a transient gravitational-wave signal. The signal sweeps upwards in frequency from 35 to 250 Hz with a peak gravitational-wave strain of 1.0×10^{-21}. It matches the waveform predicted by general relativity for the inspiral and merger of a pair of black holes and the ringdown of the resulting single black hole. The signal was observed with a matched-filter signal-to-noise ratio of 24 and a false alarm rate estimated to be less than 1 event per 203 000 years, equivalent to a significance greater than 5.1σ. The source lies at a luminosity distance of 410^{+160}_{-180} Mpc corresponding to a redshift $z = 0.09^{+0.03}_{-0.04}$. In the source frame, the initial black hole masses are $36^{+5}_{-4}M_\odot$ and $29^{+4}_{-4}M_\odot$, and the final black hole mass is $62^{+4}_{-4}M_\odot$, with $3.0^{+0.5}_{-0.5}M_\odot c^2$ radiated in gravitational waves. All uncertainties define 90% credible intervals. These observations demonstrate the existence of binary stellar-mass black hole systems. This is the first direct detection of gravitational waves and the first observation of a binary black hole merger.

DOI: 10.1103/PhysRevLett.116.061102

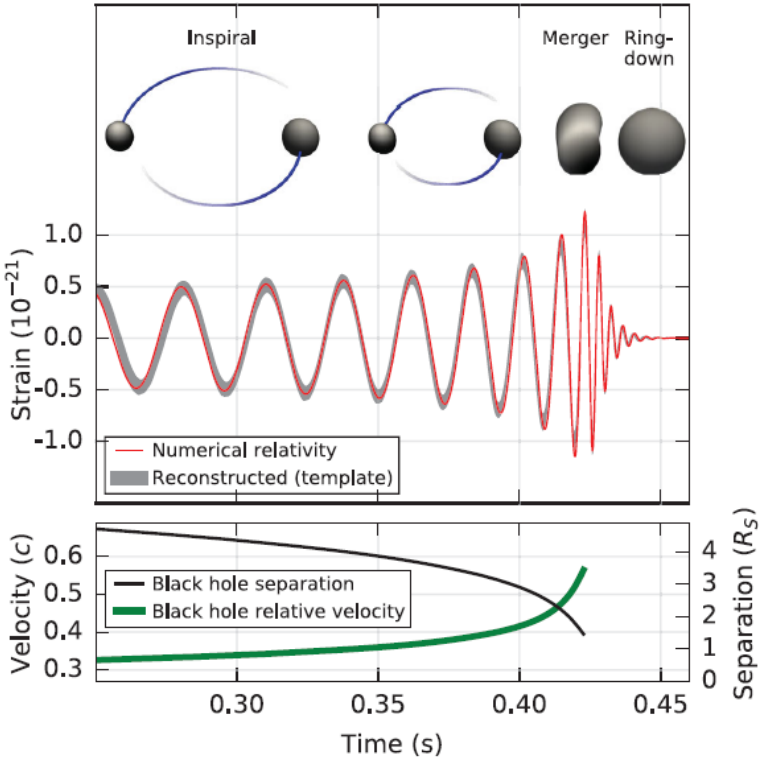

PRL **119,** 161101 (2017)

Selected for a Viewpoint in *Physics*
PHYSICAL REVIEW LETTERS

week ending
20 OCTOBER 2017

GW170817: Observation of Gravitational Waves from a Binary Neutron Star Inspiral

B. P. Abbott *et al.*[*]
(LIGO Scientific Collaboration and Virgo Collaboration)
(Received 26 September 2017; revised manuscript received 2 October 2017; published 16 October 2017)

On August 17, 2017 at 12:41:04 UTC the Advanced LIGO and Advanced Virgo gravitational-wave

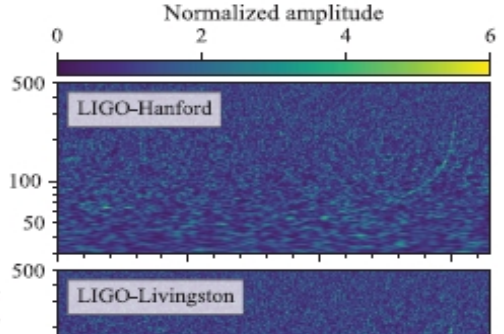

Propagation of CR, photons and neutrinos across the IM

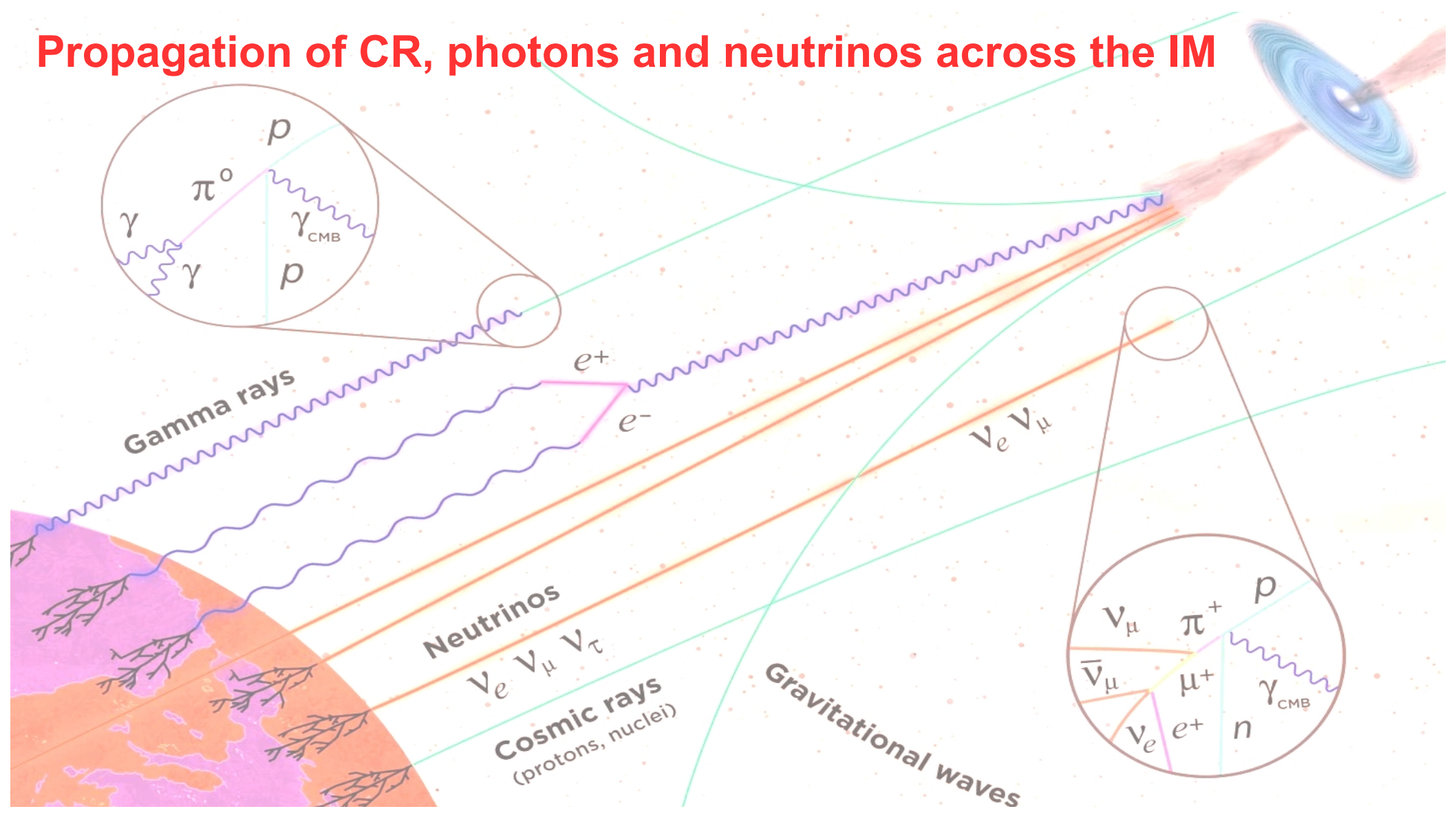

Inspecting the Cosmic Ray Realm

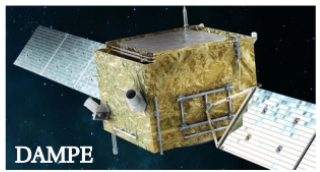

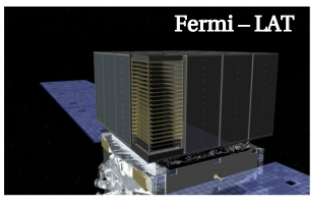

Direct experiments can currently reach up to a few hundred TeV

1. containment
2. limited effective area

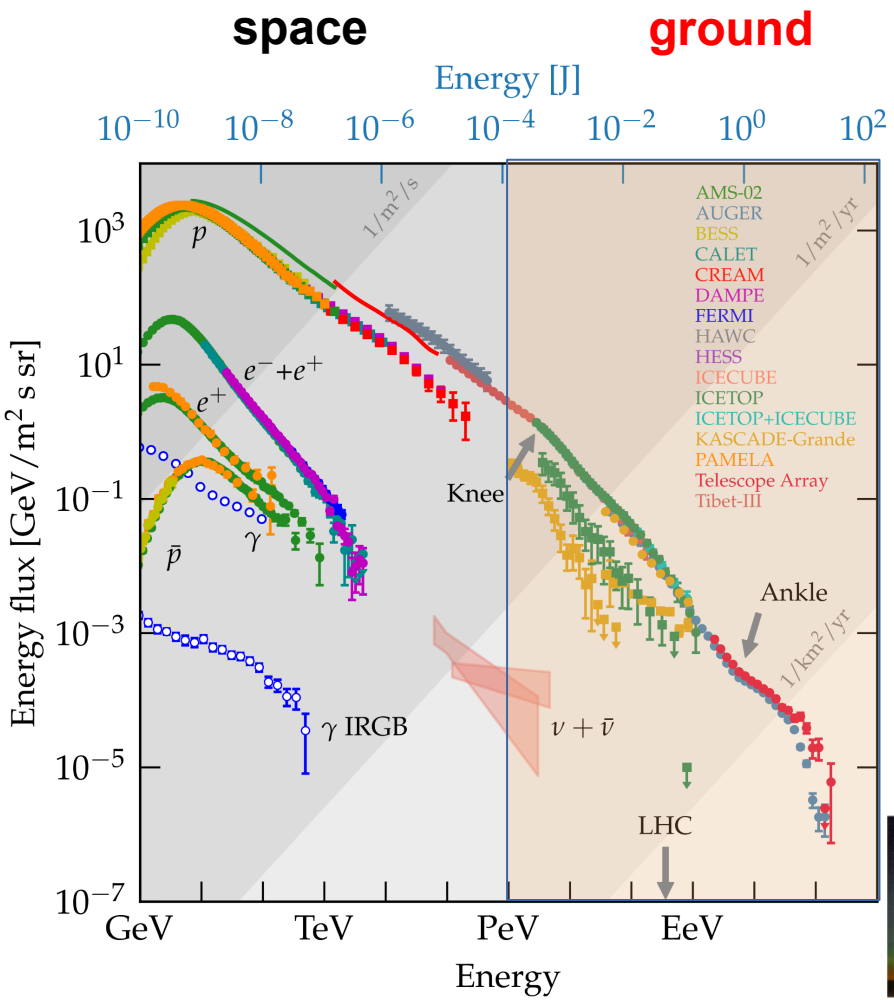

Spectral features at the highest energies can be probed using indirect detection experiments

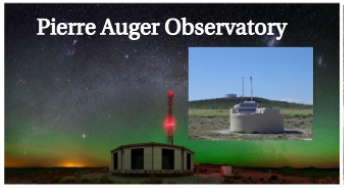

The Fermi gamma ray space telescope

Orbits Earth at ~550 km altitude in low-Earth orbit. About 4 tons

LAT (Large Area Telescope): 20 MeV – 300 GeV

- Layers of tungsten foils → incoming gamma rays hit these and convert into electron–positron pairs.
- Silicon strip detectors track their paths.
- A cesium iodide calorimeter measures the energy.
- Anti-coincidence detector helps filter out cosmic rays (so it doesn't mistake them for gamma rays).

GBM (Gamma-ray Burst Monitor): 8 keV – 40 MeV

- 14 scintillation detectors (NaI and BGO crystals).
- Covers a wider field of view than LAT.
- Specially designed to catch short bursts from all over the sky.

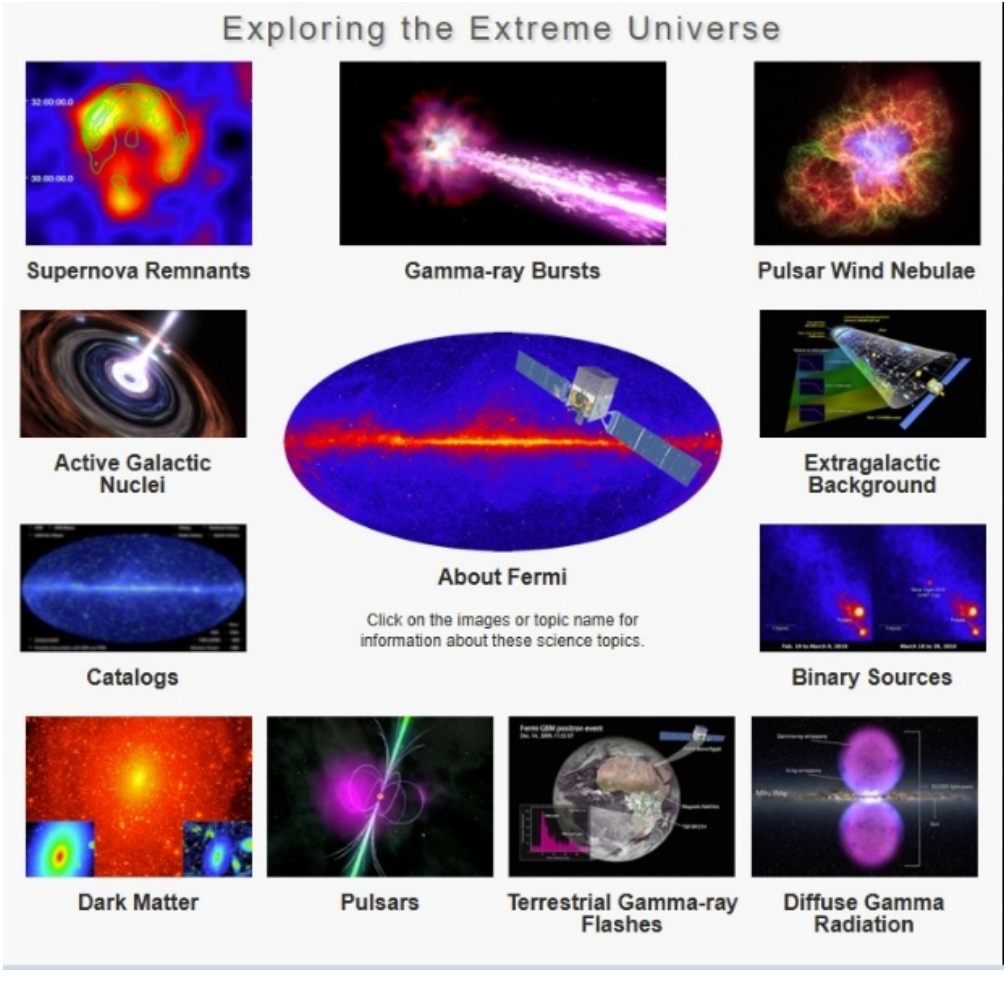

Fermi sky map after 13 years (2008-2021)

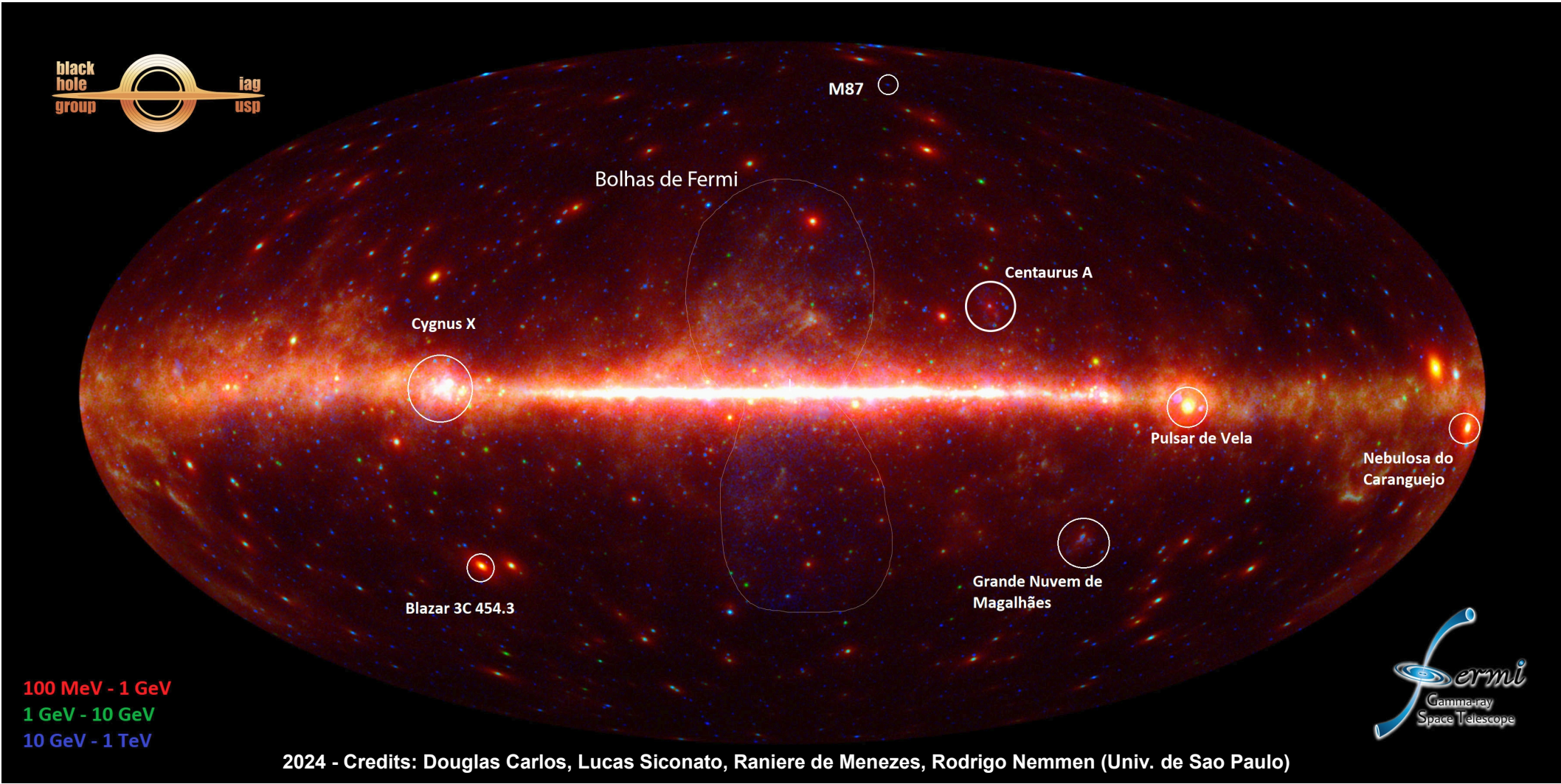

The DAMPE Mission

Orbit: Sun – synchronous, 95 min
Altitude: 500 km (LEO)
Payload: 1300 kg

Acceptance	~0.3 m^2sr
Energy Resolution	1.2% at 100 GeV (e/γ) < 40% at 800 GeV (nuclei)
e/γ Angular resolution	0.2° at 100 GeV
Energy Range	10 GeV - 10 TeV (e/γ) 50 GeV - 200 TeV (nuclei)

Launched on Dec 17th 2015

Jiuquan Satellite Launch Center
Gobi desert, China

Main scientific objectives

CRs: All-electron, proton & nucleonic spectra w/ great precision

γ – rays: Insight on high-energy γ astronomy, transient studies, etc

DM: Indirect studies on possible DM candidates

DAMPE Collaboration, Astropart. Phys., 95, 6 [2017]

The Collaboration

International synergy between Chinese, Italian & Swiss institutes/universities.

DAMPE Detector Description

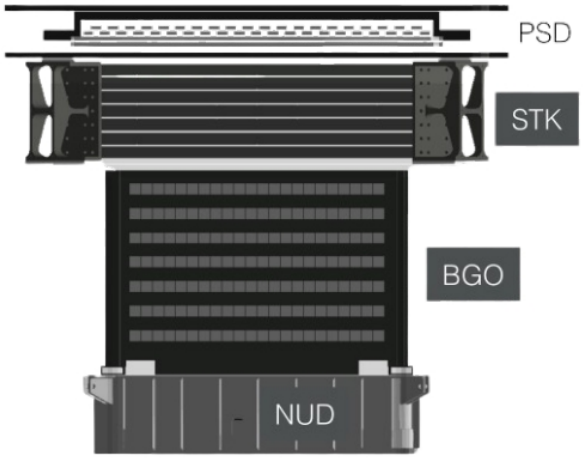

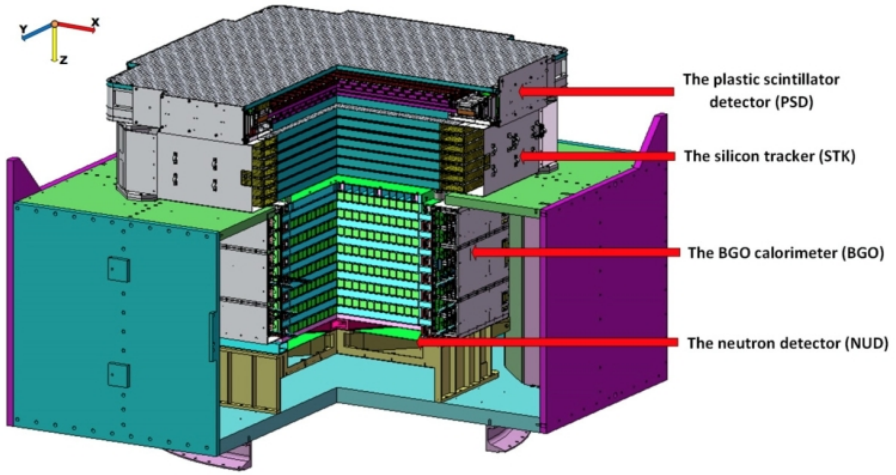

Length 1.4 m
Width 0.9
Depth 0.9
Total weight 1.9 tons

PSD: Anti – coincidence detector for gammas and charge measurement

STK: Particle tracker, photon converter & additional charge measurement

BGO: Energy measurement & particle identification via shower topology

NUD: Further particle ID from electromagnetic & hadronic showers

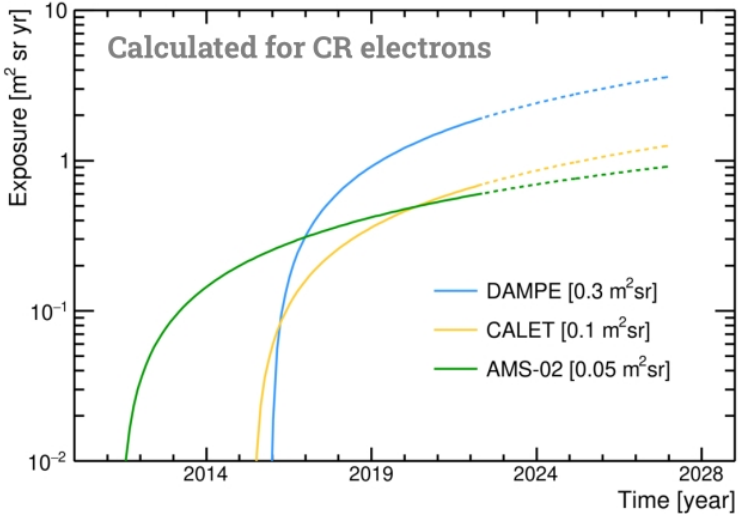

The CALOrimeter

- **14 layers of 22 BGO bars**
  - 2.5×2.5×60 cm^3 bars
  - 14 hodoscopic stacking alternating orthogonal layers
  - depth ~32X_0
- **Two PMTs coupled with each BGO crystal bar at the two ends**
- **Electronics boards attached to each side of module**

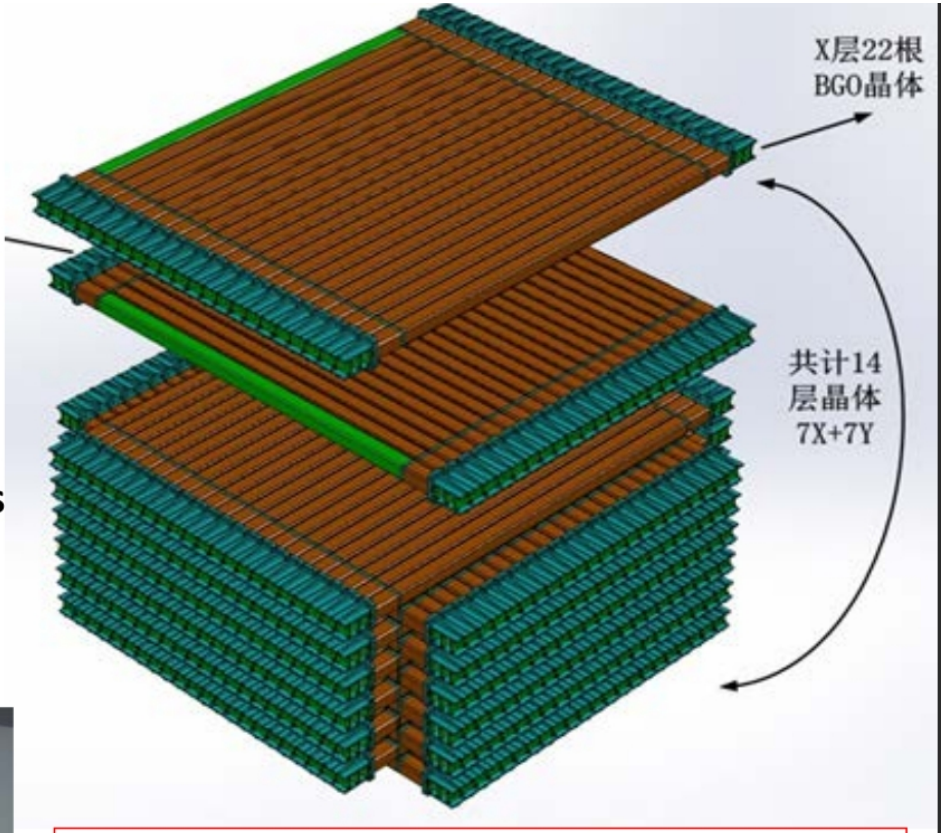

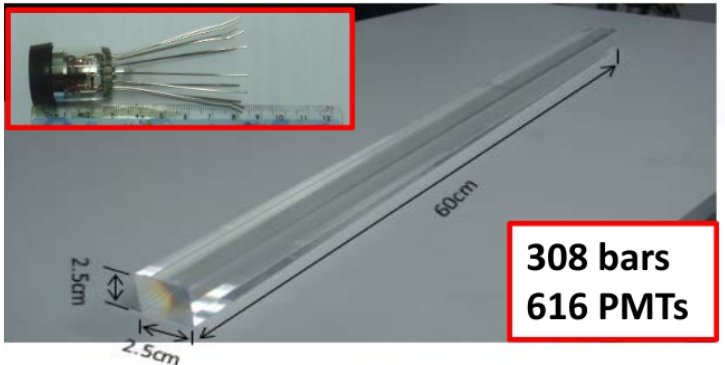

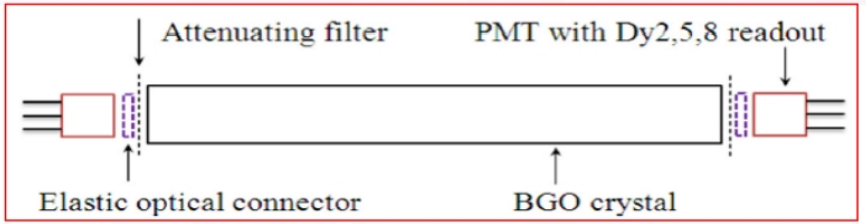

The Silicon TracKer (STK)

768 silicon sensors

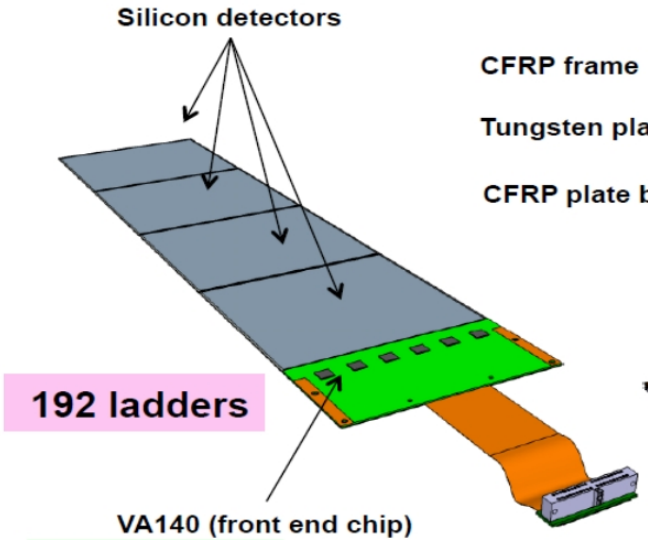

192 ladders

1152 ASICs

73728 channels

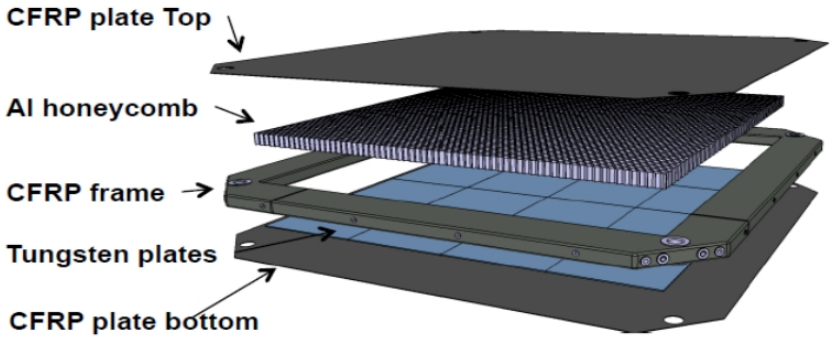

12 layers, 6-x and 6-y

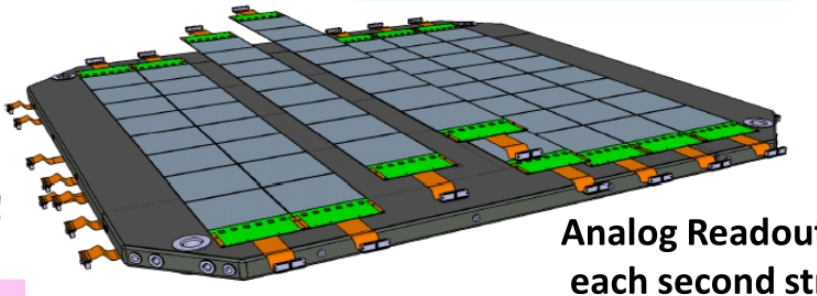

Analog Readout of each second strip:
384 channels / SSD- Ladder
Charge sharing

- 48 μm wide Si strips with 121 μm pitch
- (95 × 95 × 0.32 mm^3) Silicon Strip Detector (SSD)
- 768 strips in each SSD
- One ladder composed by 4 (SSD)
- 16 Ladders per layer (76 cm × 76 cm)
- 12 layers (6x + 6y)

The Plastic Scintillator Detector and the NeUtron Detector

PSD

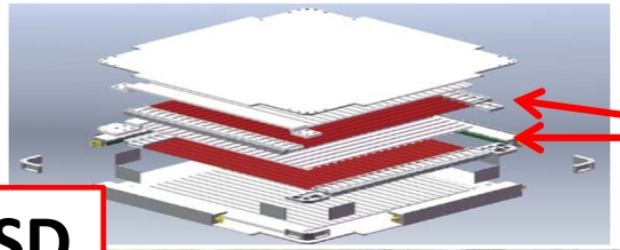

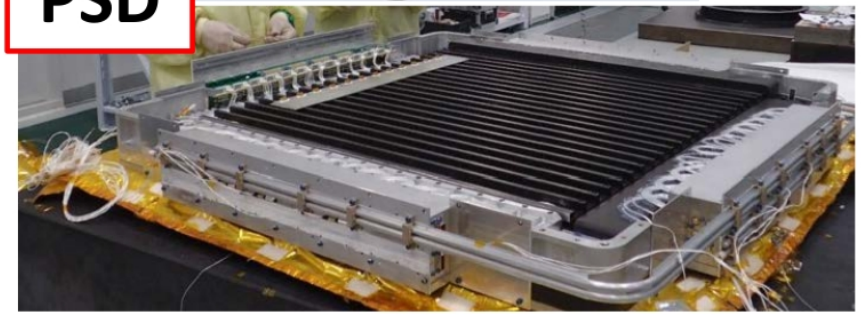

- 1.0 cm thick ,2.8cm wide and 82.0 cm long scintillator strips
- staggered by 0.8 cm in a layer
- 82 cm × 82 cm layers
- 2 layers (x and y)

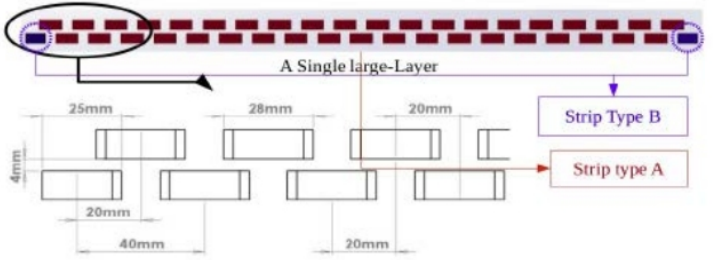

NUD

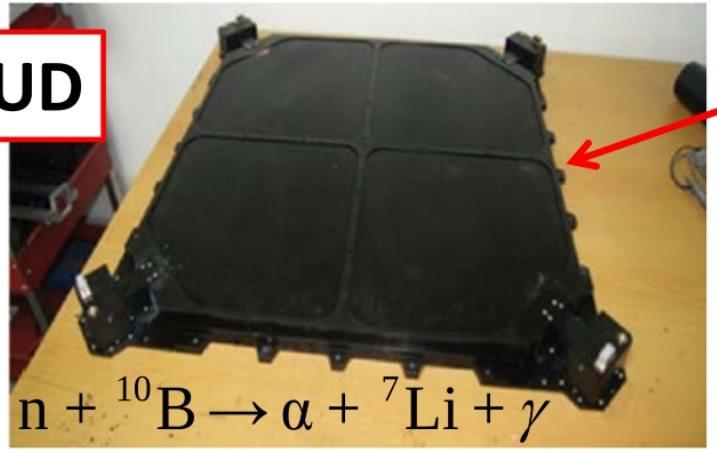

- 4 large area boron-doped plastic scintillators (30 cm × 30 cm × 1 cm)

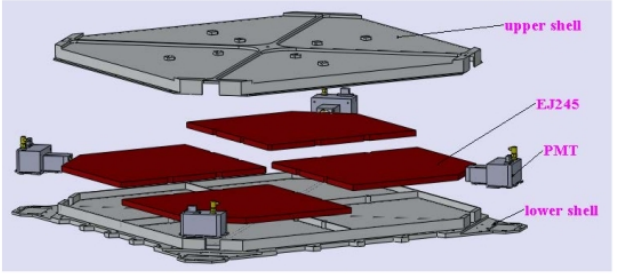

Electron IDentification

$\mathcal{F}_{\text{last}}$ = fraction of energy deposit in the last BGO layer with hits

Electron showers:
narrower and fully-contained

$$RMS_i = \sqrt{\frac{\sum_j (x_{j,i} - x_{c,i})^2 E_{j,i}}{\sum_j E_{j,i}}}$$

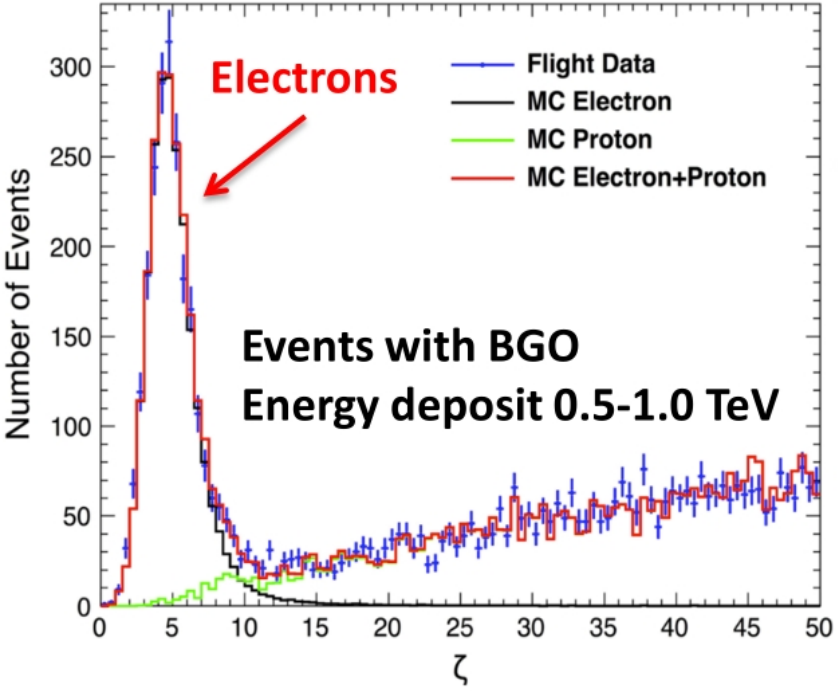

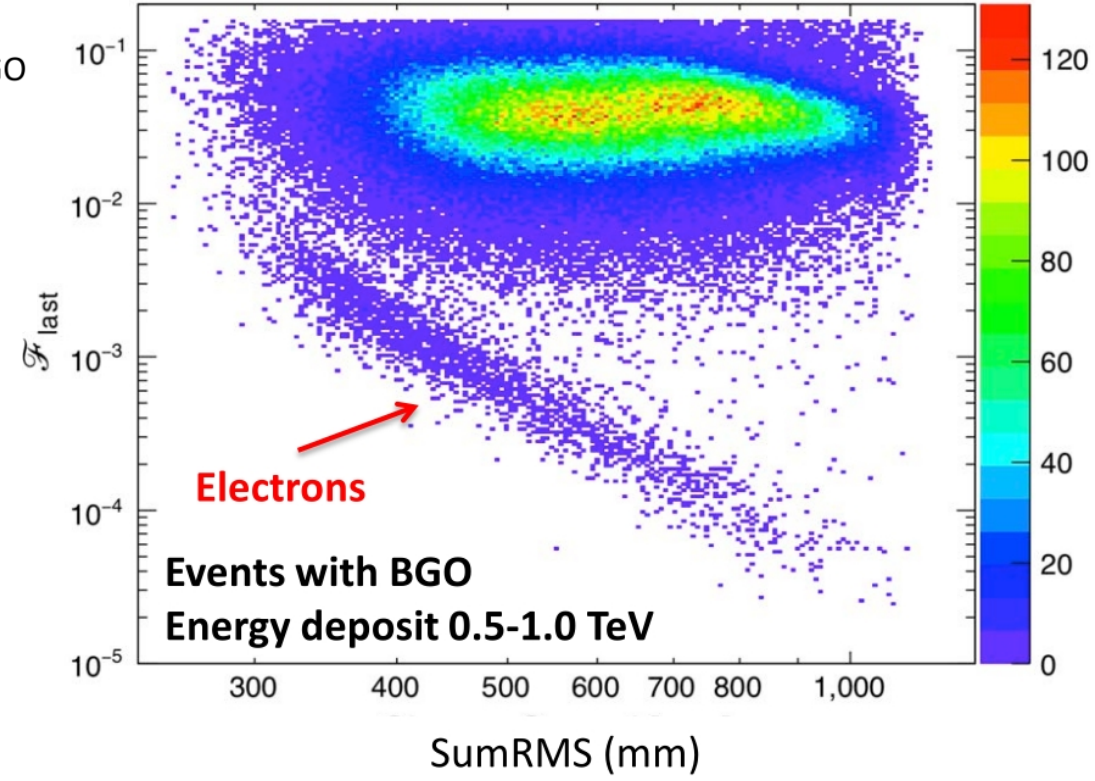

SumRMS = Sum of single layer RMS values

$$\zeta = \mathcal{F}_{\text{last}} \times (\Sigma_i RMS_i/\text{mm})^4/(8 \times 10^6)$$

The electron+positron spectrum

LETTER nature International weekly journal of science doi:10.1038/nature24475

Direct detection of a break in the teraelectronvolt cosmic-ray spectrum of electrons and positrons

DAMPE Collaboration*

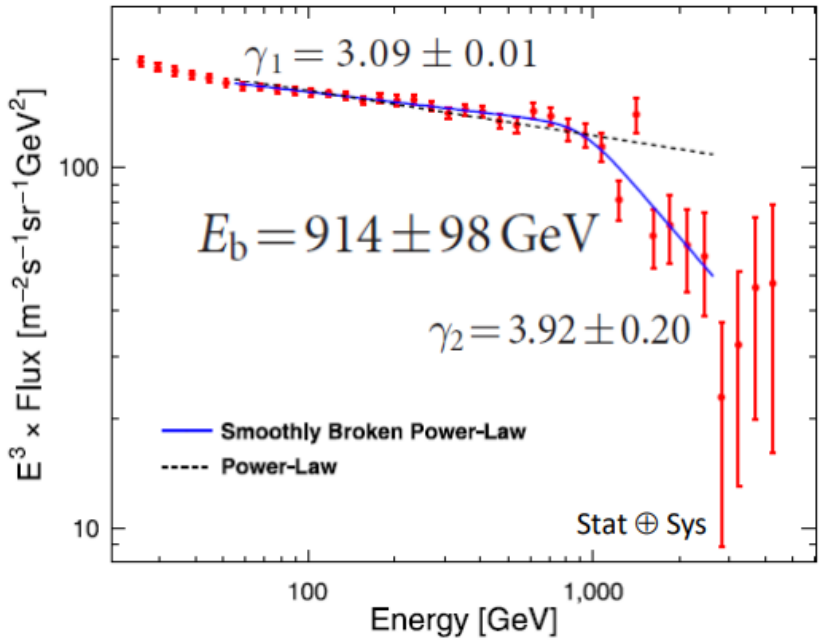

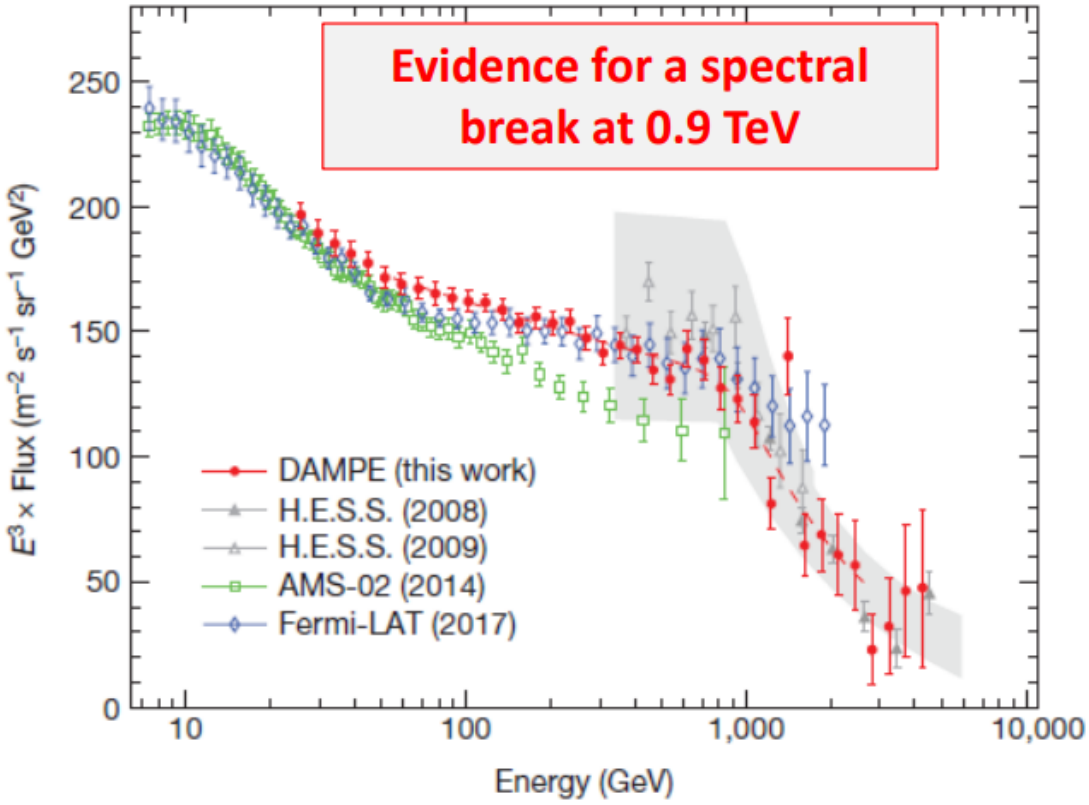

Proton and helium measured by DAMPE

PHYSICAL REVIEW LETTERS **126,** 201102 (2021)

Editors' Suggestion | Featured in Physics

Measurement of the Cosmic Ray Helium Energy Spectrum from 70 GeV to 80 TeV with the DAMPE Space Mission

May 18, 2021

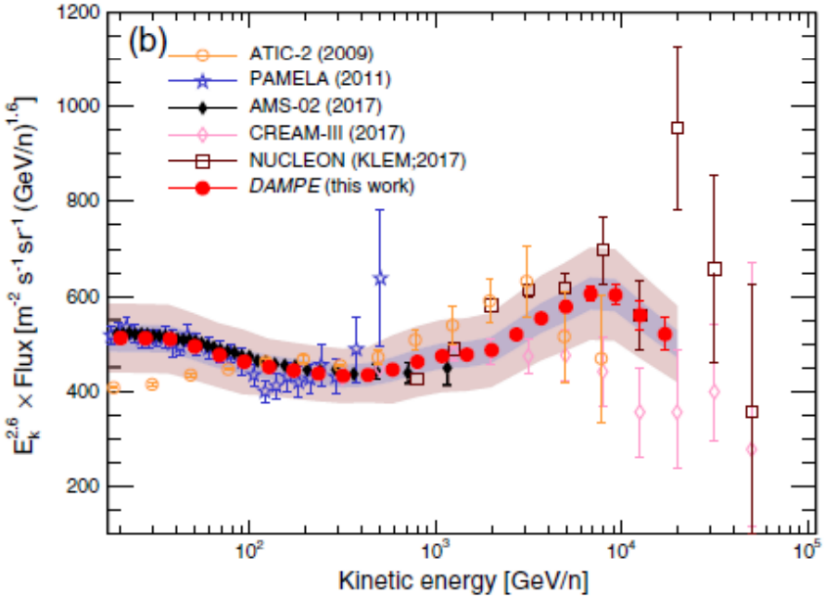

First clear evidence for a softening at about 34 TeV

Suggesting a Z dependent softening energy (~ 14 TeV for protons)

Confirmed by CALET in 2023

SCIENCE ADVANCES | RESEARCH ARTICLE

PHYSICS

September 27, 2019

Measurement of the cosmic ray proton spectrum from 40 GeV to 100 TeV with the DAMPE satellite

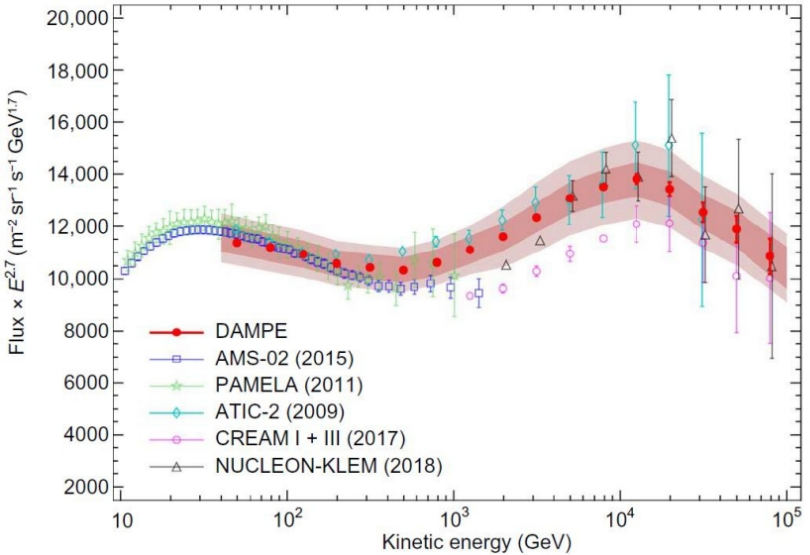

Confirmed by CALET in 2022

Heavier Nuclei Selection

Several independent analyses are ongoing from Li up to Iron
Different selection criteria to reject other nuclei and avoid charge misidentification
Different approaches to limit and better evaluate the systematics.

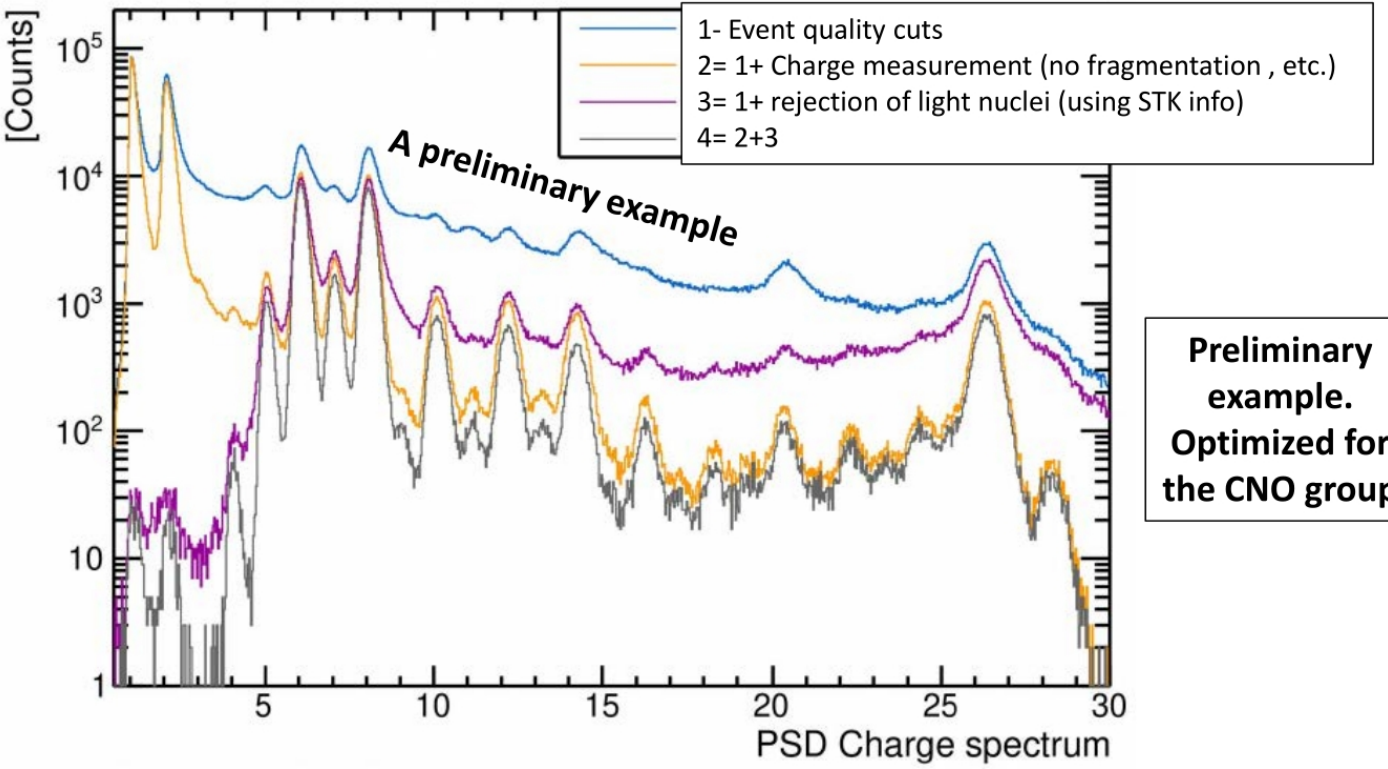

Preliminary example. Optimized for the CNO group

$$\mathrm{MPV} - 1.4\,\sigma < \mathrm{PSD\ Charge}_{Carbon} < \mathrm{MPV} + 2.7\,\sigma$$

$$\mathrm{MPV} - 1.2\,\sigma < \mathrm{PSD\ Charge}_{Oxygen} < \mathrm{MPV} + 3.5\,\sigma$$

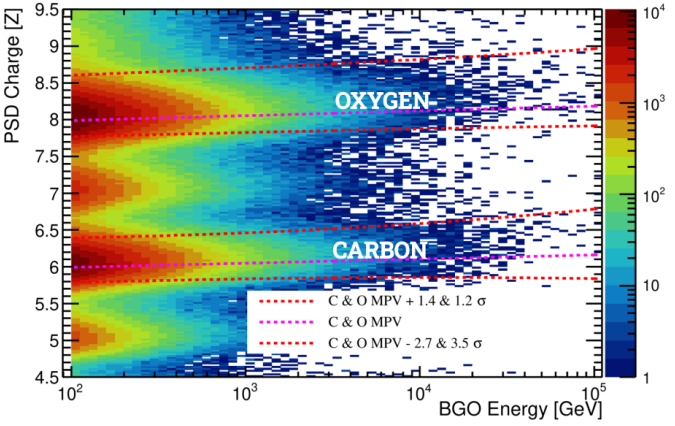

First observation of a spectral softening for heavier nuclei by DAMPE

$$\Delta\Phi\left(E_i, E_i+\Delta E_i\right)=\frac{\Delta \mathrm{N_i}}{\Delta \mathrm{E_i}\ \mathrm{A_{eff},}_i \Delta \mathrm{T}}$$

9 years of Flight Data

Good agreement among DAMPE analyses groups

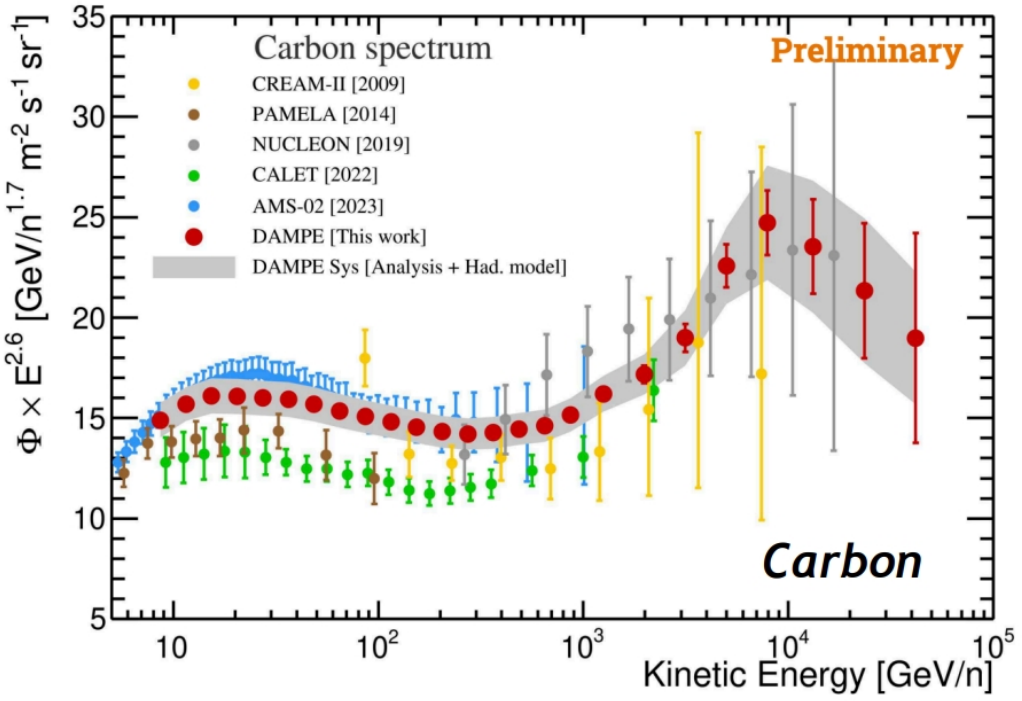

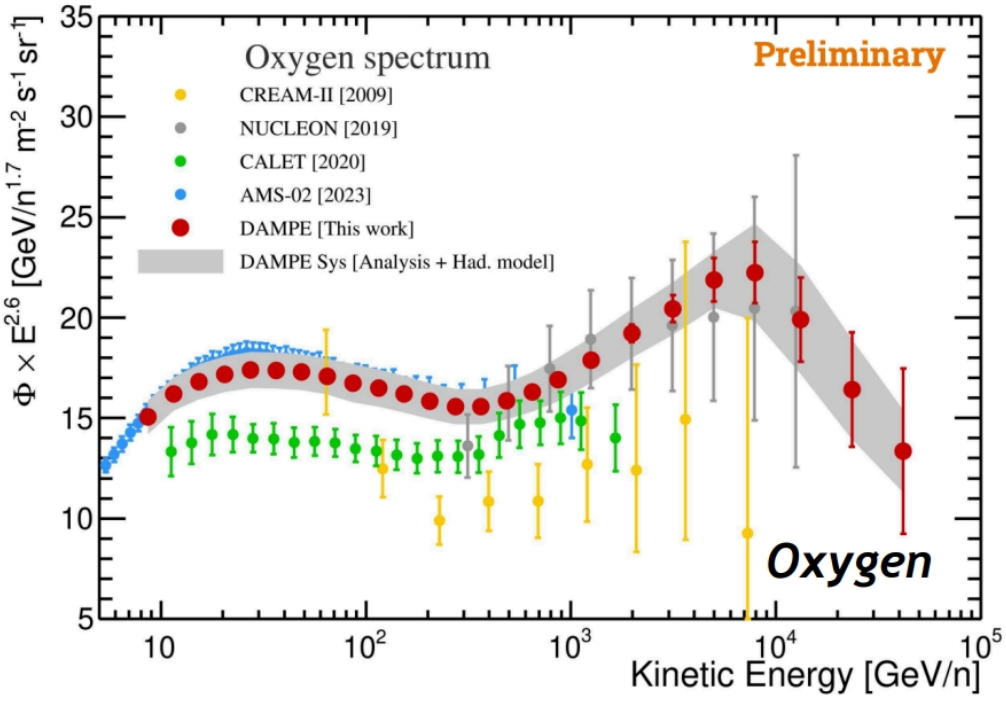

Similar hardening for other nuclei

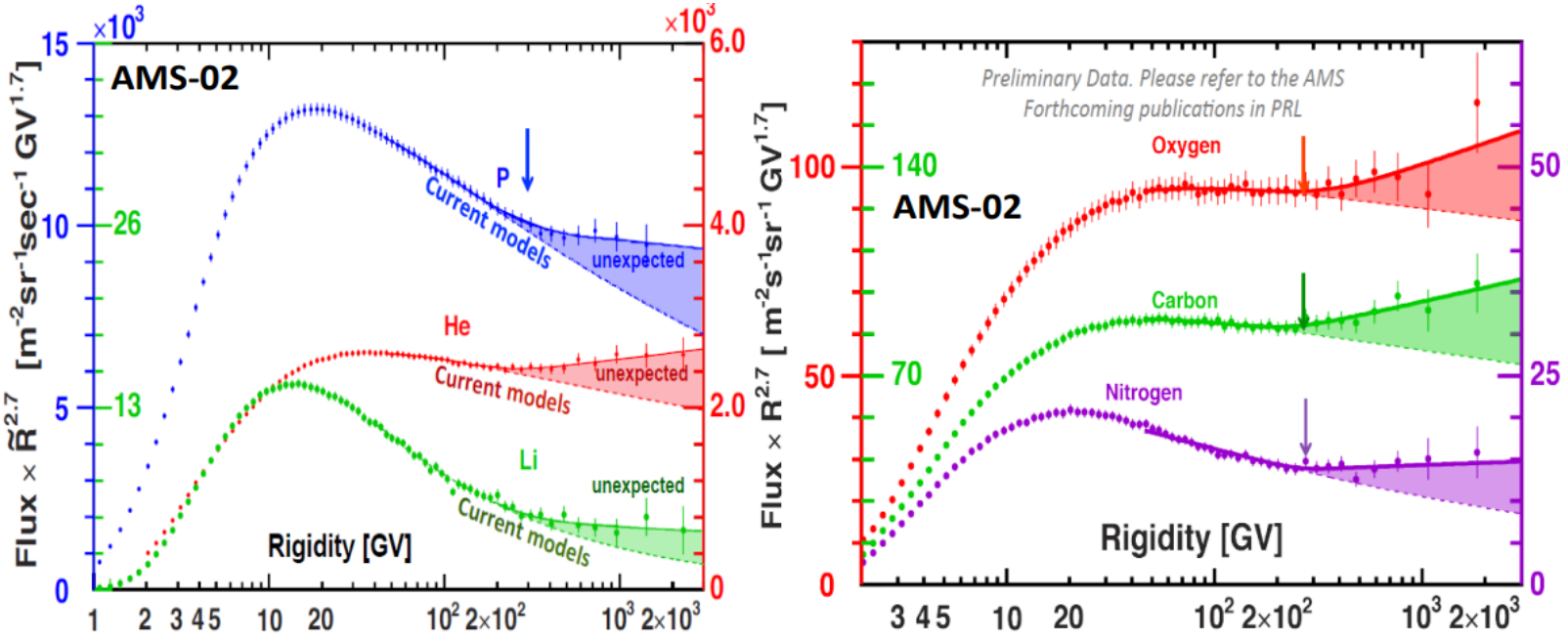

Acceleration or propagation effect ? Both ?

Need for precise measurements of secondary productions (B/C,..)

and

extensions in the 1-100 TeV energy region with large acceptance

(an good resolution) calorimeters in space

All-particle spectrum

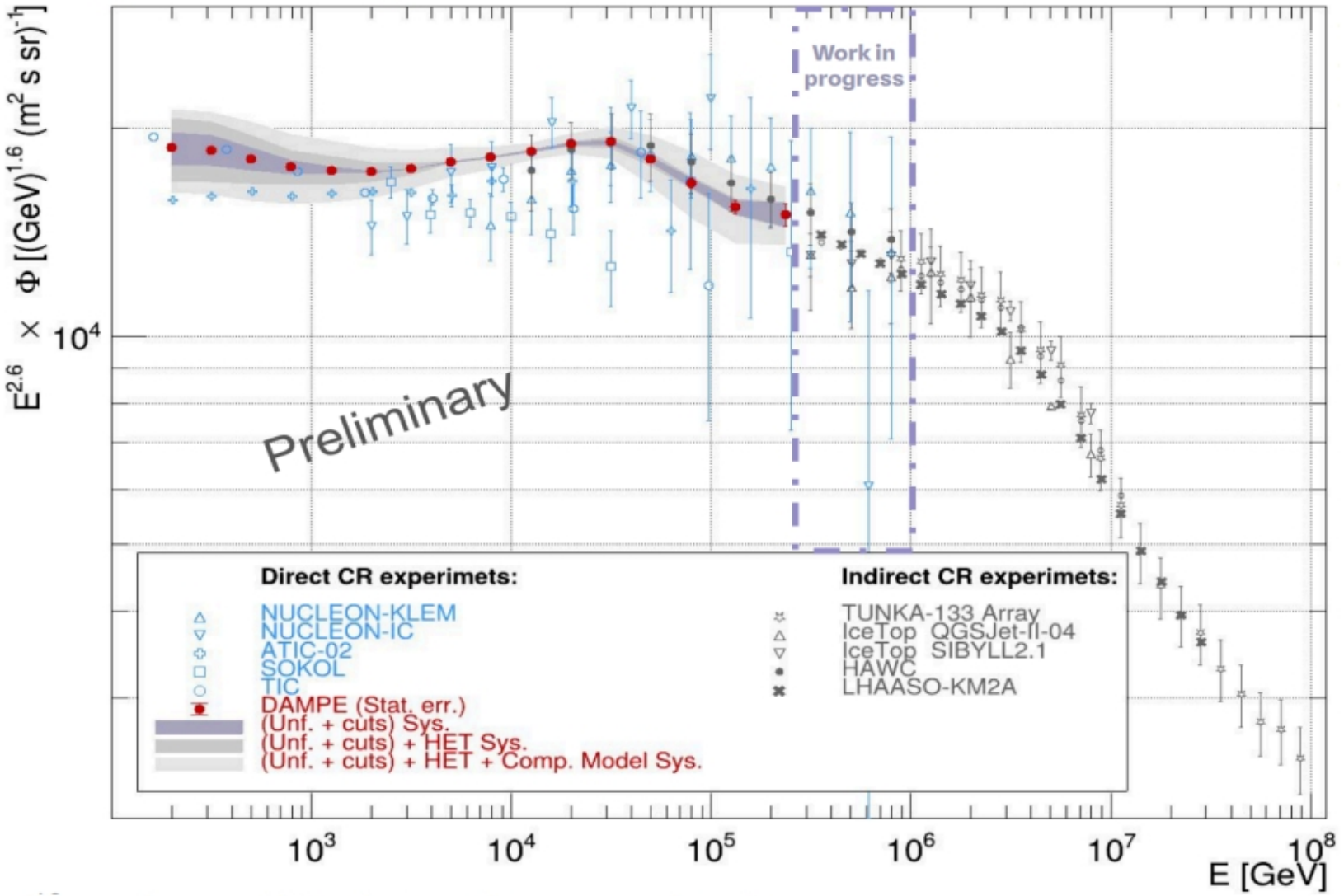

Alpha **M**agnetic **S**pectrometer
AMS-02 on the ISS

Height 5 m
Width 4 m
Depth 3 m
Mass 7.5 tons

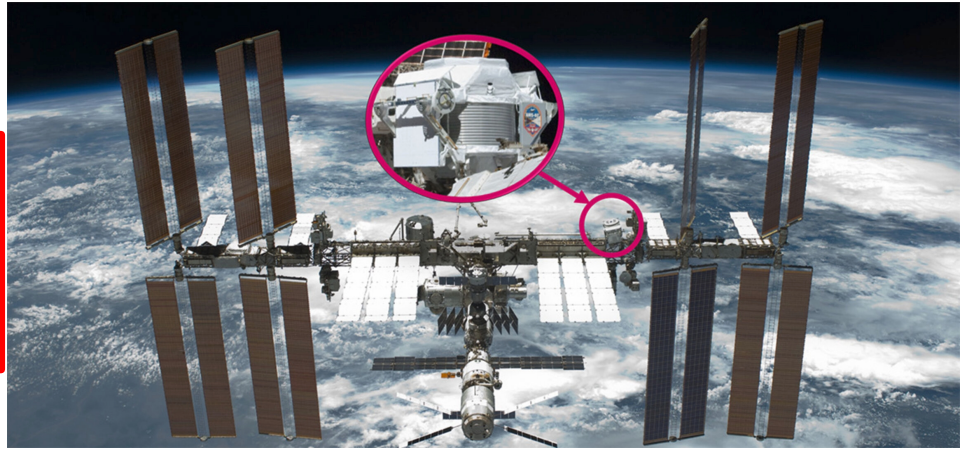

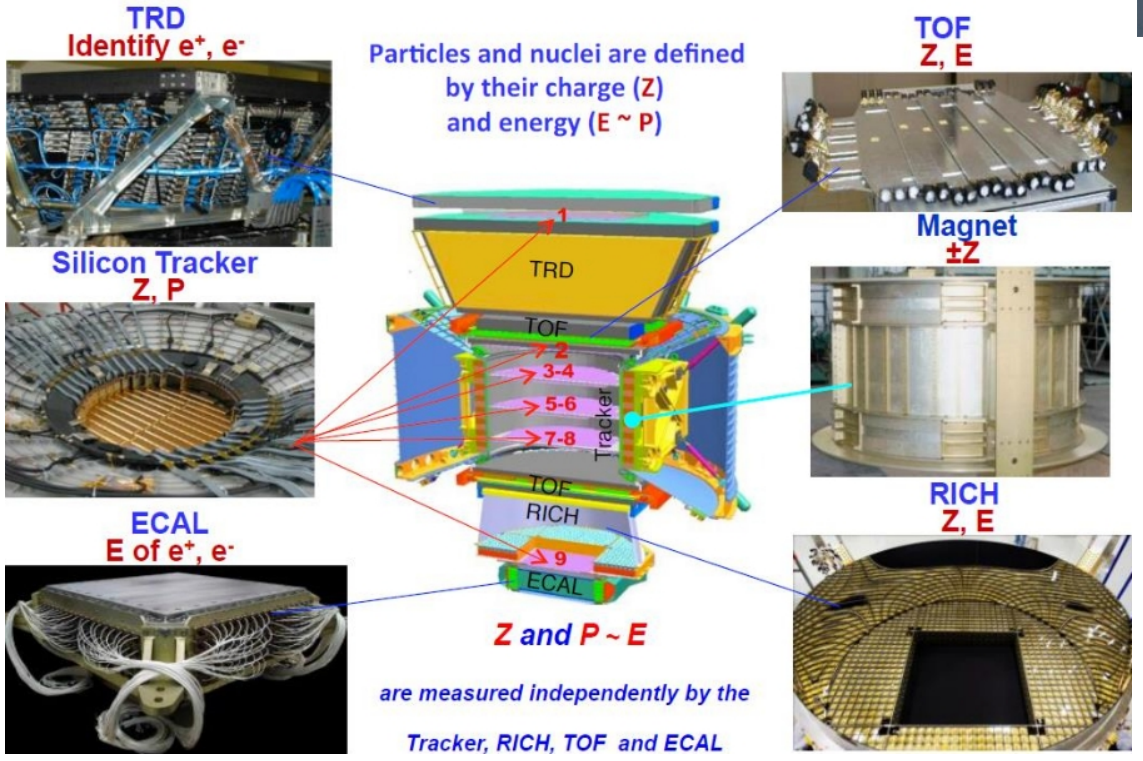

Transition Radiation Detector (TRD) – *top layer*

- Roughly 2 meters tall.
- Identifies electrons and positrons by detecting transition radiation from high-speed particles.

Time-of-Flight (TOF) Counters – *just below TRD and near the bottom*

- Two sets of scintillator panels separated by ~1.5 meters.
- Measure particle velocity and direction (upward vs. downward).
- The vertical spacing contributes to the detector's total **height**.

Magnet + Silicon Tracker – *central core*

- Originally planned with a superconducting magnet (later replaced with a permanent one).
- The **magnetic field** bends charged particles, while the **9-layer silicon tracker** (extending across ~3 meters) measures curvature → momentum.
- This central section defines most of the **depth** (front-to-back thickness).

Ring Imaging Cherenkov Detector (RICH) – *near the bottom*

- About 60 cm tall.
- Measures velocity and charge by detecting Cherenkov radiation rings.

Electromagnetic Calorimeter (ECAL) – *bottom layer*

- About 70 cm thick.
- Absorbs particles fully to measure their energy and distinguish electrons/photons from hadrons.
- Adds to both **depth** and **height**.

Antimatter: the positron fraction

Vol 458|2 April 2009|doi:10.1038/nature07942 nature

LETTERS

An anomalous positron abundance in cosmic rays with energies 1.5–100 GeV

O. Adriani[1,2], G. C. Barbarino[3,4], G. A. Bazilevskaya[5], R. Bellotti[6,7], M. Boezio[8], E. A. Bogomolov[9], L. Bonechi[1,2], M. Bongi[2], V. Bonvicini[8], S. Bottai[2], A. Bruno[6,7], F. Cafagna[7], D. Campana[4], P. Carlson[10], M. Casolino[11], G. Castellini[12], M. P. De Pascale[11,13], G. De Rosa[4], N. De Simone[11,13], V. Di Felice[11,13], A. M. Galper[14], L. Grishantseva[14], P. Hofverberg[10], S. V. Koldashov[14], S. Y. Krutkov[9], A. N. Kvashnin[5], A. Leonov[14], V. Malvezzi[11], L. Marcelli[11], W. Menn[15], V. V. Mikhailov[14], E. Mocchiutti[8], S. Orsi[10,11], G. Osteria[4], P. Papini[2], M. Pearce[16], P. Picozza[11,13], M. Ricci[17], S. B. Ricciarini[2], M. Simon[15], R. Sparvoli[11,13], P. Spillantini[1,2], Y. I. Stozhkov[5], A. Vacchi[8], E. Vannuccini[2], G. Vasilyev[9], S. A. Voronov[14], Y. T. Yurkin[14], G. Zampa[8], N. Zampa[8] & V. G. Zverev[14]

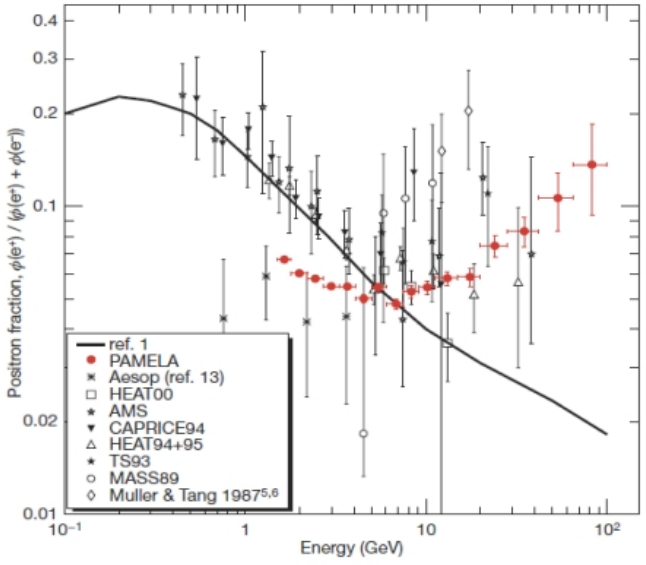

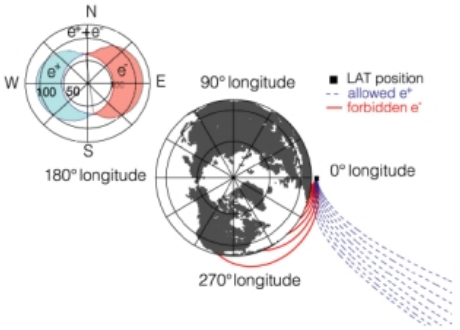

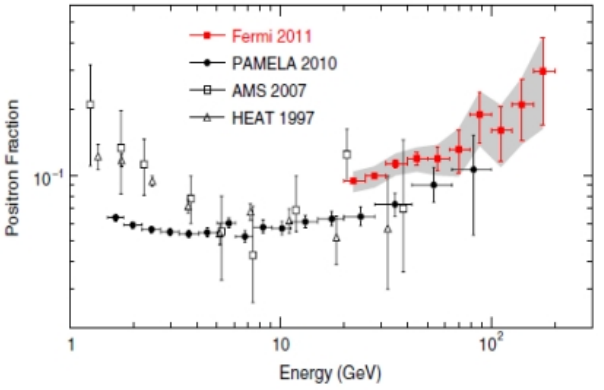

First "anomalous" results from PAMELA (april 2009)
FERMI contribution, even with large systematics.
Extended and precise measurements by AMS-02

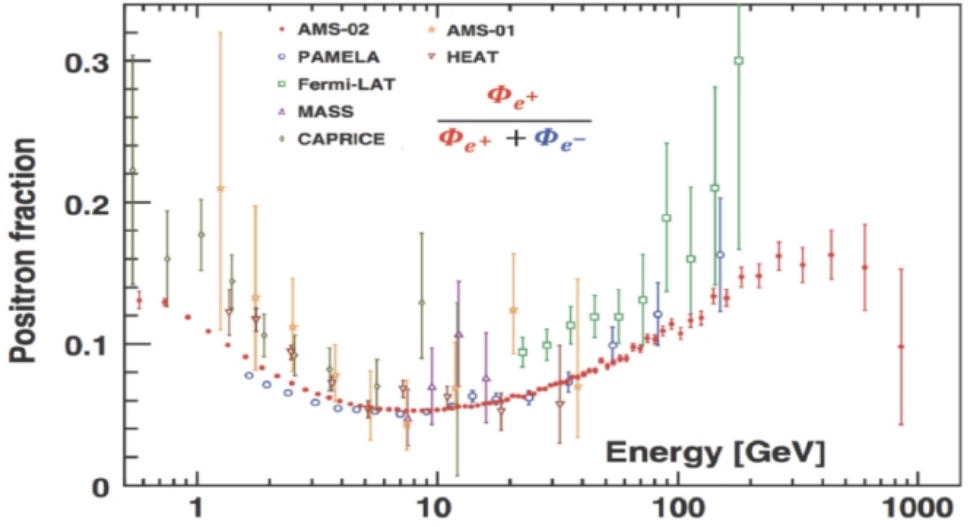

The electron and positron spectra measured by AMS-02

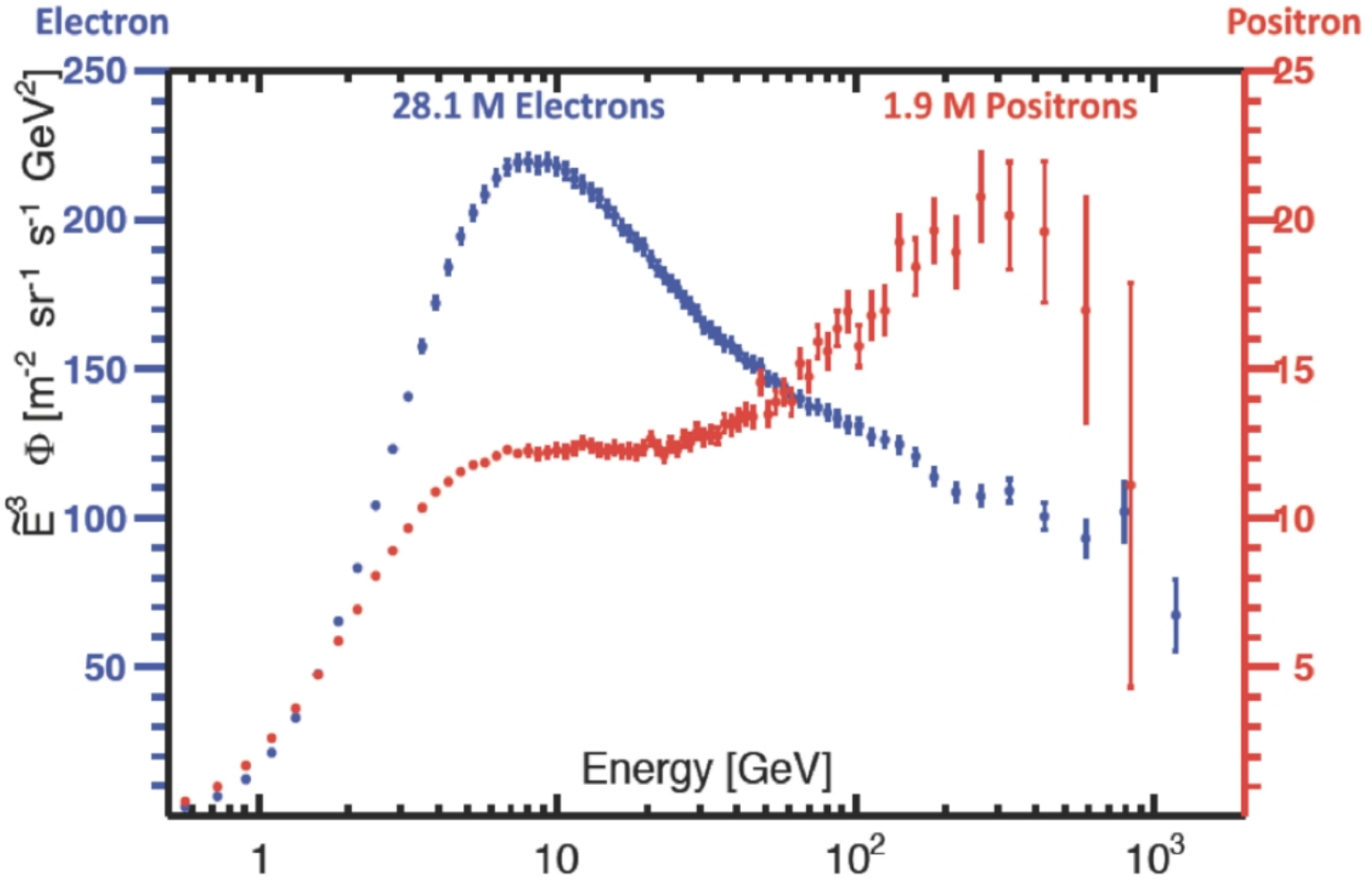

Antiprotons

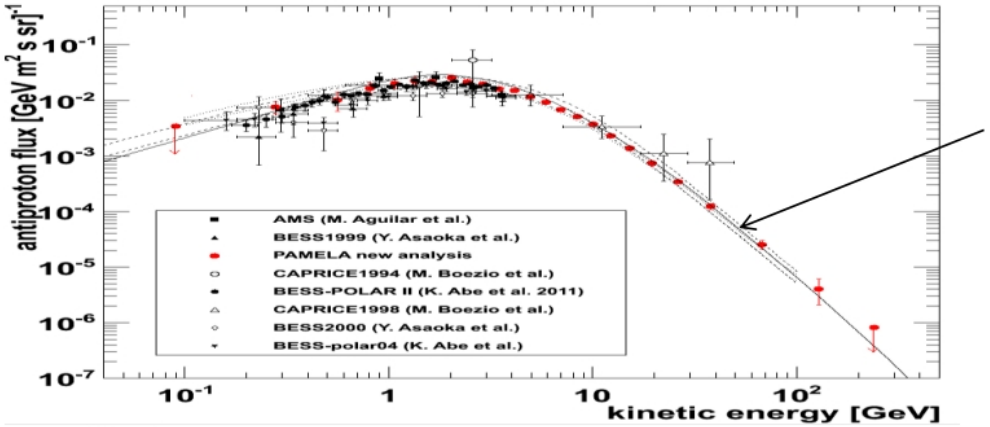

Antiproton flux consistent with secondary production calculations

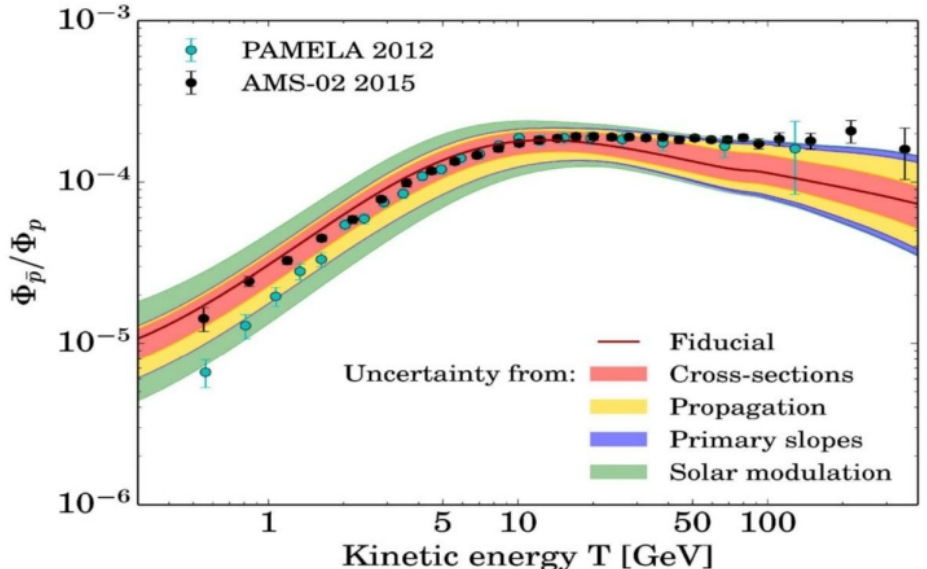

New measurements at accelerators (e.g. LHCb) in order to lower the systematic uncertainty on secondary production calculations

The NUSES mission: pathfinder for future missions

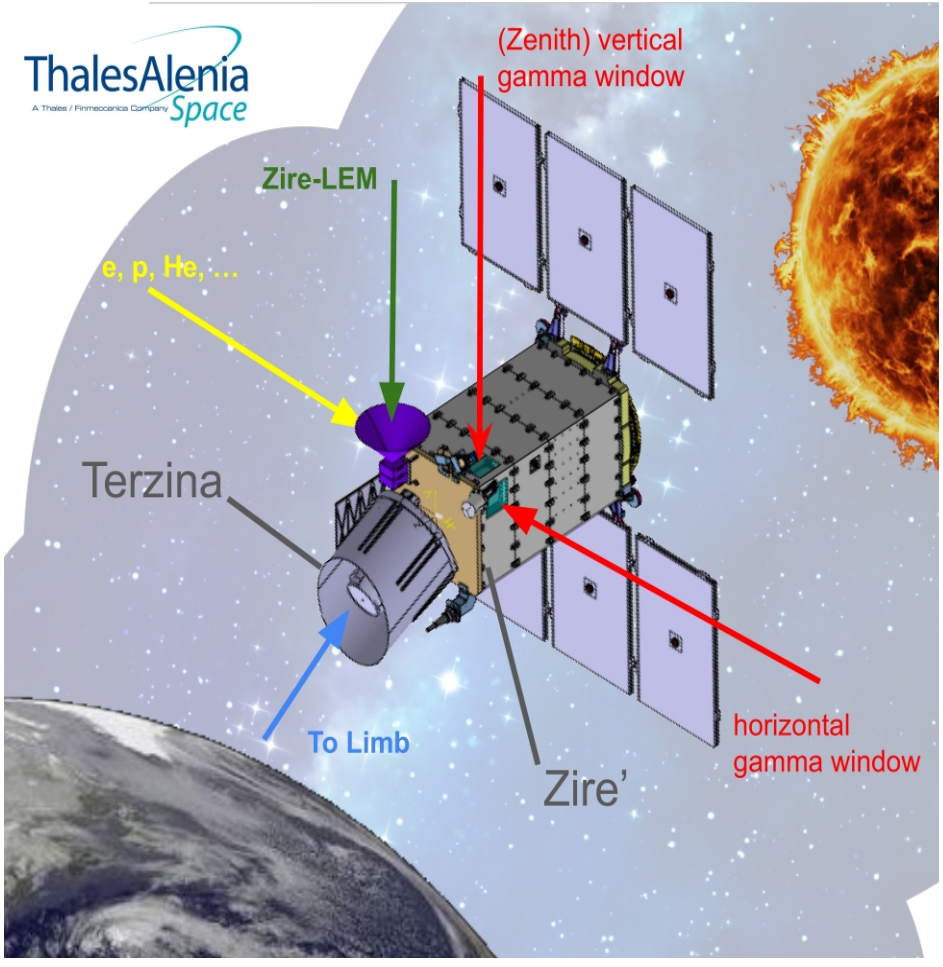

launch expected ~ 2027

Zirè

- **Measure the flux (E<300 MeV) of cosmic e⁻, p** and light nuclei of solar/galactic origin;
- Study of the cosmic radiation variability (Van Allen belt system);
- Possible correlation with seismic activity due to **Magnetosphere-Ionosphere-Lithosphere Coupling** (MILC);
- Detection of **0.1 - 30 MeV** photons for the **study of transient gamma sources**;
- Paving the way for future **applications of new technology** (SiPM, Fiber Tracker, GRB detection…);

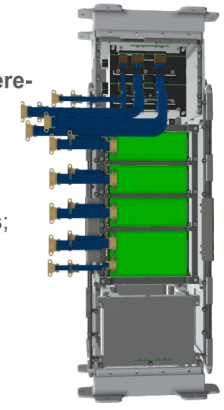

Terzina

Pathfinder for future missions devoted to UHE cosmic rays and neutrino astronomy through **space-based** atmospheric **Cherenkov light** detection.

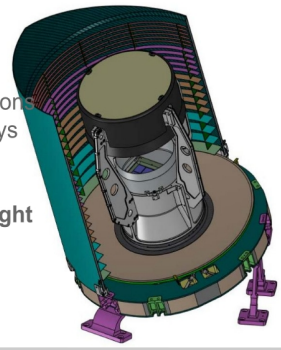

New Technologies and approaches

Development of new observational techniques, testing new sensors (e.g. **SiPM**) and related electronics, DAQ, onboard AI, for space missions. New solutions for the satellite platform.

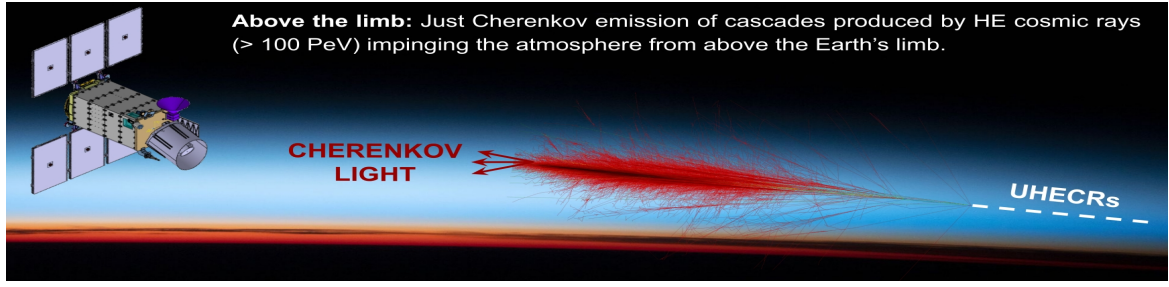


Entering the atmosphere
→ breaking into a multitude of secondary particles
Extensive Air Showers (EAS)

Extensive Air Shower (EAS)

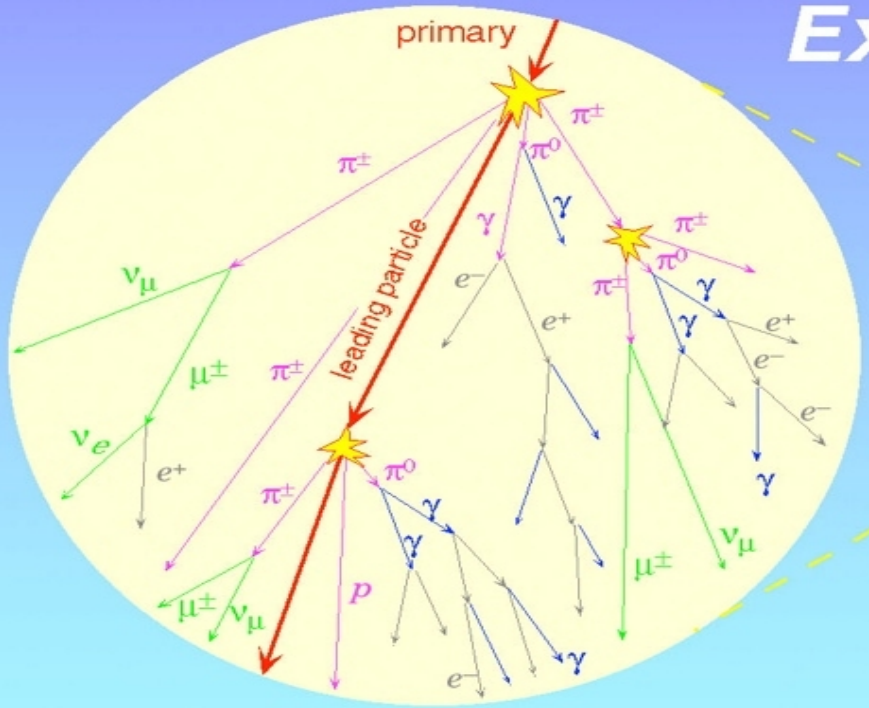

primary

≈ 20 km height

trajectory

Particle Composition at ground:
≈ 80 % photons
≈ 18 % electrons
≈ 1.7 % muons
≈ 0.3 % hadrons
≈ 10^6 secondaries for 10^{15} eV proton

+ anti-matter

+ many neutrinos and anti-neutrinos!

(very very weakly interacting)

≈ 1 m thickness

$v \approx c$

hadron calorimeter

ely detector array

Fluorescence, Cherenkov light

ca. 100-200 m

Heitler model (1944)

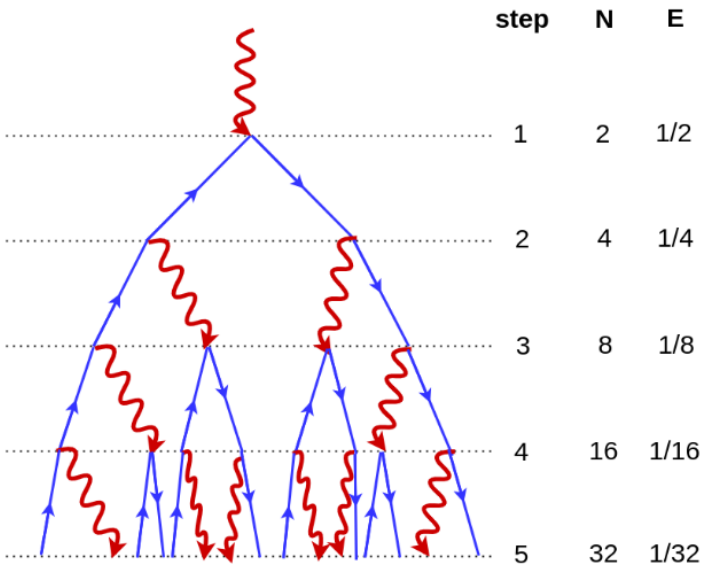

pair production and Bremsstrahlung $\lambda_r \sim 37$ g/cm^2

$$E \sim (dE/dX)_{rel} \sim N_{max}$$
$$X_{max} \sim \lambda_r \ln (E/E_c)$$

Showers development stops when the critical energy E_c (~85 MeV) is reached

Extension for hadron showers

Astrop. Phys. 387 (2005) 22

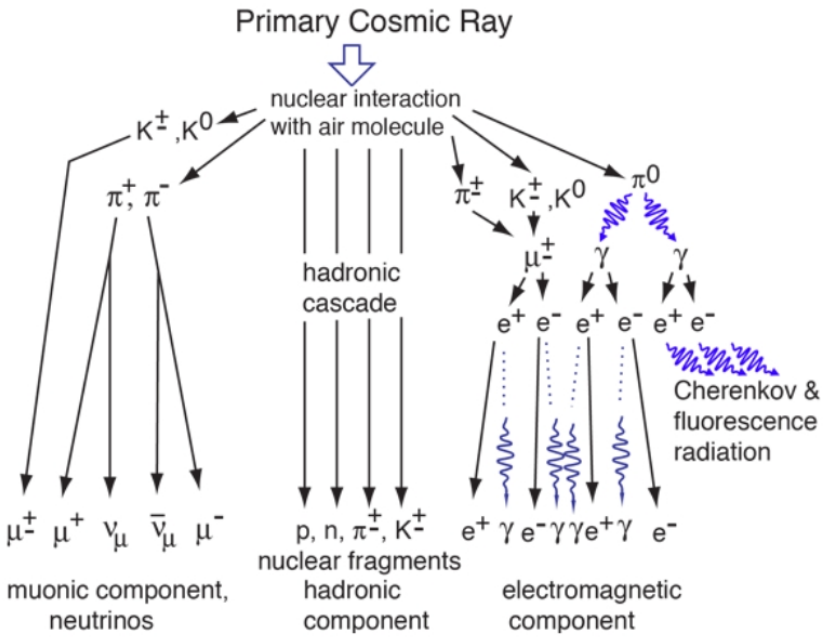

$$X_{max}^{A} \sim X_{max}^{p} - \lambda_r \ln A$$

X_{max} and its momenta relevant for understanding the nature and the composition of the primary particle

The energy spectrum of high energy cosmic rays

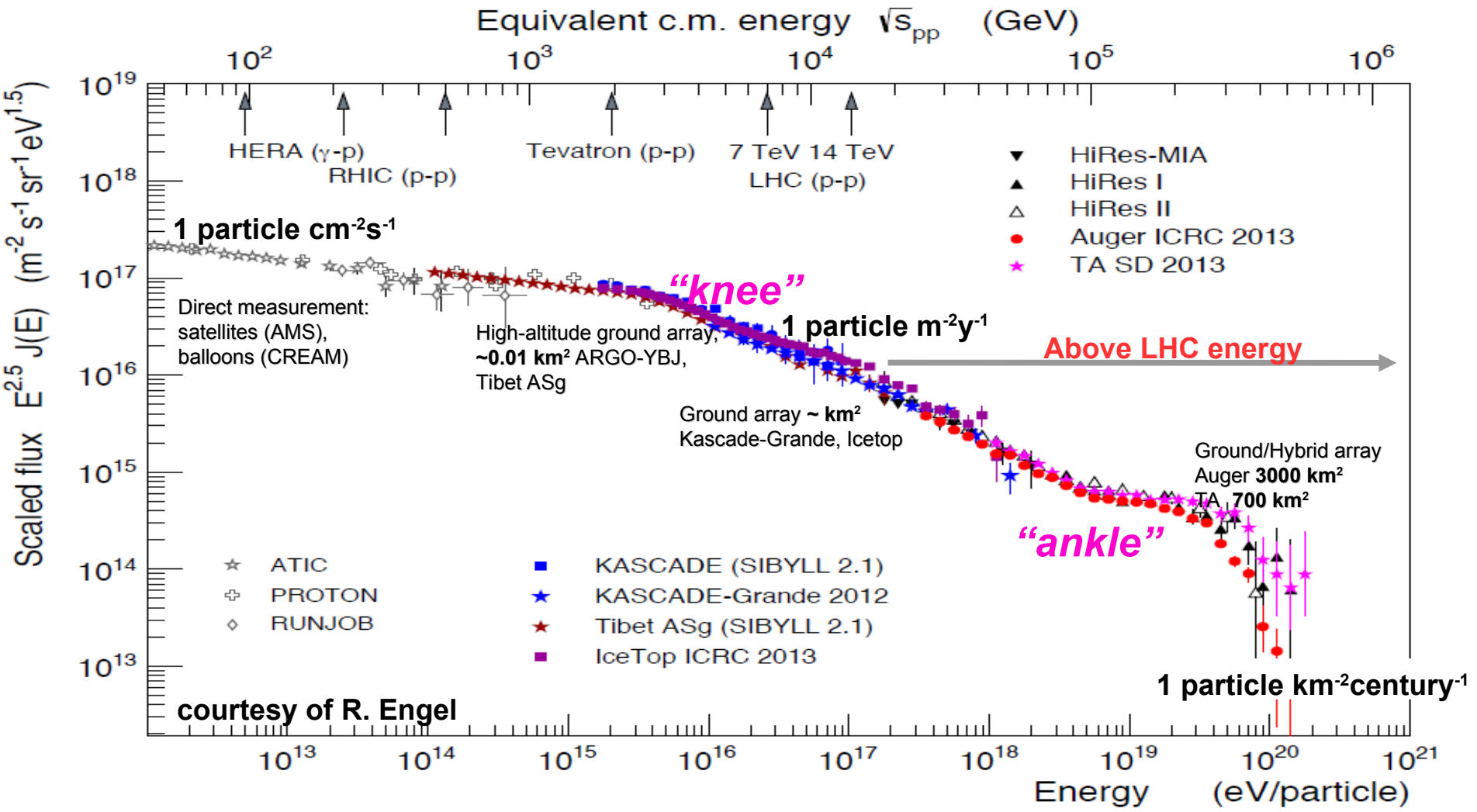

The Pierre Auger Observatory

~ 400 members, 17 countries

3000 km²

Surface detector

array of 1660 Cherenkov stations on a 1.5 km hexagonal grid of 3000 km²
Dense sub-array (750 m) of 24 km²

Fluorescence detector

4+1 buildings overlooking the array
(24 + 3 HEAT telescopes)

Radio detector

153 Radio Antenna → AERA

Muon Detectors

Buried scintillators (region of dense array)

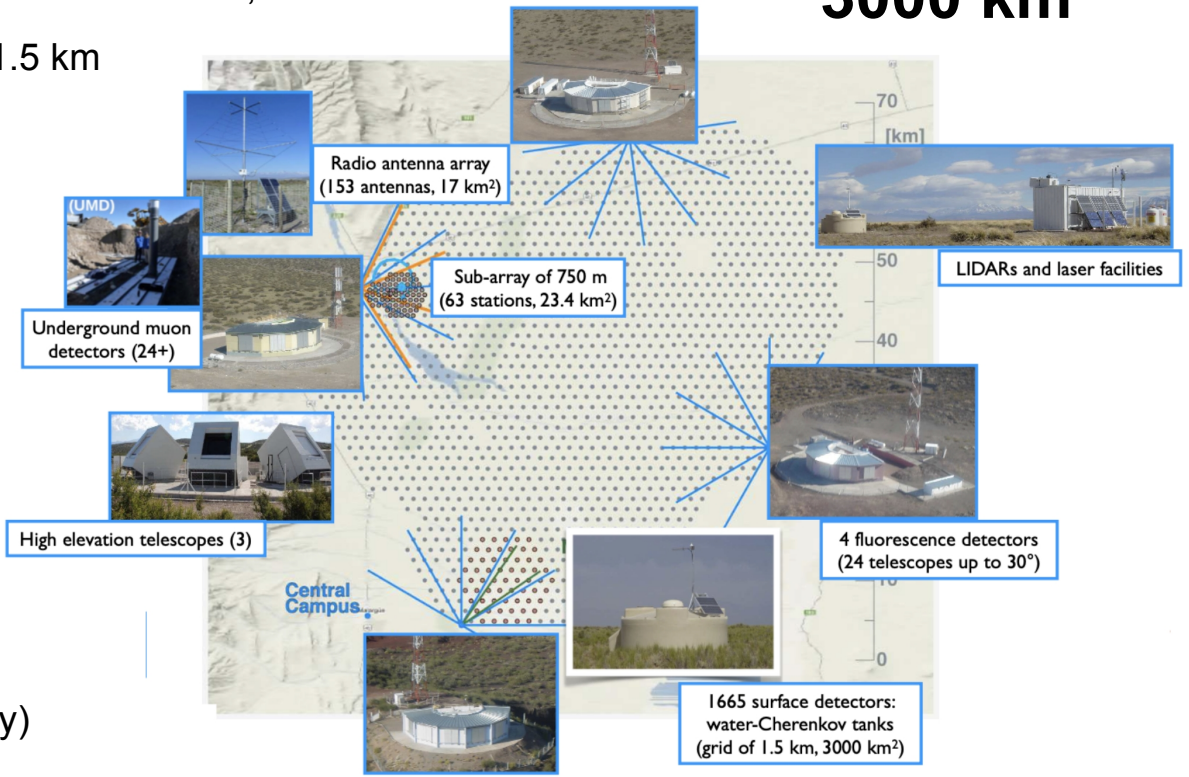

Phase 1 *: data taking from 2004 on*
(from 2008 with the full array in operation):

- Over 120.000 km² sr yr for anisotropy studies
- Over 80.000 km² sr yr for spectrum studies

Phase 2 - the AugerPrime upgrade
Data taking from 2023 to 2035…
Multiple detectors

Fluorescence detector

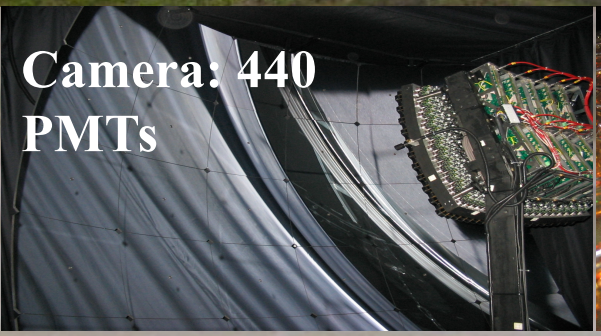

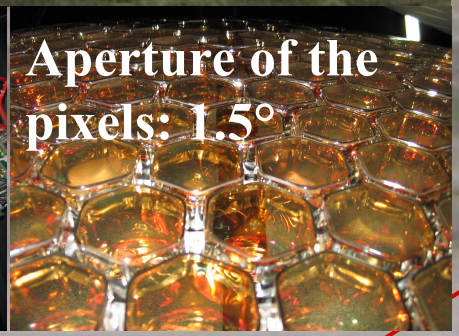

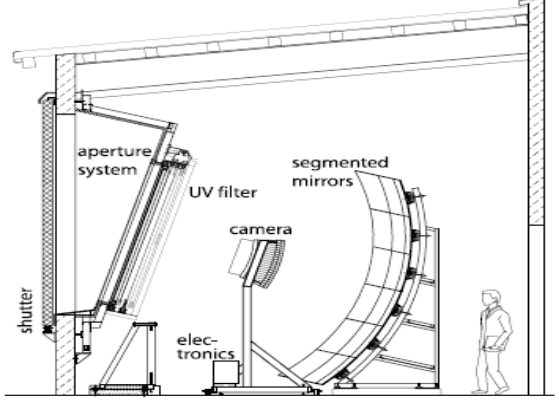

1.5 km
1.5 km
1.5 km

Surface detector

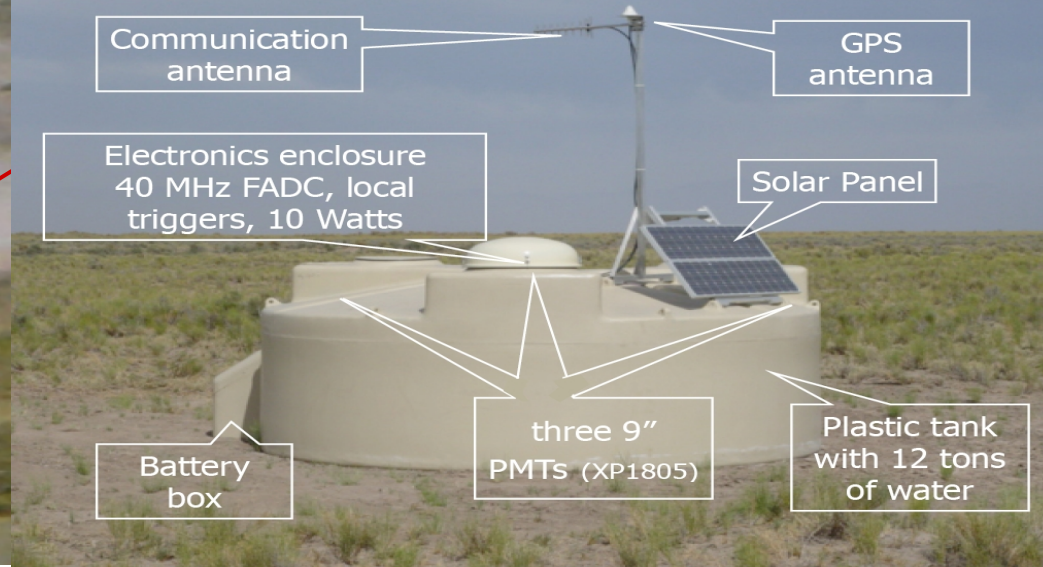

The Telescope Array project

Surface Detector: Plastic Scintillator

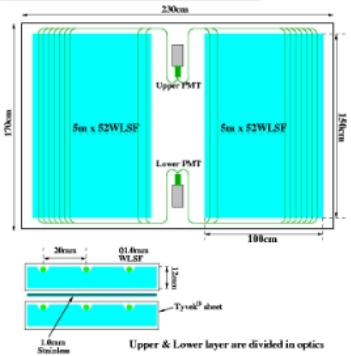

Fluorescence Detector: PMT camera

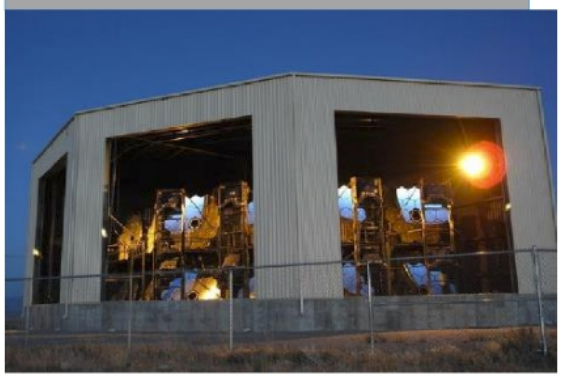

SD: 507 scintillators 3 m^2, spacing
1.2 km, Area 700 km^2

FD: 38 Telescopes in 3 stations (~30 km)

TALE (Low Extension → 2 PeV)
TALE SD (600-200-100 m)
TALE FD

TAx4, to reach 2800 km^2
spacing 2.08 km.

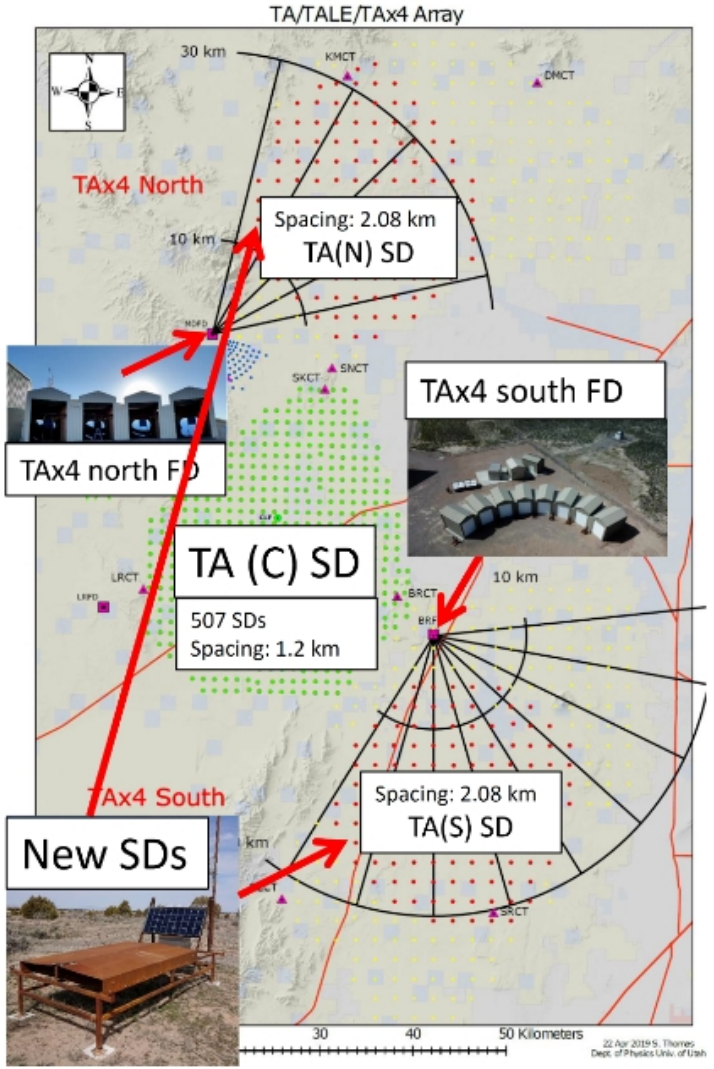

Full sky coverage with Auger and TA

Telescope Array

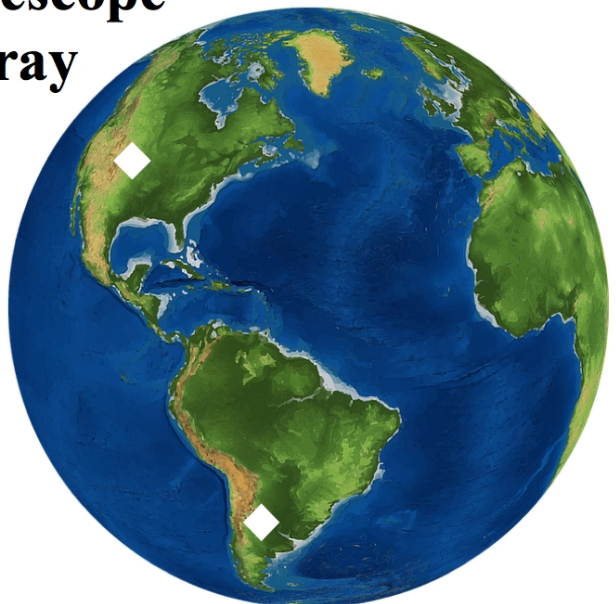

Auger

700 km²

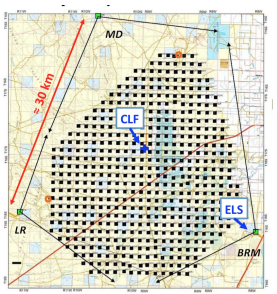

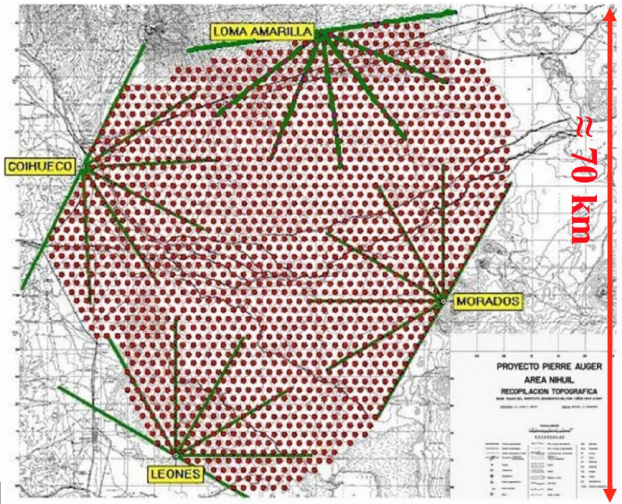

3000 km²

exposure Auger / TA ≈ 6,7

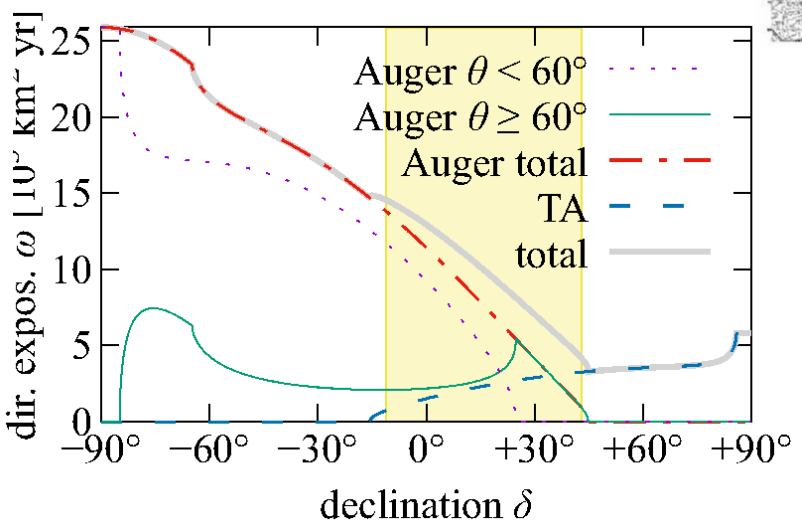

Auger/TA declination common band
$-15° < \delta < 45°$

Shower reconstruction with the Surface Detector

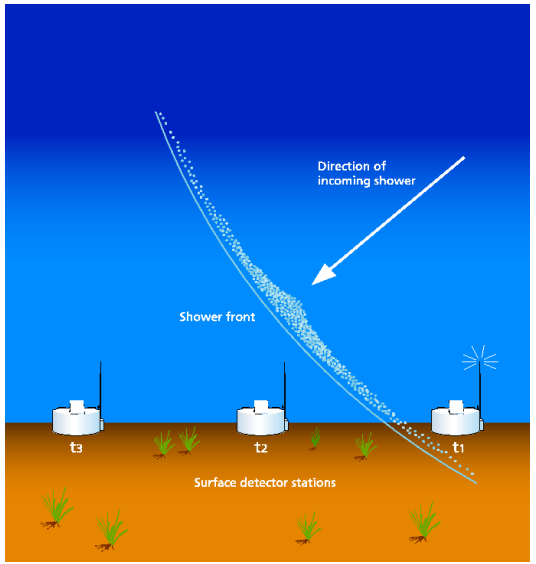

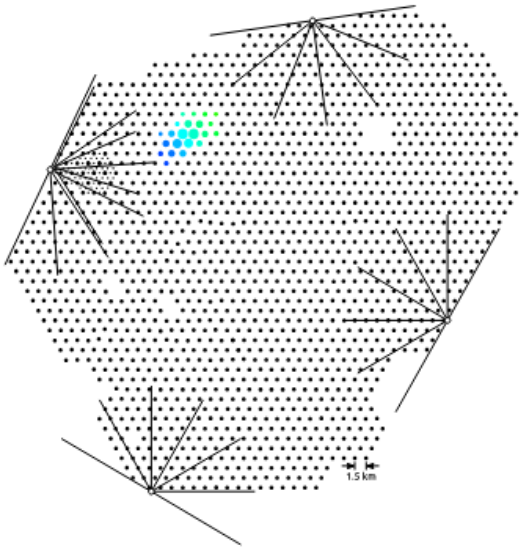

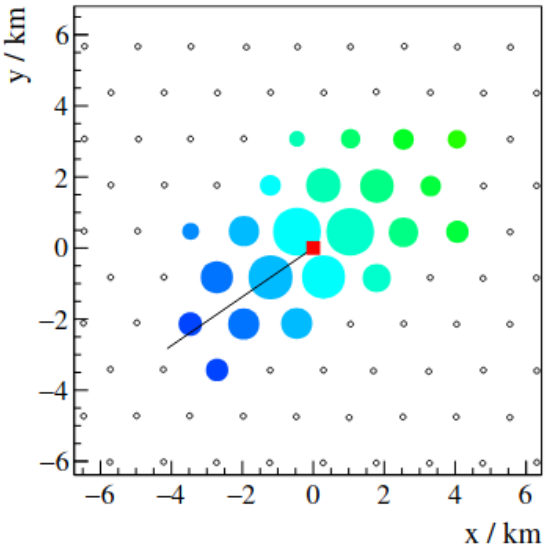

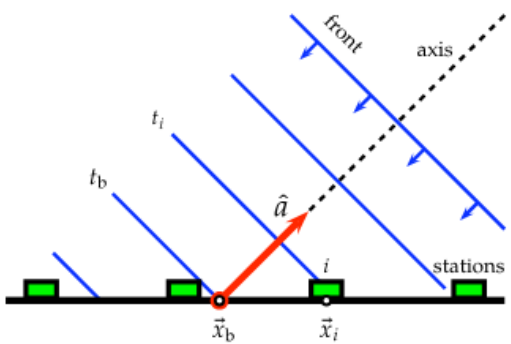

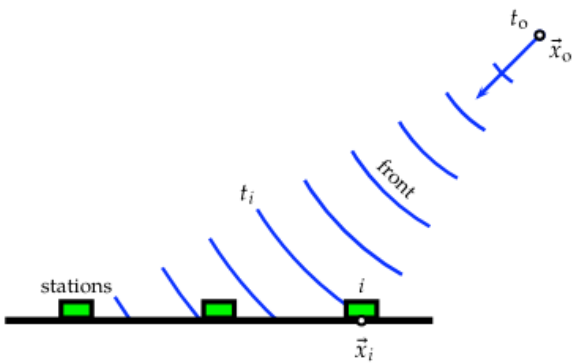

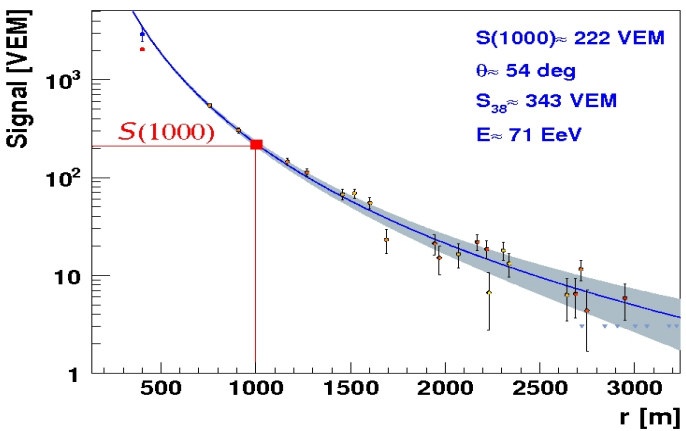

Shower reconstruction with the Fluorescence Detector

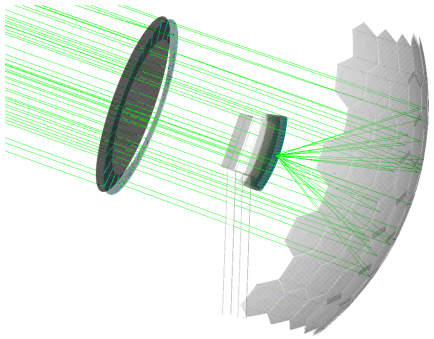

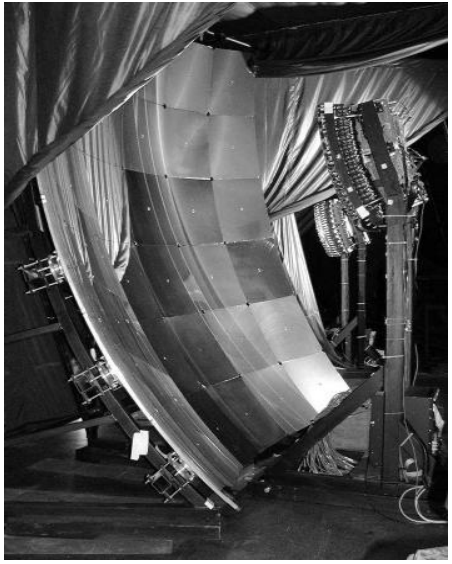

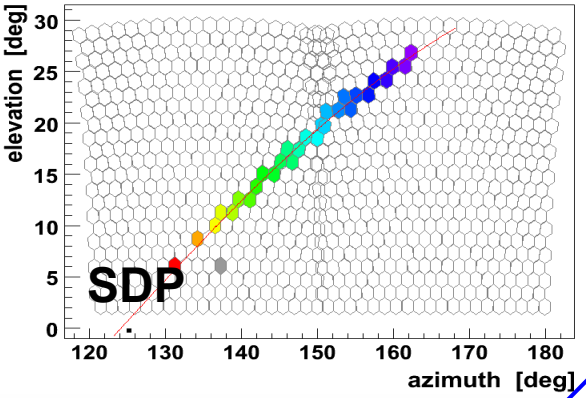

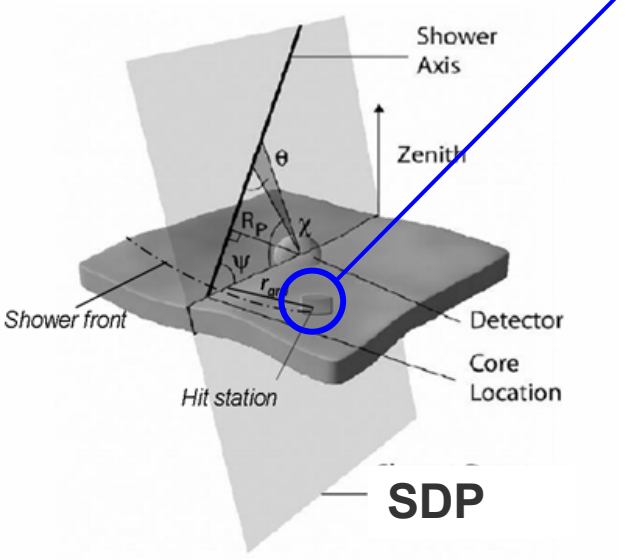

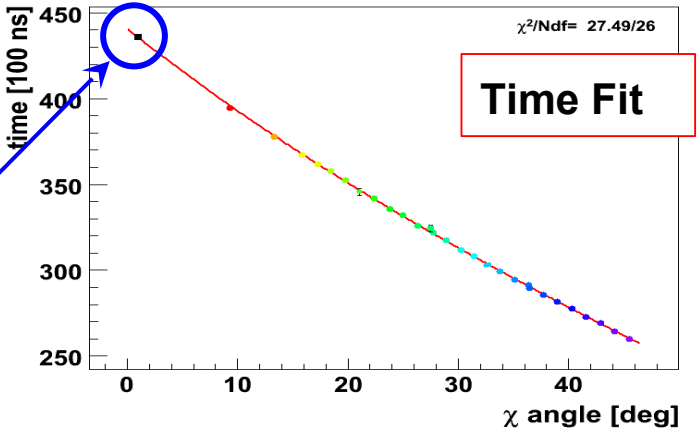

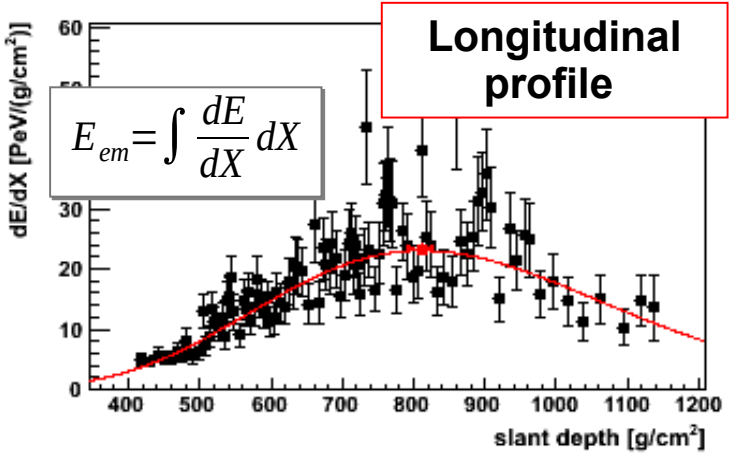

The Hybrid paradigm

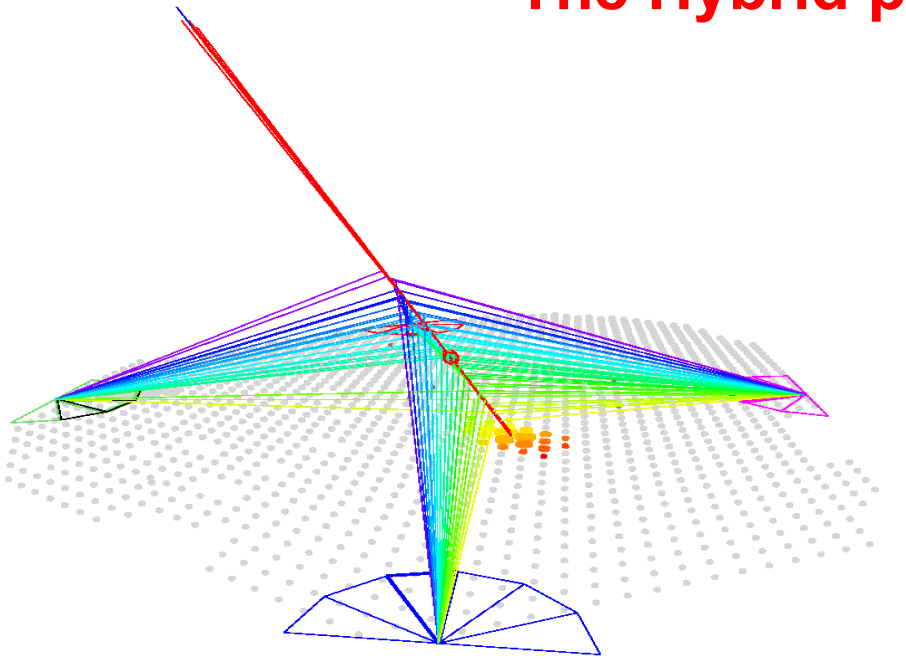

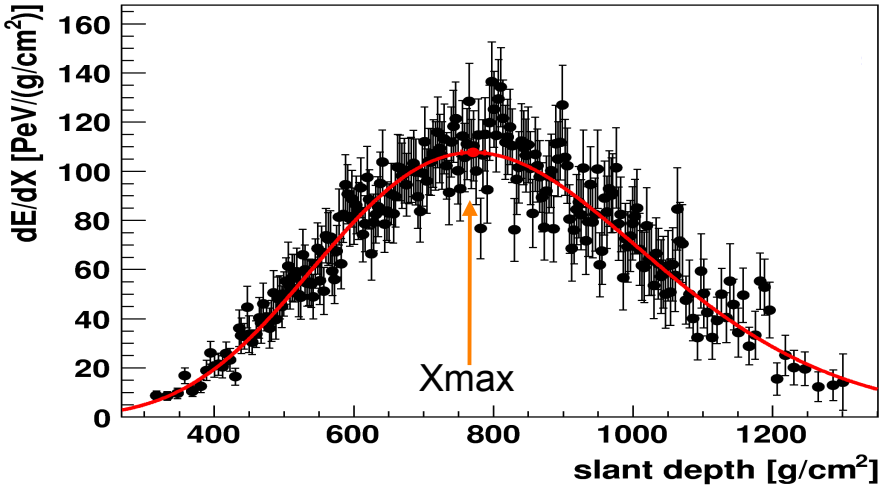

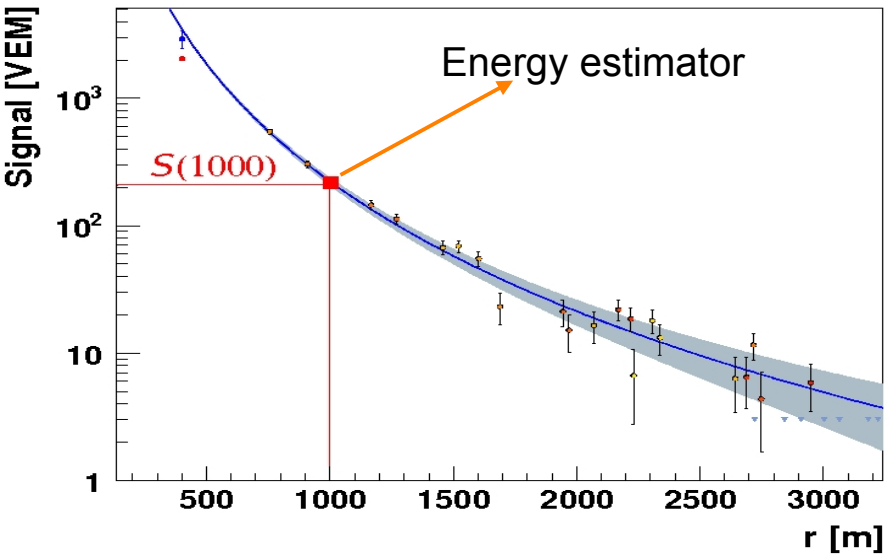

Longitudinal profile

FD - calorimetric measurement
- duty cycle 15%
- Xmax (mass composition)

Density of particles at the ground

SD - duty cycle ~ 100%

Angular resolution ~ 1°

SD rec

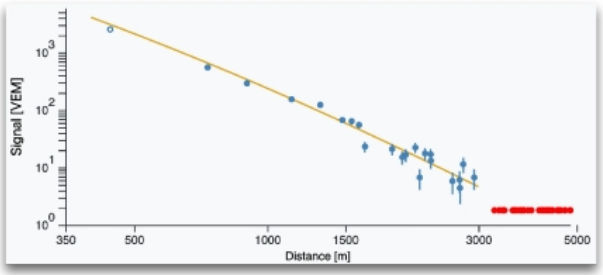

Energy	82±7 EeV
θ	53.8°
ϕ	100.6°
β	-2.1
$t_{1/2}$(1000)	127±5 ns
δ	17.8°
α	324.5°
Multiplicity	22

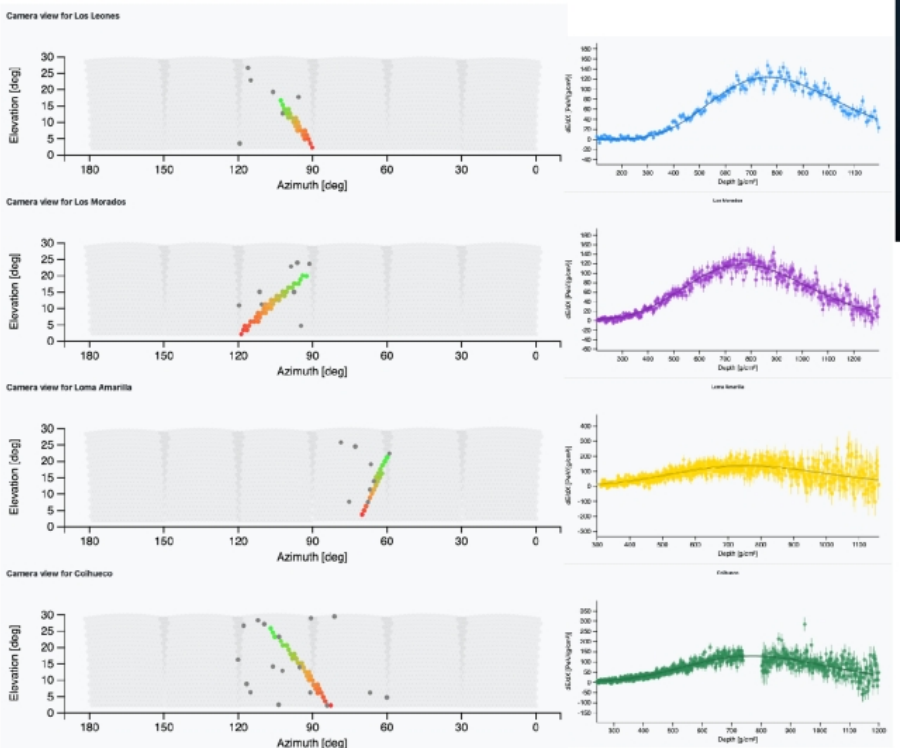

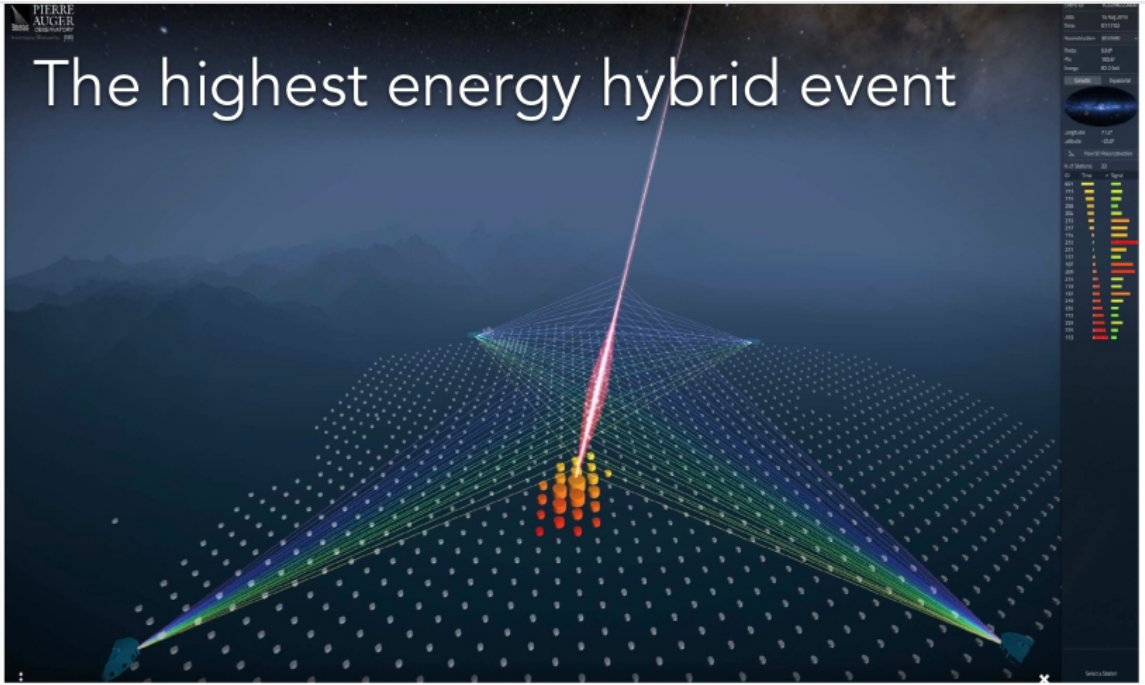

Astrophys. J. Suppl. S. 264 (2023) 50

Hybrid rec

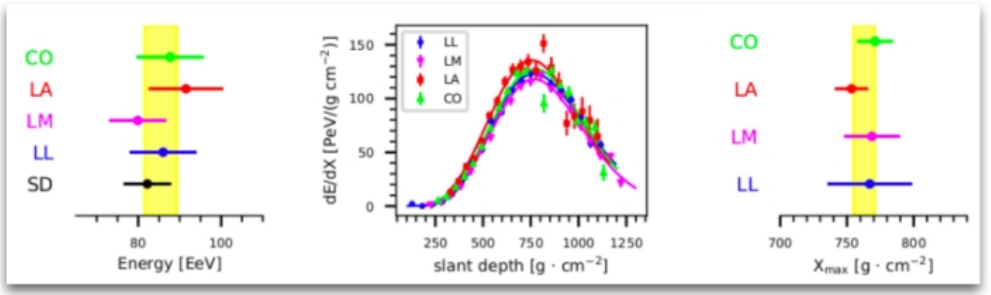

Auger: calibration with the FD energy scale

Phys. Rev. D 102 (2020) 062005

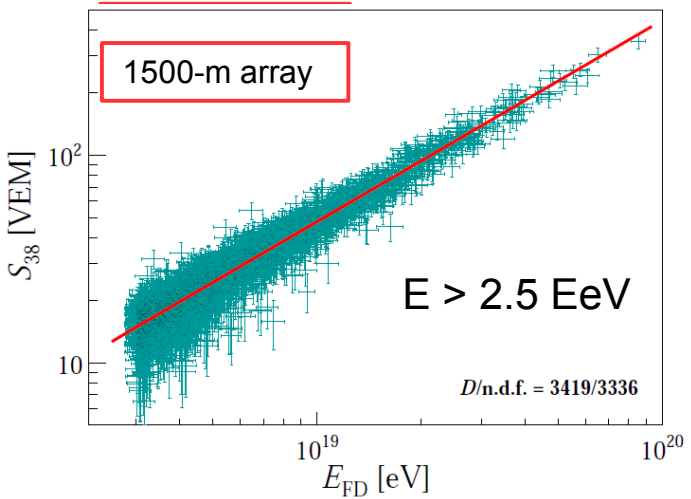

ICRC 2013

Systematic uncertainty in the energy scale	
Fluorescence yield	3.6%
Atmosphere	3.4% – 6.2%
FD calibration	9.9%
FD profile recon.	6.5% – 5.6%
Invisible energy	3% – 1.5%
Stability of energy scale	5%
TOTAL	14%

Eur. Phys J C. (2021) 81:966

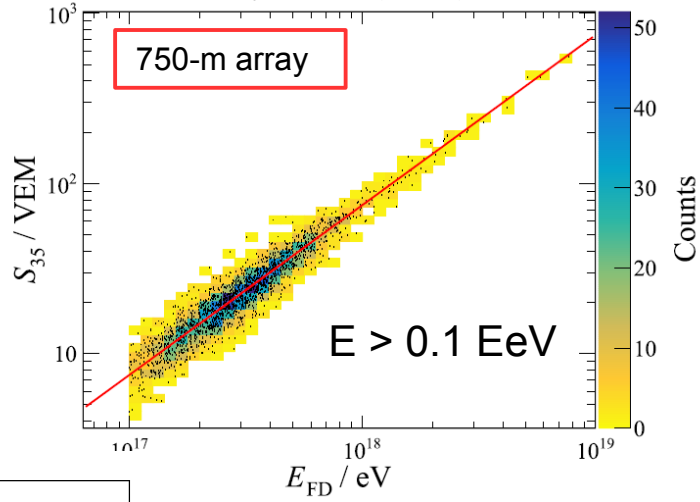

Energy resolution

SD: < 20% (zenith < 60° and)

Hybrid: 6-8 % [ICRC 2019]

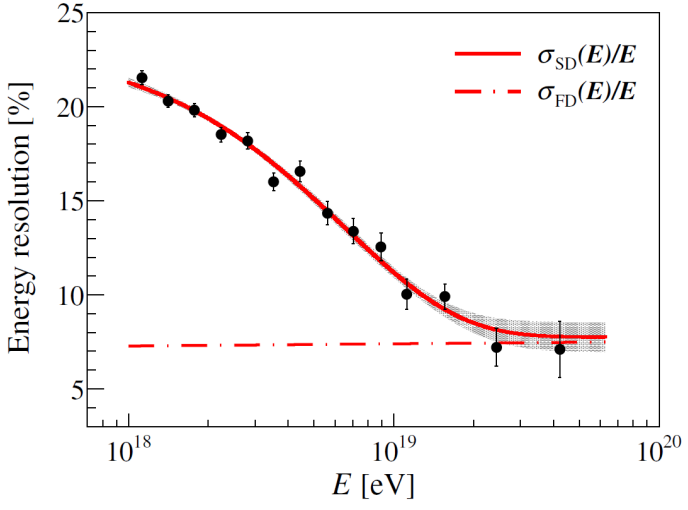

The Auger combined spectrum

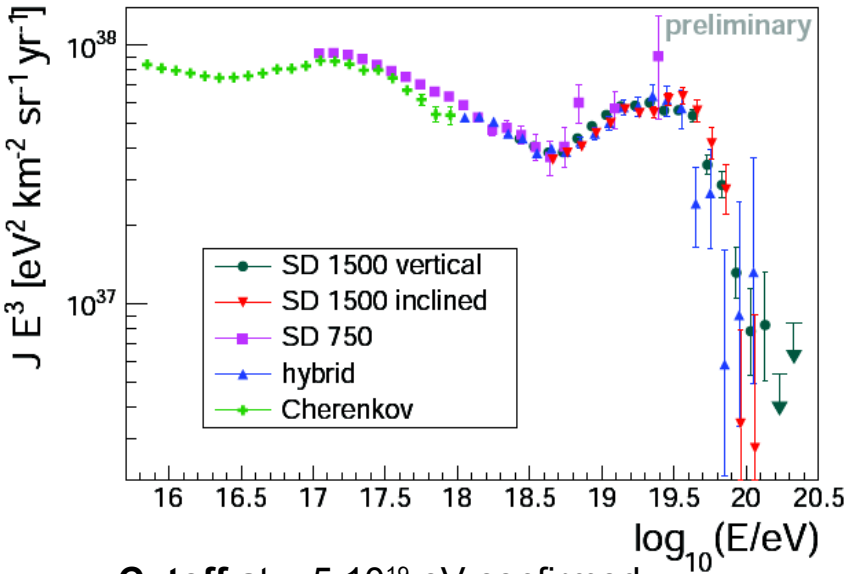

Five measurements
more than 3 order of magnitudes
same energy scale

Fluxes in agreement
within systematic uncertainties

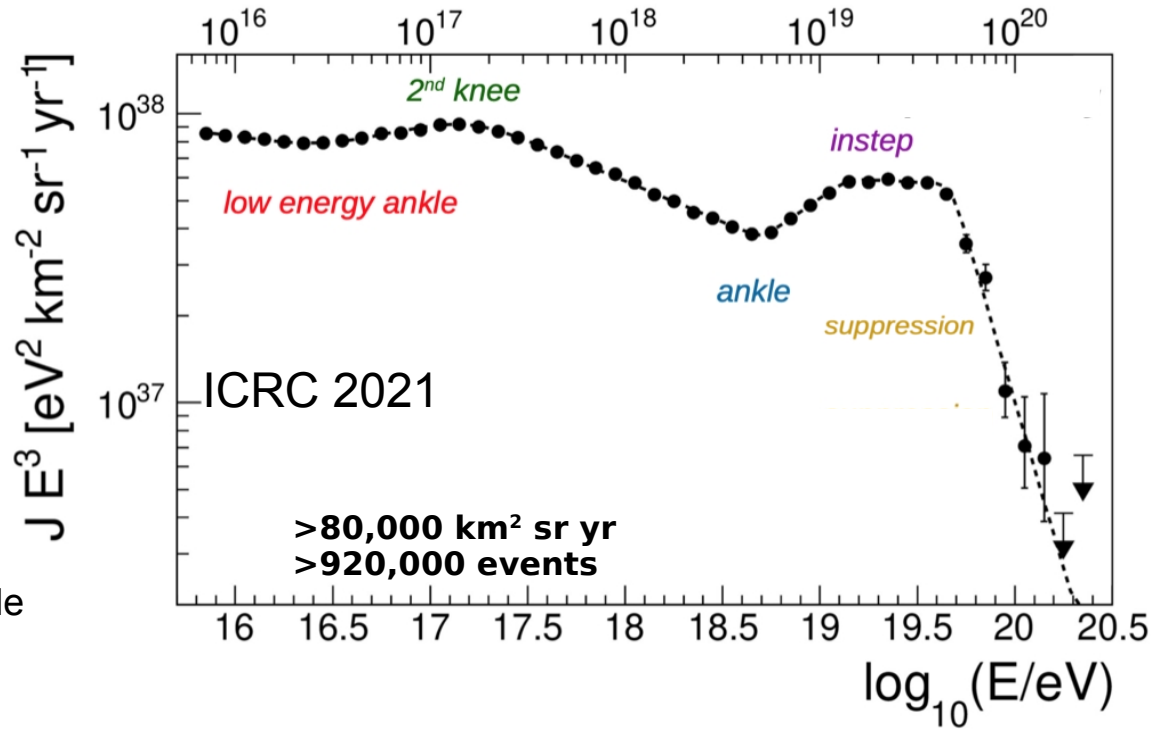

Cutoff at ~ 5 10^{19} eV confirmed

ankle at ~ 5 10^{18} eV confirmed

instep at ~ 10^{19} eV identified

2nd knee observed, hint for a low energy ankle

Independent of mass composition and model assumptions

Joint Auger TA WG on the energy spectrum

Proper data combination requires understanding the differences in energy scales

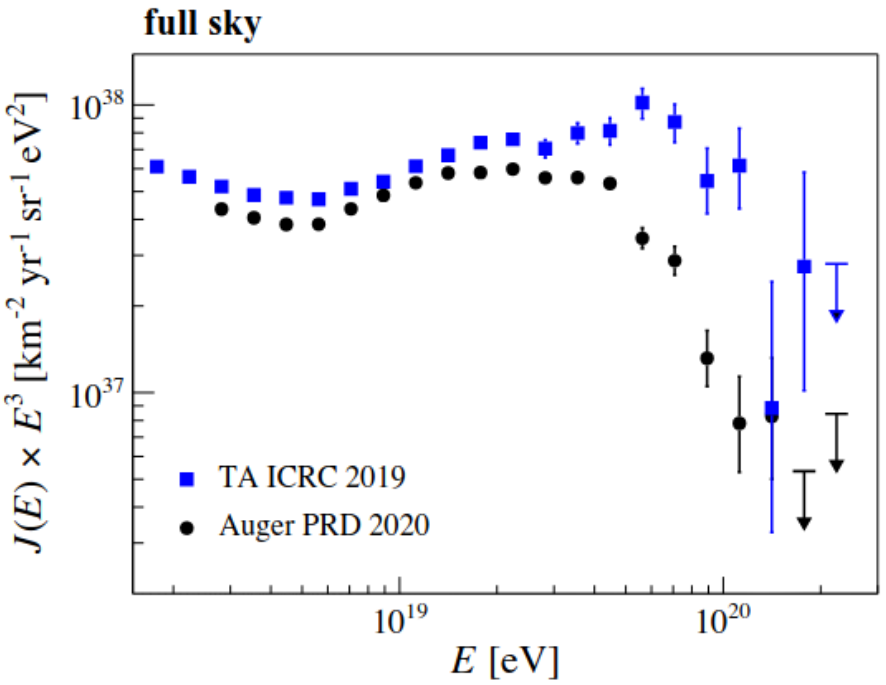

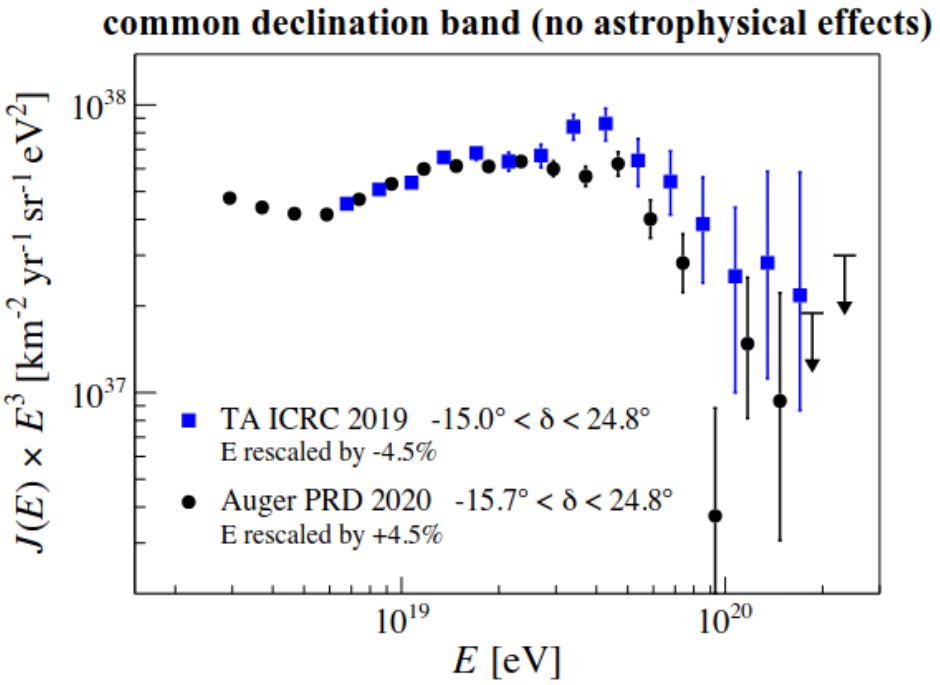

Difference at highest energies (ΔE/E = 20%/decade) not understood

Extremely Energetic Events (> 10^{20} eV)

Amaterasu particle
244 EeV

TA, Science 382, 903–907 (2023)

Time (UTC)	Energy (EeV)	S_{800} (m^{-2})	Zenith angle	Azimuth angle	R.A.	Dec.
27 May 2021 10:35:56	244 ± 29 (stat.) $^{+51}_{-76}$ (syst.)	530 ± 57	38.6 ± 0.4°	206.8 ± 0.6°	255.9 ± 0.6°	16.1 ± 0.5°

common band !

From local void. Large magnetic deflections? Physics beyond SM?

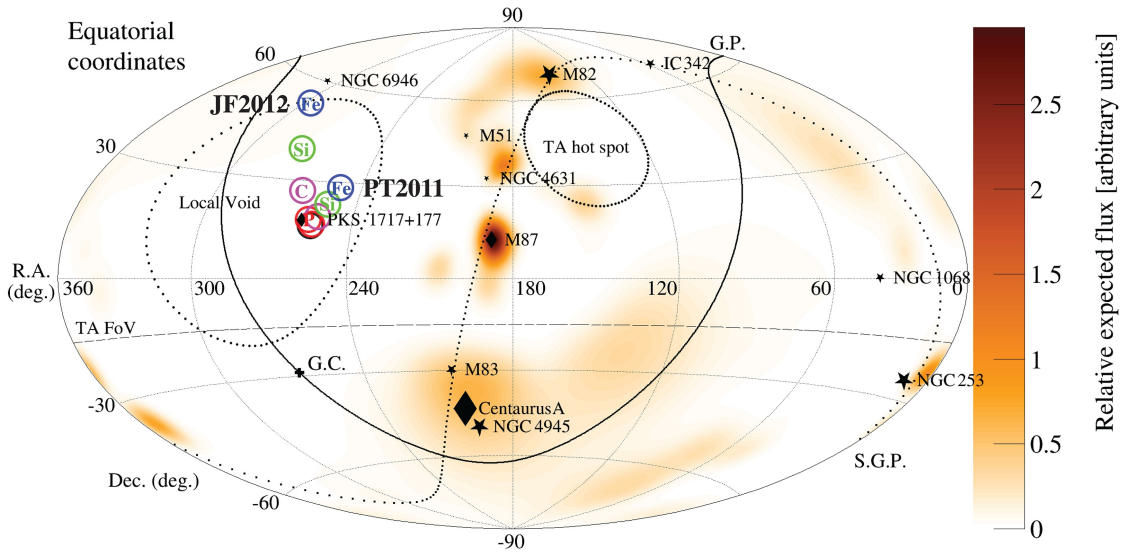

Combining Auger and TA data at extreme energies very difficult due to the mismatch in the energy scales

166 EeV: most energetic Auger event

note: exposure Auger / TA ≈ 6,7 !

energy of the Amaterasu particle at the Auger energy scale would be 154 EeV

-9% - 20%($\log_{10}$E - 19) = -37%

	E [EeV]	Dec [deg.]
PAO191110	166	-52
PAO070114	165	-21
PAO200611	155	-48
PAO141021	155	-38
TA Amaterasu	154	16

Auger, Astrophys. J. Suppl. S. 264 (2023) 50 https://opendata.auger. org/catalog/

The ultra-high energy mass composition

Phys Rev. D 111, 022003 (2025)
Phys.Rev. Lett. 134 (2025) 021001

FD → longitudinal profile

<Xmax> resol. 15 g/cm² at the highest energies

SD → temporal and lateral distributions + DNN

<Xmax> resol. 30 g/cm² at the highest energies

WITH RD!

° **<Xmax>** gets lighter up to ~2 10 [18] eV and heavier above incompatible with pure composition

° **σ (Xmax)** at the highest energy excludes a large fraction of protons and proton GZK as a dominant reason for the spectral cutoff

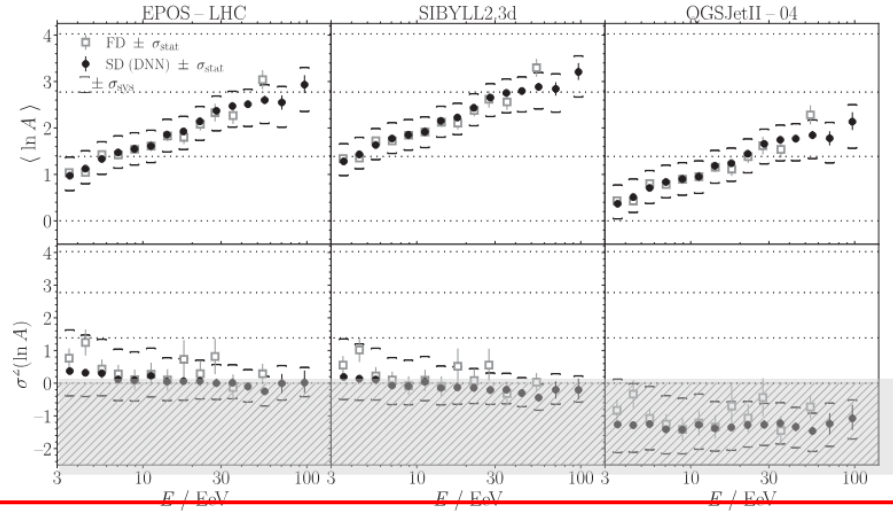

Tension with some hadronic interaction models

unphysical

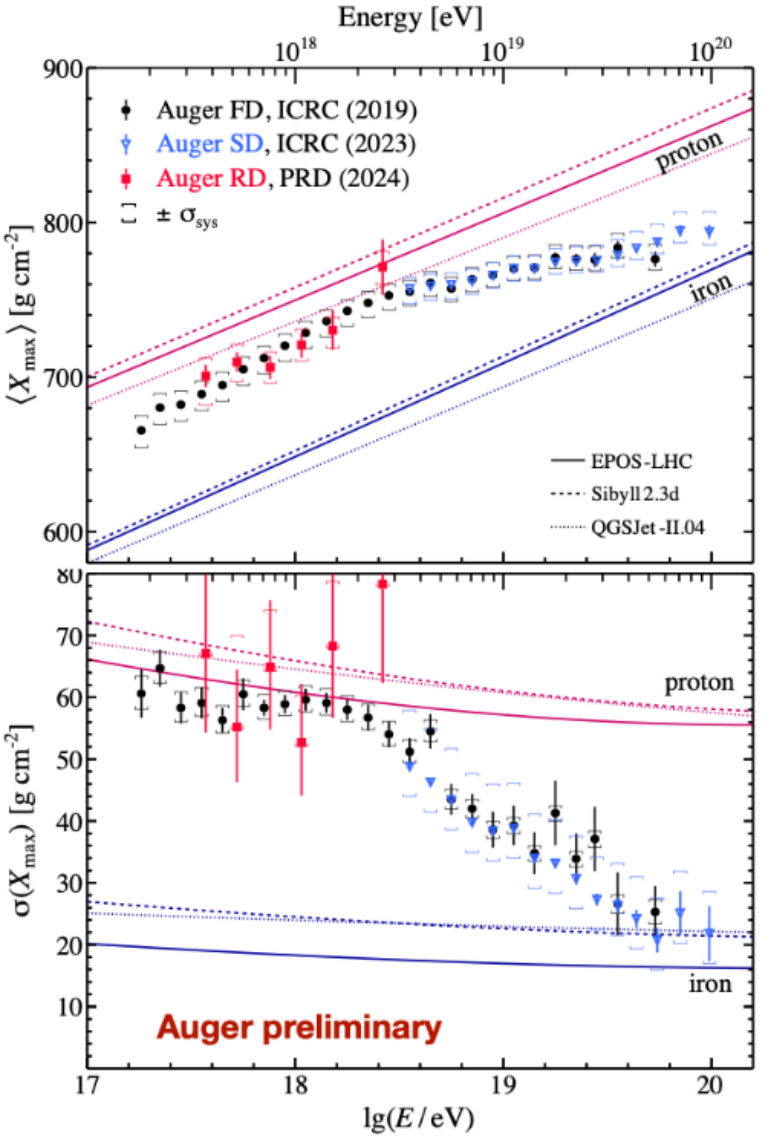

Changes in the elongation rate (SD+DNN)

Elongation rate in agreement with that found with FD

Clear evidence of a structure in ER, best described with a three-break model:

constant ER rejected at 4.4σ ⟶ ***incompatible with pure composition***

- ➡ kinks resembling the spectrum features
- ➡ supported by independent SD-based measurements (Delta method)
- ➡ in agreement with those predicted by a simplified astrophysical model

parameter val $\pm \sigma_{stat} \pm \sigma_{sys}$	3-break model val $\pm \sigma_{stat} \pm \sigma_{sys}$	energy spectrum val $\pm \sigma_{stat} \pm \sigma_{sys}$
b / g cm^{-2}	$750.5 \pm 3 \pm 13$	
D_0 / g cm^{-2} decade^{-1}	$12 \pm 5 \pm 6$	
E_1 / EeV	$6.5 \pm 0.6 \pm 1$	$4.9 \pm 0.1 \pm 0.8$
D_1 / g cm^{-2} decade^{-1}	$39 \pm 5 \pm 14$	
E_2 / EeV	$11 \pm 2 \pm 1$	$14 \pm 1 \pm 2$
D_2 / g cm^{-2} decade^{-1}	$16 \pm 3 \pm 6$	
E_3 / EeV	$31 \pm 5 \pm 3$	$47 \pm 3 \pm 6$
D_3 / g cm^{-2} decade^{-1}	$42 \pm 9 \pm 12$	

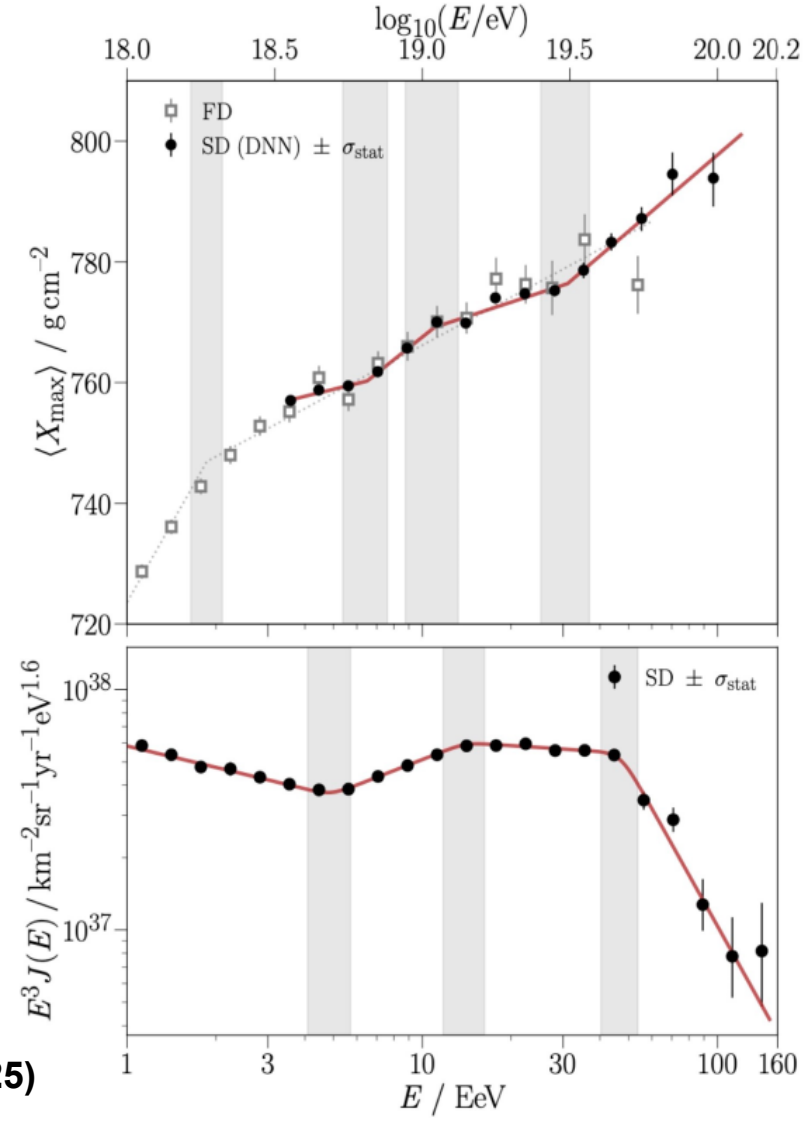

Phys. Rev. Lett. 134, 021001 (2025)

Auger Coll., JINST 16 (2021) P07019

Fractions of elements

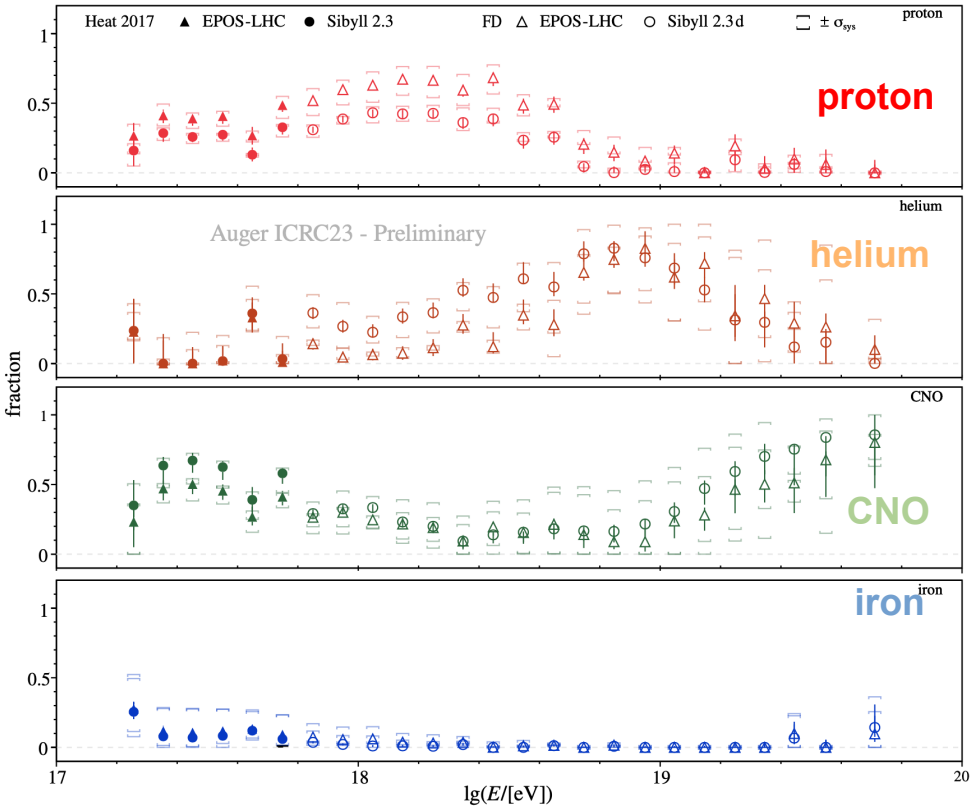

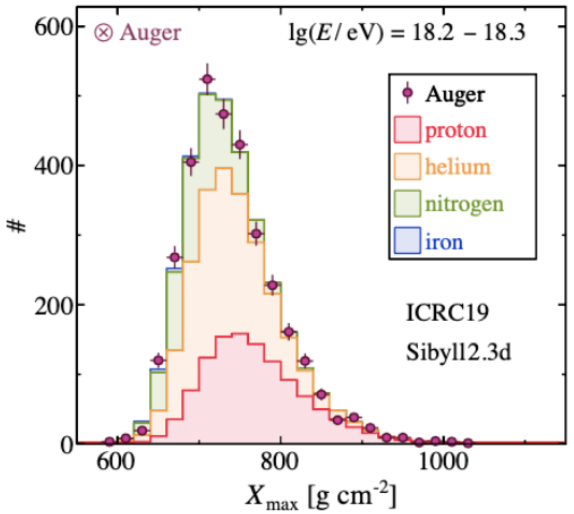

- derived from model dependent fits of the X_{max} distributions (+ many other measurements)

- they provide model dependent information on the mass evolution

Auger Coll., Phys.Rev.D102 (2020) 062005
Auger Coll., Eur. Phys. J. C 81 (2021) 966
E.Mayotte, PoS(ICRC2023)

Combined fit of Auger data (spectrum and X_{max} simultaneously) vs astrophysical scenarios

Phys. Rev. D 102(2020) 062005, Phys. Rev. Lett. 125 (2020) 121106

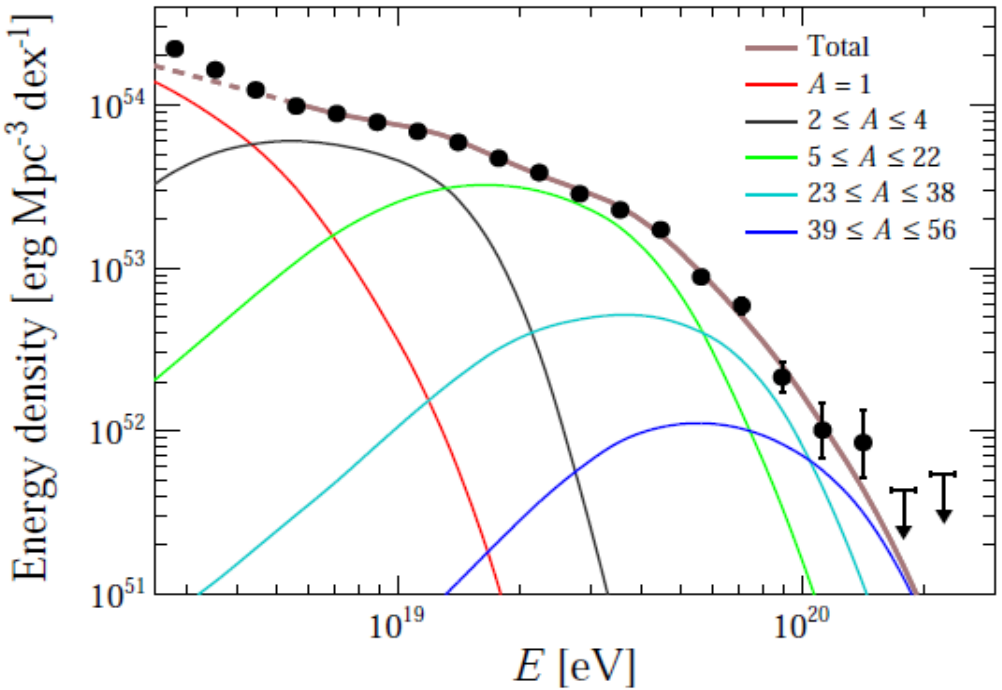

sources accelerating
only protons → **disfavored**

uniformly distributed sources accelerating nuclei [rigidity dependent] → **favored**

indication that the new feature at 10^{19} eV may be due to the interplay of He and CNO components
(individual nearby source not favored, spectrum flat in declination)

additional component required below 5 10^{18} eV (possibly a tail from galactic CR)

energy density in CR above the ankle (5.66 ± 0.03 ± 1.40) 10^{53} erg Mpc^{-3}
this constraints the luminosity density for classes of extra-galactic
→ **sources such as AGN and SB match**

Joint Auger TA WG for mass composition

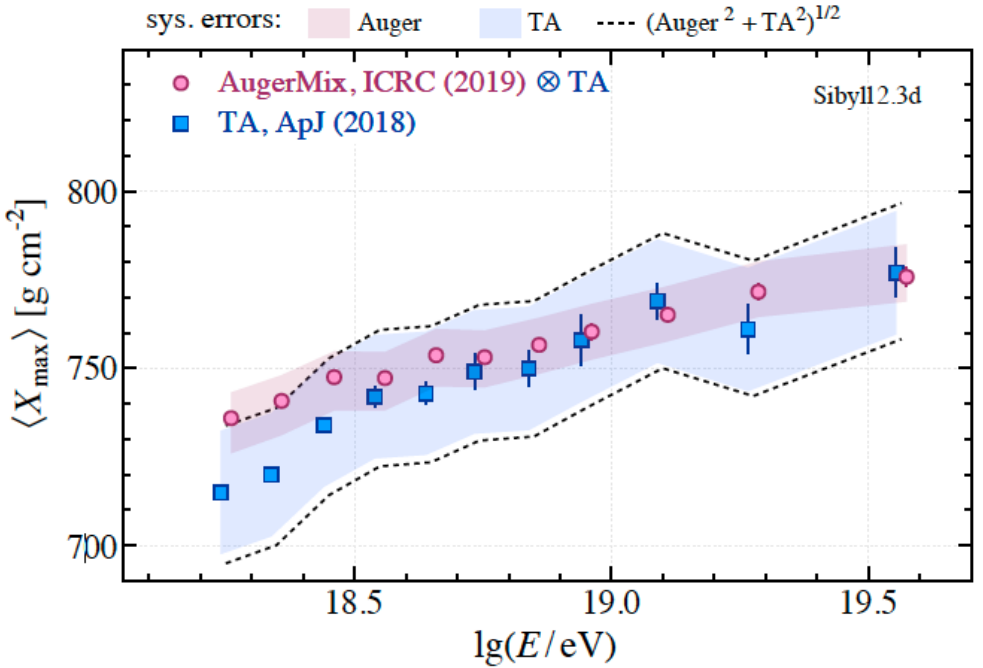

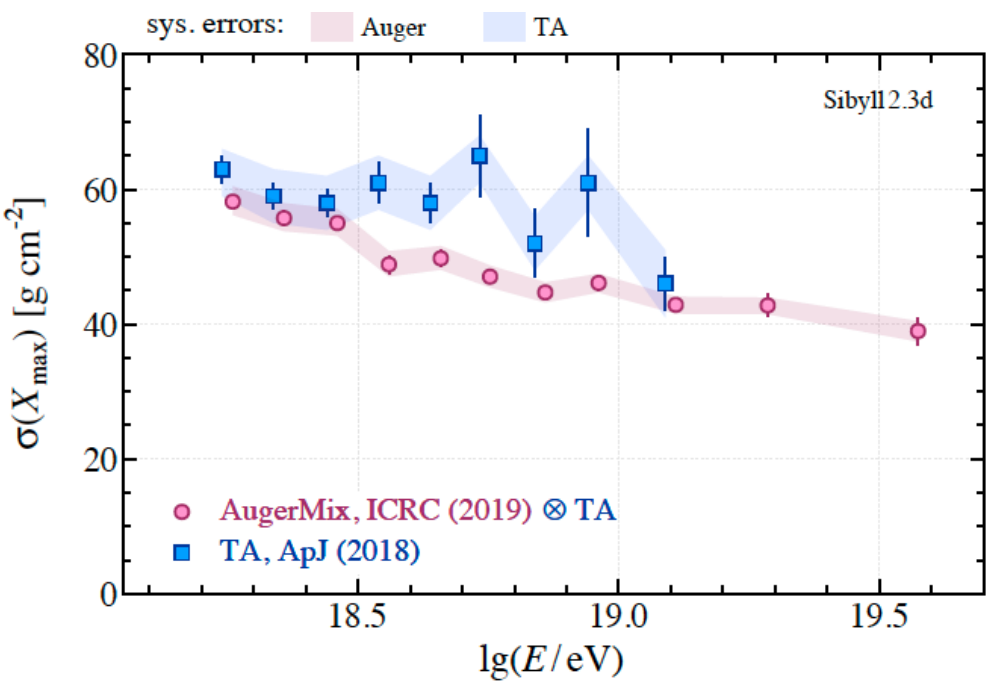

Consistency within uncertainties (larger for TA)

UHECR 2024 and paper under collaboration review

How well hadronic models match data?

Hybrid events ~ 10^{19} eV, 0°< zenith 60°

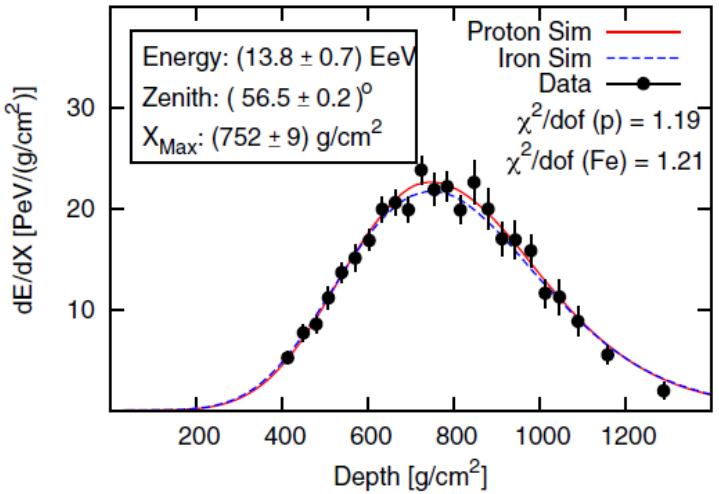

Observed longitudinal profile from FD is reproduced by simulations

Measured signal at the ground differ for data and simulations

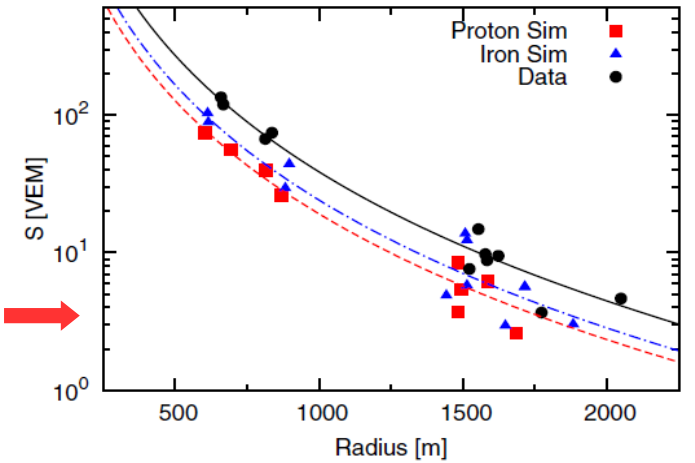

PRL 117, 192001 (2016)

R_{had} and R_E

Scaling factors to match data

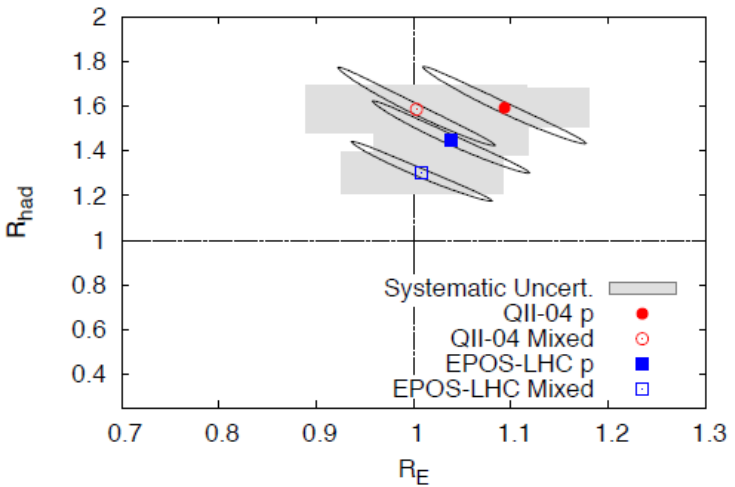

Evidence of muon excess

$1.3 < R_{had} < 1.6$

Insensitive to energy scale uncertainty

$R_E \sim 1$

Measurement of muon density and impact on models

Eur. Phys J. C (2020) 80:751: first direct measurement of muon number with UMD at Auger

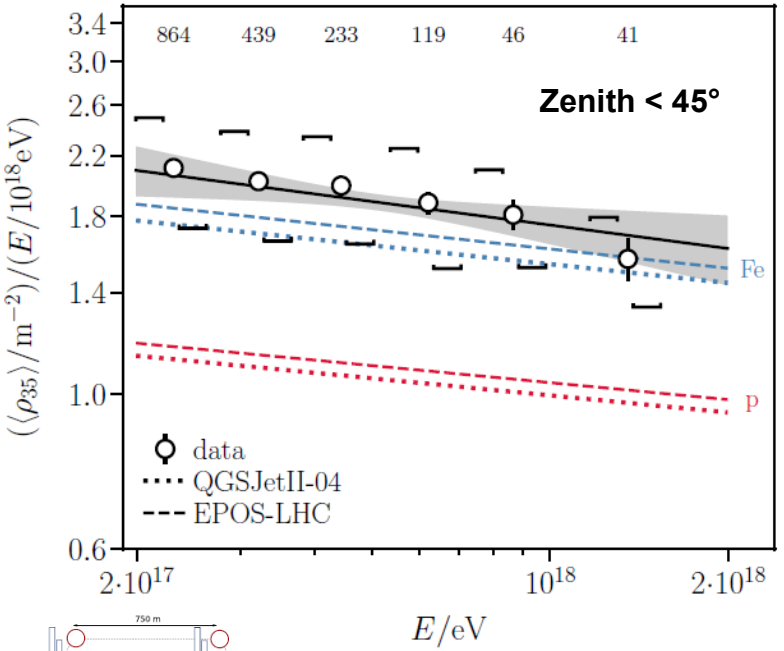

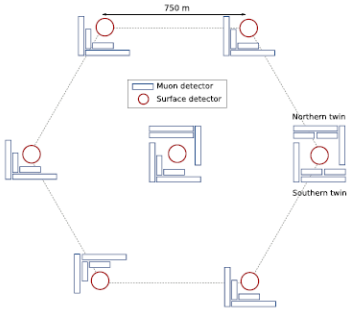

Muon number from models in tension with data

Fluctuation in agreement
(Phys. Rev. Lett. 126 (2021) 152002)

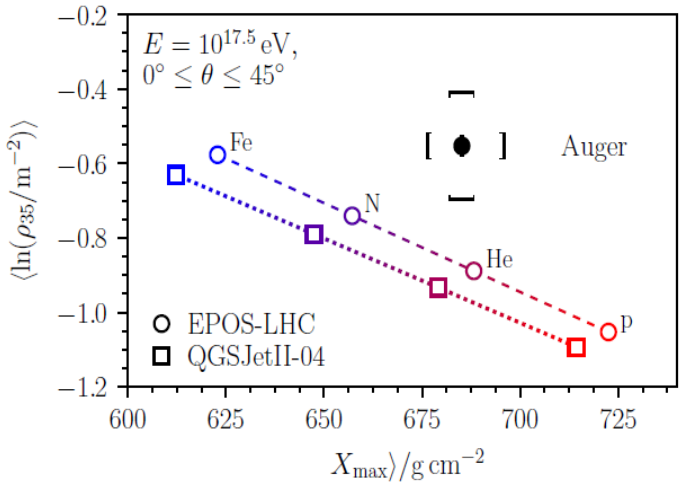

Data/Sims ~ 1.38 (1.50)
for EPOS-LHC (QGSJETII-04)

$$z = \frac{\langle \ln x \rangle - \langle \ln x \rangle_{\mathrm{p}}}{\langle \ln x \rangle_{\mathrm{Fe}} - \langle \ln x \rangle_{\mathrm{p}}}$$

EPOS-LHC

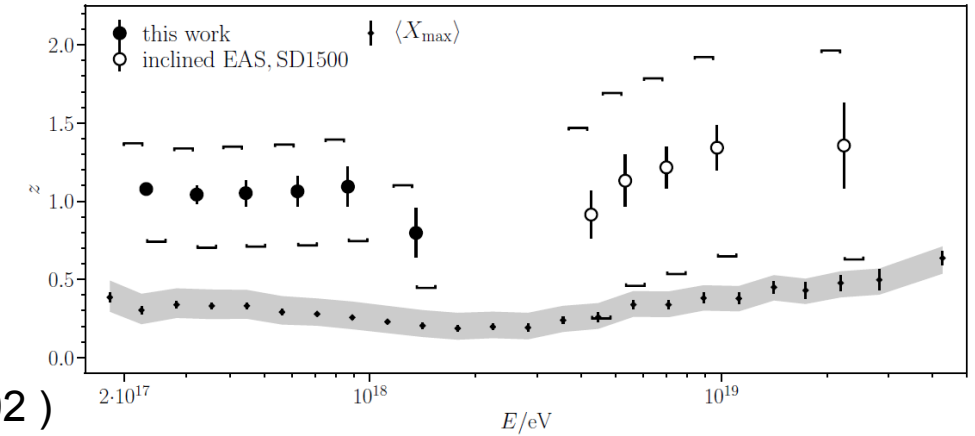

Large Scale anisotropy

E > 4 EeV, zenith < 80°
Exposure=123000 km²sr y!

Observation of dipolar anisotropy for E≳8 10^{18} eV
Significance 6.9 σ above 8 EeV, 5.7σ at E=8-16 EeV

Can be interpreted as a signature of the local large scale distribution of matter.

Not consistent with pure protons above 8 EeV
Require mixed composition

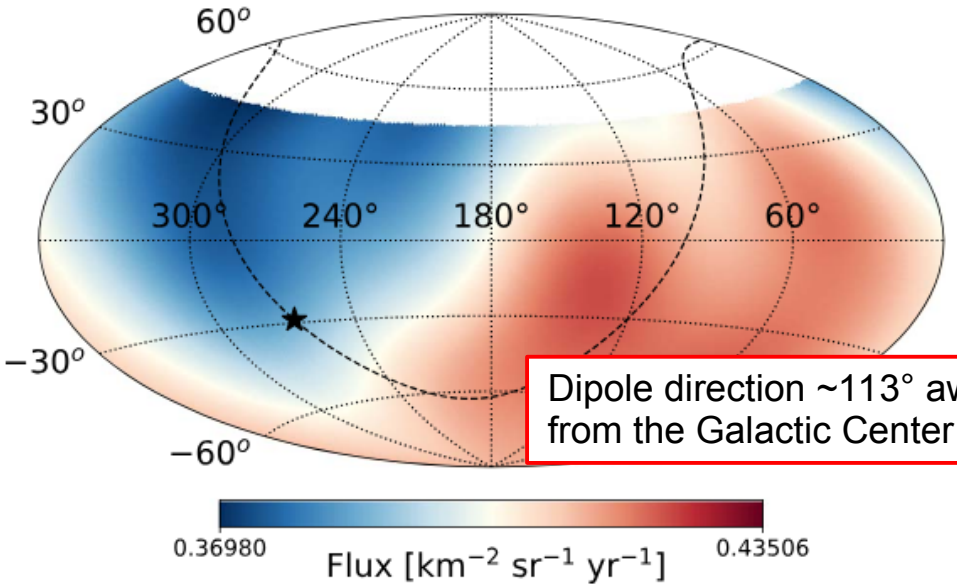

Dipole direction ~113° away from the Galactic Center

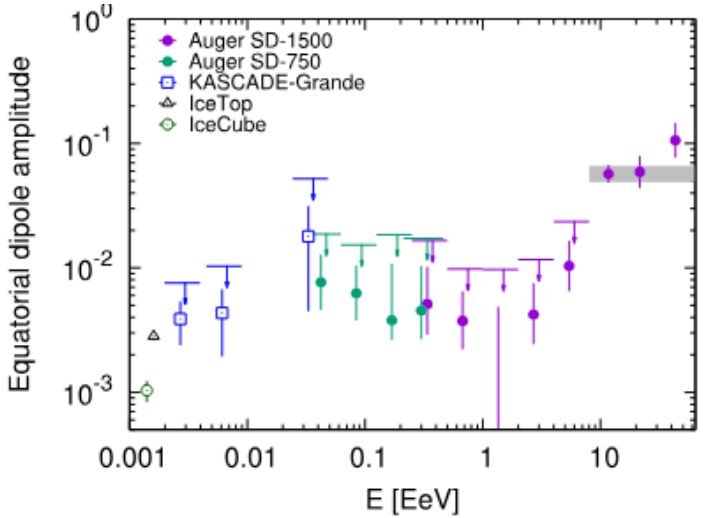

Dipole amplitude and phase

Evolution with energy of the dipole phase away from GC

→ **Extragalactic origin of UHECR above 8 EeV**

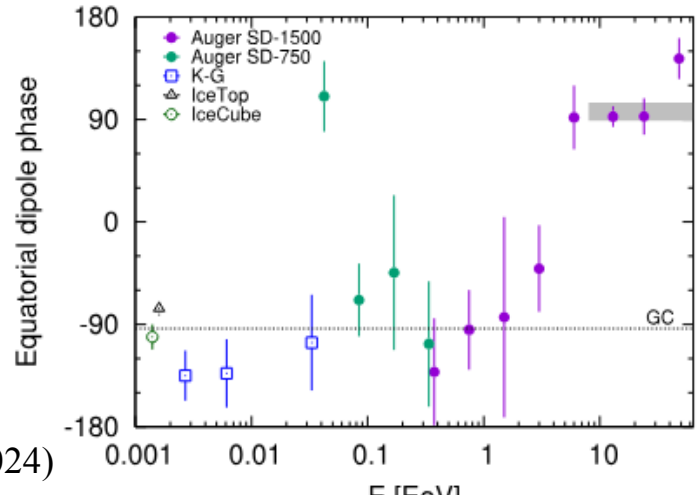

Science 315 (2017) 1266, APJ 976:48 (2024)

Anisotropy at intermediate scale

Blind search for overdensity

Energy [32-80] EeV
Zenith < 80° → 85% of the sky, declination [-90°, 45°]

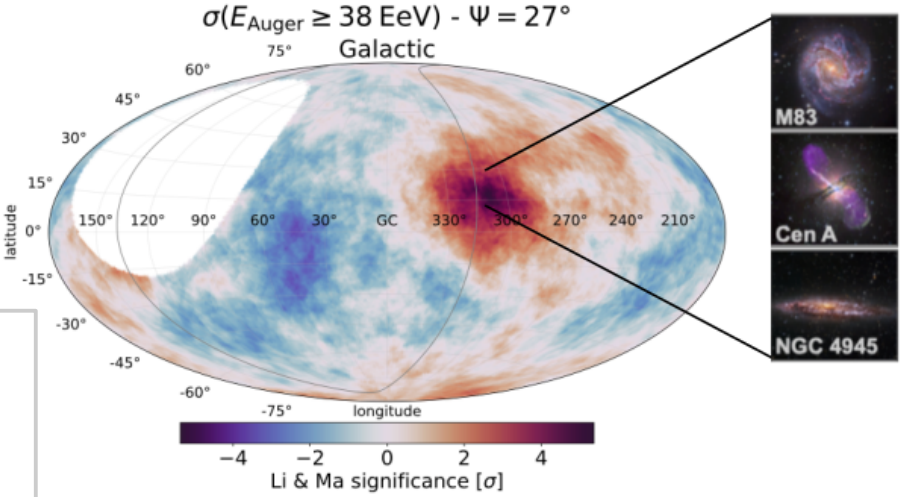

Centaurus A region:
most significant excess, p-value 2% post trial, at $\psi \sim 24°$ E > 38 EeV
direction fixed at Cen A 4 σ post trial, at $\psi \sim 27°$ E > 38 EeV

Autocorrelation with structures (GC, GP, SGP) not significant

Likelihood test for anisotropy with catalogs

Attenuation and relative weight of sources taken into account.

Catalog	$E_{\rm th}$ [EeV]	Ψ[°]	α[%]	TS	Post-trial p-value
All galaxies (IR)	38	24^{+15}_{-8}	14^{+8}_{-6}	18.5	6.3×10^{-4}
Starbursts (radio)	38	25^{+13}_{-7}	9^{+7}_{-4}	23.4	6.6×10^{-5}
All AGNs (X-rays)	38	25^{+12}_{-7}	7^{+4}_{-3}	20.5	2.5×10^{-4}
Jetted AGNs (γ-rays)	38	23^{+8}_{-7}	6^{+3}_{-3}	19.2	4.6×10^{-4}

Significance
3.8 σ for SB

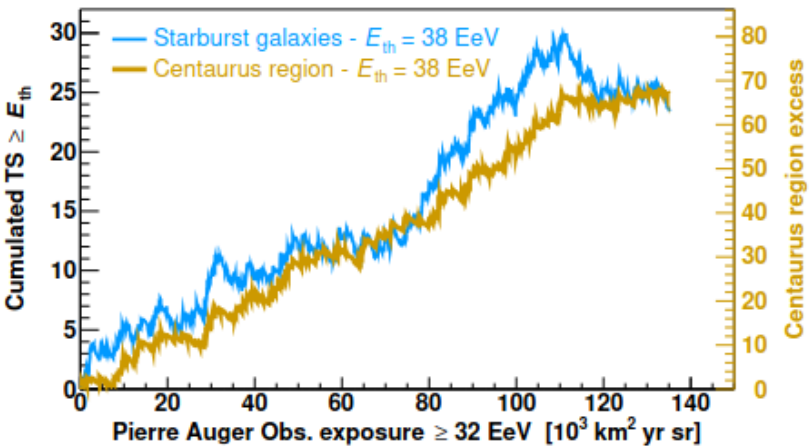

The Astrophysical Journal 935 (2022)170, PoS(ICRC2023) 252

Multi-messenger physics (diffuse, targeted and follow up)

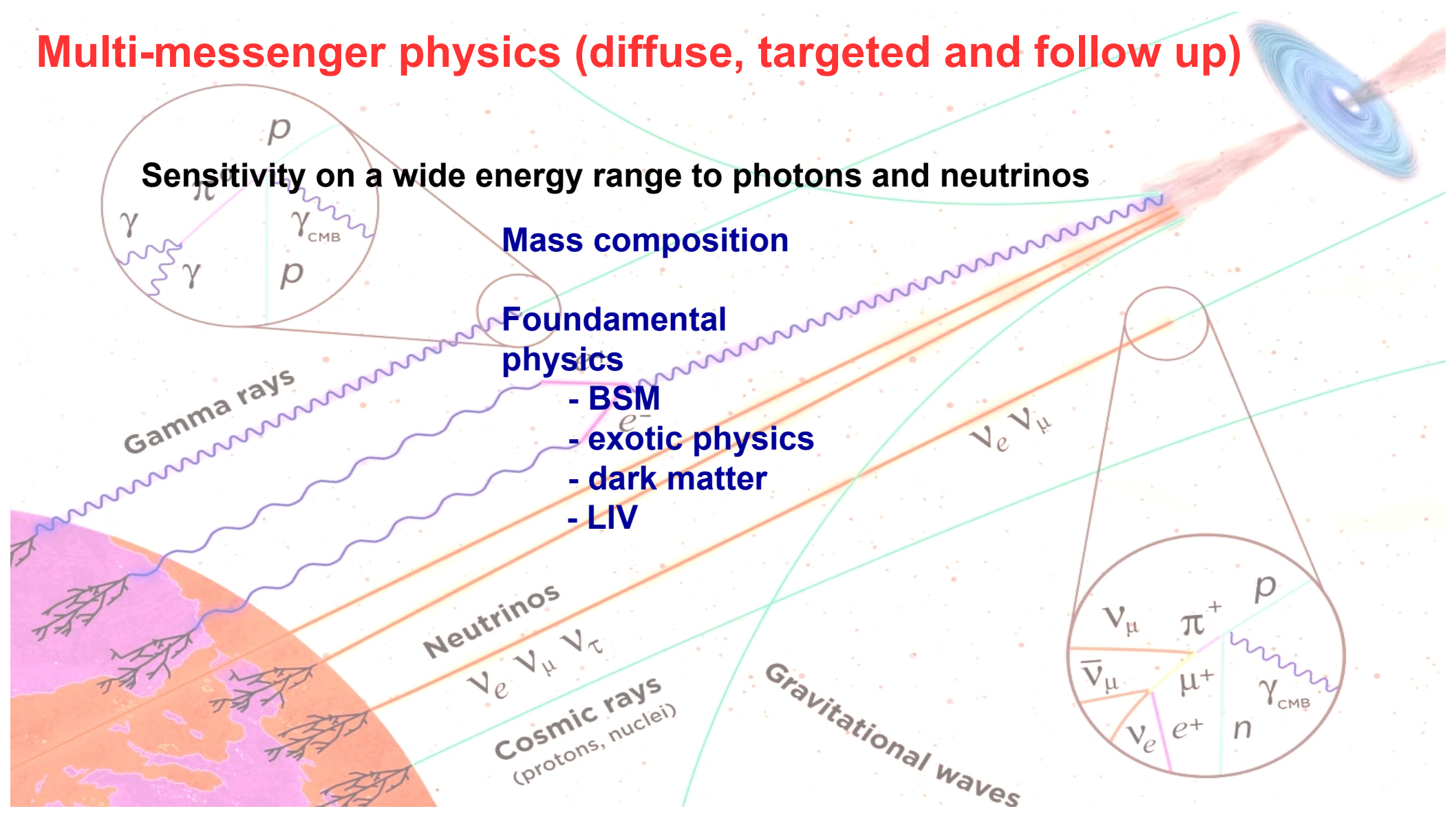

Auger: A 4π MM Observatory

1 Neutrons and charged CRs: $\Theta \leq 80°$

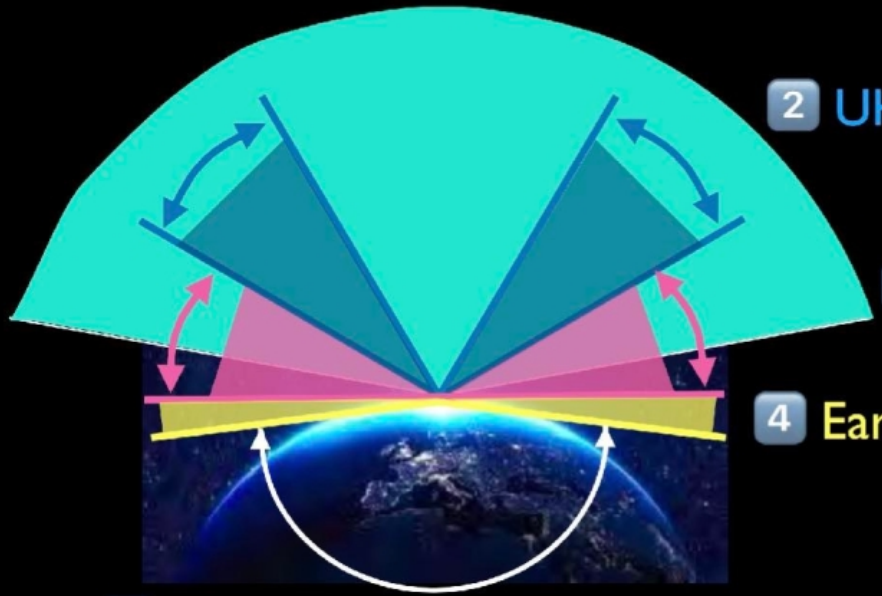

2 UHE Photons: $30° \leq \Theta \leq 60°$

3 Down-Going Neutrinos: $60° \leq \Theta \leq 90°$

4 Earth Skimming Neutrinos: $90° \leq \Theta \leq 95°$

5 HE BSM Particles: $\Theta > 95°$

UHE Photon induced cascades

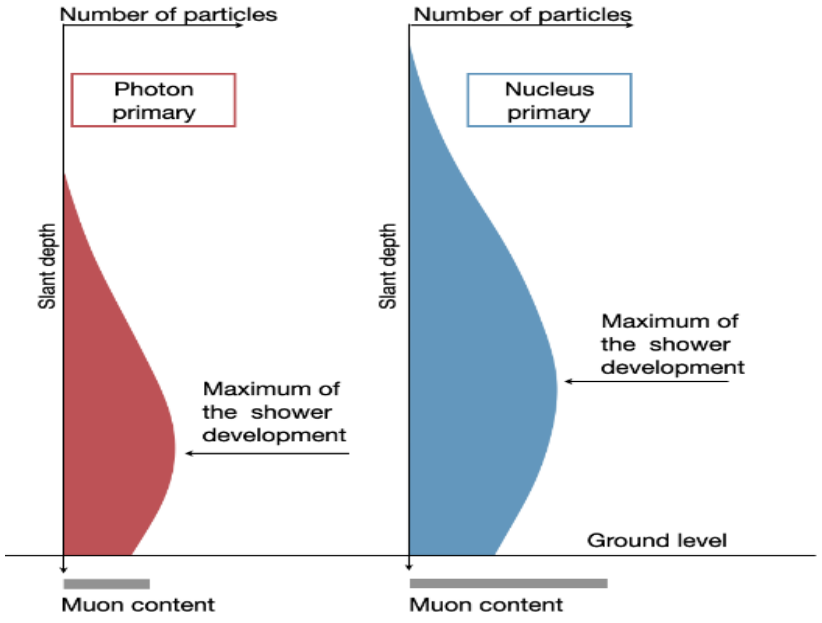

Photon EAS distintive signature:
→ delayed shower developement
→ smaller muon content

observable characteristics:
- deeper <Xmax>
- steeper LDF
- smaller footprint
- broader signal

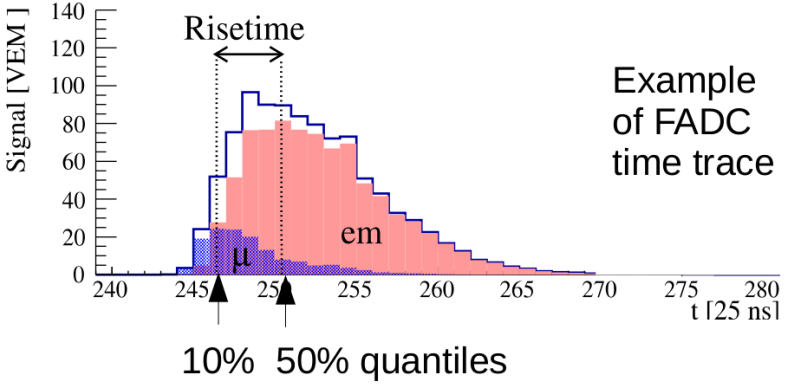

Example of FADC time trace

steeper LDF

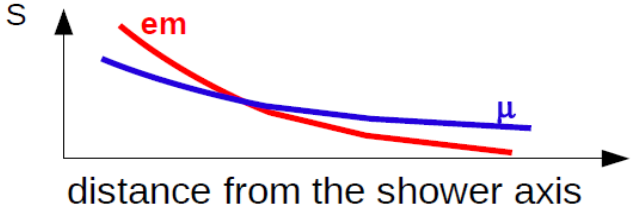

longer rise-time

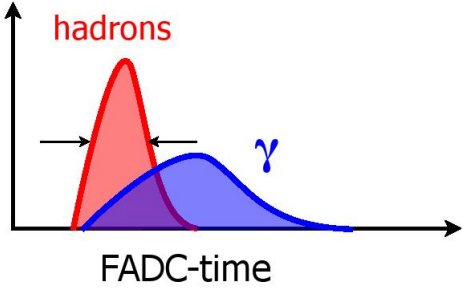

Auger: Hybrid and SD photon search

Phys. Rev. D 110, 062005 (2024)

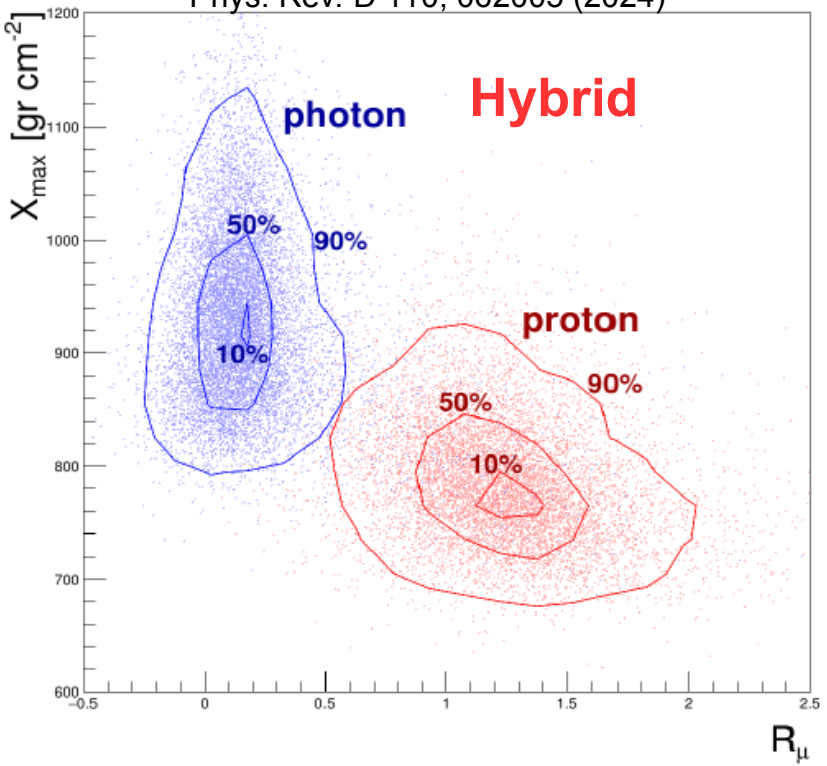

Maximum of shower development: $\mathbf{X_{max}}$

Muon content of the shower (universality): R_μ

ApJ. 933 (2022)125

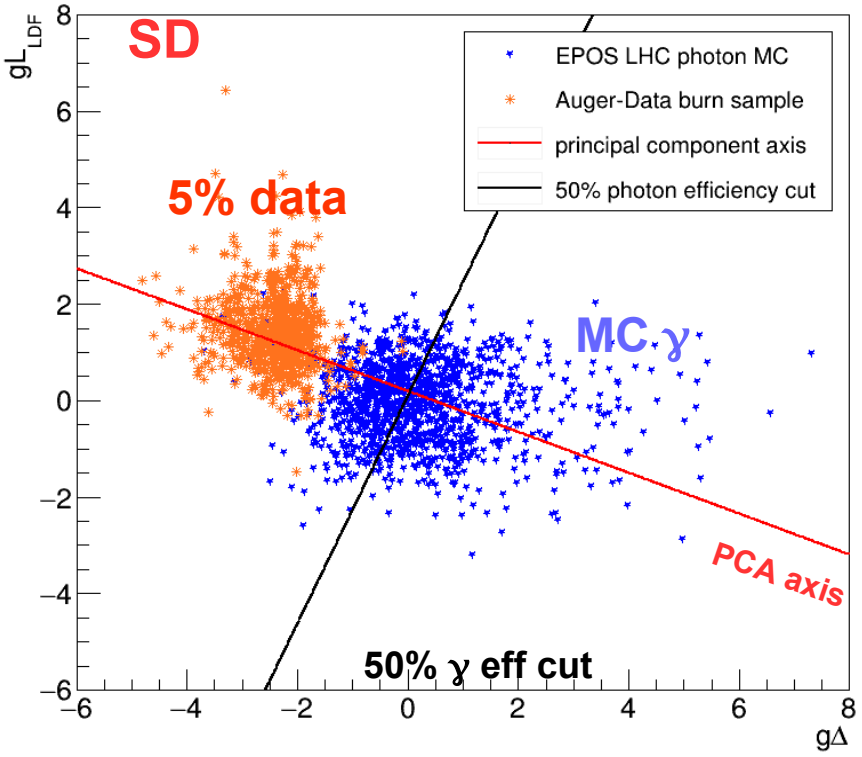

Deviation from data <LDF>: $\mathbf{gL_{LDF}}$

rise-time rel. event-wise quantity: $\mathbf{g_\Delta}$

Upper limits on diffuse photon flux

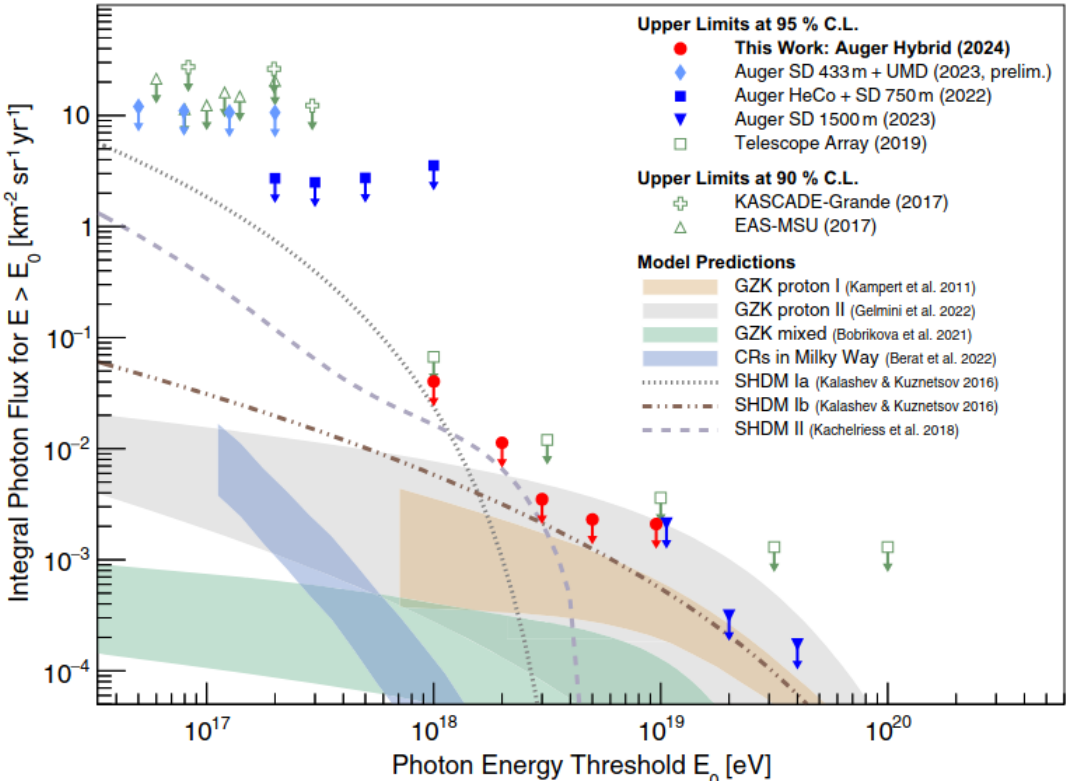

ApJ. 933 (2022)125

Phys. Rev. D 110, 062005 (2024)

Strictest limits at E> 0.2 EeV

11 candidates > 10 EeV (SD)

22 candidates > 1 EeV (Hybrid)

Targeted search

- In coincidence of known sources including CenA and the Galactic Center [UL extrapolating HESS flux]
- GW follow-up

No candidates found

- Top-down model disfavored

- CR proton dominated scenario (also the most pessimistic cases) disfavoured
- constraining mass and lifetime of dark matter particles →
- Auger Phase II: additional information for better photon/hadron separation or photon discovery

Auger: UHE neutrinos with the SD

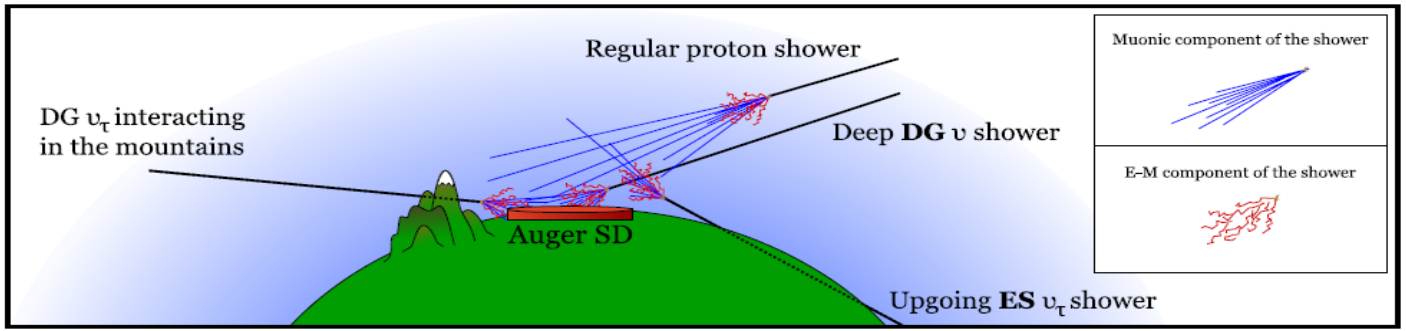

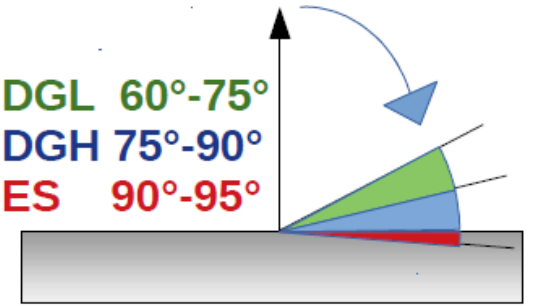

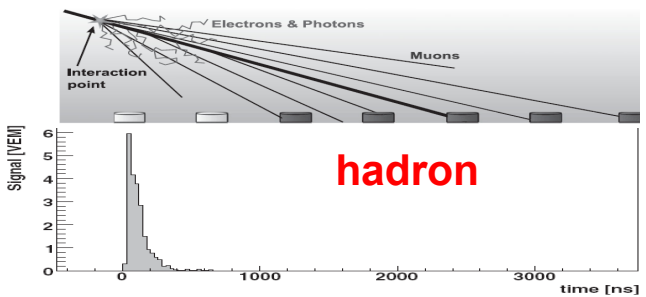

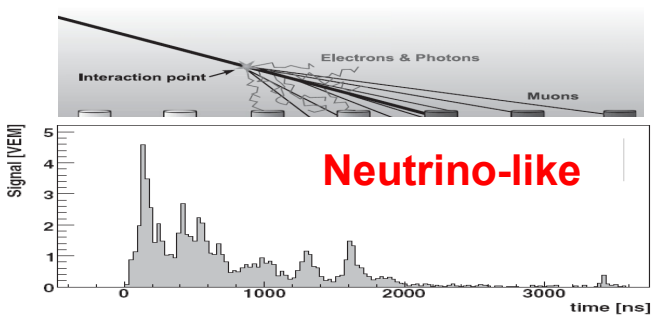

Sensitivity to different channels

ES 79.4%
DGH 17.6%
DGL 3.0%

ν_τ ES sensitivity dominant

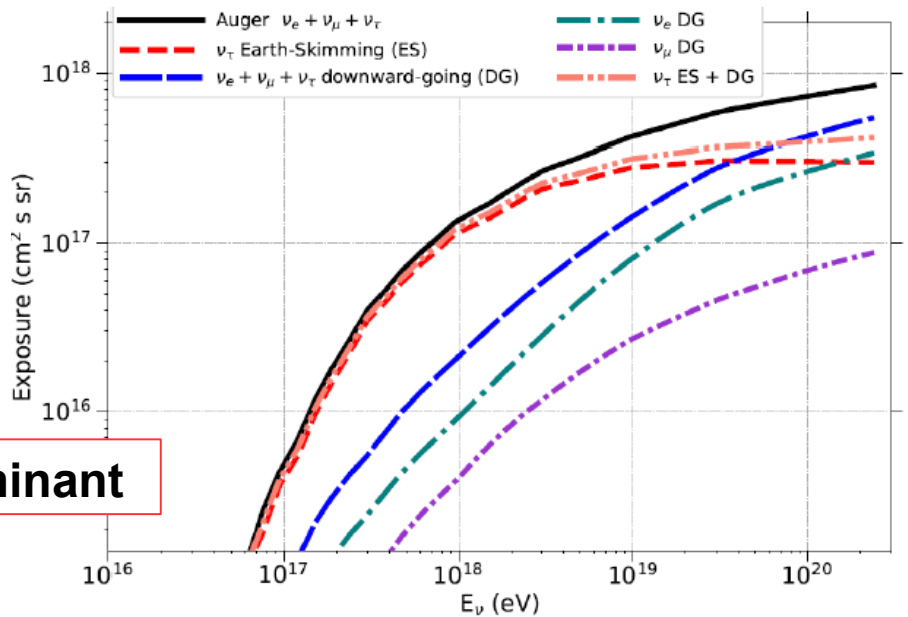

Search for neutrinos with the SD: signature

typical signal shapes

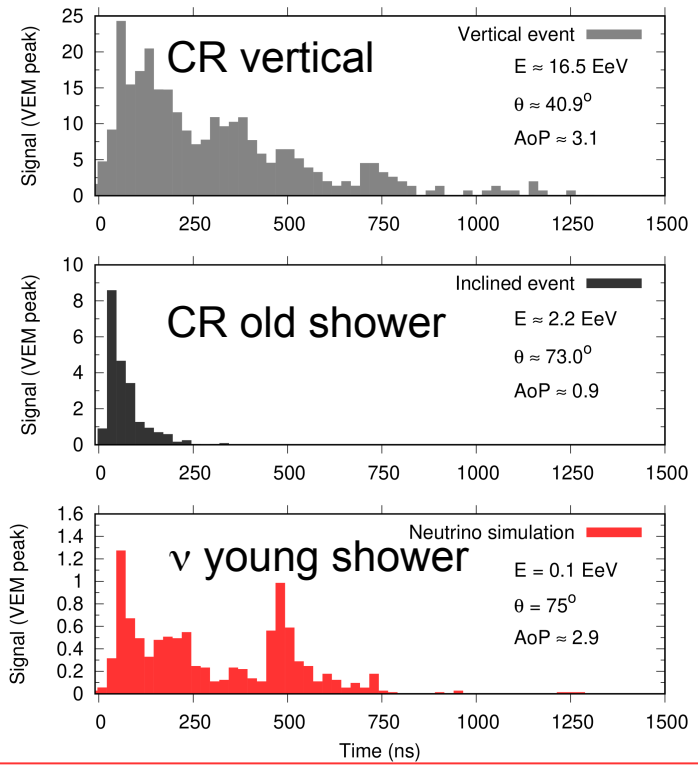

Signature:

"young shower" → with large electromagnetic component

inclined event with slow rising and broad signal

larger Area-over-Peak (**AoP**)

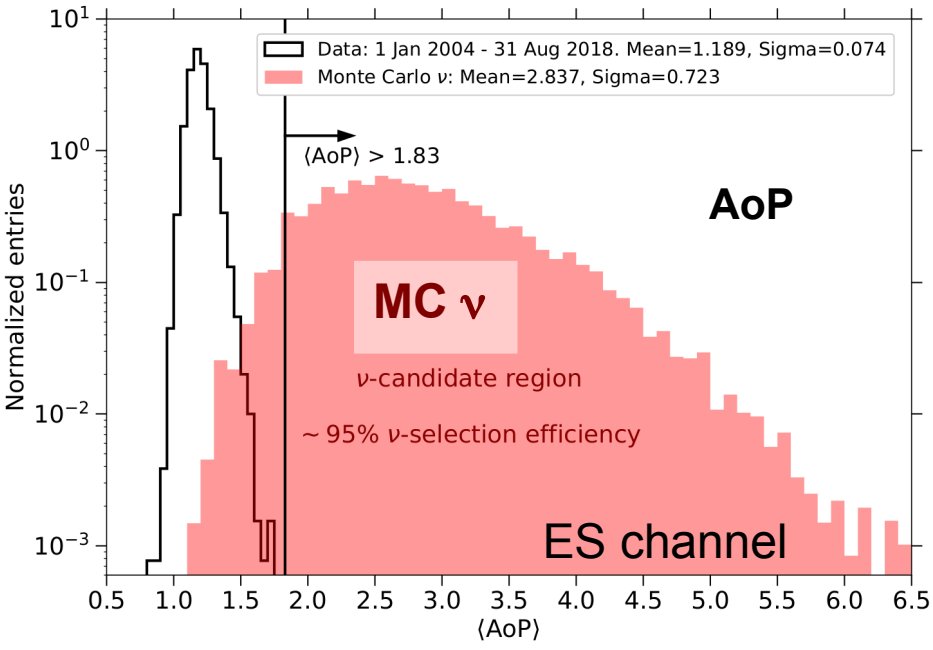

Data 2004 – 2018: 14.7 yr

→ **bkg expected: <1 event in 50 years!**

NO Candidates found

Bounds on neutrino fluxes from cosmic rays

tension with models assuming pure proton and spectrum shaped by GZK
[up to 6 neutrino expected vs 0 observed]

Upper limits on the diffuse neutrino flux

Pierre Auger Coll., JCAP 10 (2019) 02, PoS(ICRC2023)1488

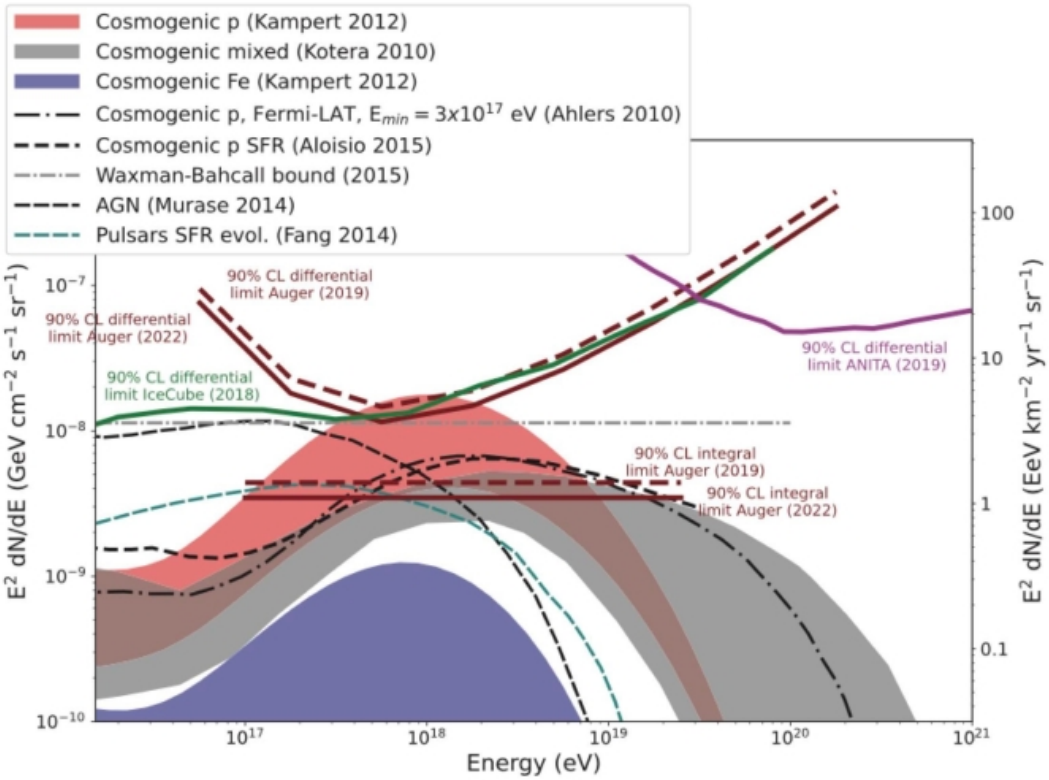

Maximum sensitivity **~ 1 EeV**

Point-like sources

also in coincidence with observations by other experiments
For example TXS 0506+056

Coincidence with GW

For example GW170817
GW follow-up (62 events, stack analysis)

NO Candidates found

Constraining models assuming sources of CRs accelerating only protons

UHE neutrinos: point sources sensitivity

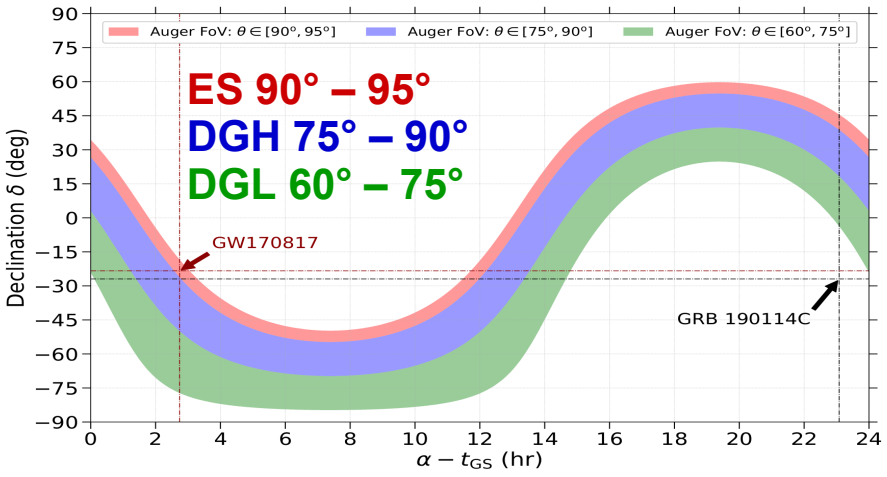

point sources transit through the field of view of each detection channel

→ sensitivity strongly depends on source location and event timing

Pierre Auger Coll., JCAP 11 (2019) 004

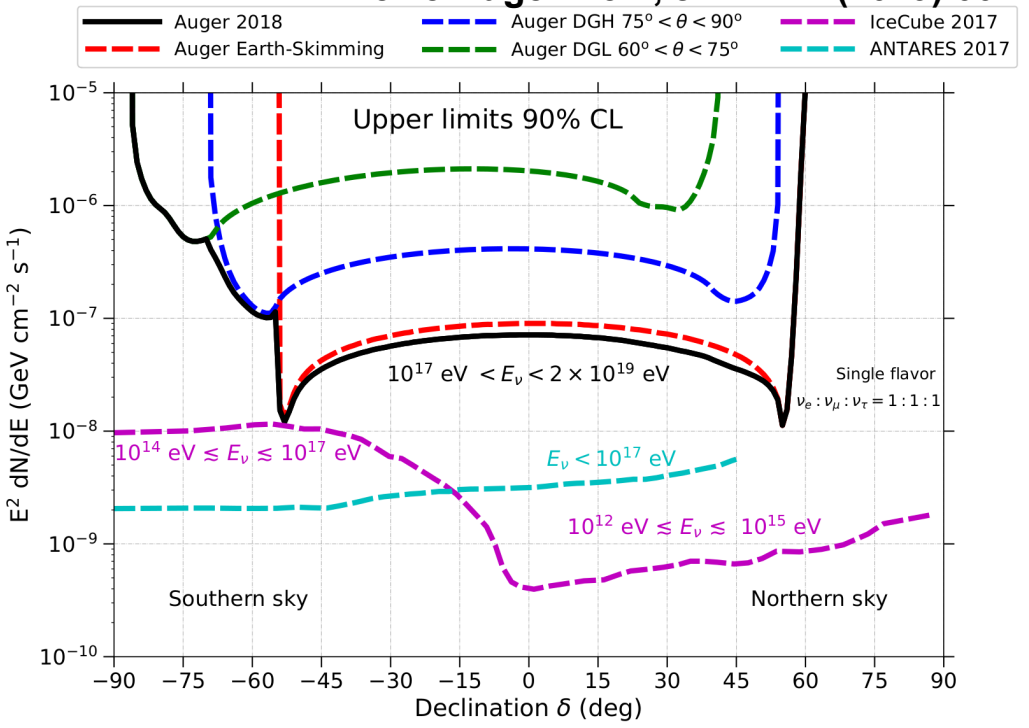

Auger follow-up searches: GW170817

LIGO/Virgo BNS GW170817 & Fermi sGRB 170817A
→ EM counterpart Optical/IR KiloNova AT2017GFO

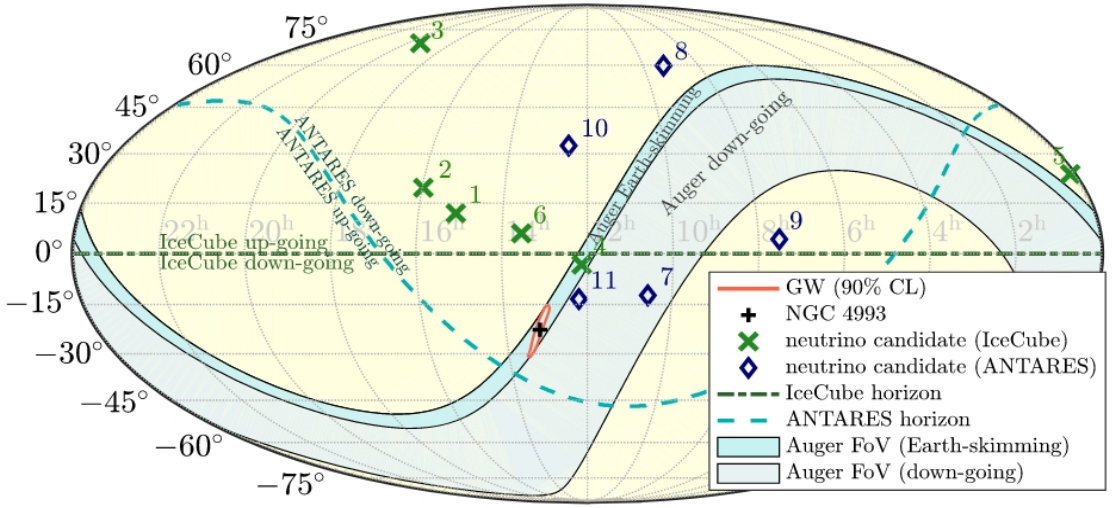

→ excellent visibility of the merger:
90% CL GW event location in FoV of ES channel

→ time dependent exposure leads to substantially lower 14-day neutrino fluence limits wrt to prompt

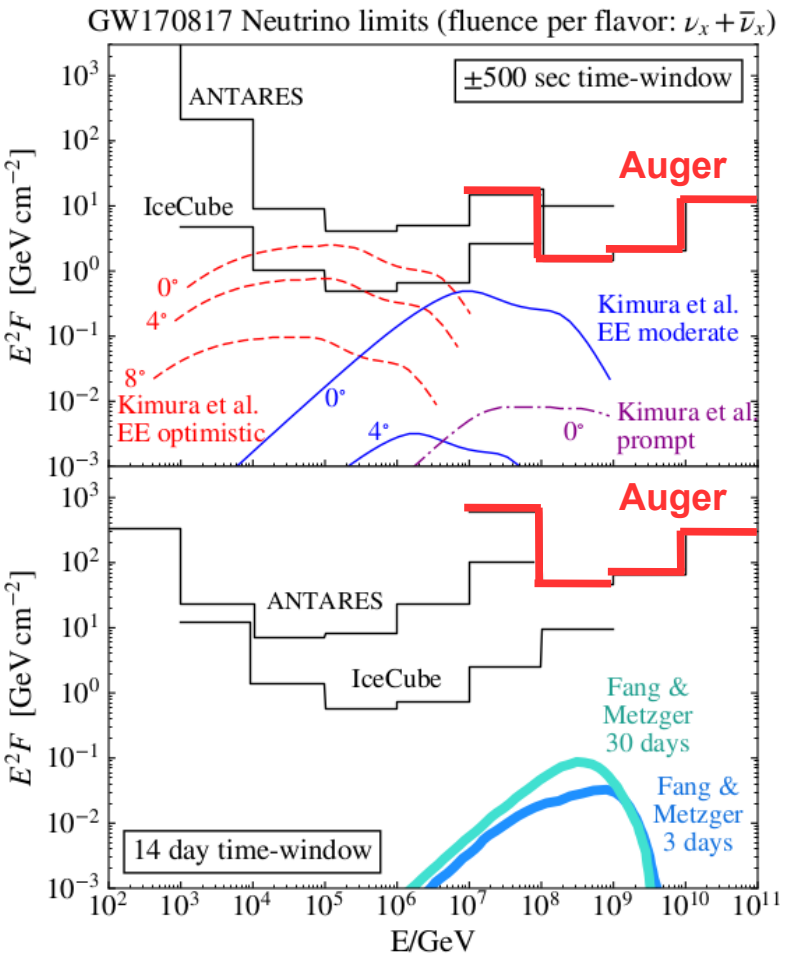

The neutrino event KM3-230213A

Energy ~ 120 PeV !!

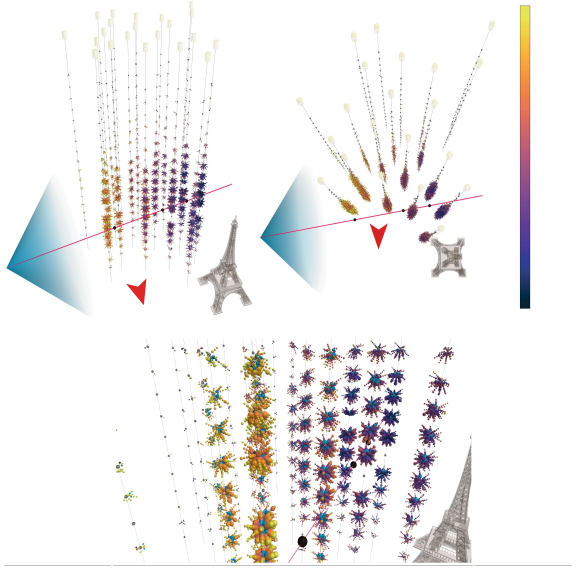

Nature | Vol 638 | 13 February 2025

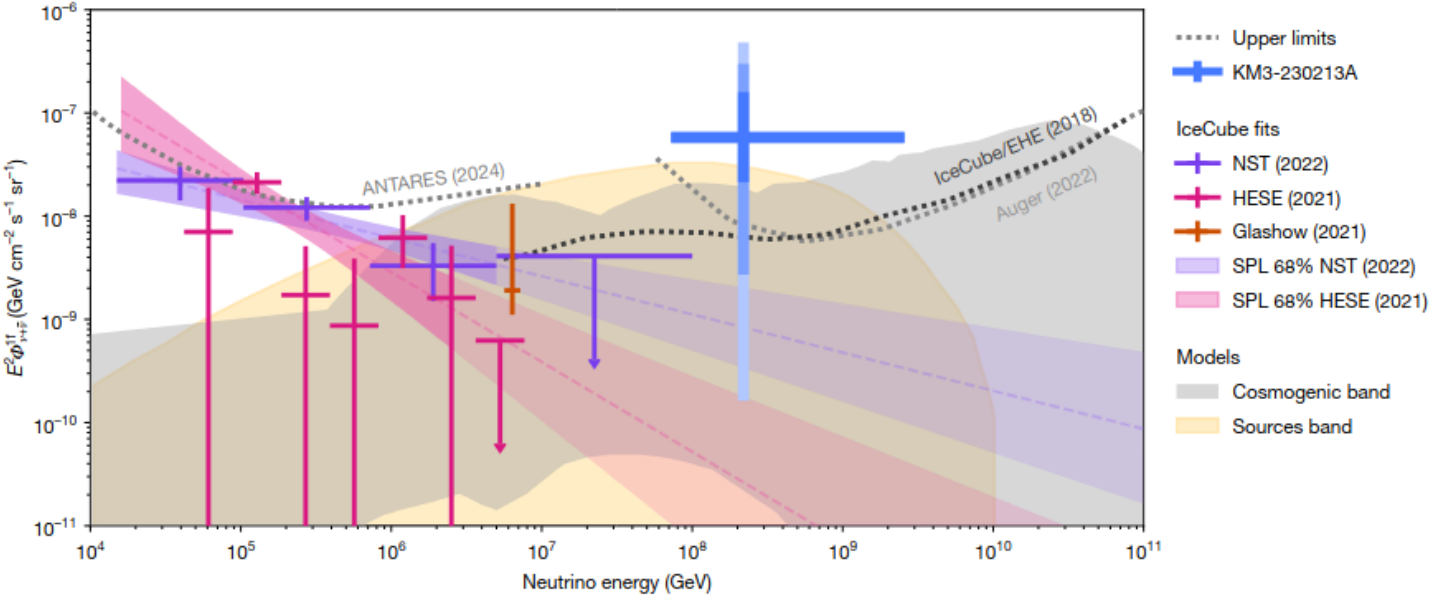

Astrophysical or cosmogenic?

→ **it's a breakthrough**

UHE neutrinos: point sources sensitivity

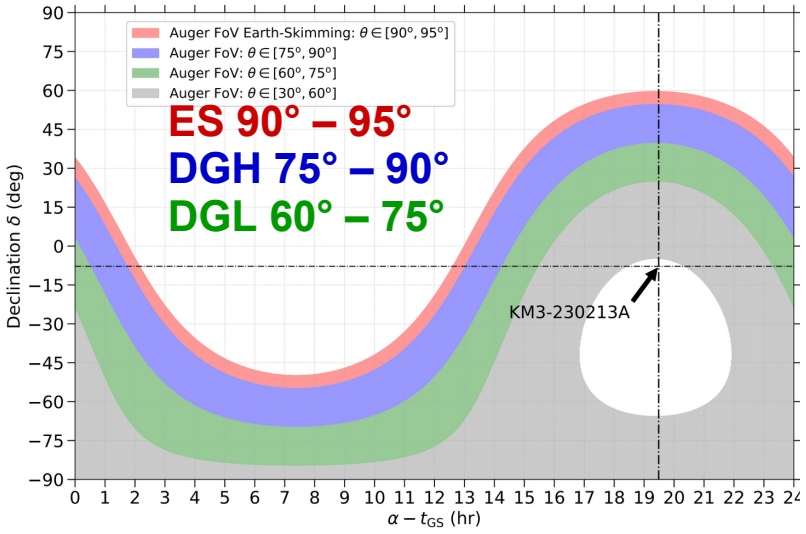

point sources transit through the field of view of each detection channel

→ sensitivity strongly depends on source location and event timing

Pierre Auger Coll., JCAP 11 (2019) 004

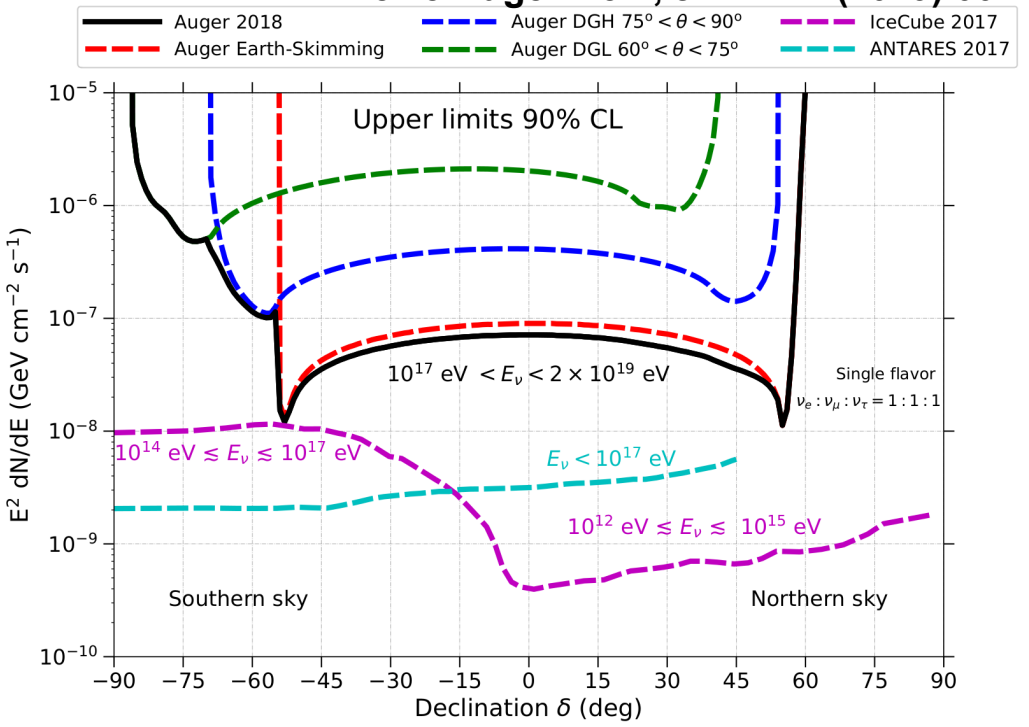

Search for neutrinos using the Auger FD detector

FD Energy > 0.1 EeV, zenith > 110°, 14 years of FD data

Accepted for publication on PRL 2025

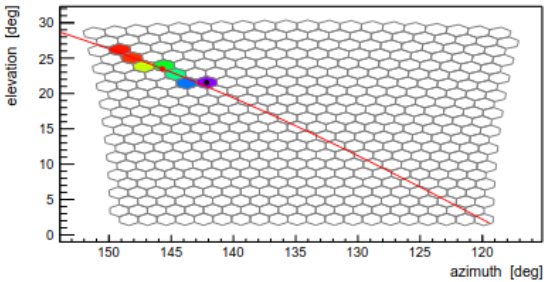

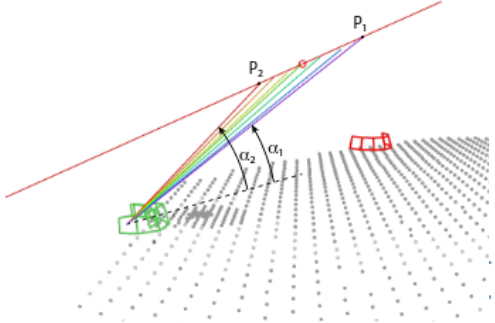

FD only reconstruction challenging for specific event topologies

Debate triggered by the claim done by the ANITA collaboration

Exposure (energy, height of first interaction)

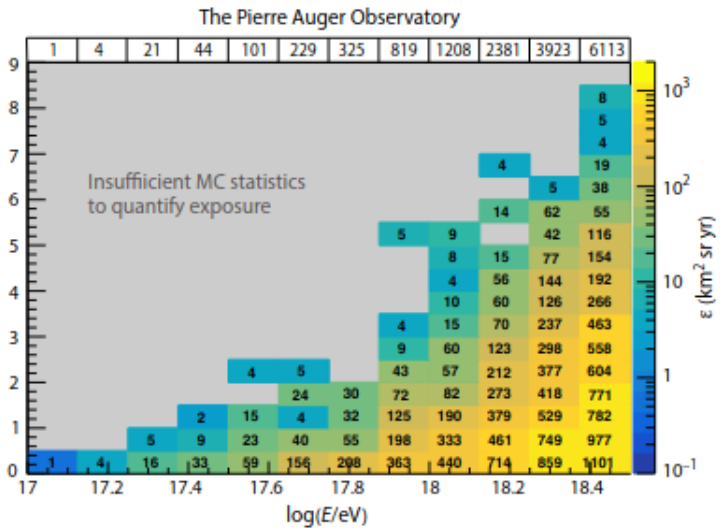

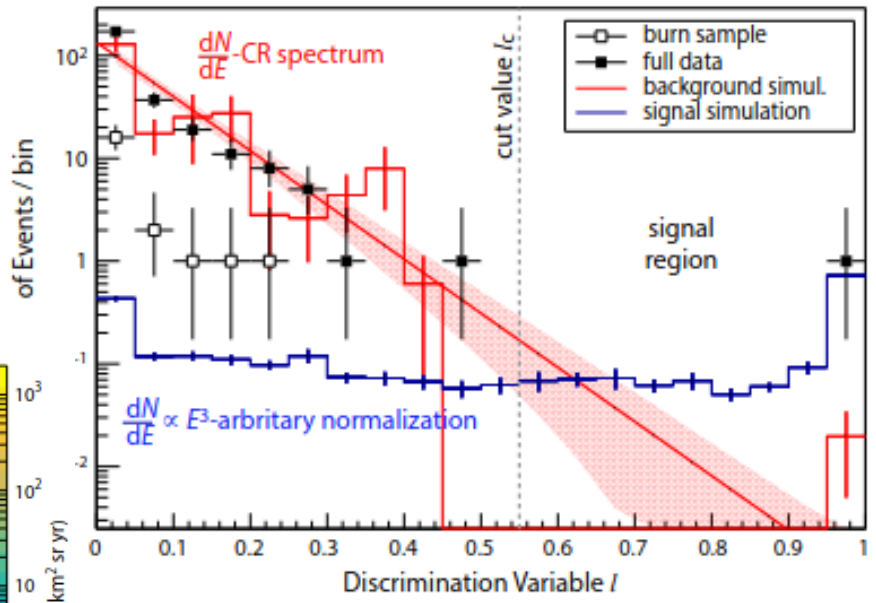

1 candidate consistent with the background (~0.3)

Tau scenarios and BSM constrained (modified deep inelastic cross-sections)

Search for neutrinos using the FD detector

PoS(ICRC2023)1095

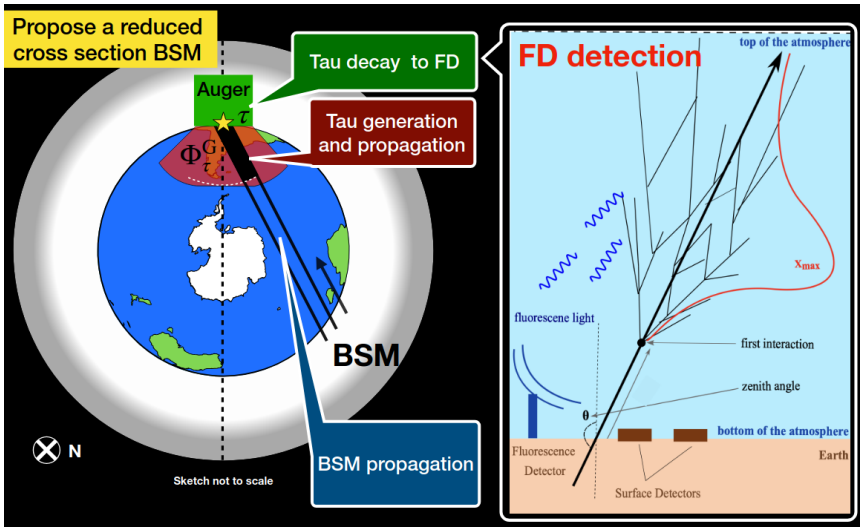

Upper limits for a specific tau scenario in the context of BSM

Best UL for 3% of the standard cross section

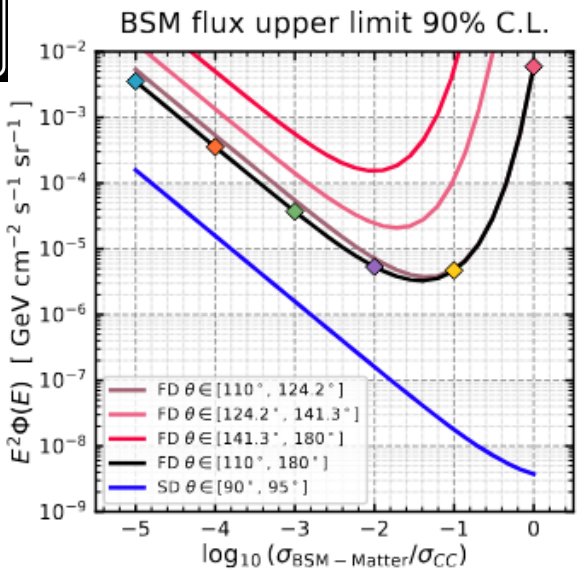

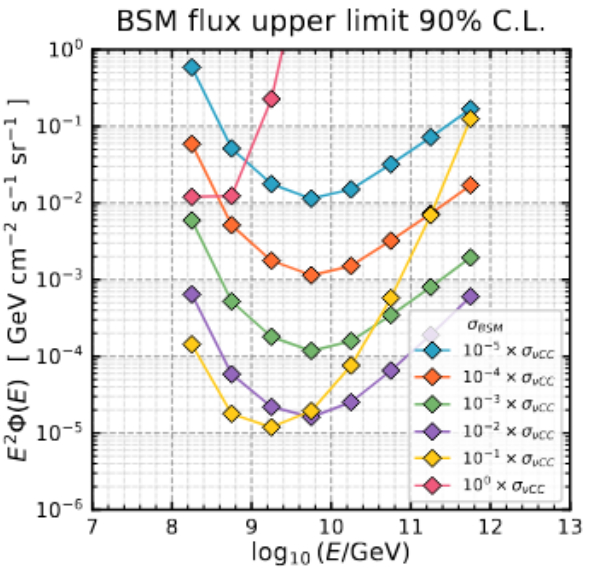

FD: best upper limits for a modified deep inelastic cross-section of about 3% of the standard charge current

FD: zenith > 110°
SD: 90°<zenith<95°
→ complementary in zenith

proton-air cross-section

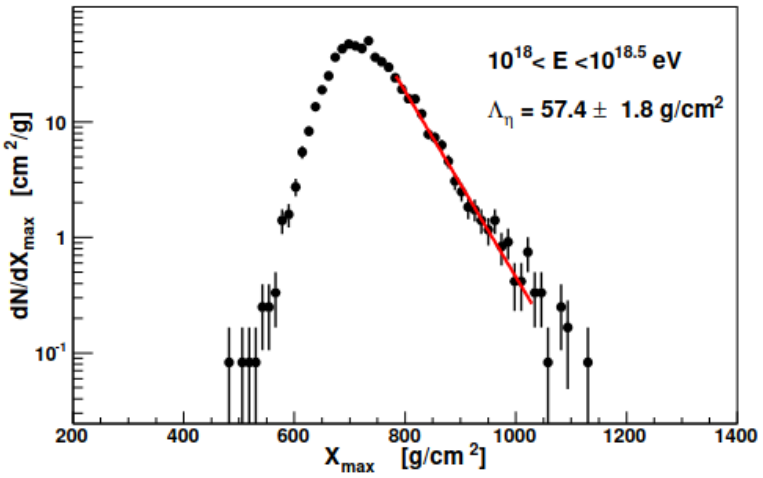

Fit to the tail of the Xmax distribution and converting into cross-section using simulations

- depends on composition

- depends on model

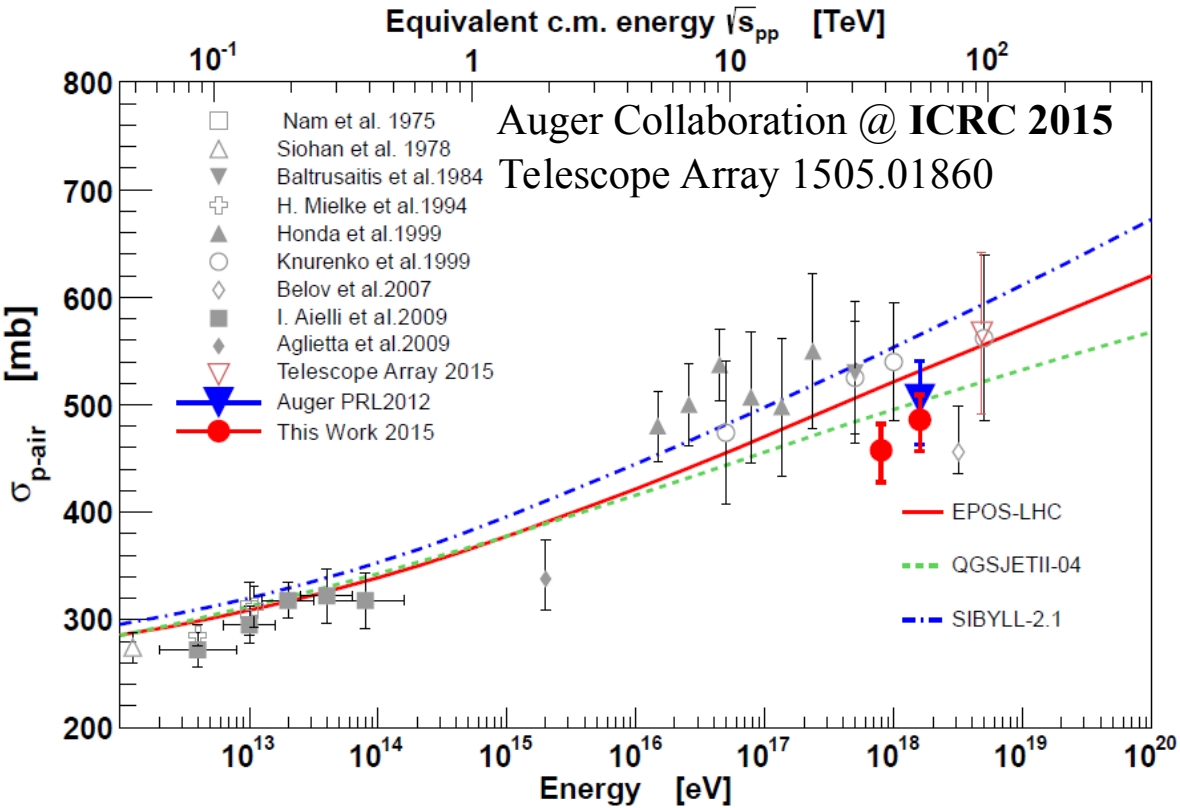

Lower energy [457 ± 18(stat)+19/-25(syst)] mb
Higher energy [486 ± 16(stat)+19/-25(syst)] mb

AugerPrime 2025→ 2035

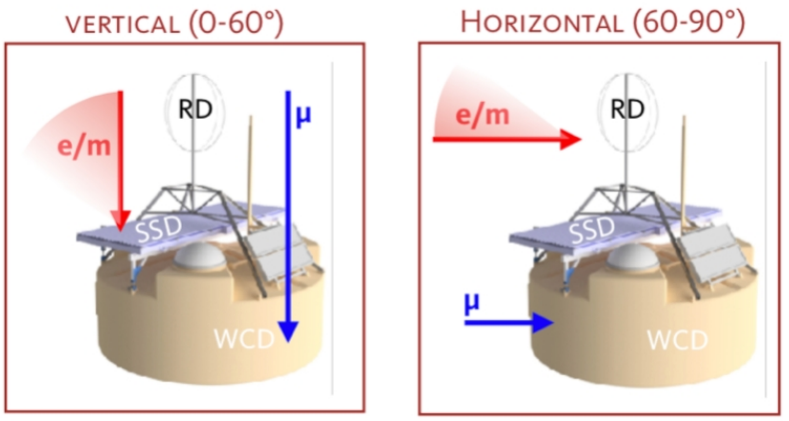

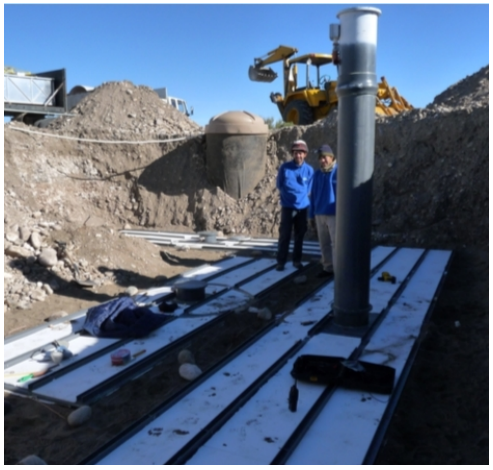

Multi-hybrid measurements

scintillator layers added on top of WCD
→ better separation electromagnetic/muonic
faster electronics
→ improve on signal characterization, higher sensitivity
low gain PMTs added
→ measurement closer to shower axis
radio antennas
→ horizontal events
muon detectors in infill area (installed 75%)
→ direct measurement

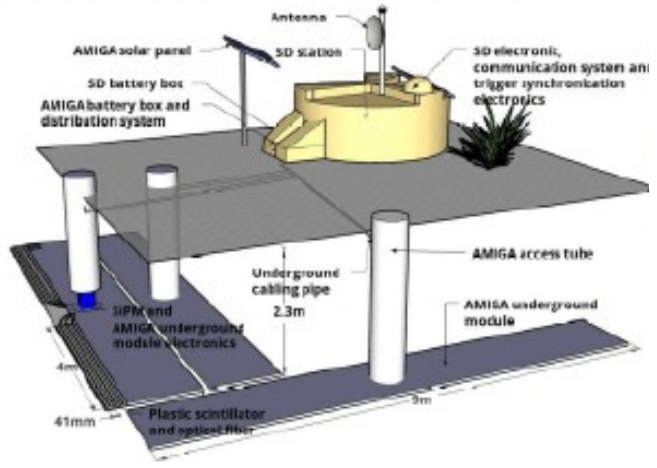

RADIO Detection of cosmic rays is a mature technique!

AERA engineering array placed at the Pierre Auger Observatory

→ electromagnetic component of EAS
→ Xmax measurement
Phys. Rev. Lett. 132 (2024)

AugerPrime include radio antenna on the entire array!

→ inclined events

GRAND → Future 10.000 km² !

A look into the future for UHECRs

EPJ Web of Conferences 283, 01001 (2023)

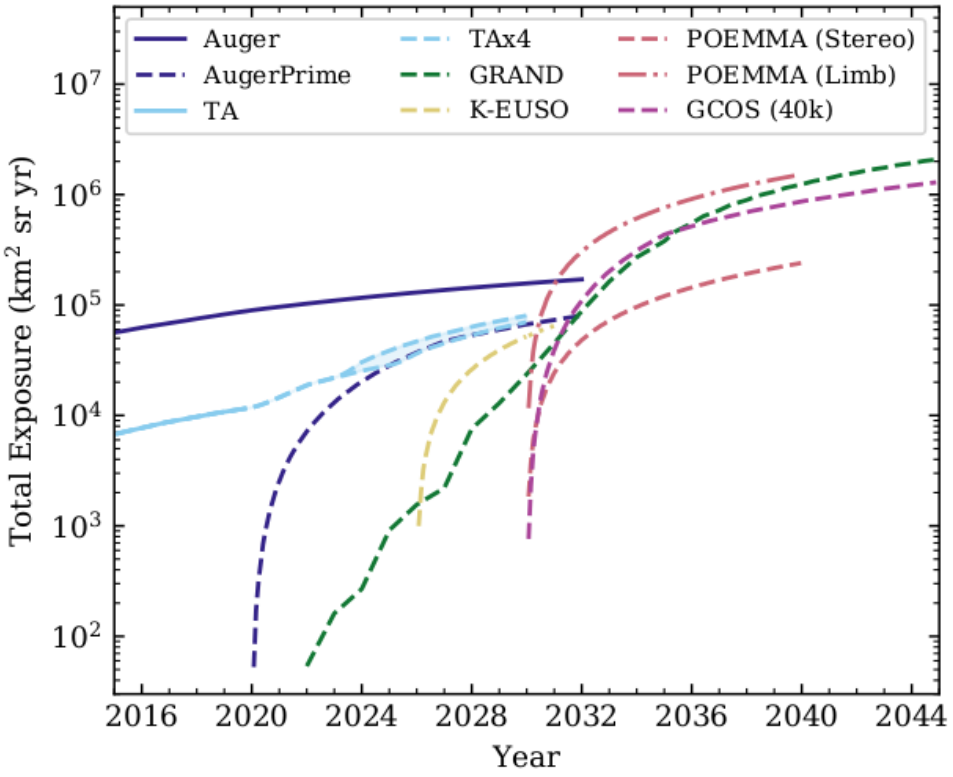

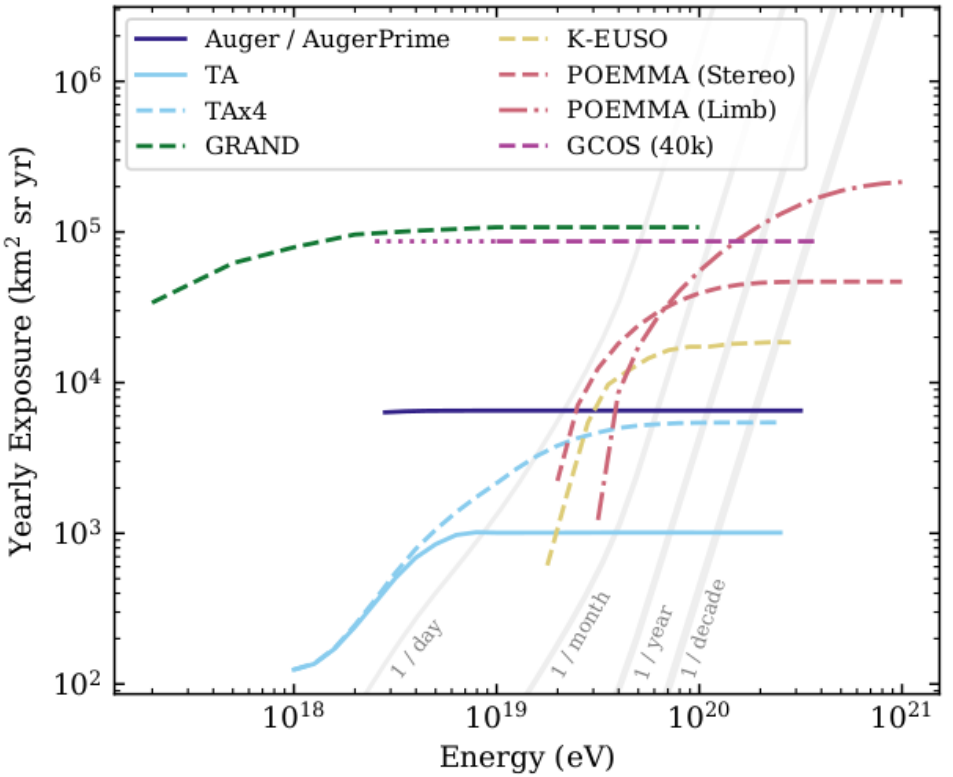

Pierre Auger Observatory Open Data

March 2024 release

https://opendata.auger.org

doi 10.5281/zenodo.4487613

10% cosmic ray data → 30% at the end of 2024
100% atmospheric data

Close to raw data and higher level reconstruction

Surface and Fluorescence Detectors

JSON and summary CSV files

Python code for data analysis

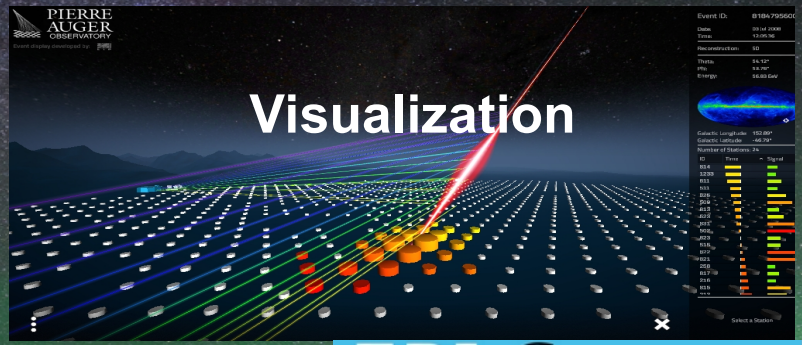

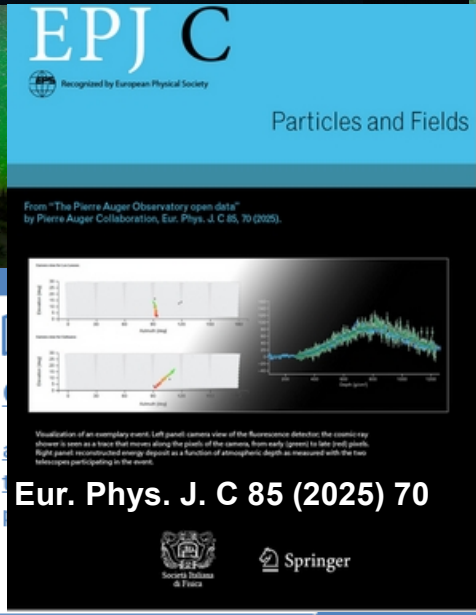

Datasets

the released datasets and their complementary data

Visualize

an online look at the released pseudo raw cosmic-ray data

Analyze

example analysis codes in online python notebooks to run on the datasets

Detecting cosmic rays and gammas: particle detector arrays and IACT

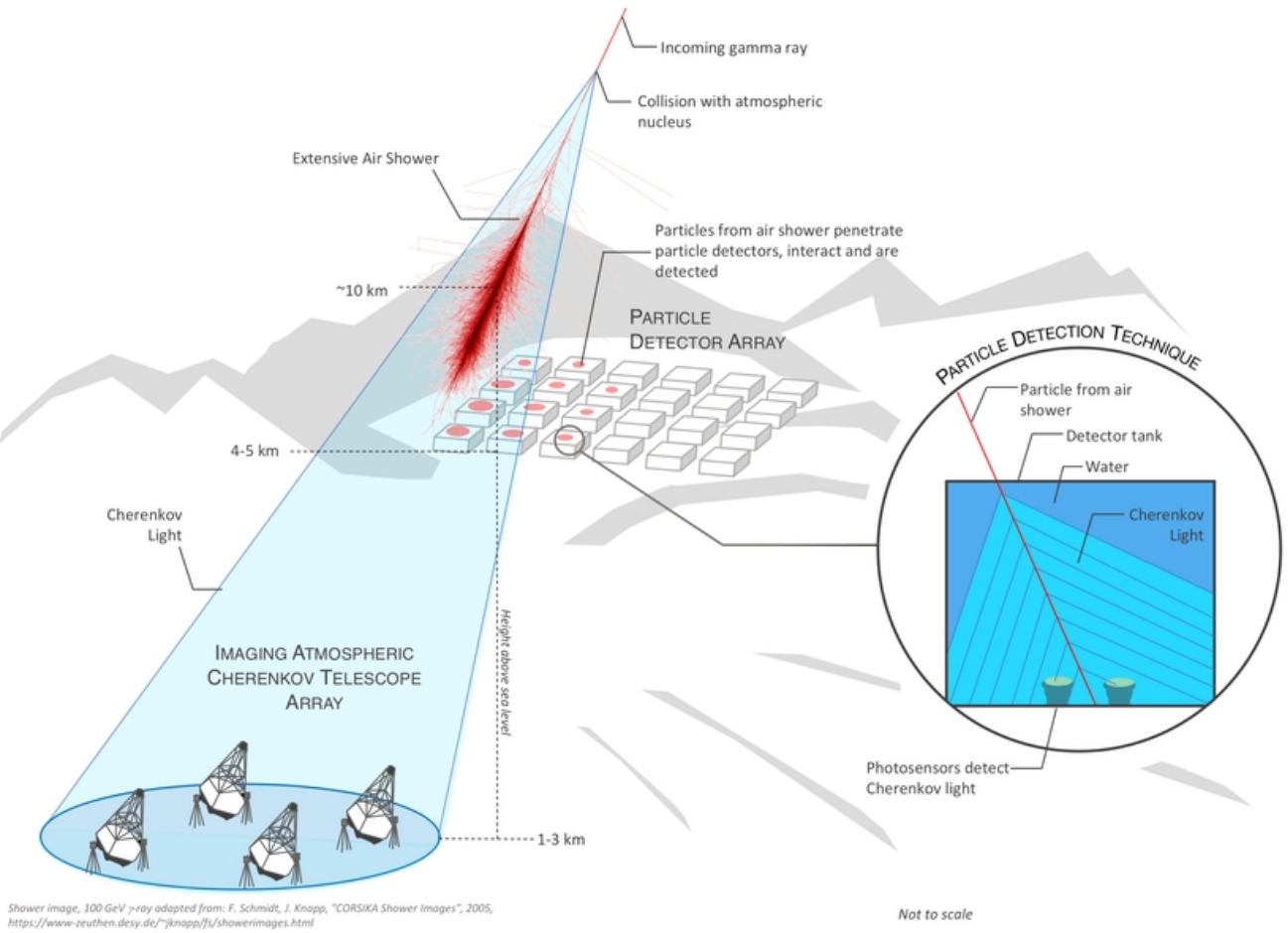

EAS-array
Extensive Air Shower arrays

IACT → Imaging Atmospheric Cherenkov Telescopes

→ complementary techniques

	IACT	EAS Arrays
Field of view	3°-10°	90°
Duty Cycle	10% - 30%	>95%
Energy range	30 GeV - >300 TeV	500 GeV – PeV
Angular resolution	0.05° – 0.02°	0.4° – 0.1°
Energy resolution	≈10%	60% - 20%
Background rejection	>95%	90% - 99.8%

EAS-array
→ large field of view ~2 sr
100% duty cycle
IACT
→ high sensitivity for point-like source
excellent angular resolution

Gamma and CR ground telescopes/array world map

Large High Altitude Air Shower Observatory (LHAASO)

Three detectors
WCDA
KM2A
WFCTA

4400 m asl

Energy 0.1 TeV – 1000 PeV

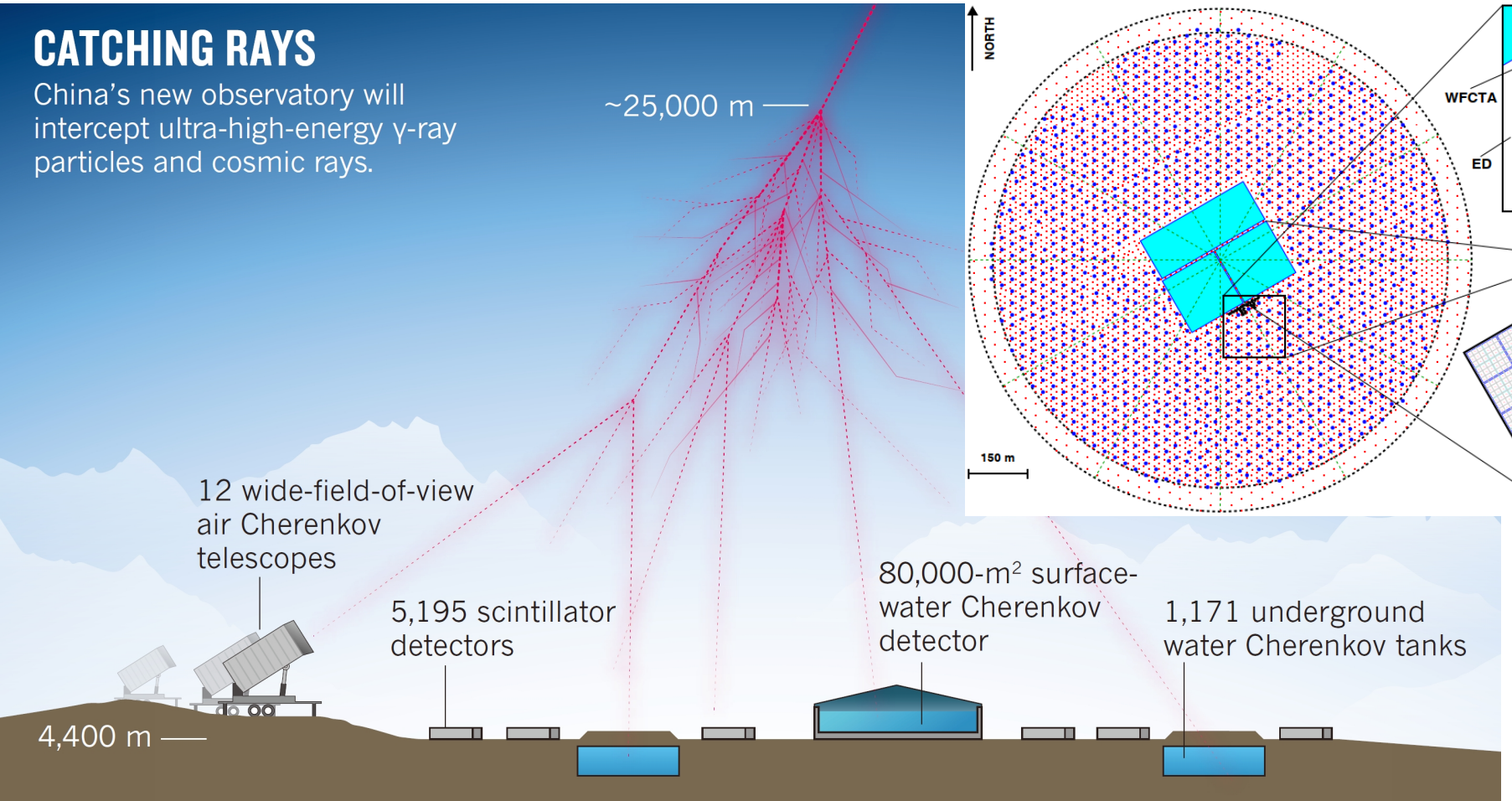

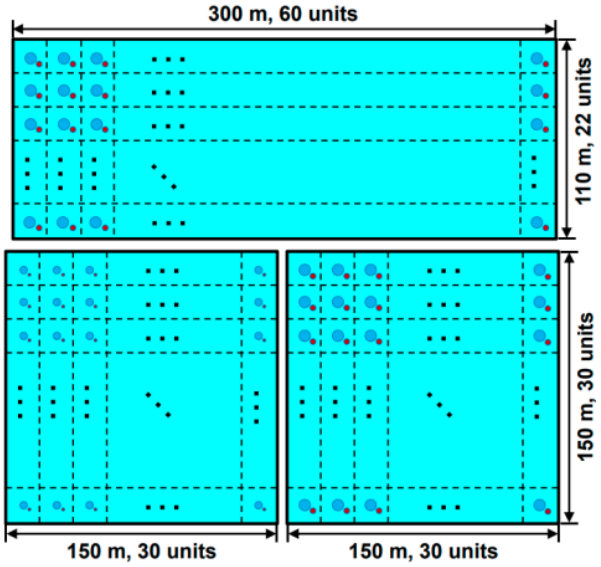

WCDA Water Cherenkov Detector Array

3 ponds, total area of 78000 m^2
→ water depth 4.5 m
→ 3120 units 5x5 m^2
2 PMTs (20''+3''or 8''+1.5''
Ethr = 100 GeV, 600 GeV)

Angular resolution: ~ 0.2°
Energy range 0.1 TeV – 10 PeV
Energy resol. < 20%
γ/hadron → compactness

KM2A
square kilometer array
(1km^2 + 0.3km 2 external ring)
Electromagnetic Detector (ED)
→ 1 m^2 x 5195
Muon Detector (MD)
→ 36 m^2 x1188

Energy range 10 TeV – 100 PeV
γ/hadron → muon content

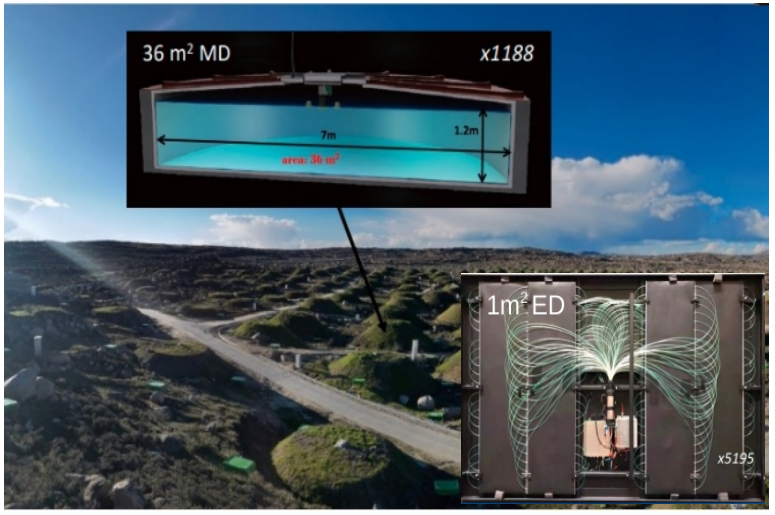

WFCTA Wide Field of view Cherenkov Telescope Array
18 telescopes, near WCDA
→ 32 × 32 SiPMs array
→ fov 0.5°× 0.5° for pixel and
→ total fov 16°× 16°

Energy range 10 TeV -100 PeV

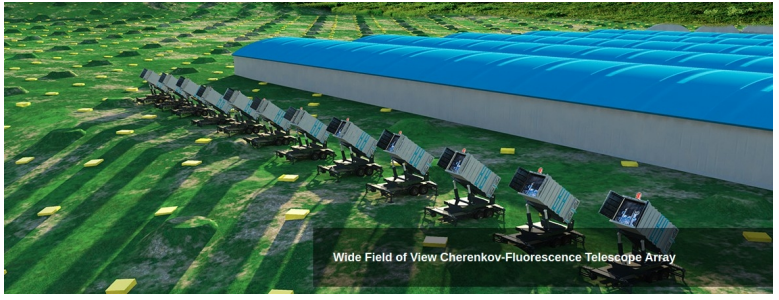

KM2A → 99.4% duty cycle and event rate 2x10^8 /day
WCDA → 98.4% and event rate 3x10^9 /day
WFCTA → >1400 hrs and number of matched events ~70 million

Ultrahigh-energy photons up to 1.4 petaelectronvolts from 12 γ-ray Galactic sources

Nature | Vol 594 | 3 June 2021

KM2A
12 gamma rays above 100 TeV > 7 σ

Set a precedent!

Indication of hadronic processes

crab →

1.4 PeV →

Table 1 | UHE γ-ray sources

Source name	RA (°)	dec. (°)	Significance above 100 TeV (×σ)	E_{max} (PeV)	Flux at 100 TeV (CU)
LHAASO J0534+2202	83.55	22.05	17.8	0.88 ± 0.11	1.00(0.14)
LHAASO J1825-1326	276.45	−13.45	16.4	0.42 ± 0.16	3.57(0.52)
LHAASO J1839-0545	279.95	−5.75	7.7	0.21 ± 0.05	0.70(0.18)
LHAASO J1843-0338	280.75	−3.65	8.5	$0.26^{+0.16}_{-0.10}$	0.73(0.17)
LHAASO J1849-0003	282.35	−0.05	10.4	0.35 ± 0.07	0.74(0.15)
LHAASO J1908+0621	287.05	6.35	17.2	0.44 ± 0.05	1.36(0.18)
LHAASO J1929+1745	292.25	17.75	7.4	$0.71^{+0.16}_{-0.07}$	0.38(0.09)
LHAASO J1956+2845	299.05	28.75	7.4	0.42 ± 0.03	0.41(0.09)
LHAASO J2018+3651	304.75	36.85	10.4	0.27 ± 0.02	0.50(0.10)
LHAASO J2032+4102	308.05	41.05	10.5	1.42 ± 0.13	0.54(0.10)
LHAASO J2108+5157	317.15	51.95	8.3	0.43 ± 0.05	0.38(0.09)
LHAASO J2226+6057	336.75	60.95	13.6	0.57 ± 0.19	1.05(0.16)

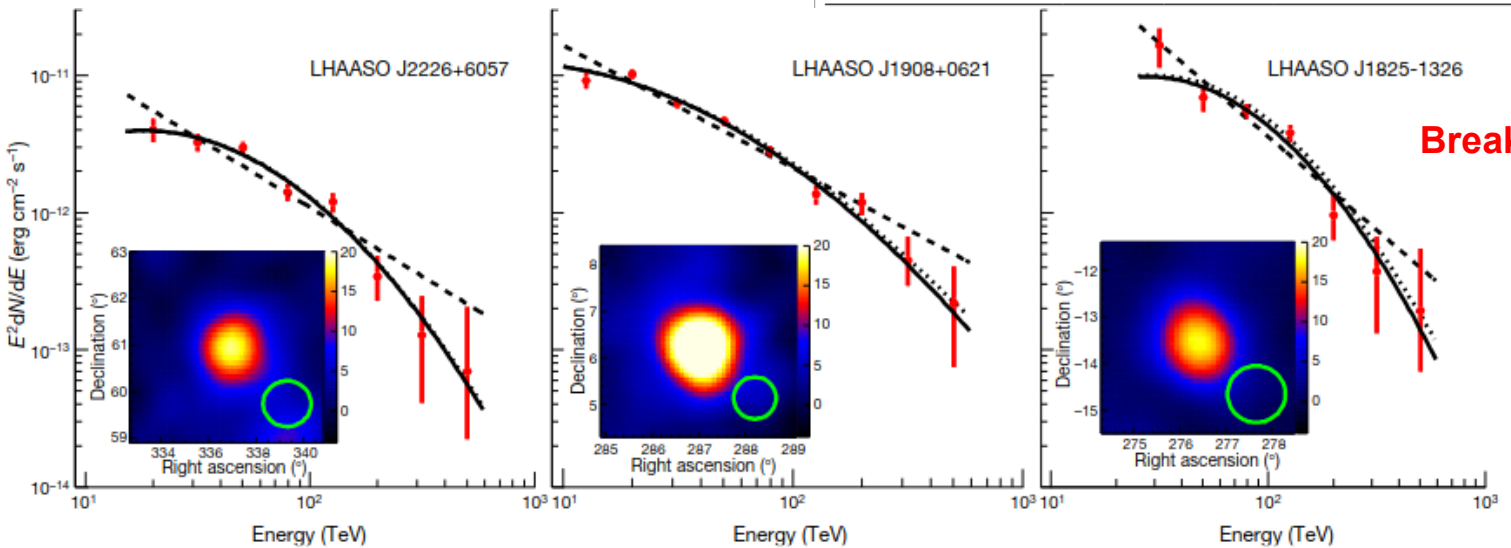

Breakthrough for the field!

LHAASO J2032+4102
Max Energy 1.4 PeV

Close to the Cygnus Cocoon that surrounds Cygnus OB2

→ evidence of the operation of massive stars as hadronic PeVatrons.

→ leptonic (inverse Compton) origin of radiation unlikely because of the lack of brightening of the γ-ray image towards Cygnus OB2.

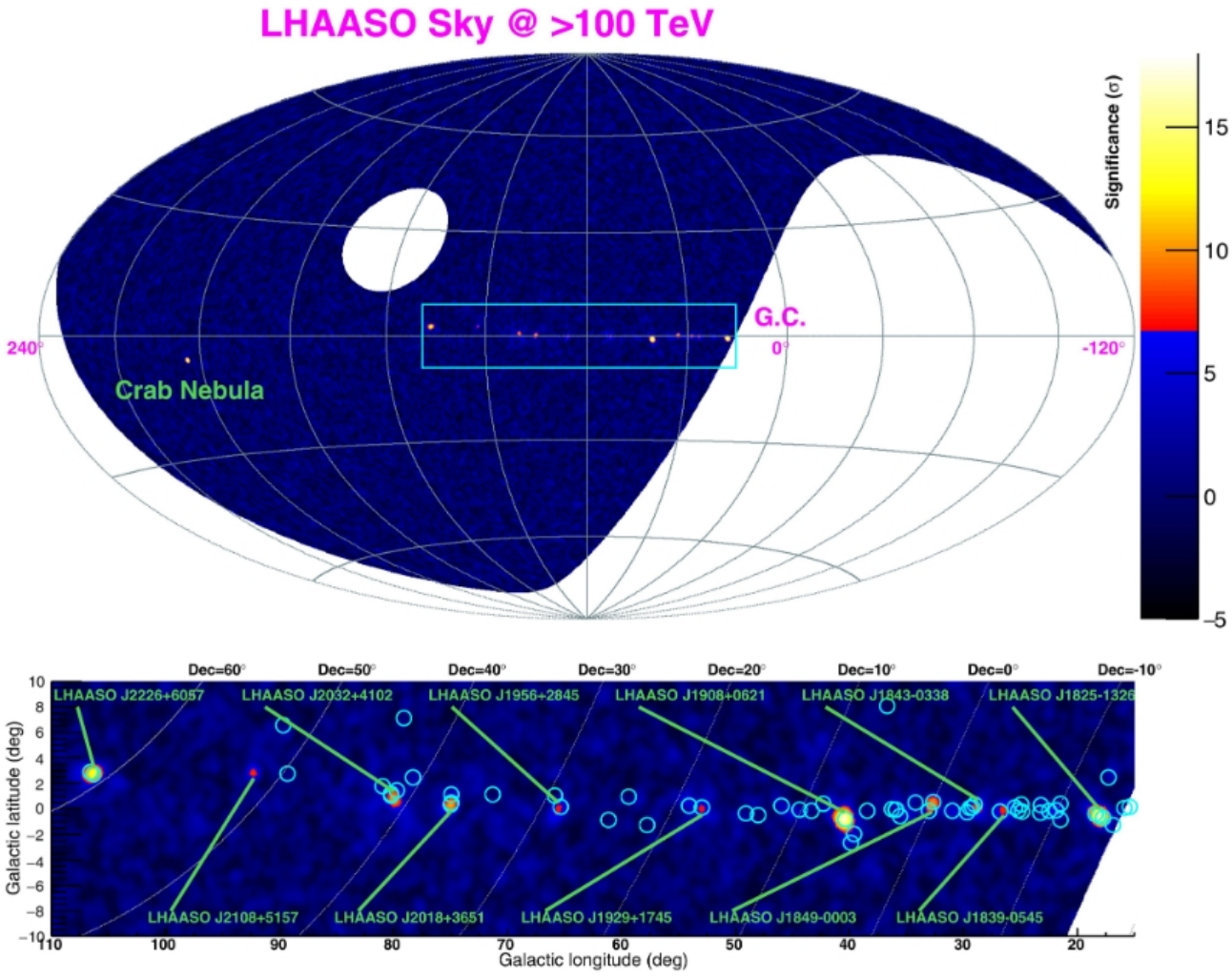

All particle spectrum and <ln(A)> between 0.3 and 30 PeV

KM2A (ED and MD), 10°<zenith<30° 1.2 years

Phys. Rev Lett 132, 131002 (2024)

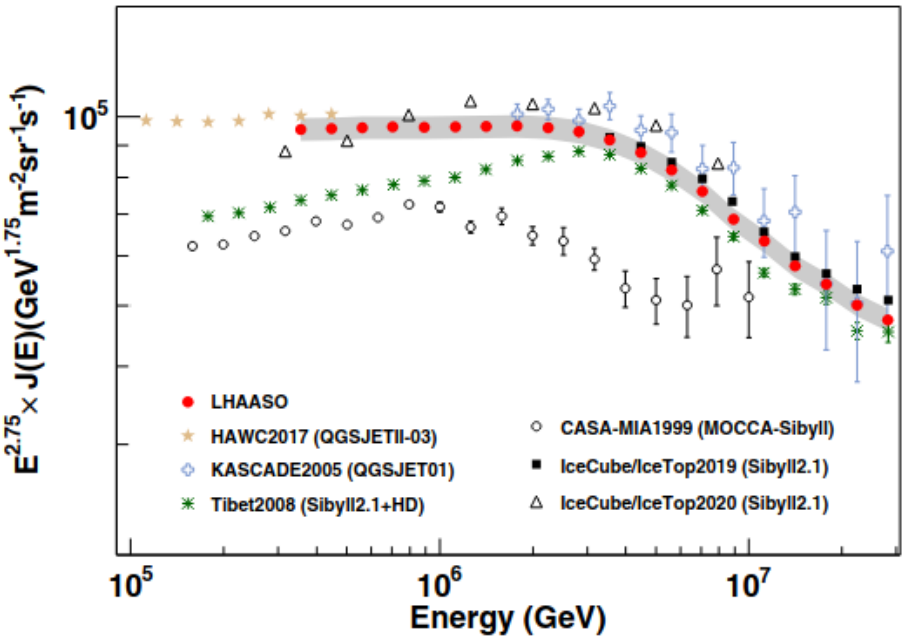

knee 3.67 ± 0.05 PeV
spectral index change from -2.74 to -3.12

Slight decrease of the <ln(A)> before the knee, then increase

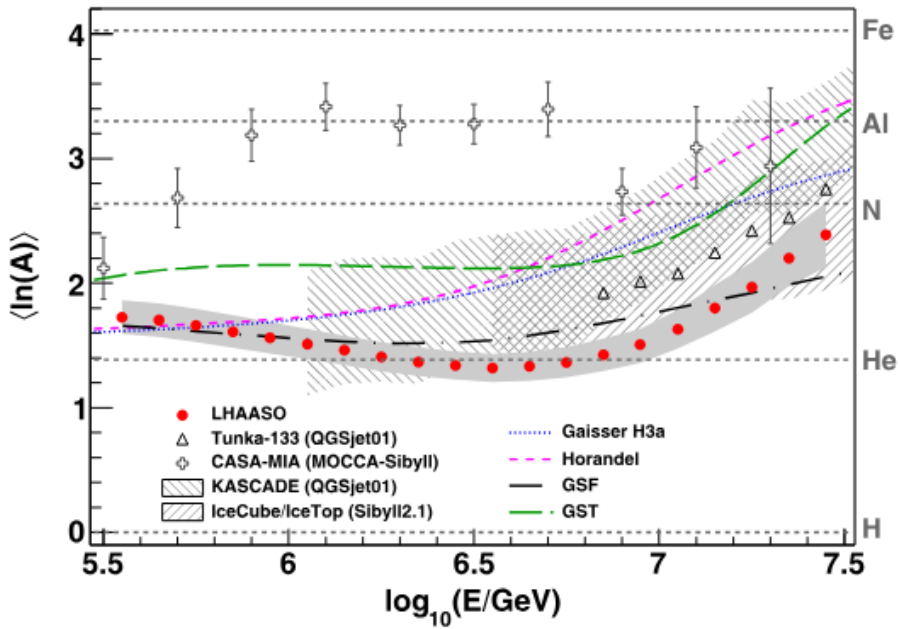

Correlation with an evolution of mass composition

High Altitude Water Cherenkov (HAWC) detector

Pico de Orizaba
5636

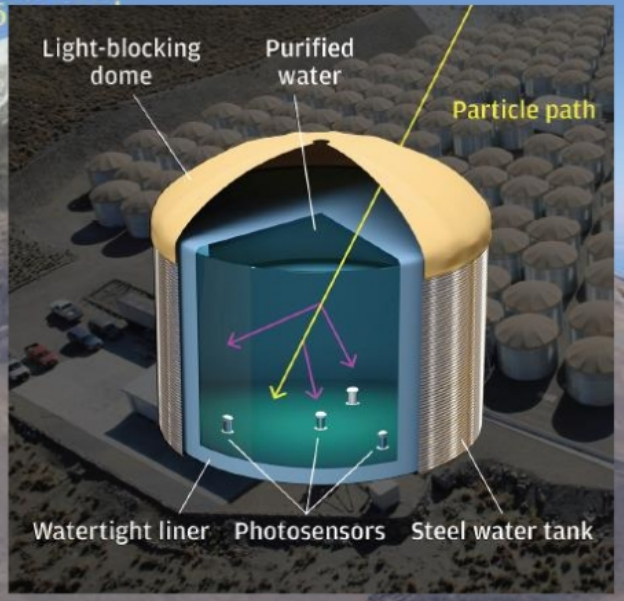

FoV: ~2 sr

Sierra Negra
Alfonso Serrano
Large Millimetric Telescope
4640 m a.s.l.

HAWC
4100 m a.s.l.

~24000 m^2

- 300 close-packed optically isolated water Cherenkov detectors
- Full detector inaugurated March 2015
- Funding from a combination of US and Mexican agencies
- High energy extension: Outrigger array, since summer 2018
- Takes data with >95 on time
- ~5 trillion triggers to date - 7PB of data

Sierra Negra Volcano (Mexico)
◎ 4100 m a.s.l.
◎ Operating since 2016
◎ Water Cherenkov Detectors
→ Inner 300 tanks 7m (d) 4.5m (h)
→ 4 PMT/tank
→ ≈ 22000 m^2
→ Outer 350 tanks 1.5m (d) 1.4m (h)
→ 1 PMT/tank

HAWC
High Altitude Water Cherenkov
Gamma-Ray Observatory

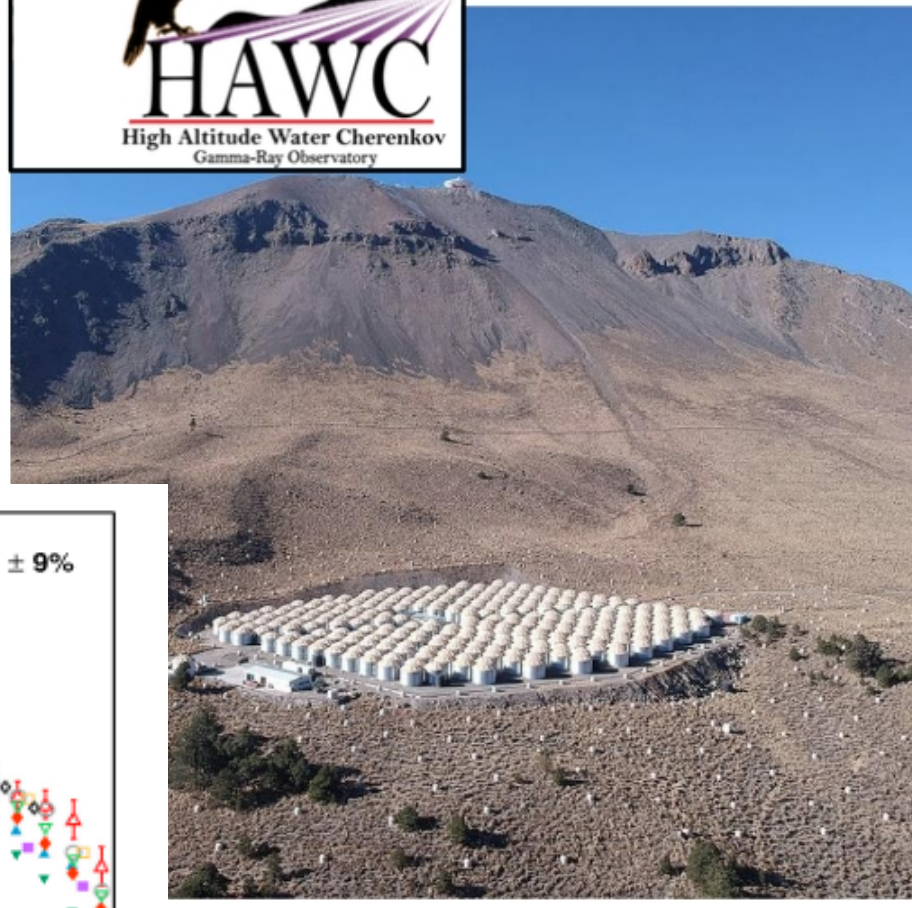

Astropart. Phys 167 (2025) 103077

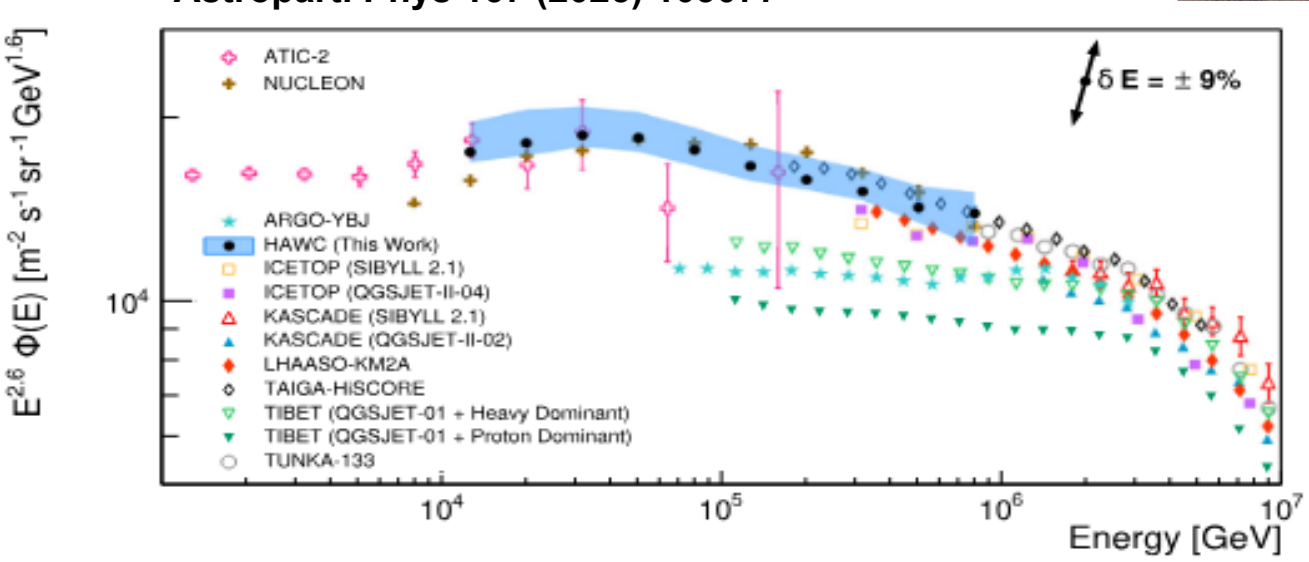

The SWGO experiment: a wide field of view observatory exploring the Southern hemisphere between 100 GeV and 10 PeV

- HAWC + SWGO
  → full sky coverage

- SWGO:
  → Southern sky (GC)

- Area ~ LHAASO KM2A

- Complementary to CTA-South

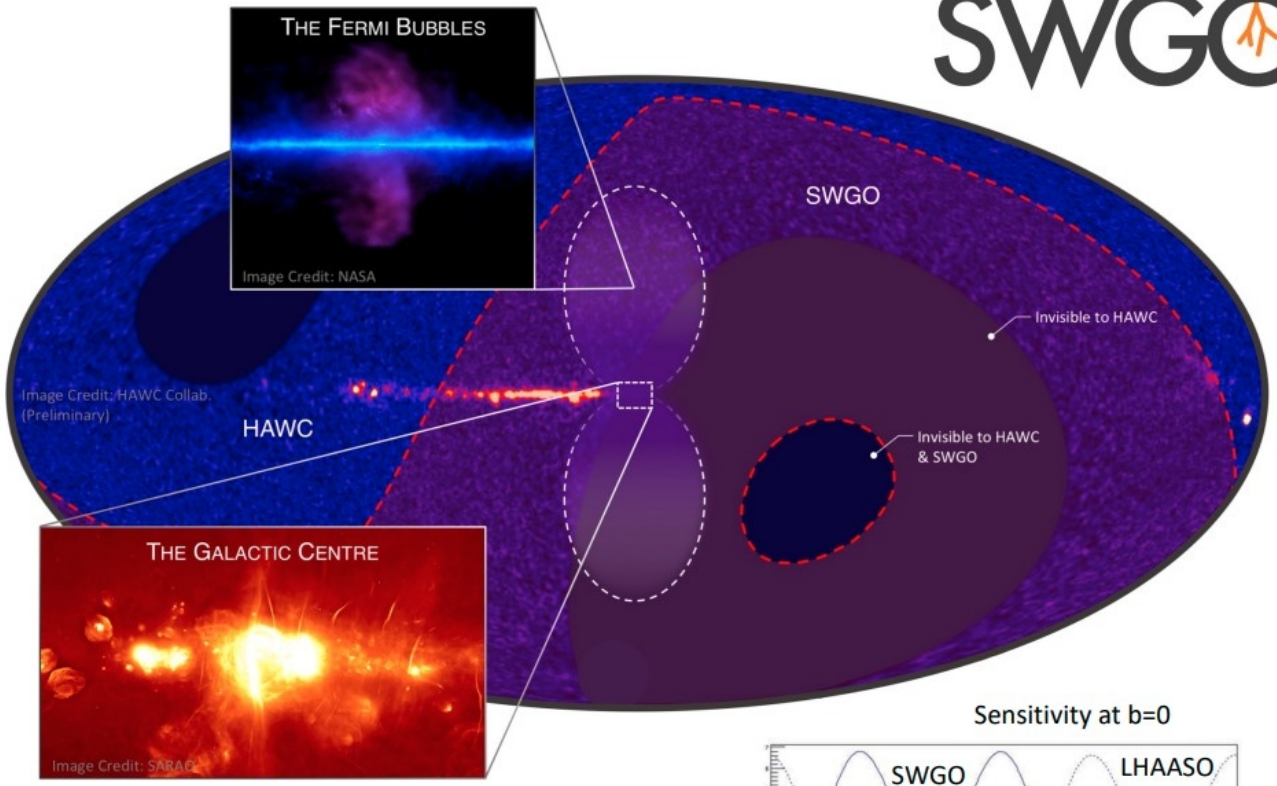

The site: Atacama Astronomical Park

- 4770 a.s.l.
- 23˚ South, 68˚ West

50 Km from San Pedro de Atacama (2400 a.s.l.)
1.5 hour from the closest airport

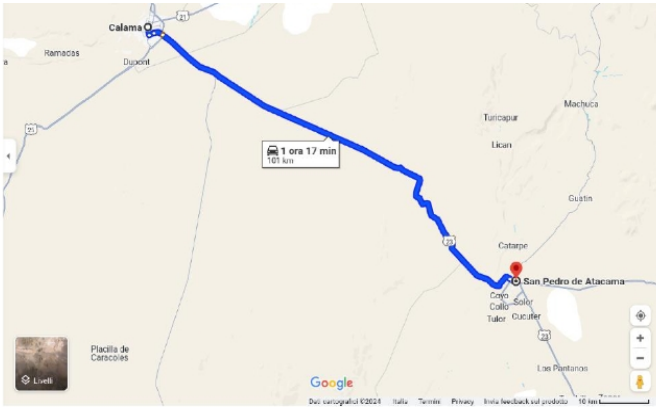

Water transported from Calama (1.5 h)

IACT: Imaging Atmospheric Cherenkov Telescopes

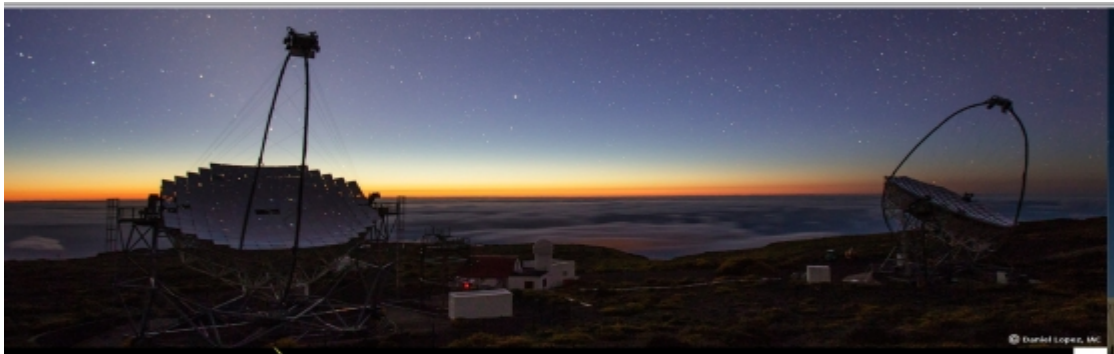

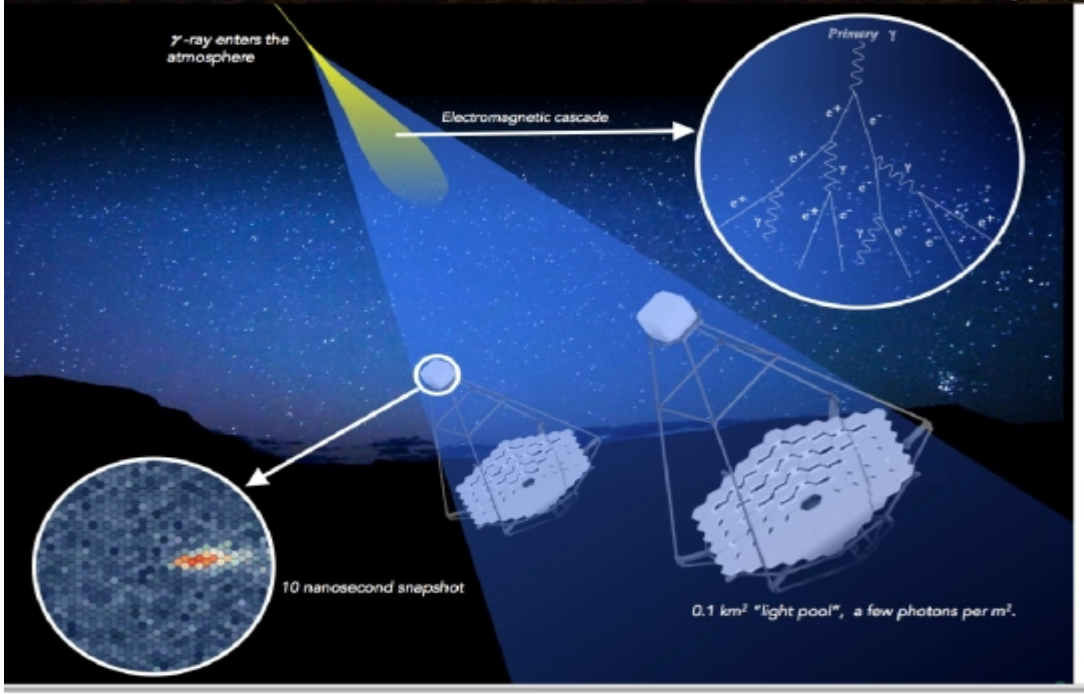

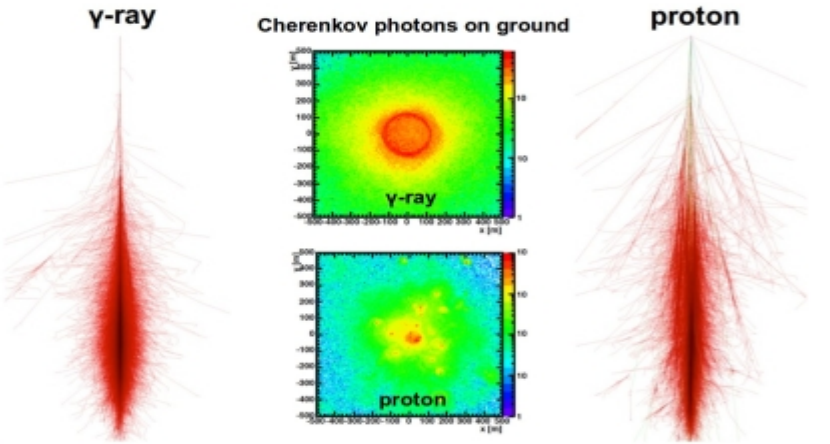

MAGIC

Major **A**tmospheric **G**amma-ray
Imaging **C**herenkov Telescopes

La Palma (28° N),
Canary Islands, Spain. 2200 m a.s.l.

Stereo system of 2 telescopes
→ 17m diameter
→ 1039 PMTs. FoV = 3.5°
Angular res <0.08°
Energy res.: 15-25%
Fast repositioning 25 s
Energy range: 30 GeV – 100 TeV

- astrophysics
  Steady and transient sources

- fundamental physics
  Search for Gamma-Ray Spectral Lines from Dark Matter Annihilation up to 100 TeV toward the Galactic Center with MAGIC
  Phys Rev. Lett. 130, 061002 (2023)

MAGIC detection of GRB 201216C at z = 1.1

Hunt for fast transients continues
Record distance for IACT

arXiv:2310.06473v1

Also the “historical” observation of
GRB 190114C → **up to TeV!**

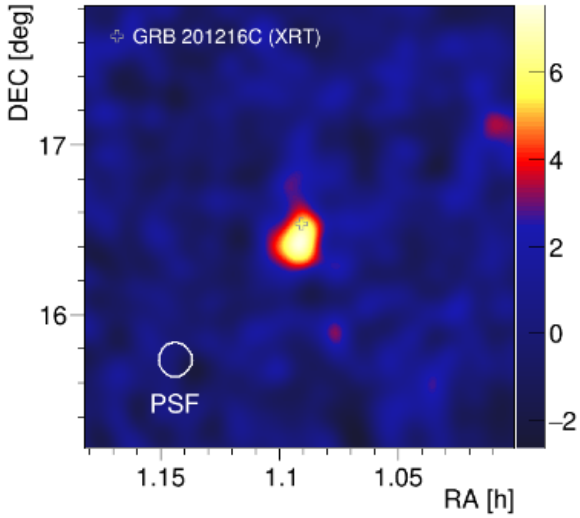

Emission above 70 GeV well described by SSC mechanism

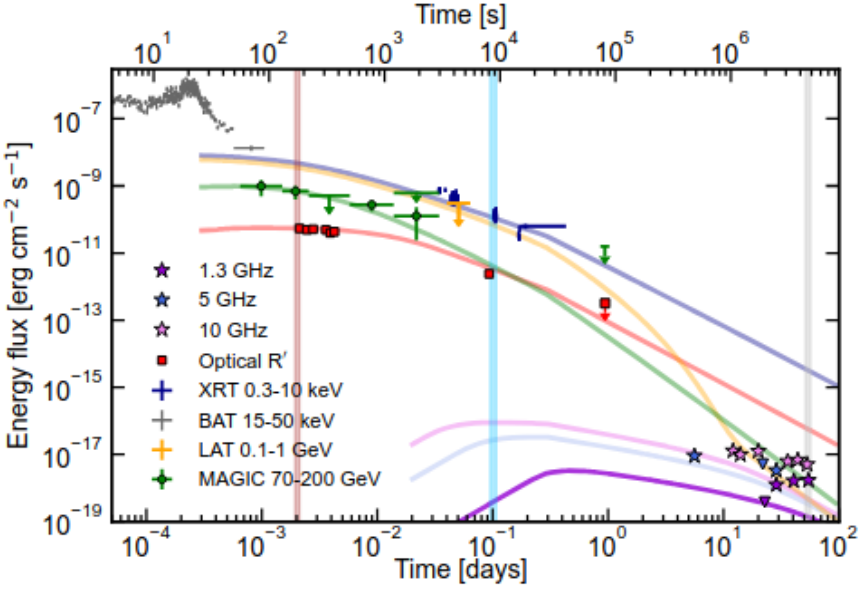

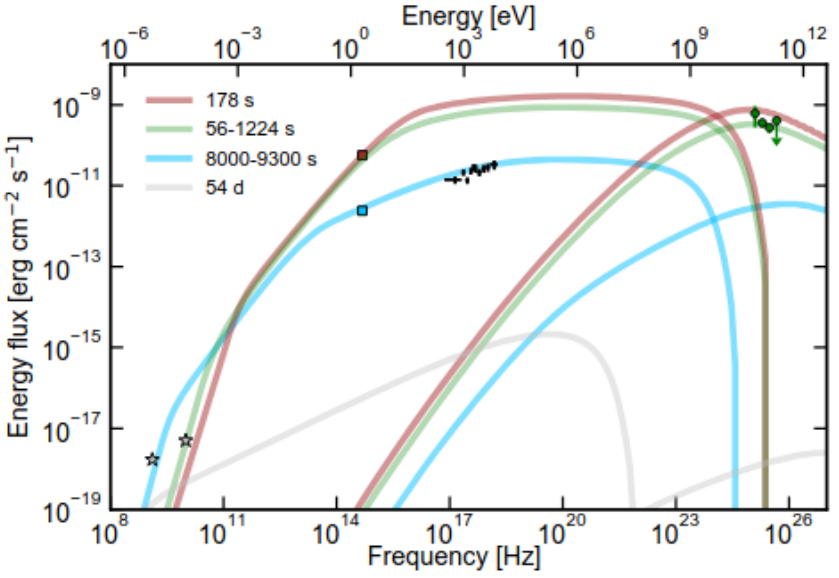

Layout of the CTAO array

North: low and mid energy range (20 GeV – 5 TeV)

→ extragalactic physics

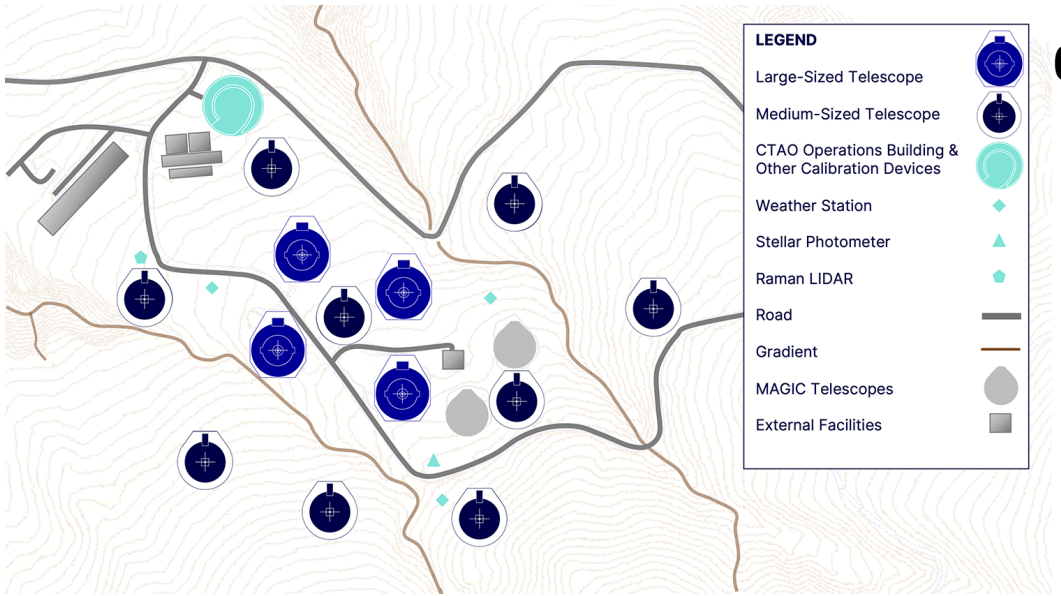

0.5 km²

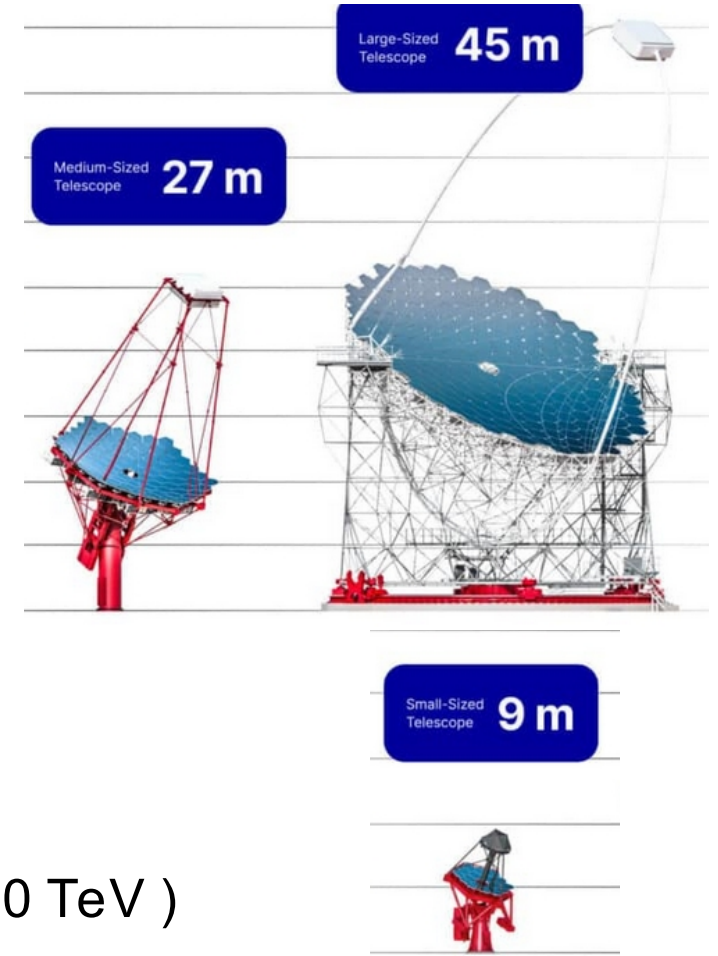

South: low mid and high energy range (20 GeV – 300 TeV)

CTAO:
array sites

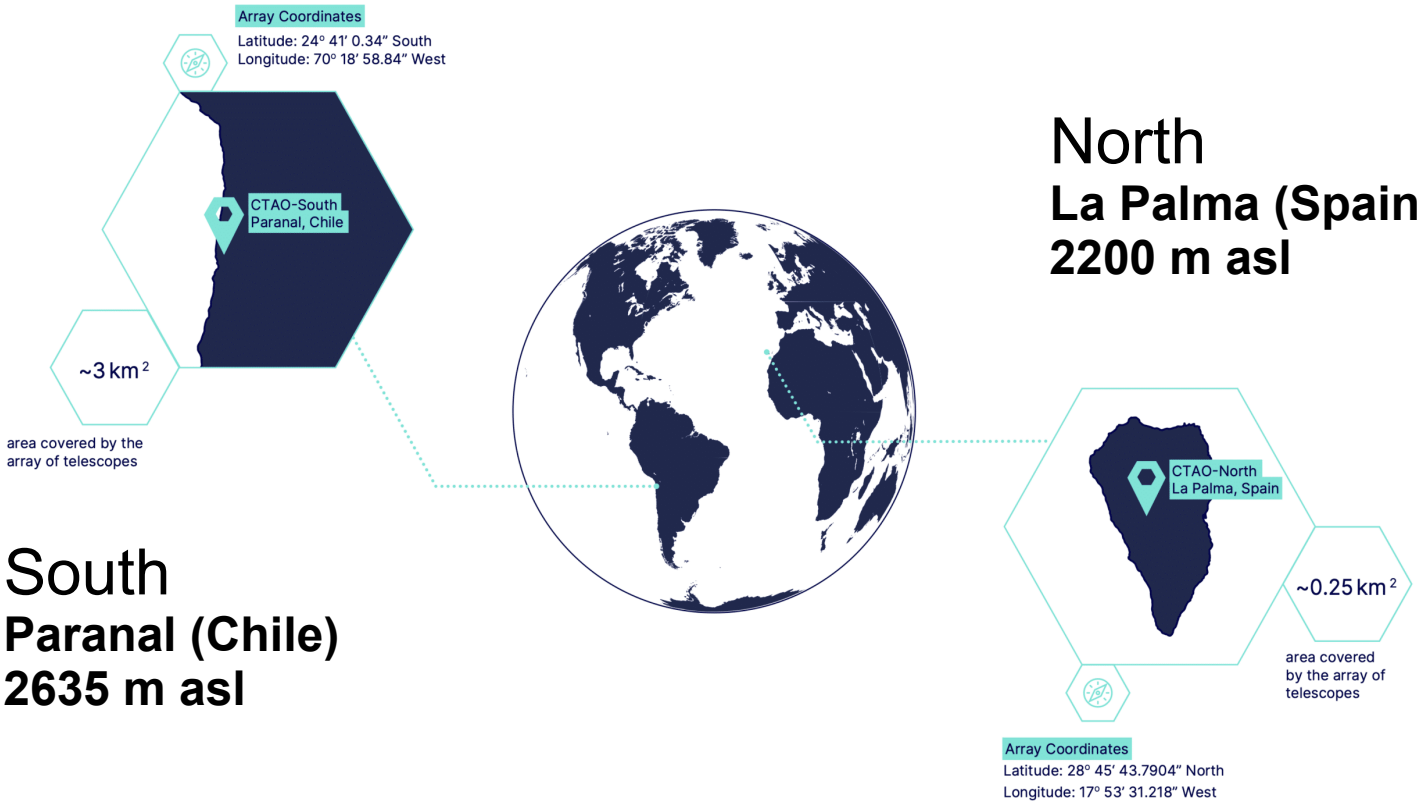

CTA sito Nord

Fall 2024

La Palma, Canary Islands
→ 2200 m a.s.l.

Largest telescope of the CTA

Camera:
→ 1855 PMTs (4.5° FoV)

Focal length of 28 m

Mirror area 400 m^2

Trigger threshold ~20 GeV
→ up to 300 GeV

Fast repositioning: 20s

LSTs:
CDR passed in Sept. 24

CTA: expected sensitivity

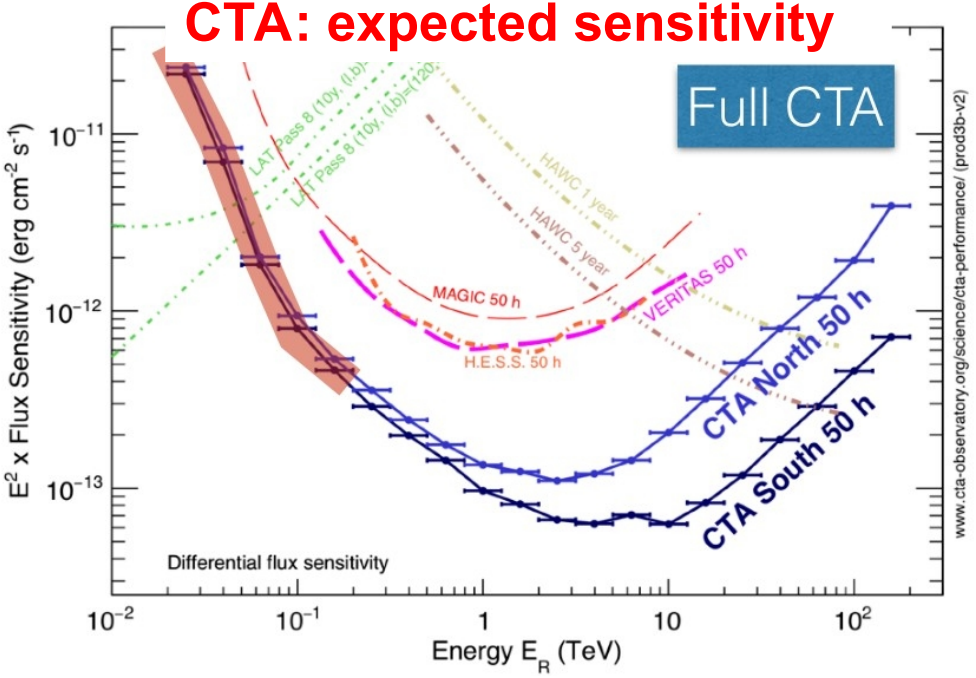

Instrument	energy range	Effective area (m^2)	sensitivity (milli-CU†)	energy resolution (%)	PSF (°)	FoV (sr)	duty cycle (%)
Fermi-LAT[a)]	20 MeV - 300 GeV	~ 0.95	10 - 30	8 - 18	0.15 - 3.5	~ 2.4	~ 60
H.E.S.S.[b)]	10 GeV - 50 TeV	$\sim 10^5$	~ 5	15	< 0.1	~ 0.03	$\sim$10
MAGIC[c)]	$\geq$ 30 GeV	$\sim 10^5$	~ 7	16	≤ 0.07	0.02	$\sim$18
VERITAS[d)]	50 GeV - 50 TeV	$\sim 10^5$	~ 5	10 - 15	0.08 - 0.13	0.02	10-14
CTA-LST1[e)]	20 GeV - 300 GeV	$\sim 10^4$	~ 10	10 - 30	0.05 - 0.1	0.02	$\sim$10
ASγ[f)]	10 TeV - 1 PeV	$\sim 7 \times 10^4$	~ 200	20 - 40	~ 0.8	~ 2.0	90
ARGO-YBJ[g)]	50 GeV - 10 TeV	$\sim 0.8 \times 10^4$	~ 300	>13	~ 0.5	~ 2.0	86
HAWC[h)]	100 GeV - 100 TeV	$\sim 3 \times 10^4$	~ 50	20 - 50	~ 0.69	> 1.5	95
LHAASO-WCDA[i)]	100 GeV - 20 TeV	$\sim 0.8 \times 10^5$	~ 12	$\sim$33	0.2 - 0.84	~ 2.0	95
LHAASO-KM2A[i)]	10 TeV - 4 PeV	$\sim 10^6$	~ 12	15 - 40	0.2 - 0.6	~ 2.0	95

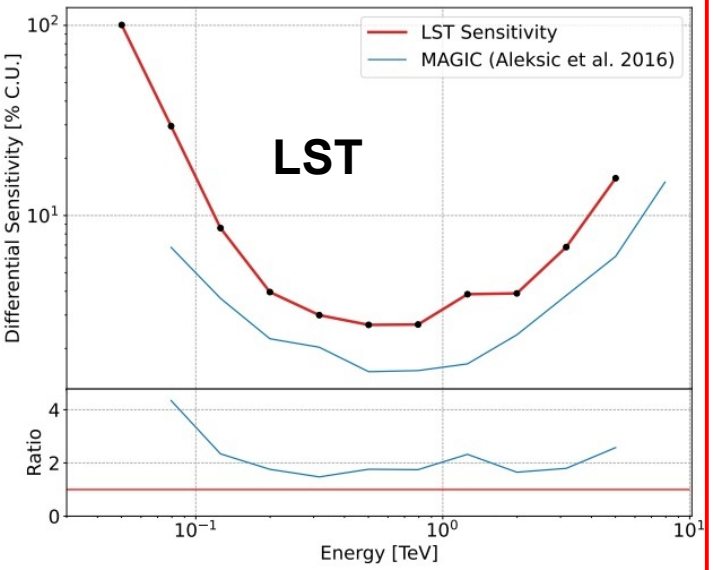

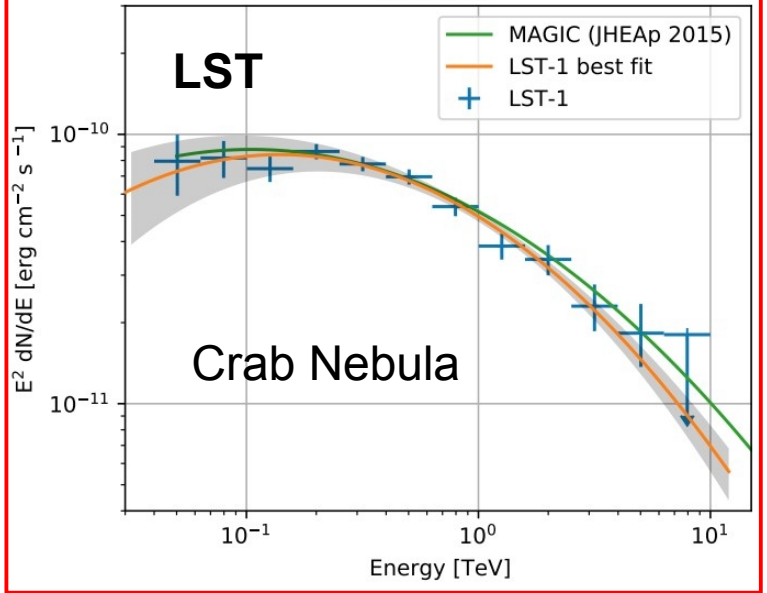

BACKUP

The Silicon TracKer (STK)

768 silicon sensors

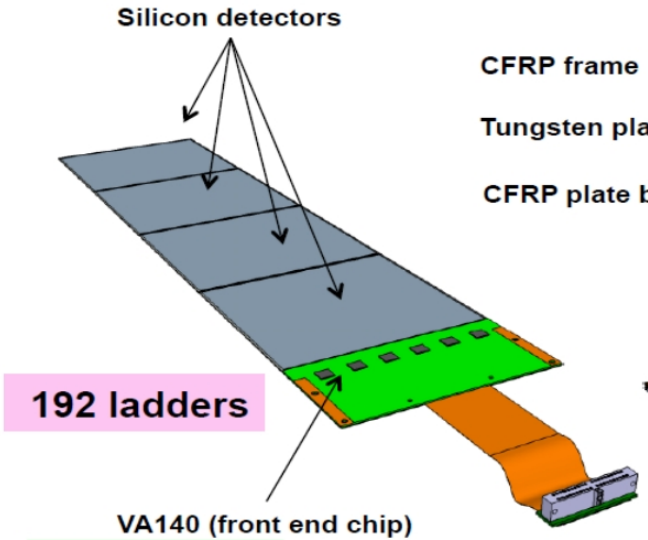

192 ladders

1152 ASICs

73728 channels

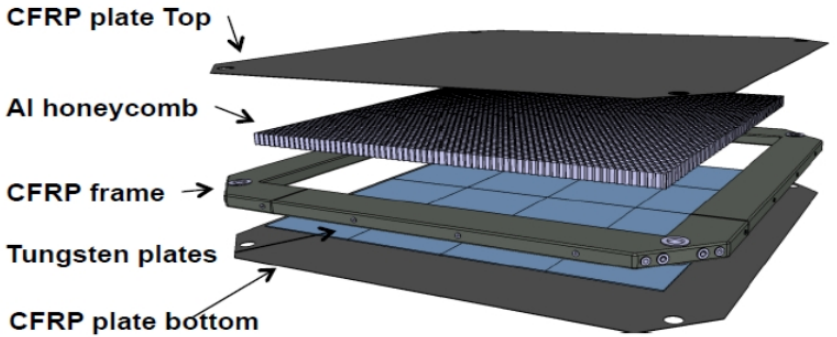

12 layers, 6-x and 6-y

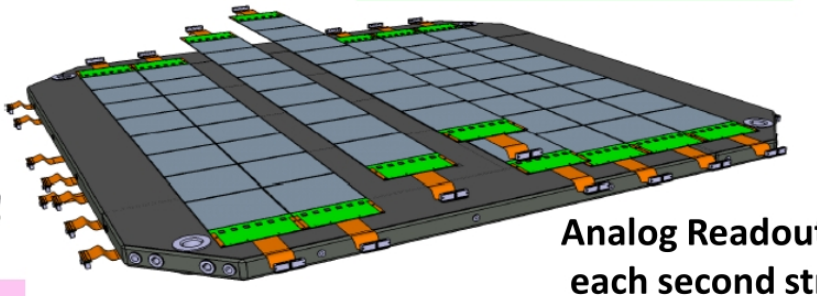

Analog Readout of each second strip:
384 channels / SSD- Ladder
Charge sharing

- 48 μm wide Si strips with 121 μm pitch
- (95 × 95 × 0.32 mm^3) Silicon Strip Detector (SSD)
- 768 strips in each SSD
- One ladder composed by 4 (SSD)
- 16 Ladders per layer (76 cm × 76 cm)
- 12 layers (6x + 6y)

The CALOrimeter

- **14 layers of 22 BGO bars**
  - 2.5×2.5×60 cm^3 bars
  - 14 hodoscopic stacking alternating orthogonal layers
  - depth ~32X_0
- **Two PMTs coupled with each BGO crystal bar at the two ends**
- **Electronics boards attached to each side of module**

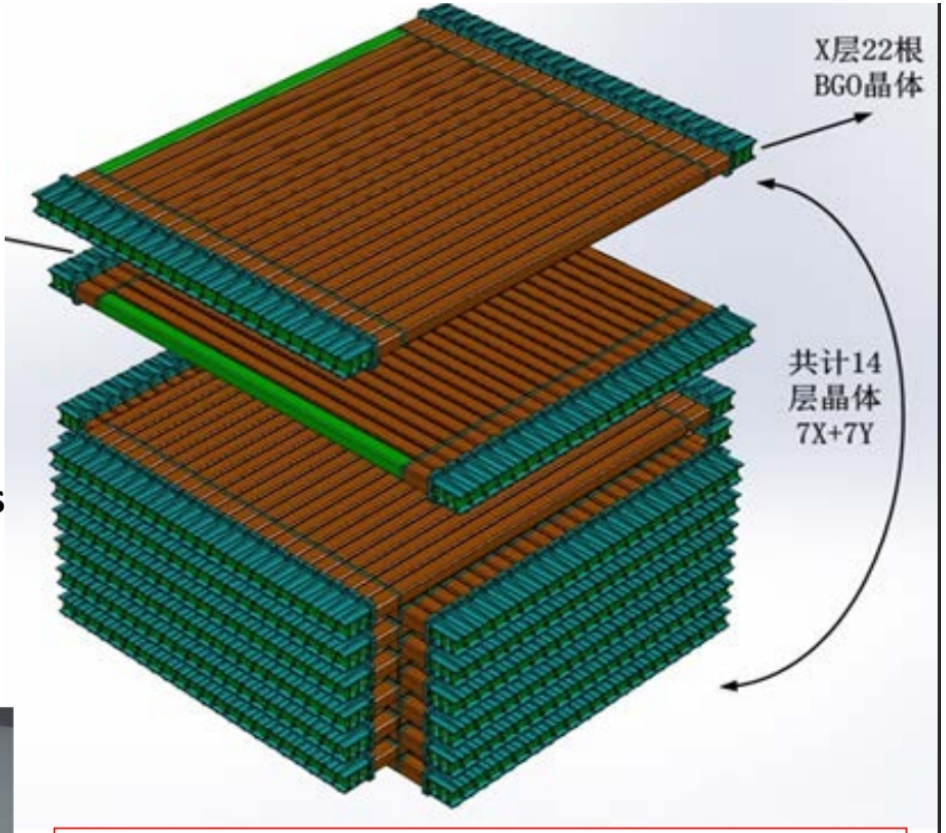

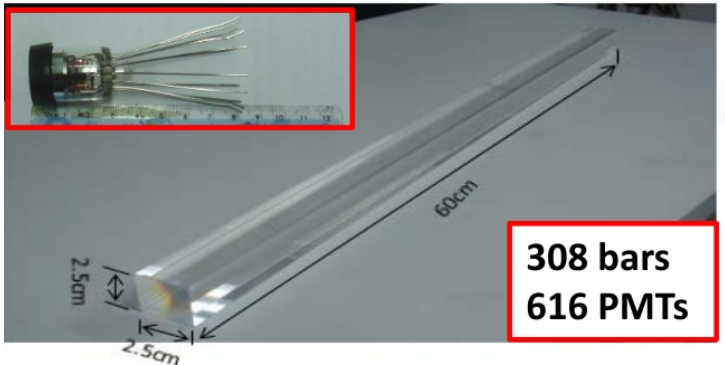

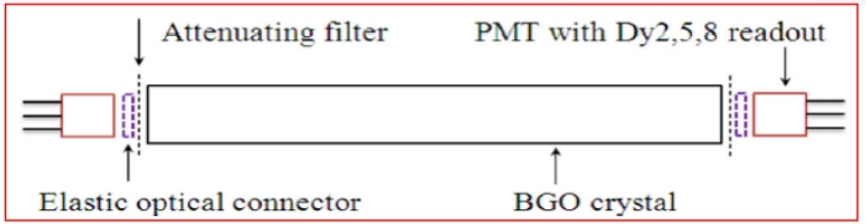

The Plastic Scintillator Detector and the NeUtron Detector

PSD

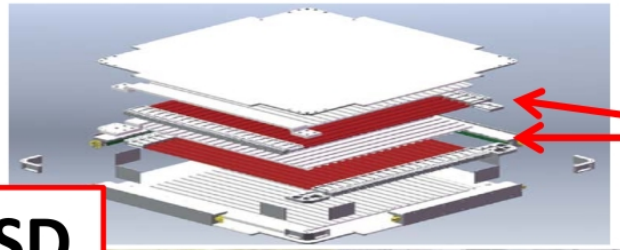

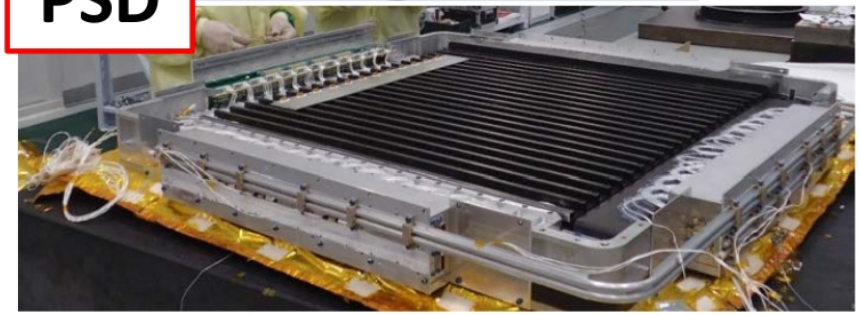

- 1.0 cm thick ,2.8cm wide and 82.0 cm long scintillator strips
- staggered by 0.8 cm in a layer
- 82 cm × 82 cm layers
- 2 layers (x and y)

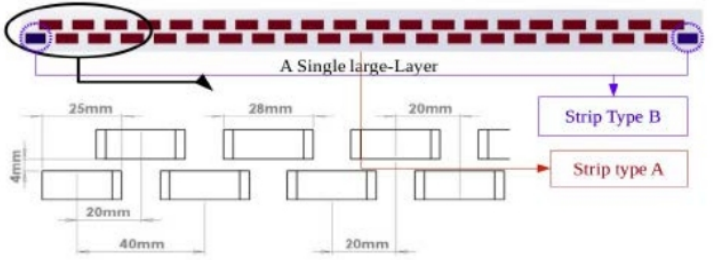

NUD

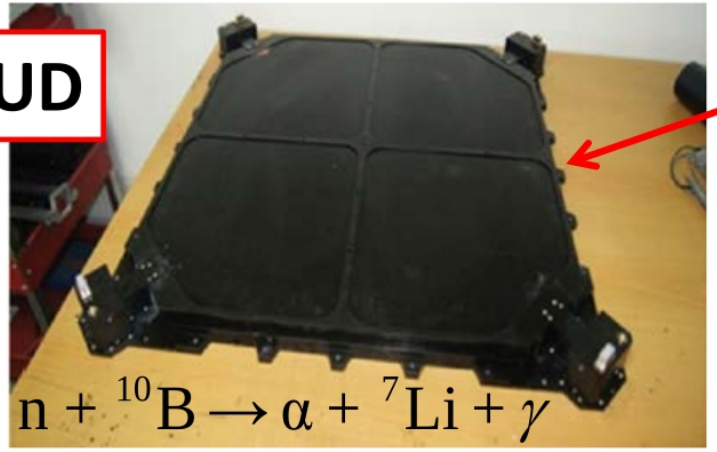

- 4 large area boron-doped plastic scintillators (30 cm × 30 cm × 1 cm)

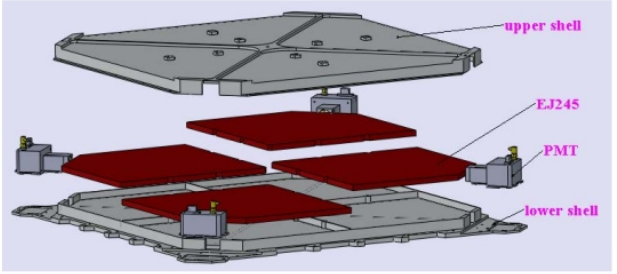

gamma ray emission of the blazar PKS 2155-304

arXiv:1709.07997

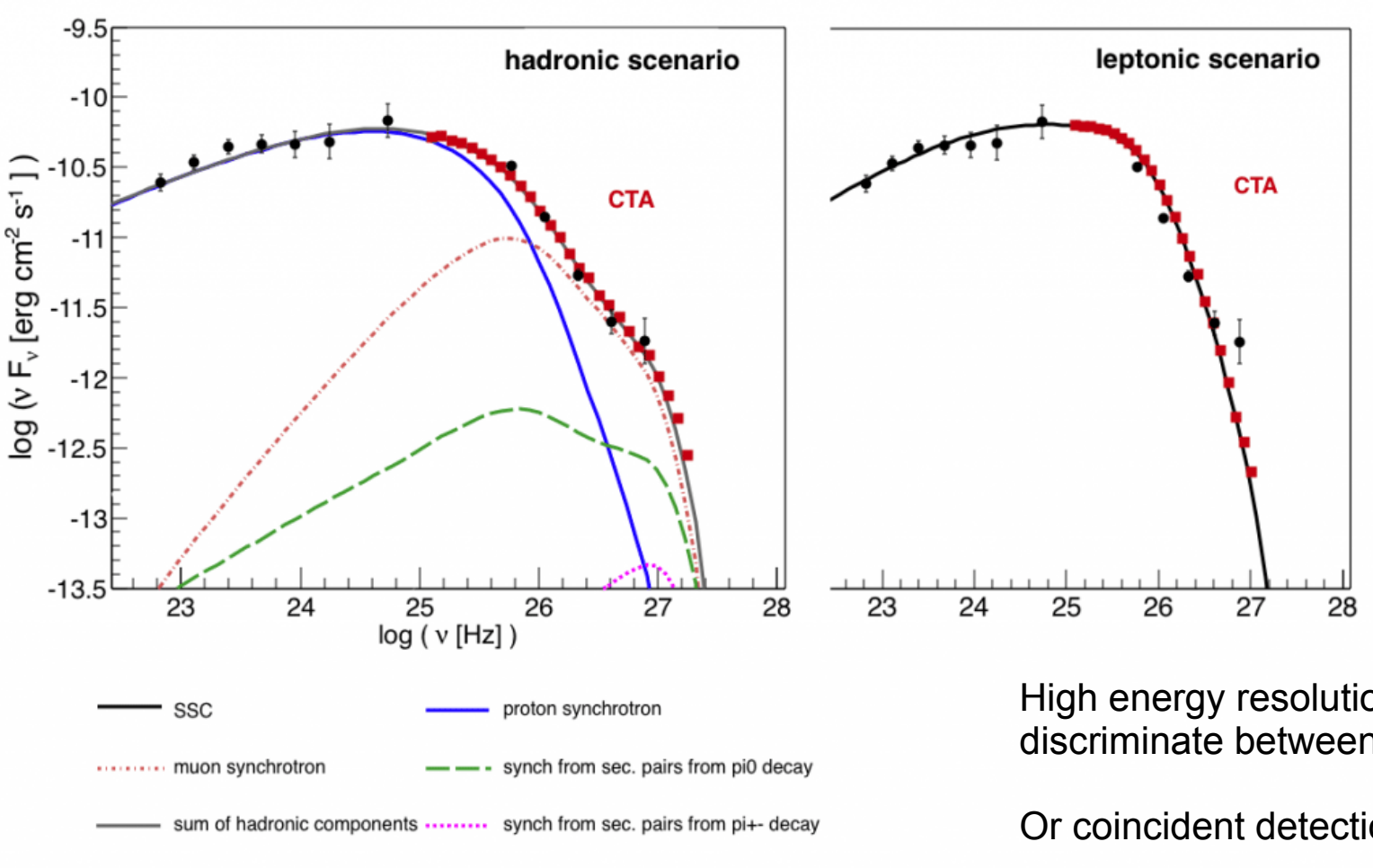

High energy resolution required to discriminate between the two scenarios

Or coincident detection of neutrinos

The Launch Dec 17th 2015, 0:12 UTC

Jiuquan Satellite Launch Center
Gobi desert

CZ-2D rocket

Mass: 1850 kg (scientific payload 1400 kg)
Power : 640 W (scientific payload 400 W)
Orbit: sun syncronous
Altitude: 500km
Inclination: 97.41°
Period: 95 minutes
Downlink: 16 GB / day
Lifetime: > 3 years

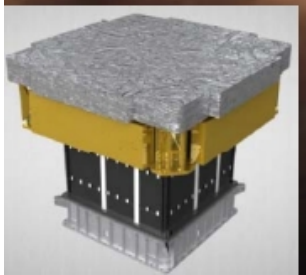

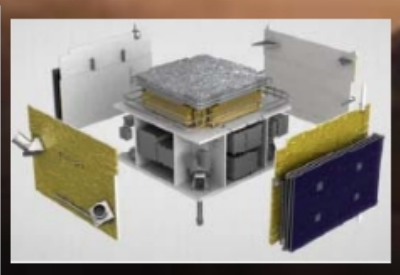

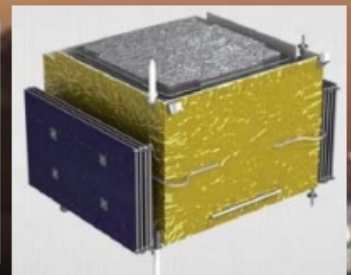

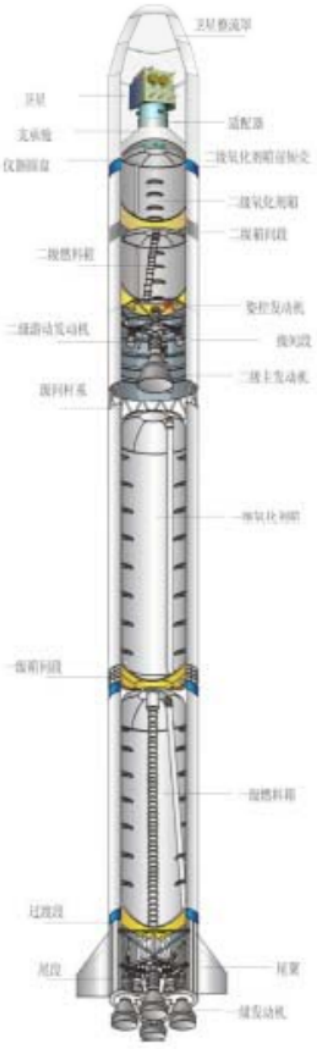

The electron+positron

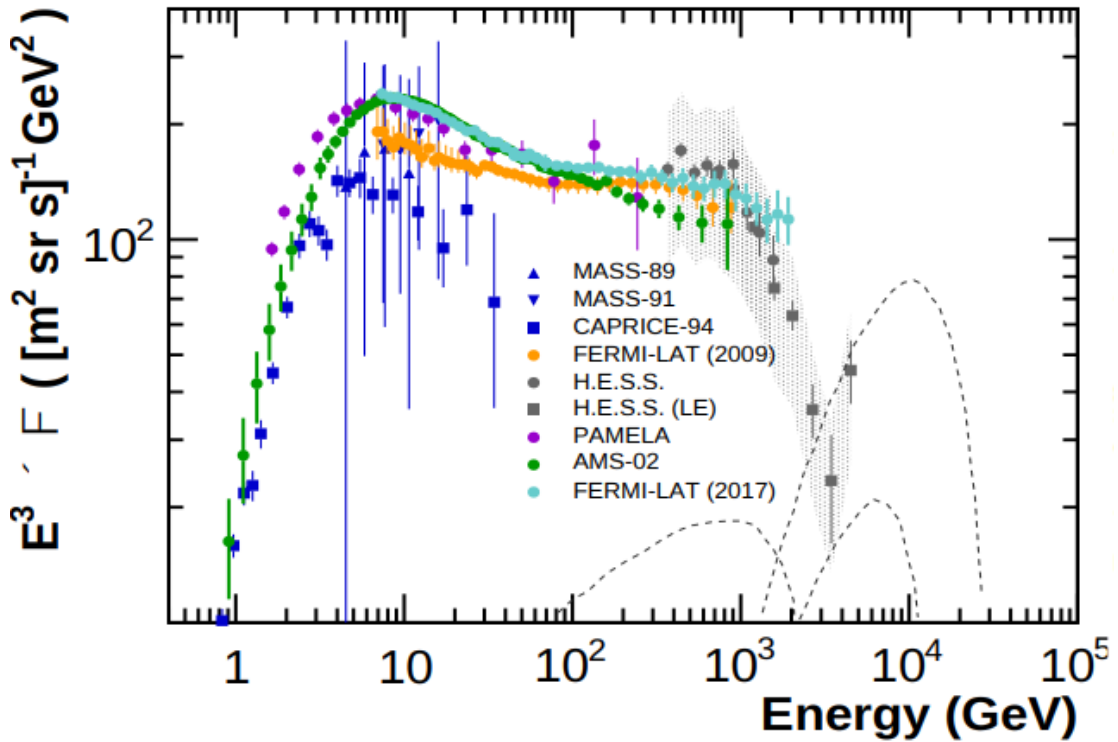

- Small fluxes and ~ E^{-3} spectra
- Cut-off at about 1 TeV?

TeV sources:
- T < 10^5 yr and D < 1 kpc
- Nearby CR sources: large anisotropies?
- Contributions from DM annihilation/decay?

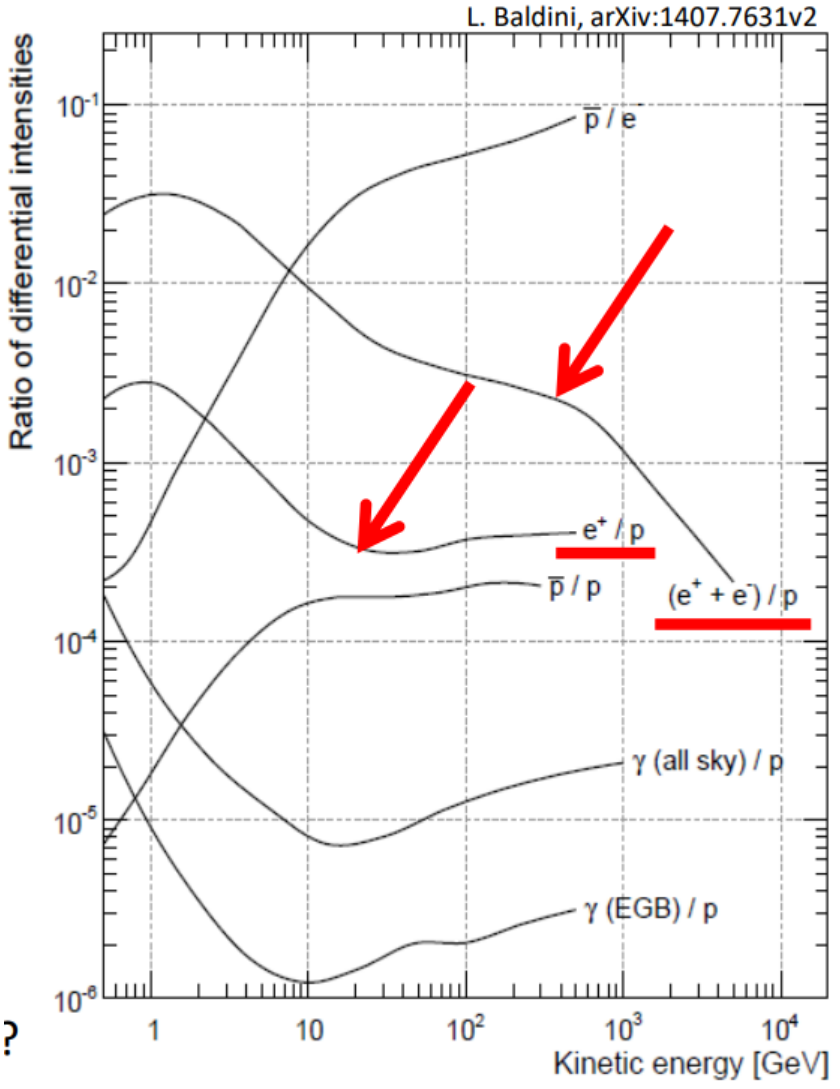

Proton and helium: (discrepant)

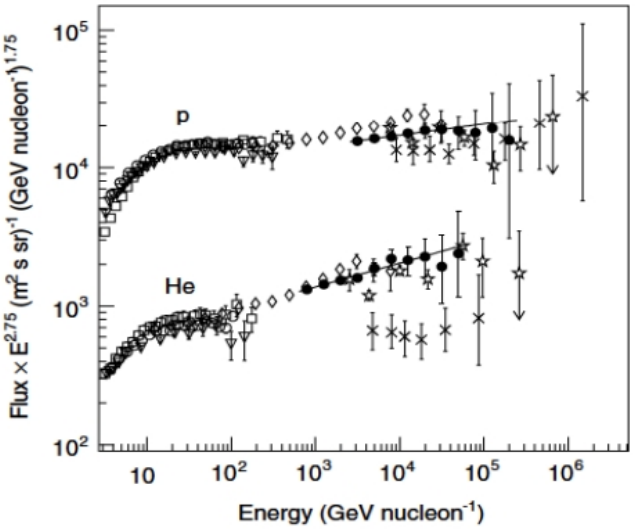

CREAM
First hints for Hardenings.

PAMELA and AMS
Direct detection fo the break at about 250GeV/n

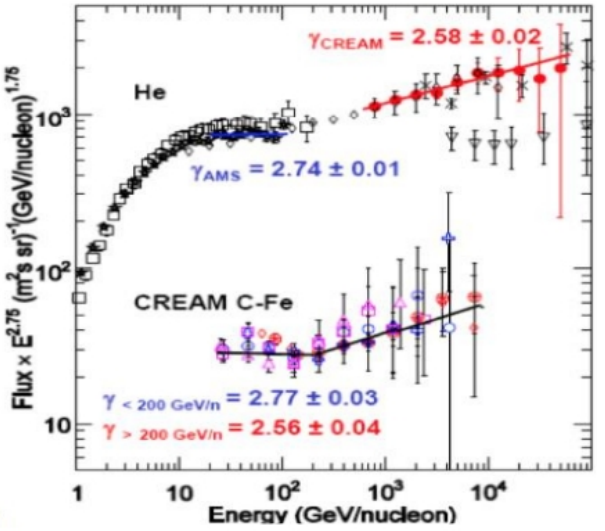

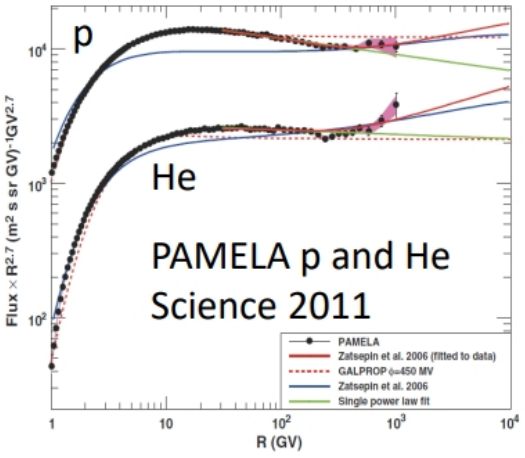

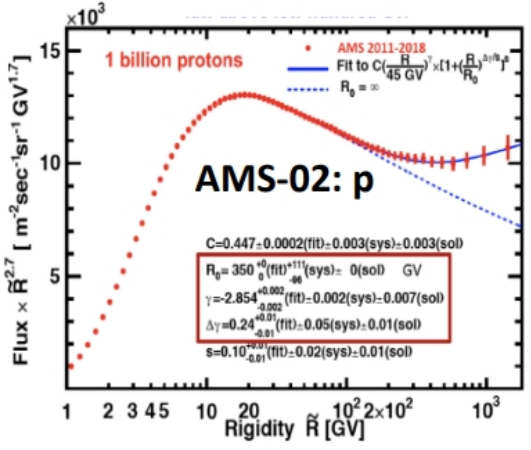

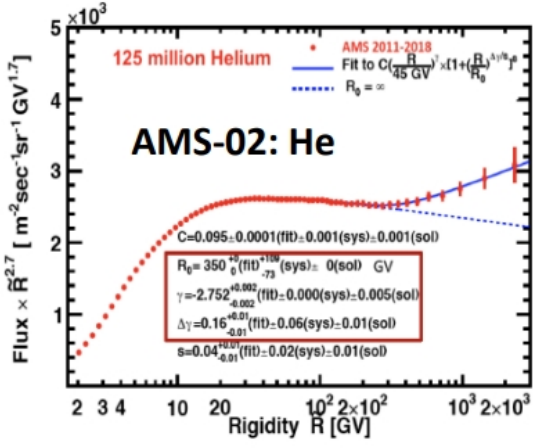

The ultra-high energy mass composition

Phys Rev. D 111, 022003 (2025)
Phys.Rev. Lett. 134 (2025) 021001

FD → longitudinal profile

<Xmax> resol. 15 g/cm^2 at the highest energies

SD → temporal and lateral distributions + DNN

<Xmax> resol. 30 g/cm^2 at the highest energies

° **<Xmax>** gets lighter up to ~2 10 ^{18} eV and heavier above incompatible with pure composition

° **σ (Xmax)** at the highest energy excludes a large fraction of protons and proton GZK as a dominant reason for the spectral cutoff

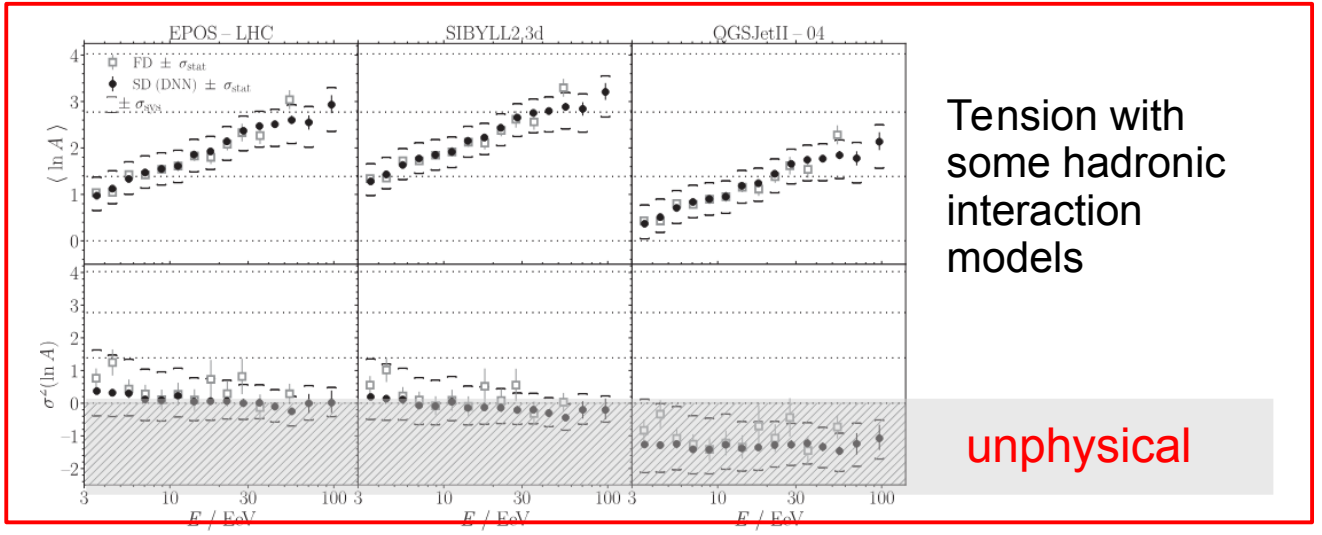

Tension with some hadronic interaction models

unphysical

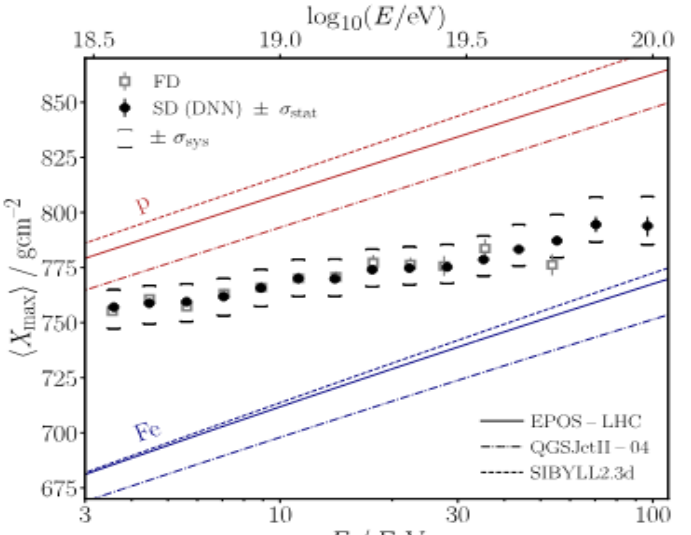

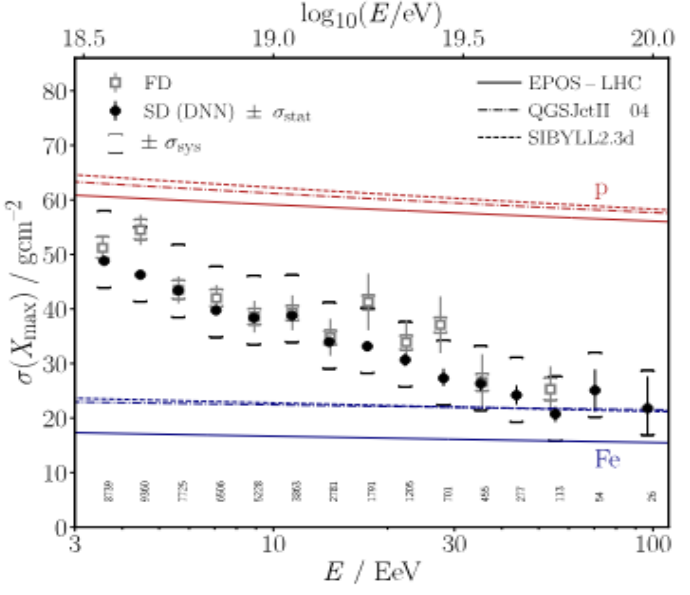

Beyond the standard model

Search for Lorentz invariance violation

Effects suppressed for low energy and short travel distances : UHECRs !!!

$$E_i^2 - p_i^2 = m_i^2 + \sum_{n=0}^{N} \delta_i^{(n)} E_i^{2+n} = m_i^2 + \eta_i^{(n)} \frac{E_i^{2+n}}{M_{Pl}^n}$$

$$\gamma_{\mathrm{LIV}} = \frac{E}{m_{\mathrm{LIV}}} \qquad \tau = \gamma_{\mathrm{LIV}} \tau_0$$

In air shower development
for $\eta^{(n)}<0$, decay of π^0 forbidden
EM component decreasing, hadronic one increasing

$\pi^0 \to \gamma\gamma$ $\quad \tau_0 = 8.4 \cdot 10^{-17}\mathrm{s}$

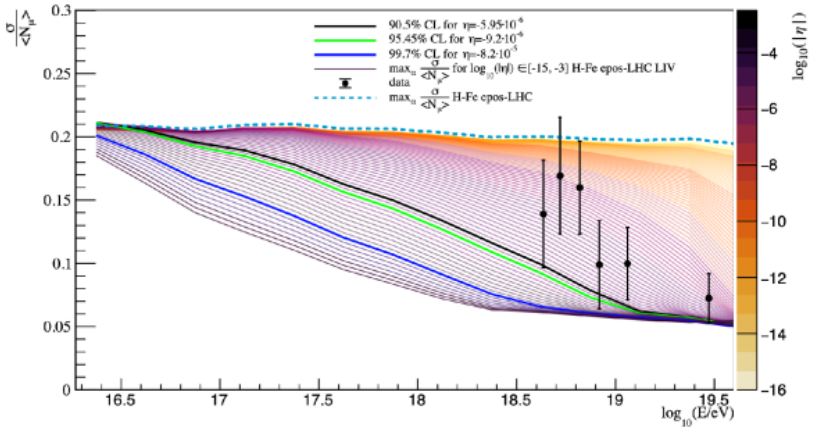

*C.Trimarelli, EPJ Web of Conf. **283**, 05003 (2023)*
Auger Coll., JCAP 01 (2022) 023

Super-heavy dark matter searches

Overdensity of SHDM in the galatic halo:

$$\delta = \frac{\delta_X^{halo}}{\rho_X^{extr}} = \frac{\rho_{DM}^{halo}}{\Omega_{DM}\rho_c} \simeq 2 \times 10^5$$

Berezinsky V. et al., Phys.Rev.Lett.79 (1997) 4302

Flux of secondaries from SHDM decay ($i = \gamma, \nu, \overline{\nu}, N, \overline{N}$):

$$J_i^{\mathrm{gal}}(E) = \frac{1}{4\pi M_X c^2 \tau_X} \frac{\mathrm{d}N_i}{\mathrm{d}E} \int_0^\infty \mathrm{d}s\, \rho_{\mathrm{DM}}(\mathbf{x}_\odot + \mathbf{x}_i(s;\mathbf{n})).$$

Free parameters

$$\tau_X = \hbar M_X^{-1} \exp(4\pi/\alpha_X)$$

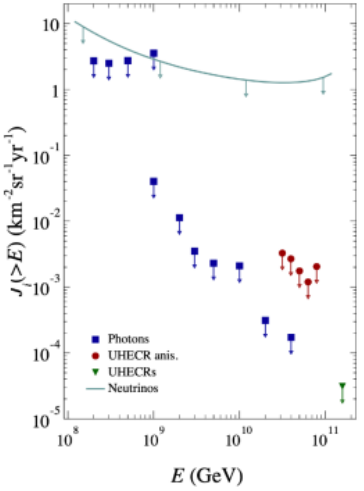

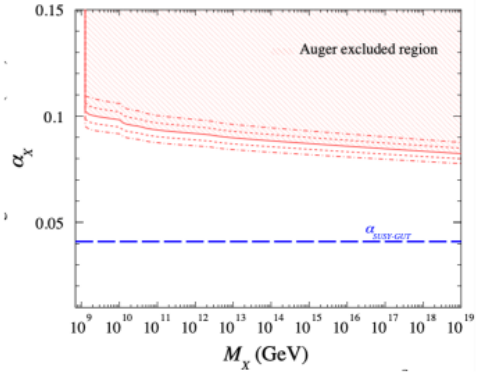

Auger Coll., Phys. Rev. D 107 (2023) 042002
Auger Coll., Phys. Rev. Lett. 130 (2023) 061001
Auger Coll., Phys. Rev. D 109 (2024) L081101

TA Hotspot & Perseus-Pisces supercluster excess

J. Kim, PoS(ICRC2023)244

25°-radius oversampling

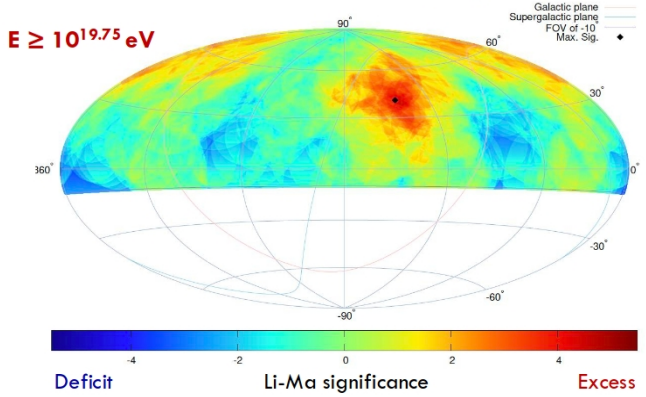

- 216 events (15-year TA SD data)
- Max local sig.: **4.8σ** at (144.0°, 40.5°)
- Post-trial prob.: $P(S_{MC} > 4.8\sigma)$=2.7×10^{-3}→ **2.8σ**

20°-radius oversampling

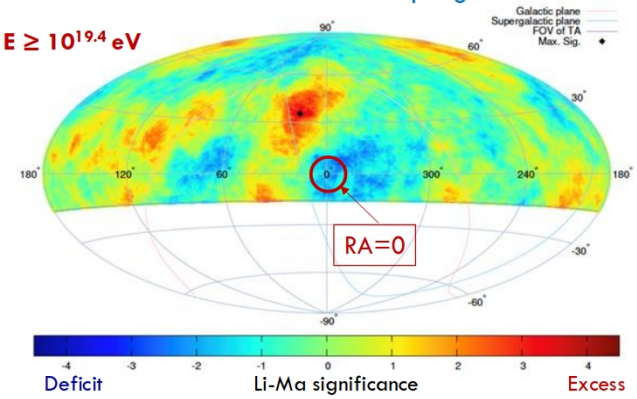

- 1125 events (15-year TA SD data)
- Max local sig.: **4.0σ** at (17.9°, 35.2°)
- Chance probability of having equal or higher excess close to the PPSC → **3.3σ**

Declination Auger/TA common band

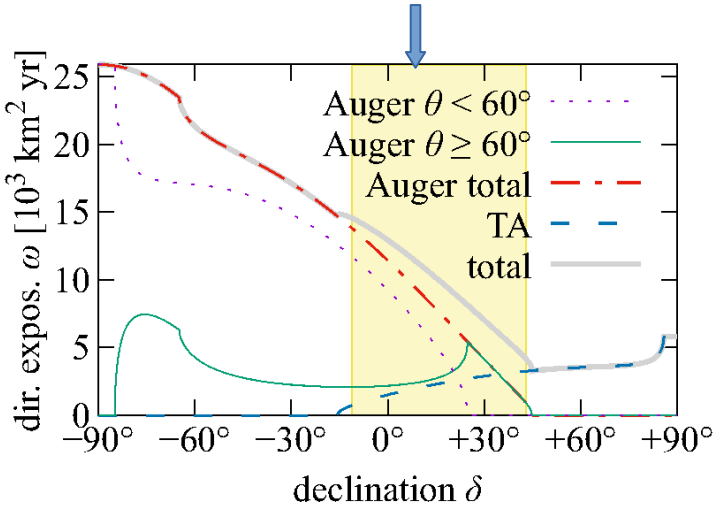

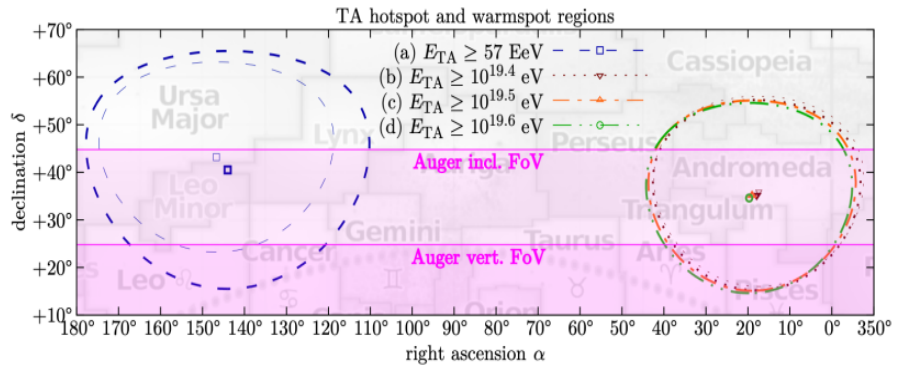

TA "Hot Spot" and PPSC excess not confirmed by Auger

PoS(ICRC2023) 252

	(α_0, δ_0)[°]	E^{TA}	N^{TA}_{obs}	N^{TA}_{exp}	σ^{TA}_{post}	E^{Auger}	N^{Auger}_{obs}	N^{Auger}_{exp}	σ^{Auger}_{Li-Ma}
PPSC	(17.4, 36.0)	25.1	95	61.4	3.1σ	20.1	68	69.3	−0.2σ
	(19.0, 35.1)	31.6	66	39.1	3.2σ	25.3	40	45.2	−0.8σ
	(19.7, 34.6)	39.8	43	23.2	3.0σ	31.8	27	26.5	0.1σ
TA hot spot	(144.0, 40.5)	57	44	16.9	3.2σ	45.6	7	10.1	−1.0σ

Search for neutrinos with the SD: signature

typical signal shapes

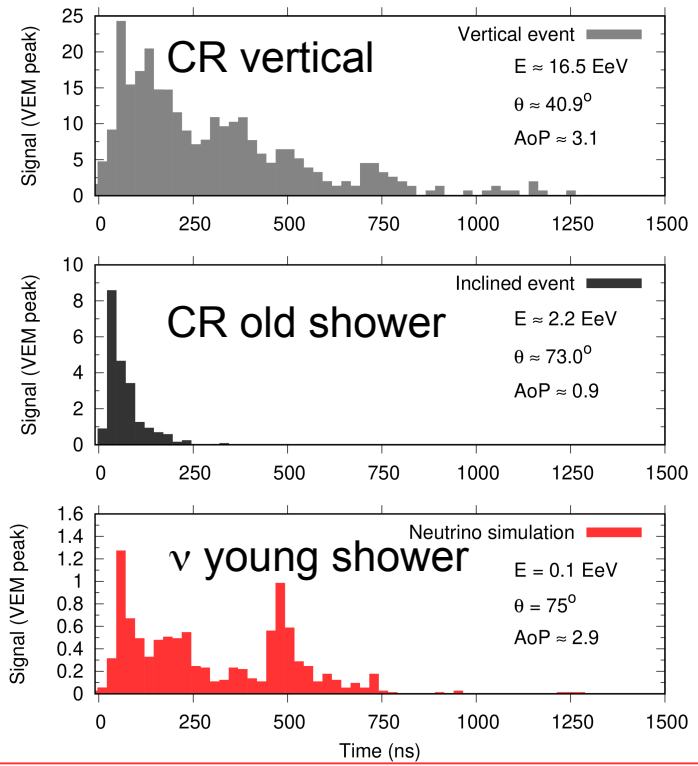

Signature:

"young shower" → with large electromagnetic component

inclined event with slow rising and broad signal

larger Area-over-Peak (**AoP**)

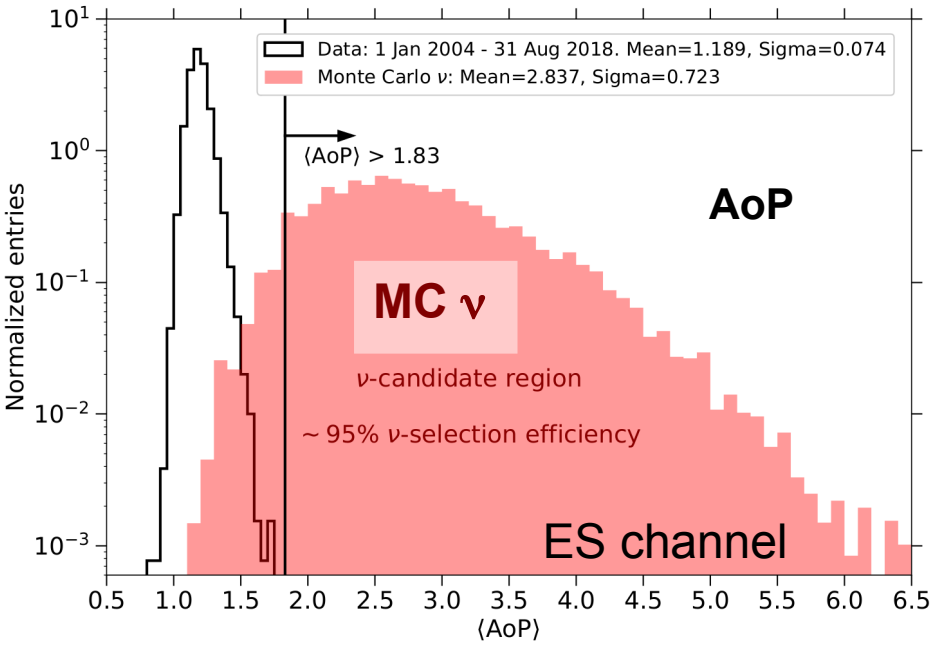

Data 2004 – 2018: 14.7 yr

→ **bkg expected: <1 event in 50 years!**

NO Candidates found

Bounds on neutrino fluxes from cosmic rays

tension with models assuming pure proton and spectrum shaped by GZK
[up to 6 neutrino expected vs 0 observed]

Joint Auger TA WG in the search for anisotropy signals

Reports at UHECR and ICRC conferences, journal publications

large scale (dip. + quad.)

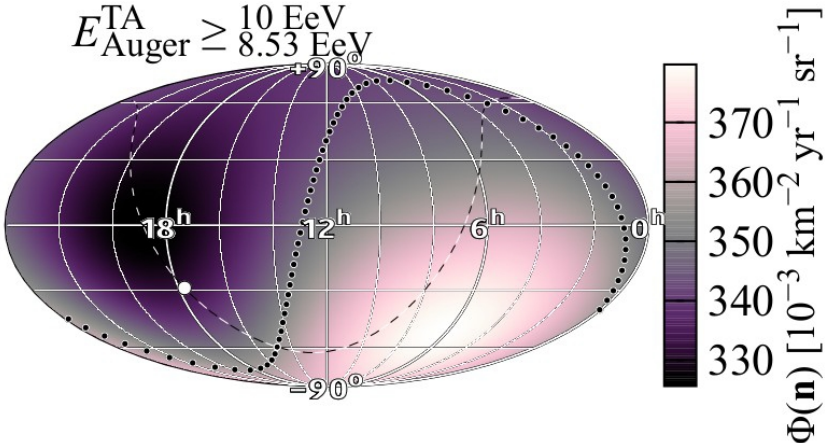

equatorial coordinates

medium scale

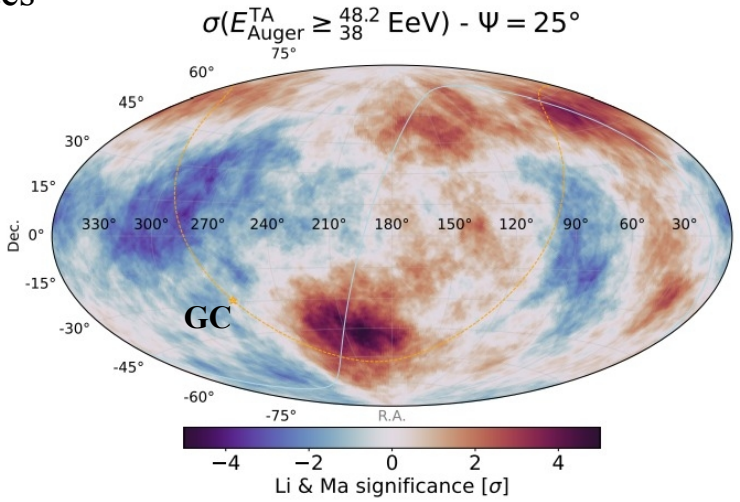

Cen A

studies limited by TA statistics

TAx4 under construction

ICRC2023, UHEC2024

Correlation with starburst galaxies $1\,\mathrm{Mpc} \leq D < 130\,\mathrm{Mpc}$ (Lunardini+ '19 catalog)

dataset	$E^{\rm min}_{\rm Auger}$	$E^{\rm min}_{\rm TA}$	Θ	f	TS	post-trial
ICRC 2023	38 EeV	48.2 EeV	$(15.4^{+5.2}_{-3.0})°$	$(11.7^{+4.7}_{-2.9})\%$	30.5	4.6σ
UHECR 2024	38 EeV	47.8 EeV	$(15.0^{+5.0}_{-2.9})°$	$(11.1^{+4.4}_{-2.8})\%$	29.5	4.4σ

Starbust galaxies: Auger only 4σ Auger+TA 4.4σ

Most likely configuration

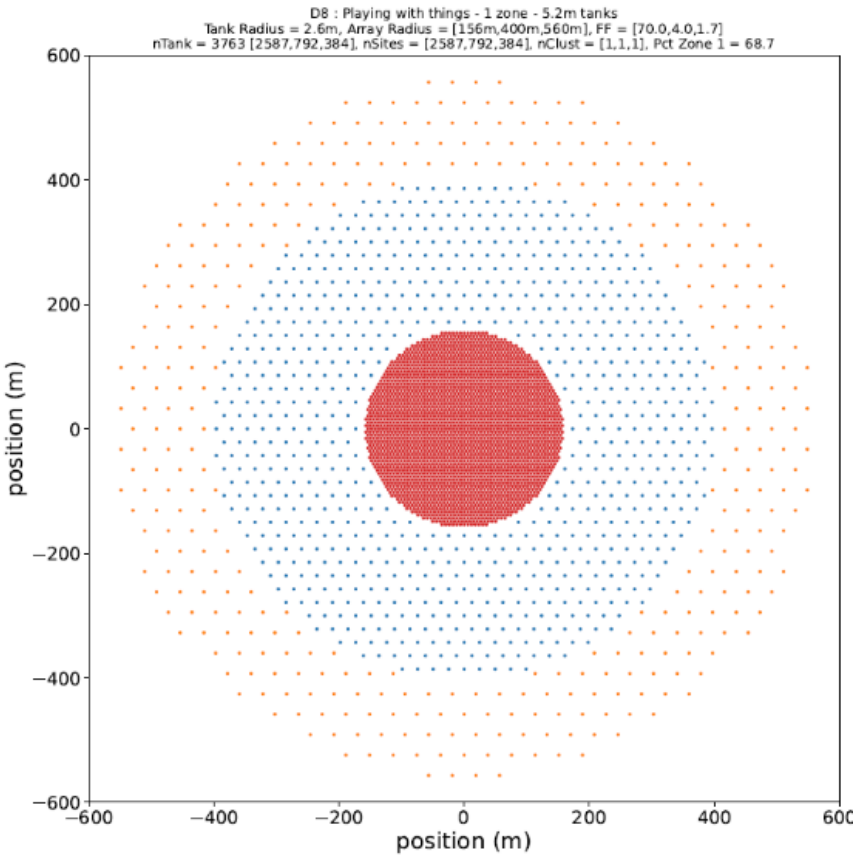

Inner Array

- 160m radius; Fill Factor between 60% and 70%
- Double Layer Metallic Tanks
- 5.2m diameter. Height: 3.42m Upper Layer, 0.68m Lower Layer
- Approximately 87 m^3 water/tank
- If FF=70% 2587 Tanks
- Single central PMT in each layer, 8″ or 10″
- Signals transmitted, maximum cable length 130m, by cable to one of the collection points (Field Nodes, about 50 tanks each) and digitized there

Outer Array

- 2 zones: 160<r<400m 4% Fill Factor; 400<r<560m 1.7% Fill Factor
- Single Layer Rotomolded Tanks
- 3.6m diameter. Height 1.70m
- Approximately 17.3 m^3 water/tank
- Approximately 1470 tanks in the first zone and approximately 710 in the second
- Multi-PMT: 7 3″ PMTs contained in a plastic hemisphere
- Locally digitized signals transmitted via Fiber Optics

MAGIC as a stellar intensity interferometer

- Special hardware setup developed for MAGIC: real-time, dead-time-free, 4-channel, GPU-based correlator
- **22 stellar diameters** published, 9 corresponding to reference stars with previous comparable measurements, and 13 with no prior measurements
- Exploiting this technique to make IACTs competitive optical Intensity Interferometers with minimal hardware adjustments.

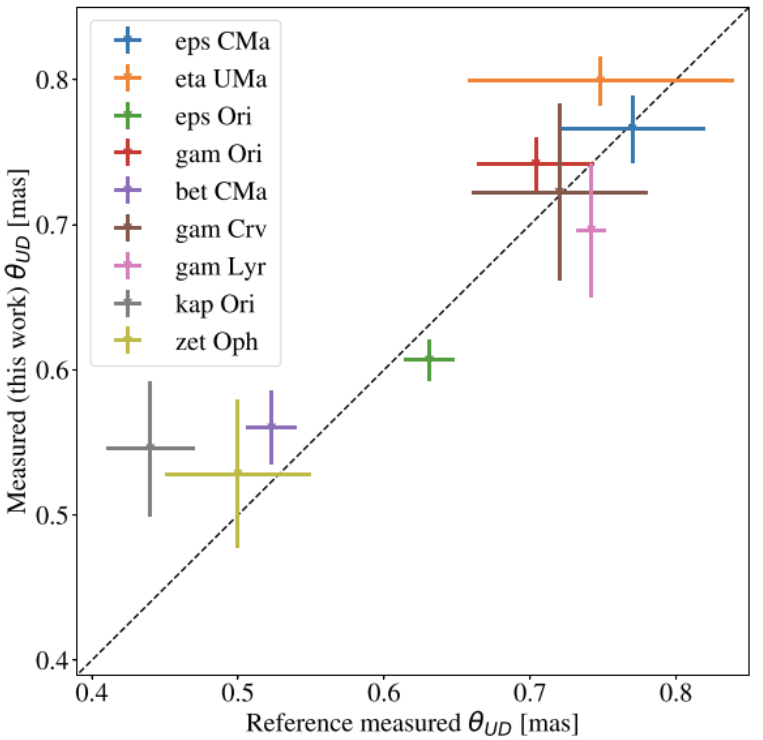

comparison measured-reference diameters

- Sky observation at High Energies
  - → Extragalactic Sources and Transients
  - → Galactic Sources
    - ✓ Pulsars Halos
    - ✓ Galactic PeVatrons
    - ✓ Galactic Diffuse Emission and Fermi Bubbles
    - ✓ Galactic center observ

Science case and sensitivity

- Fundamental Physics
  - → Primordial Black Holes
  - → Dark Matter annihilation and decay
  - → Axion like particles
  - → Lorentz Invariance Violation
- Cosmic Ray Physics
  - → Composition dependent anisotropy

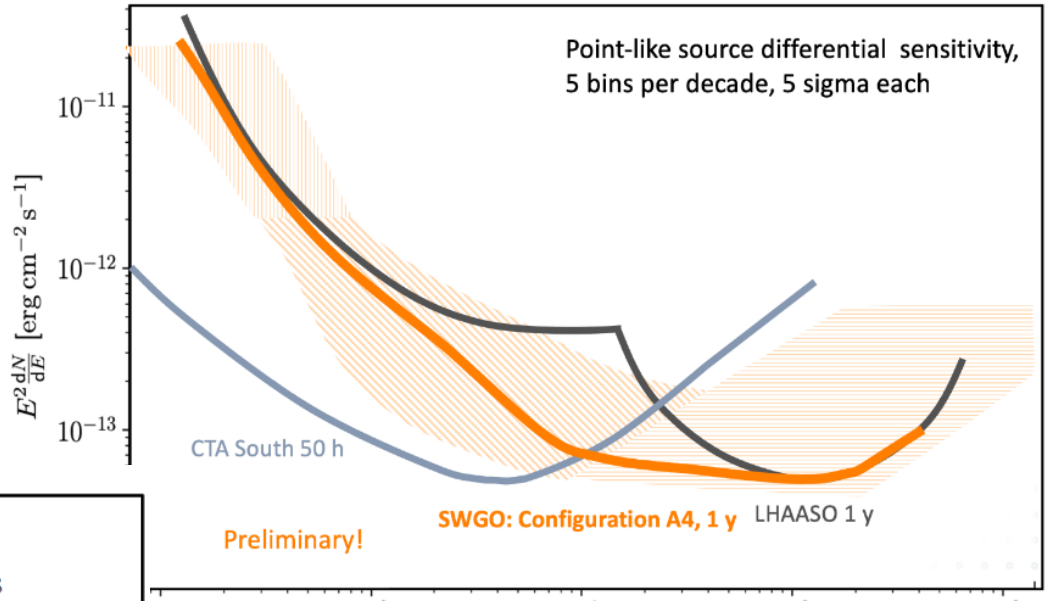

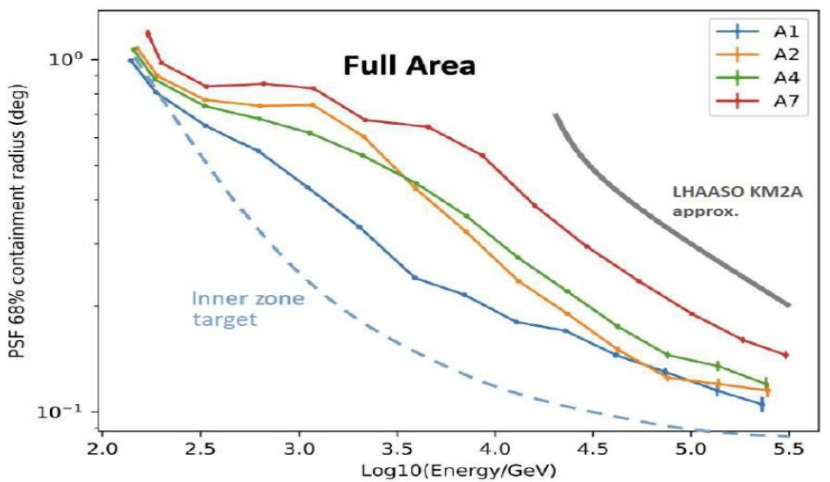

CTA: expected sensitivity

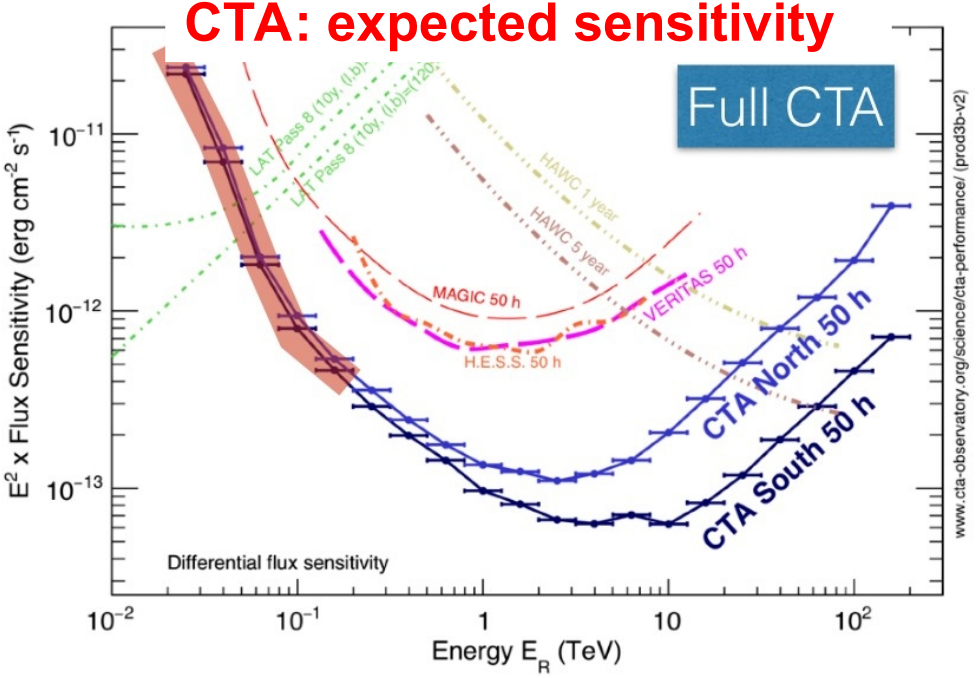

Instrument	energy range	Effective area (m^2)	sensitivity (milli-CU†)	energy resolution (%)	PSF (°)	FoV (sr)	duty cycle (%)
Fermi-LAT[a)]	20 MeV - 300 GeV	~ 0.95	10 - 30	8 - 18	0.15 - 3.5	~ 2.4	~ 60
H.E.S.S.[b)]	10 GeV - 50 TeV	$\sim 10^5$	~ 5	15	< 0.1	~ 0.03	$\sim$10
MAGIC[c)]	$\geq$ 30 GeV	$\sim 10^5$	~ 7	16	≤ 0.07	0.02	$\sim$18
VERITAS[d)]	50 GeV - 50 TeV	$\sim 10^5$	~ 5	10 - 15	0.08 - 0.13	0.02	10-14
CTA-LST1[e)]	20 GeV - 300 GeV	$\sim 10^4$	~ 10	10 - 30	0.05 - 0.1	0.02	$\sim$10
ASγ[f)]	10 TeV - 1 PeV	$\sim 7 \times 10^4$	~ 200	20 - 40	~ 0.8	~ 2.0	90
ARGO-YBJ[g)]	50 GeV - 10 TeV	$\sim 0.8 \times 10^4$	~ 300	>13	~ 0.5	~ 2.0	86
HAWC[h)]	100 GeV - 100 TeV	$\sim 3 \times 10^4$	~ 50	20 - 50	~ 0.69	> 1.5	95
LHAASO-WCDA[i)]	100 GeV - 20 TeV	$\sim 0.8 \times 10^5$	~ 12	$\sim$33	0.2 - 0.84	~ 2.0	95
LHAASO-KM2A[i)]	10 TeV - 4 PeV	$\sim 10^6$	~ 12	15 - 40	0.2 - 0.6	~ 2.0	95

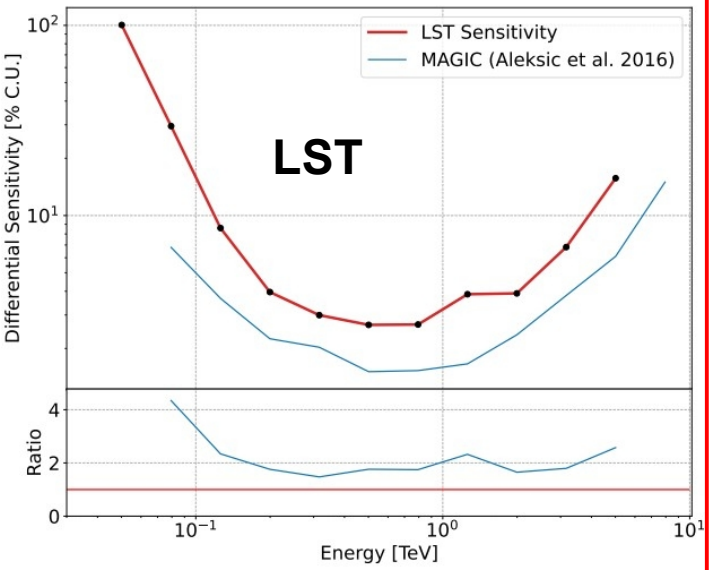

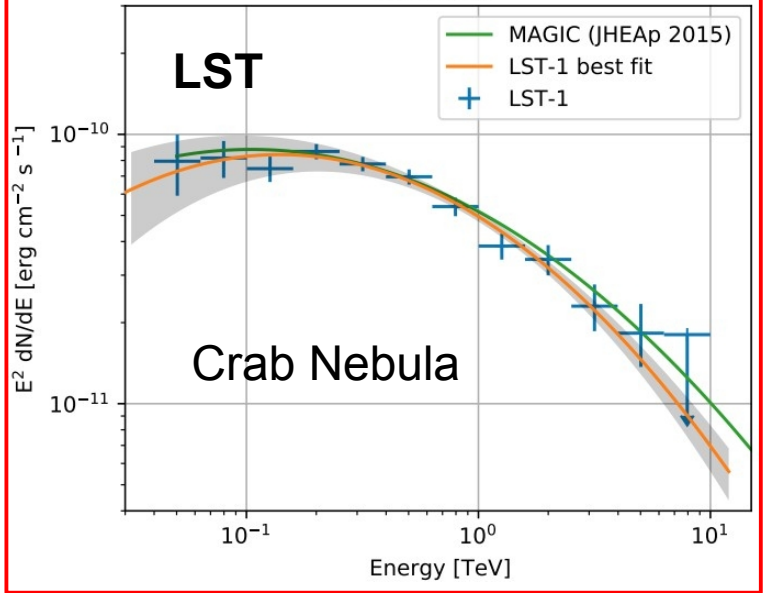

Summary of main facts for UHECRs

UHECRs NOT predominantly protons, fraction of heavier nuclei increases with energy above ~2 EeV
→ spectrum features reflect the evolution of mass composition
→ different and independent measurements
→ non observation of photons and neutrinos from CRs

Spectrum features are clearly identified without relying on hypotheses on composition or sources
The shape of the spectrum reflects the different contributions in mass

Observation of a dipolar anisotropy > 8 EeV → EG origin
no hints for anisotropy in Northern sky up to 45° in declination (vertical+inclined events)
hints of correlation with the SBGs above 40 EeV

No composition difference from Northern to Southern hemisphere below $10^{19.5}$ eV
The transition region is placed around the second knee. Supported by
— the measured composition, which becomes lighter above the 2nd knee up to $\sim 2\times10^{18}$ eV
— the smooth transition from isotropy to a dipolar anisotropy above 8 EeV
— the exclusion of H+He mix in the ankle region at >5σ

Valuable information about hadronic interactions at UHE:
μ deficit in models due to pile-up effects along the shower development

Constraints to effects of **physics beyond standard model**

Cosmological implications of photon-flux upper limits at ultrahigh energies in scenarios of Planckian-interacting massive particles for dark matter

Using the data of the Pierre Auger Observatory, we report on a search for signatures that would be suggestive of super-heavy particles decaying in the Galactic halo. From the lack of signal, we present upper limits for different energy thresholds above $\gtrsim 10^8$ GeV on the secondary by-product fluxes expected from the decay of the particles. Assuming that the energy density of these super-heavy particles matches that of dark matter observed today, we translate the upper bounds on the particle fluxes into tight constraints on the couplings governing the decay process as a function of the particle mass. Instantons, which are nonperturbative solutions to Yang-Mills equations, can give rise to decay channels otherwise forbidden and transform stable particles into metastable ones. Assuming such instanton-induced decay processes, we derive a bound on the reduced coupling constant of gauge interactions in the dark sector: $\alpha_X \lesssim 0.09$, for $10^9 \lesssim M_X/\mathrm{GeV} < 10^{19}$. Conversely, we obtain that, for instance, a reduced coupling constant $\alpha_X = 0.09$ excludes masses $M_X \gtrsim 3 \times 10^{13}$ GeV. In the context of dark matter production from gravitational arameter space that involves, eheating efficiency, and the

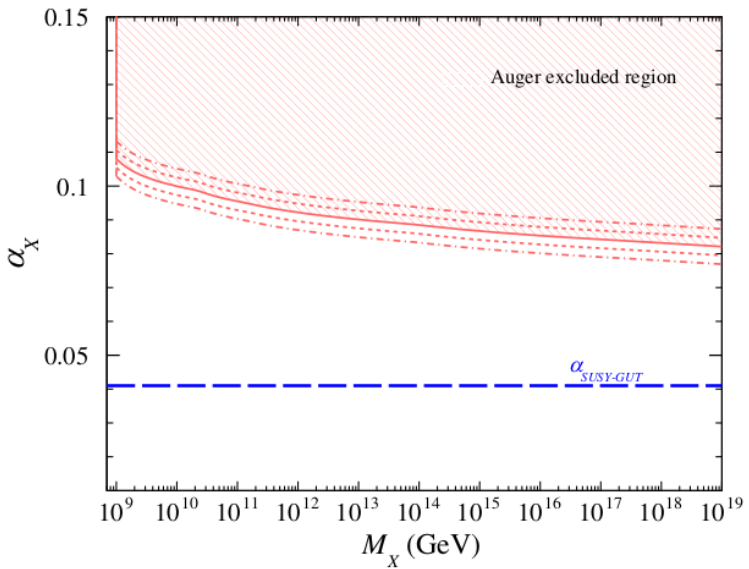

SHDM scenario assuming dark matter interaction (lifetime stabilized) with SM particles using photon upper limits

Flux of secondaries from SHDM decay ($i = \gamma, \nu, \overline{\nu}, N, \overline{N}$):

$$J_i^{\mathrm{gal}}(E) = \frac{1}{4\pi M_X c^2 \tau_X} \frac{\mathrm{d}N_i}{\mathrm{d}E} \int_0^\infty \mathrm{d}s\, \rho_{\mathrm{DM}}(\mathbf{x}_\odot + \mathbf{x}_i(s;\mathbf{n})).$$

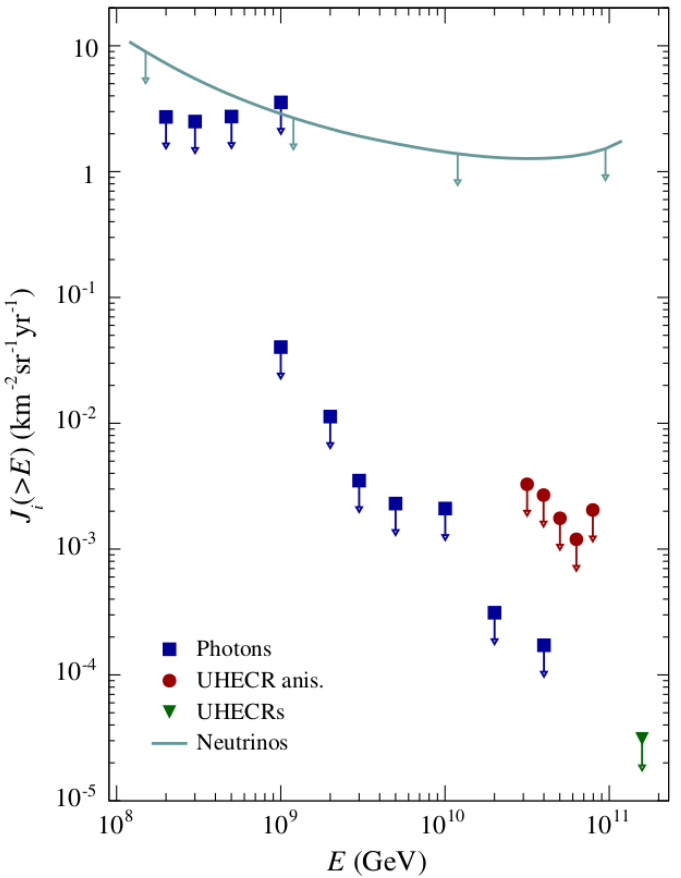

FIG. 3. Upper limits on secondaries produced from the decay of SHDM particles.

Auger Collaboration Phys. Rev. D 102 (2020) 062005

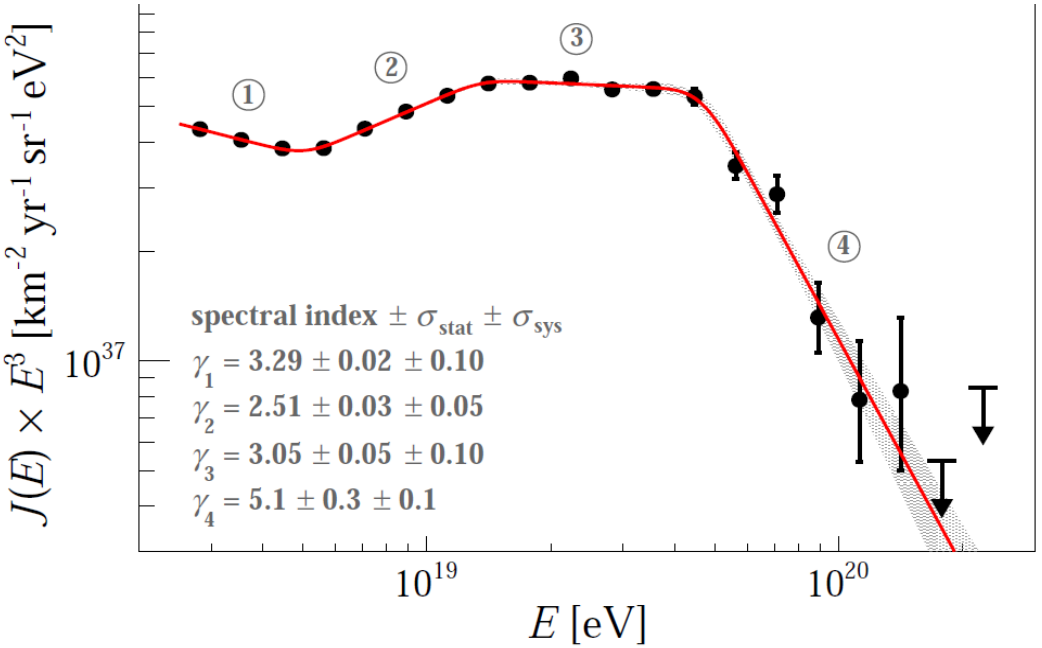

Cutoff at ~ 5 10^{19} eV confirmed

Ankle at ~ 5 10^{18} eV confirmed

new feature instep at ~ 10^{19} eV identified

SD1500, zenith < 60°

Data sample:
215030 events 1/1/2004 – 31/8/2018
Exposure:
60400 km^2 sr y

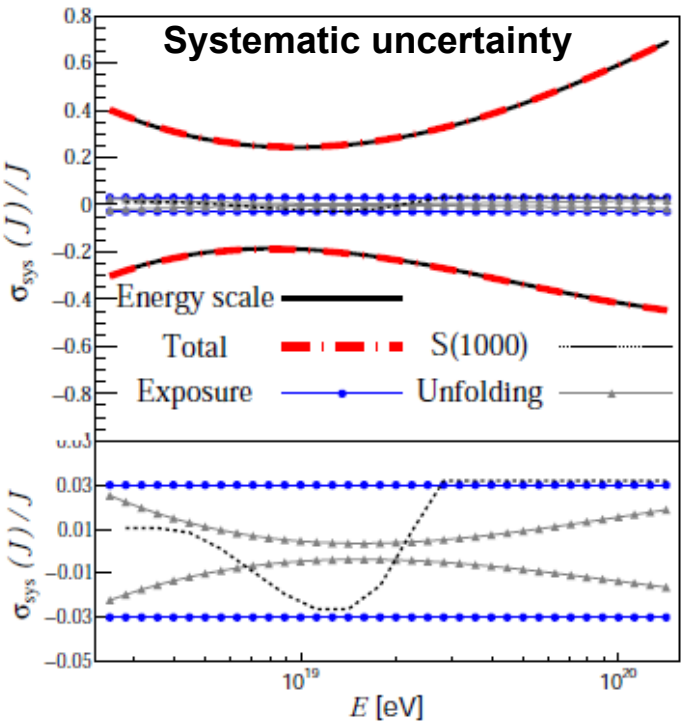

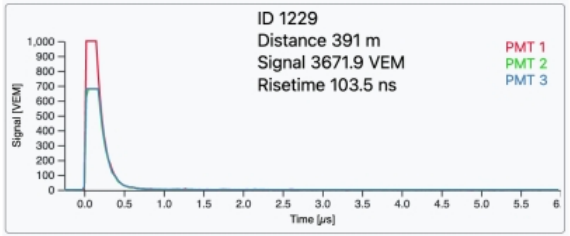

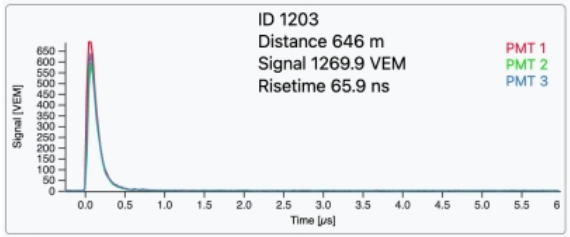

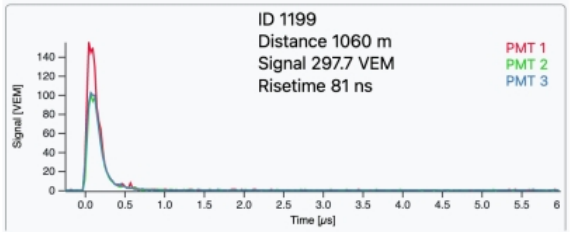

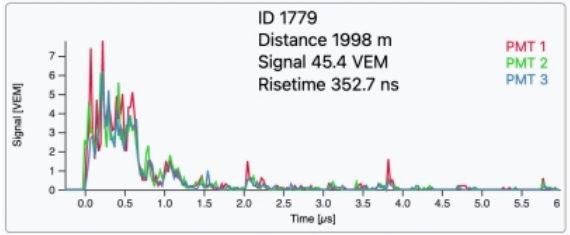

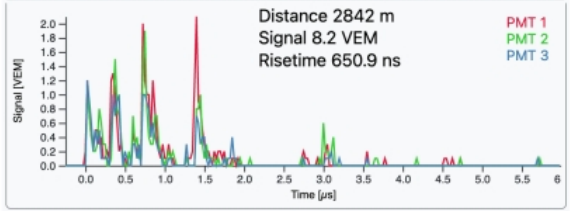

The highest energy event

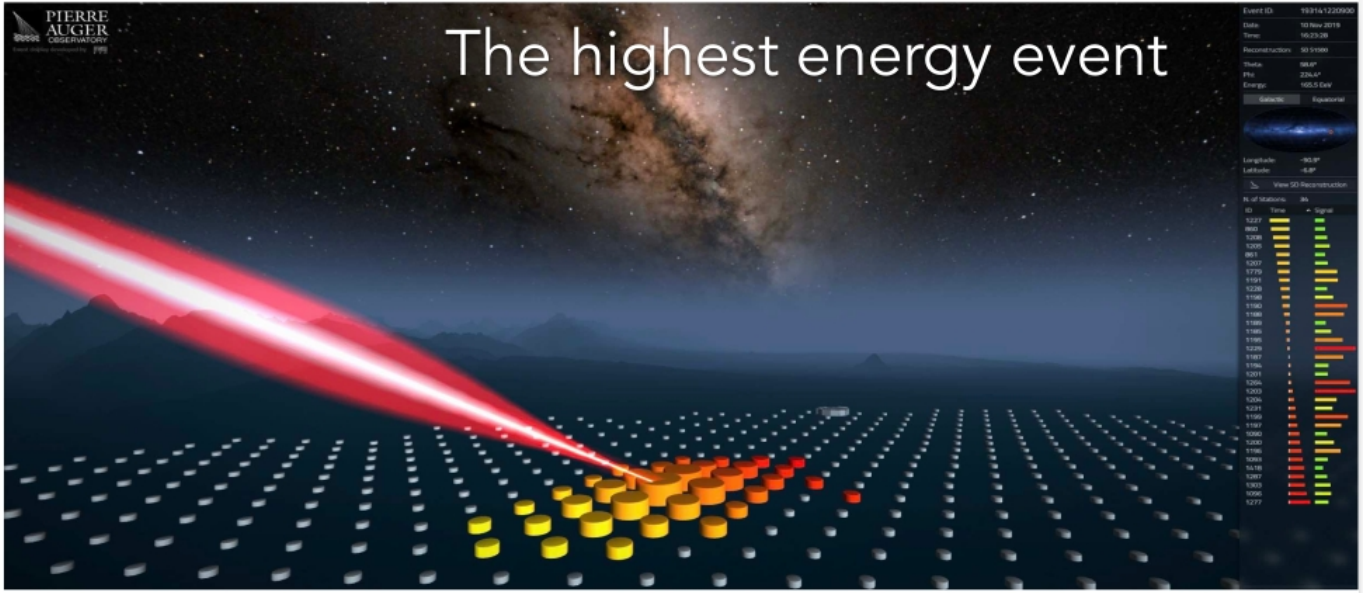

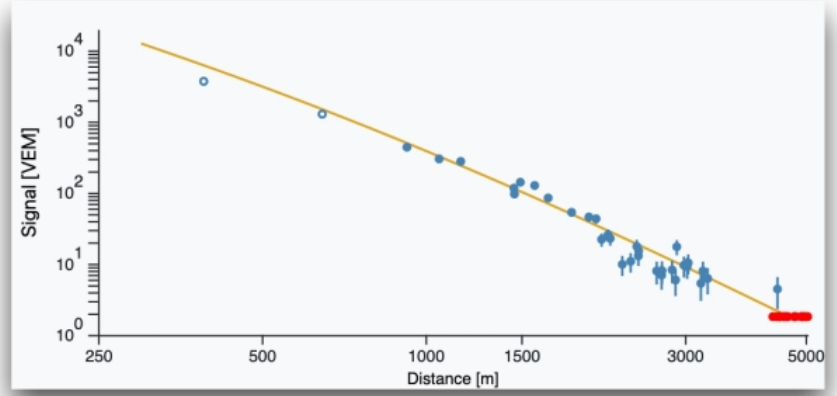

Date	2019-11-10
Energy	166±13 EeV
θ	58.6°
ϕ	224.4°
β	-2.0
$t_{1/2}(1000)$	98±3 ns
δ	-52.0°
α	128.9°
Multiplicity	34

ICRC 2021, JCAP05(2023)024

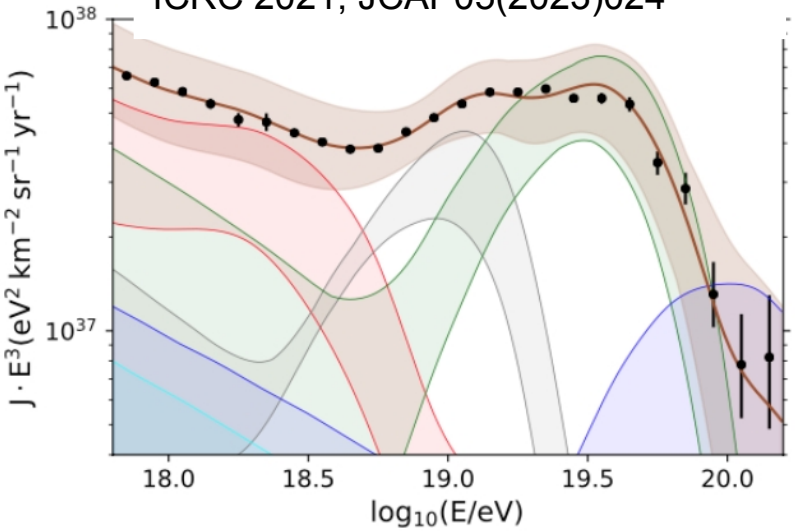

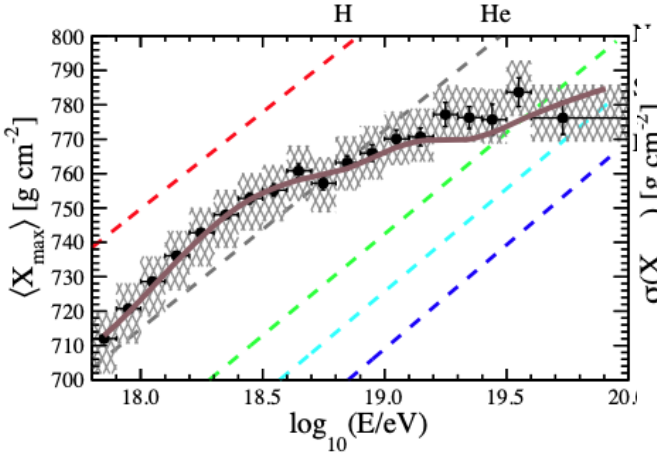

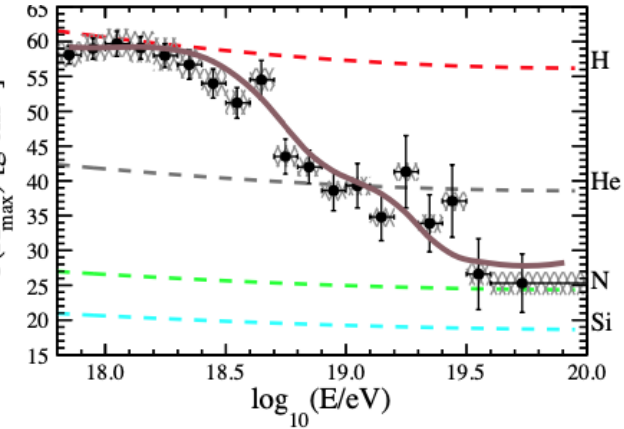

BEST FIT

1) EG: hard HE component + soft LE component
2) possible Galactic component (N)

Scenarios compatible within systematics

Dominant experimental systematics
Only propagation, no magnetic fields

	1st scenario		2nd scenario	
Galactic contribution (at Earth)	N+Si		-	
J_0^{gal} [eV^{-1} km^{-2} sr^{-1} yr^{-1}]	$(1.07 \pm 0.06) \cdot 10^{-13}$		-	
$\log_{10}(R_{cut}^{gal}/V)$	17.48 ± 0.02		-	
f_N (%)	93.0		-	
EG components (at the sources)	Low energy	High energy	Low energy	High energy
$\mathcal{L}_0$ [erg Mpc^{-3} yr^{-1}]	$7.28 \cdot 10^{45}$	$4.4 \cdot 10^{44}$	$1.7 \cdot 10^{46}$	$4.5 \cdot 10^{44}$
γ	3.30 ± 0.05	-1.47 ± 0.12	3.49 ± 0.02	-1.98 ± 0.10
$\log_{10}(R_{cut}/V)$	24 (lim.)	18.19 ± 0.02	24 (lim.)	18.16 ± 0.01
I_H (%)	100 (fixed)	0.0	49.87	0.0
I_{He} (%)	-	27.17	10.92	28.60
I_N (%)	-	69.86	36.25	69.05
I_{Si} (%)	-	0.0	0.0	0.0
I_{Fe} (%)	-	2.97	2.96	2.35
D_J (N_J)	49.5 (24)		60.1 (24)	
$D_{X_{max}}$ ($N_{X_{max}}$)	593.8 (329)		554.8 (329)	
D (N)	643.3 (353)		614.9 (353)	

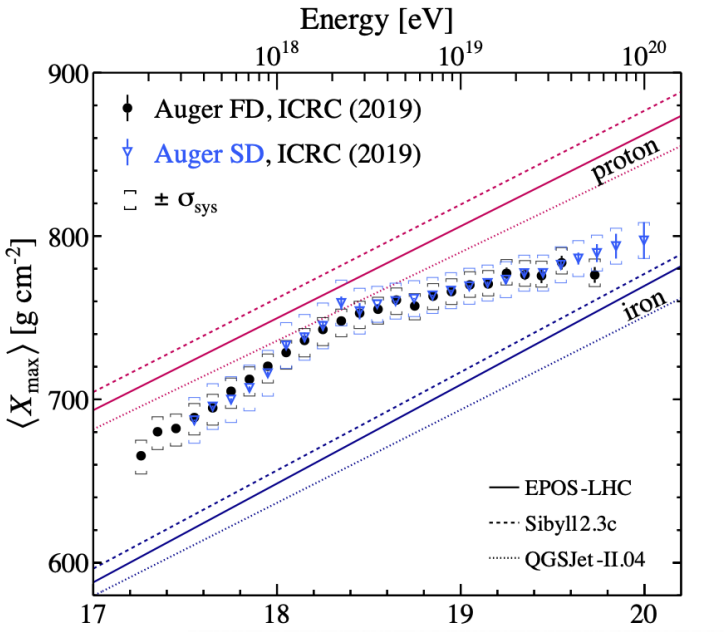

SD can extend the measurement of <Xmax> (worse resolution)

Neural network approach tested with hybrid events

Promising in view of the additional info provided by the upgraded SD detector

The Pierre Auger Collaboration, JINST (2021) 16 P07019

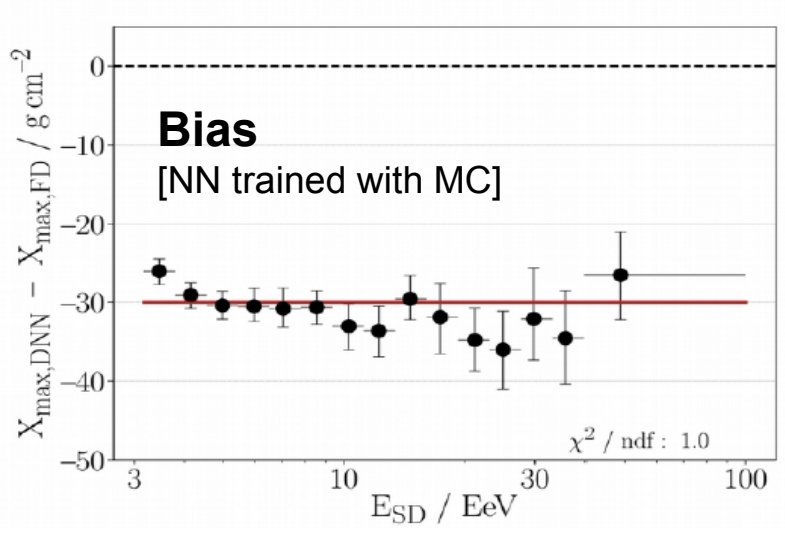

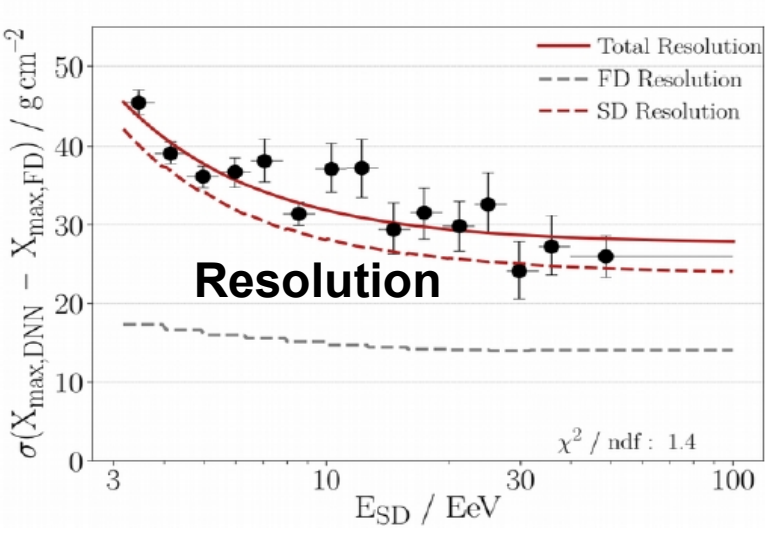

Depth of shower maximum - world data set

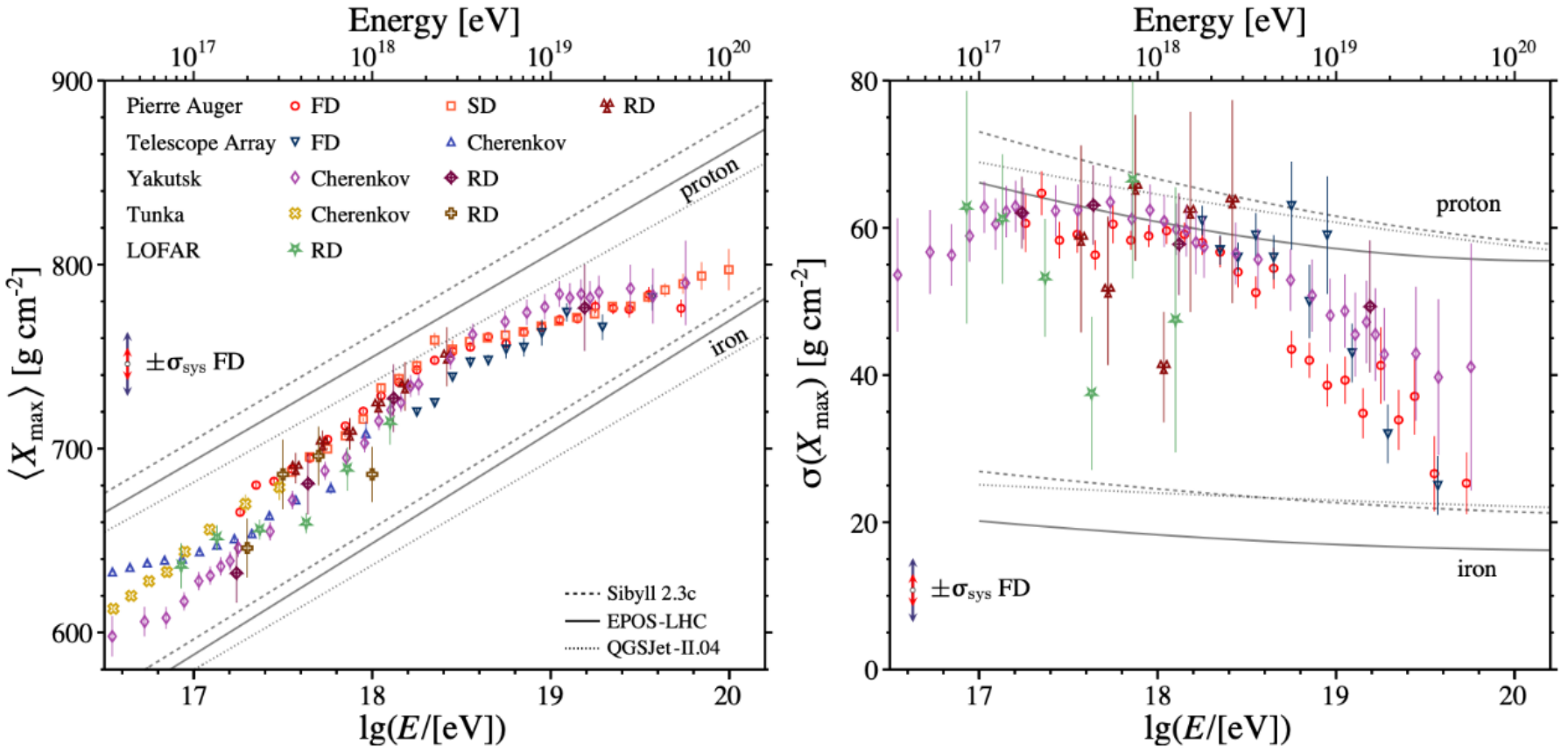

Compilation from A.Coleman et al., Snowmass - Astrop.Phys.147 (2023) 102794

Joint searches (UHECR and neutrinos)

Antares, **I**ce**C**ube, **A**uger, **T**elescope **A**rray

APJ 934 (2022)164

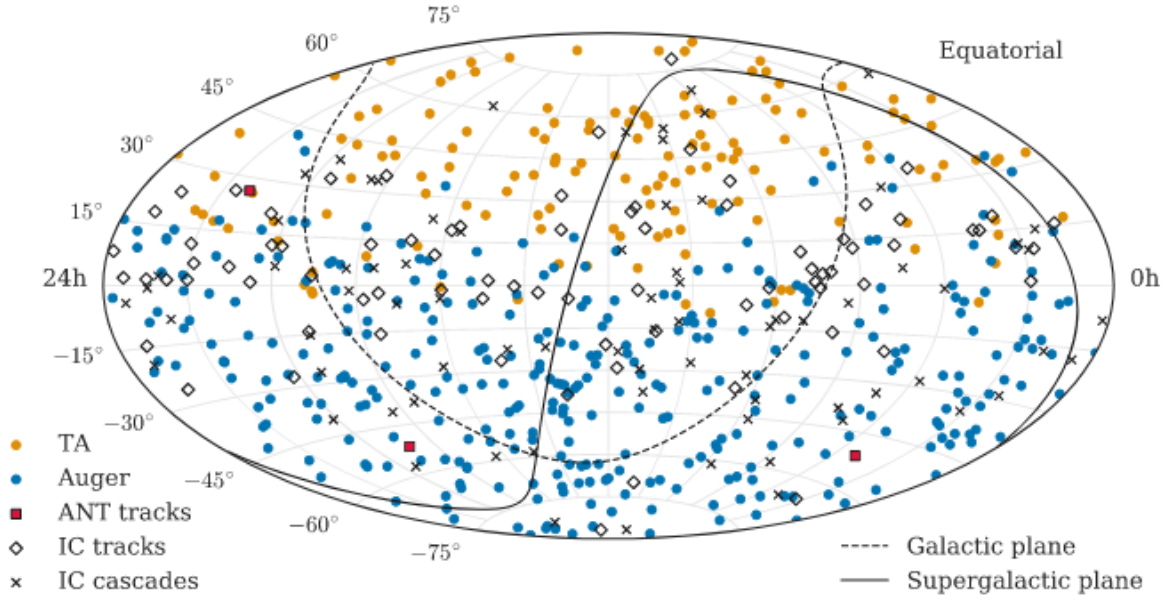

Three analyses strategies:

- UHECR-neutrino cross-correlation
- Neutrino-stacking correlation with UHECRs
- UHECR-stacking correlation with neutrinos

All compatible with background

Auger-TA comparison : the energy spectrum

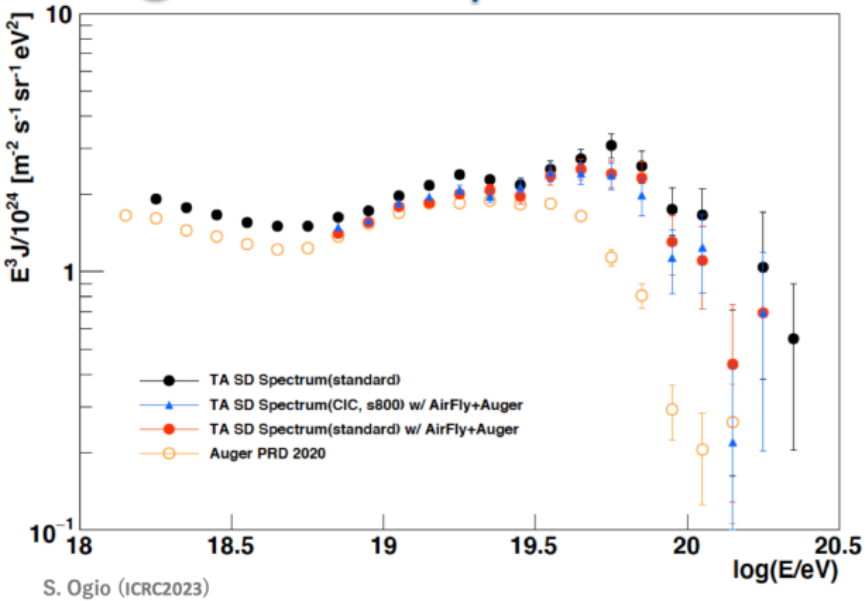

Good example of common working group

TA now using
— the same fluorescence yield (previously off by ~ -14%)
— the invisible energy (data-driven) correction of Auger (previously off by ~ +7%)

➡ E≲$10^{19.5}$ eV : good agreement (~1% difference)

S.Ogio, PoS(ICRC2023) 400
K.Fujisue, TeVPA2023

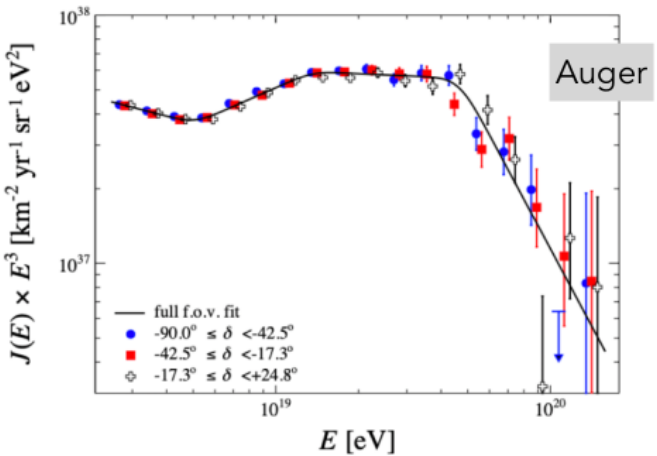

A.Aab et al., PRD 102 (2020) 062005

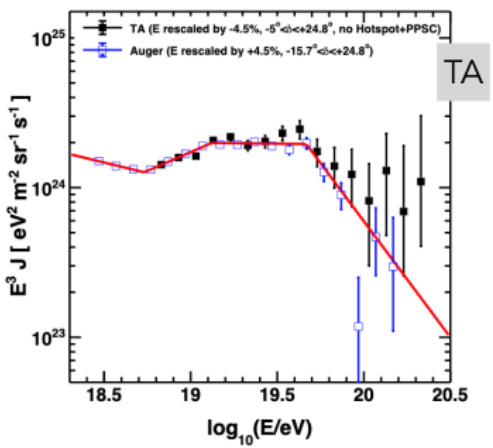

R.Abbasi et al., arXiV:2406.08612

➡ E>$10^{19.5}$ eV: persistent difference.
— no declination dependence found in Auger
— TA first claim of a declination dependence (3.5σ):
$\log_{10}E_{break}$=19.64±0.04 for lower δ
$\log_{10}E_{break}$=19.84±0.02 for higher δ
TA second claim: 1.8σ difference in common decl.band if subtracting spots

Instrument	**energy range**	**Effective area** (m^2)	**sensitivity** (milli-CU[†])	**energy resolution** (%)	**PSF** (°)	**FoV** (sr)	**duty cycle** (%)
Fermi-LAT[a)]	20 MeV - 300 GeV	~ 0.95	10 - 30	8 - 18	0.15 - 3.5	~ 2.4	~ 60
H.E.S.S.[b)]	10 GeV - 50 TeV	$\sim 10^5$	~ 5	15	< 0.1	~ 0.03	$\sim$10
MAGIC[c)]	$\geq$ 30 GeV	$\sim 10^5$	~ 7	16	≤ 0.07	0.02	$\sim$18
VERITAS[d)]	50 GeV - 50 TeV	$\sim 10^5$	~ 5	10 - 15	0.08 - 0.13	0.02	10-14
CTA-LST1[e)]	20 GeV - 300 GeV	$\sim 10^4$	~ 10	10 - 30	0.05 - 0.1	0.02	$\sim$10
ASγ[f)]	10 TeV - 1 PeV	$\sim 7 \times 10^4$	~ 200	20 - 40	~ 0.8	~ 2.0	90
ARGO-YBJ[g)]	50 GeV - 10 TeV	$\sim 0.8 \times 10^4$	~ 300	>13	~ 0.5	~ 2.0	86
HAWC[h)]	100 GeV - 100 TeV	$\sim 3 \times 10^4$	~ 50	20 - 50	~ 0.69	> 1.5	95
LHAASO-WCDA[i)]	100 GeV - 20 TeV	$\sim 0.8 \times 10^5$	~ 12	$\sim$33	0.2 - 0.84	~ 2.0	95
LHAASO-KM2A[i)]	10 TeV - 4 PeV	$\sim 10^6$	~ 12	15 - 40	0.2 - 0.6	~ 2.0	95

Auger UHE window: TXS0506

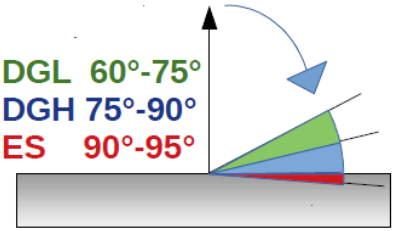

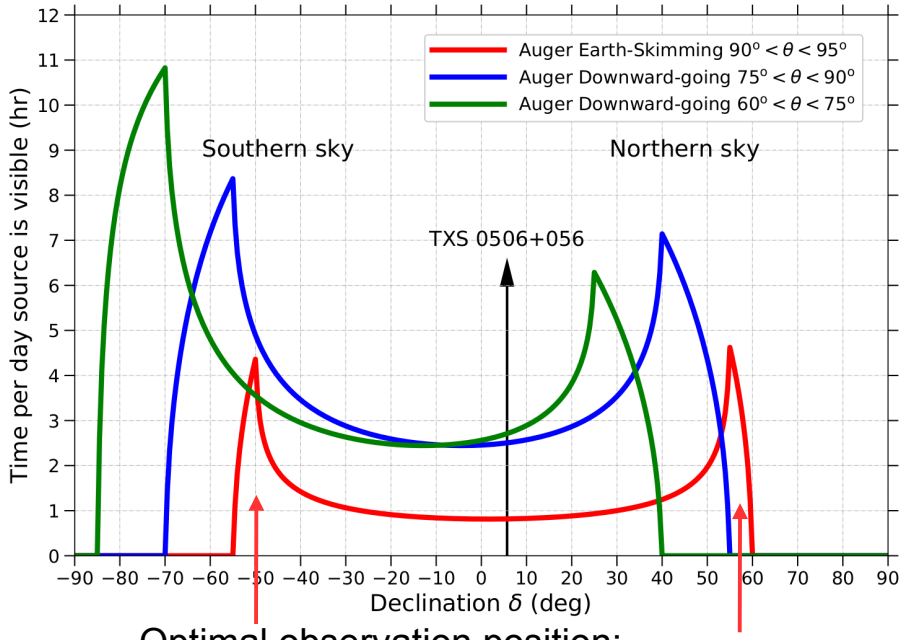

Optimal observation position: source δ in FOV of the Earth-skimming channel (right below the horizon)

TXS0506+056 declination = 5.7°
→ Non optimal sensitivity of the source in all channels

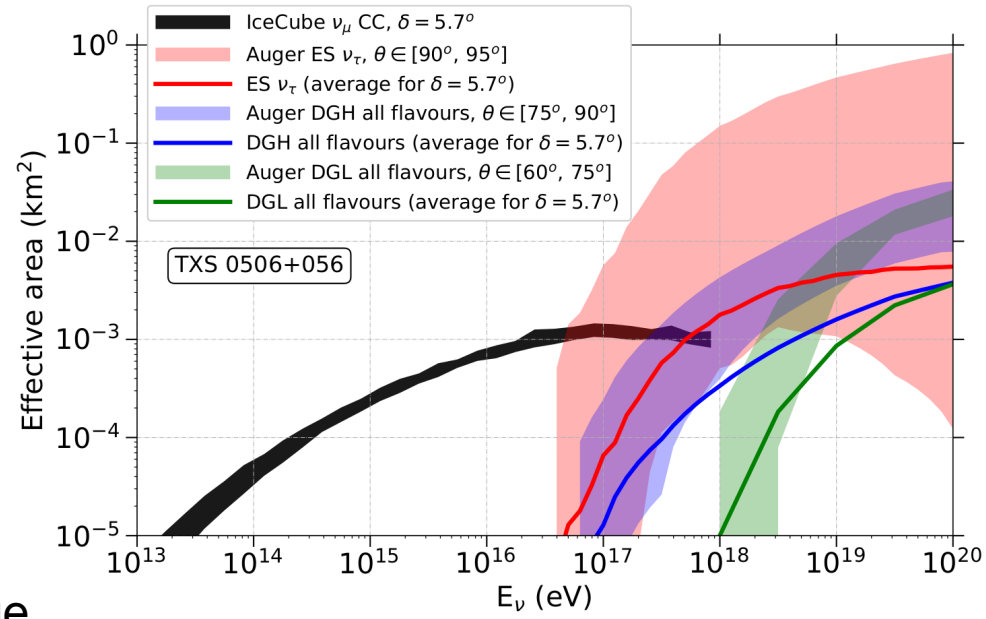

→ complementary to IceCube in the EeV range

Follow-up searches: TXS0506+056

IceCube observed a 290 TeV ν in the direction of TXS0506+056 during flaring state

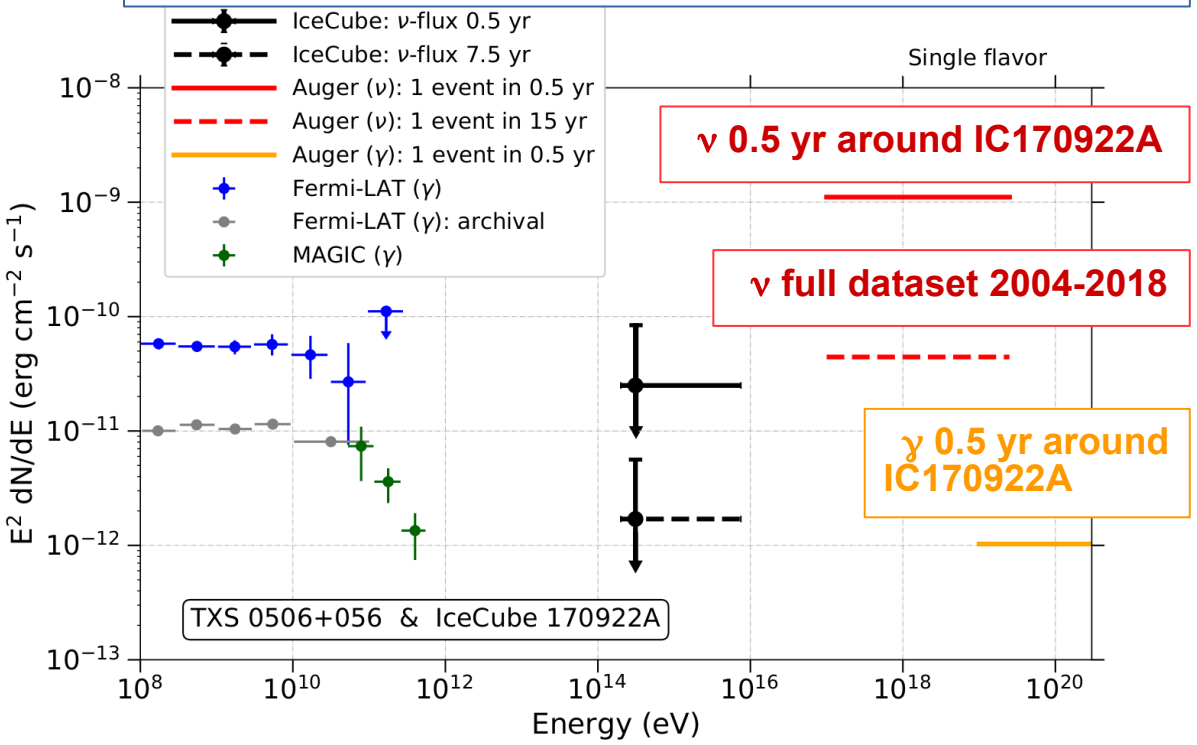

Pierre Auger Coll., Ap. J., 902:105 (2020)

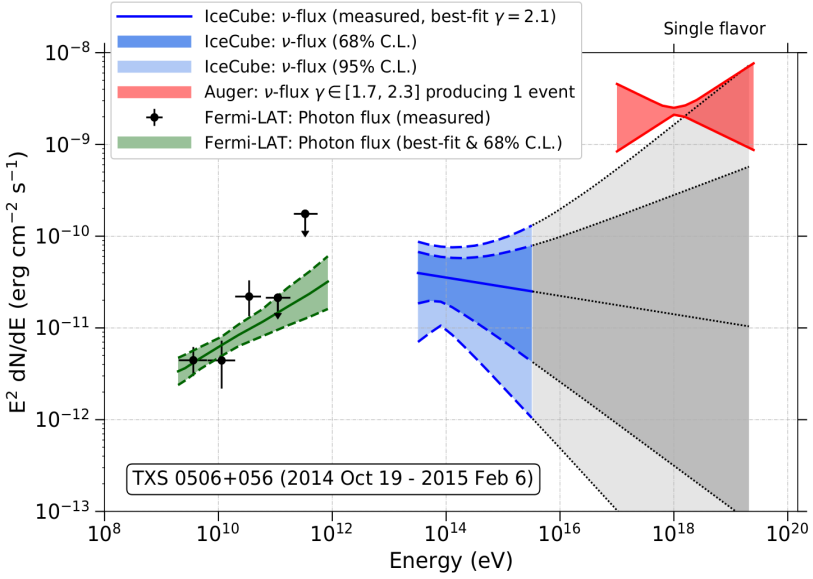

TXS0506 not in the most sensitive region

The Telescope Array project

Surface Detector: Plastic Scintillator

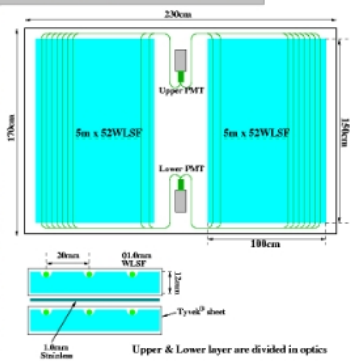

Fluorescence Detector: PMT camera

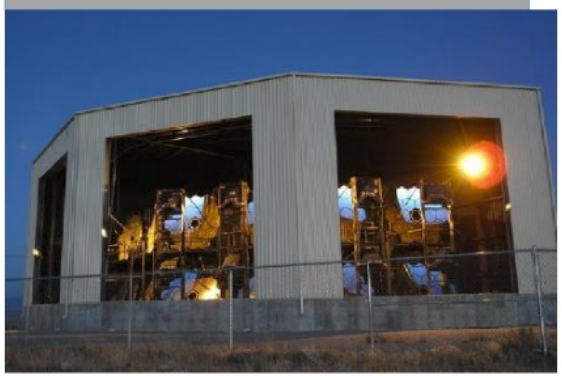

SD: 507 scintillators 3 m^2, spacing
1.2 km, Area 700 km^2

FD: 38 Telescopes in 3 stations (~30 km)

TALE (Low Extension → 2 PeV)
TALE SD (600-200-100 m)
TALE FD

TAx4, to reach 2800 km^2
spacing 2.08 km.